CELLULAR INTERACTIONS WITH HYDROGELS

RICHARD JOHN EDWARDS

Doctor of Philosophy

ASTON UNIVERSITY

September 2001

Aston University

CELLULAR INTERACTIONS WITH HYDROGELS

Richard John Edwards

Doctor of Philosophy

2001

Thesis summary

An efficient means of evaluating potential biomaterials is to use the *in vitro* fibroblast cell culture model. However, the chemistry which influences cell adhesion on polymer substrates is poorly understood. The work in this thesis aims to rationalise several theories of current opinion and introduce new chemical techniques that may predict cellular behaviour. The keratoprosthesis is a typical example of the need to be able to manipulate cell adhesion of materials since both adhesive and non adhesive sections are needed for proper integration and optical function.

Calcein AM/ethidium homodimer-1 and DAPI assays were carried out using 3T3 and EK1.BR cells. Poly(HEMA) was found to be the most cell adhesive hydrogel tested. The reactivity of monomers and the resulting sequence distribution were found to affect surface properties and this may explain the poor levels of cell adhesion seen on NVP/MMA copolymers. Surface free energy is shown to be dependent on the polar and non polar groups present along the backbone chain of the polymers. Dehydrated and hydrated contact angle measurements show the effect of rotation of surface groups around the backbone chain. This effect is most apparent on hydrogels containing methacrylic acid. Dynamic contact angle measurements confirm sequence distribution irregularities and demonstrate the mobility of surface groups. Incorporation of NVI or DEAEMA into the hydrogels does not affect the mobility of the surface groups despite their bulkiness. Foetal calf serum was used for the first time as a test solution in an attempt to mimic a biological environment during surface experiments. A Vroman effect may be present, and may involve different surface proteins for each material tested.

This interdisciplinary study combines surface characterisation and biological testing to further the knowledge of the biomaterial/host interface. Surface chemistry techniques appear to be insufficiently sensitive to predict cellular behaviour. The degree of ionisation of hydrogels containing ionic groups depends on the nature of the functional groups as well as the concentration and this is an important parameter to consider when comparing charged materials.

Keywords: cell adhesion, hydrogel, keratoprosthesis, biomaterial, chemistry

For my family

ACKNOWLEDGEMENTS

I would like to thank Professor Brian Tighe for the opportunity to study in the Biomaterials Research Unit and for his encouragement throughout the course of this research.

I am especially grateful to Dr Steve Tonge for most interesting discussions during my time at Aston, for his advice, and for reading the draft of this thesis.

I am grateful to Professor Andrew Lloyd and Dr Susi Sandeman for allowing me to carry out the DAPI assays in their laboratories at the School of Pharmacy and Biomolecular Sciences, University of Brighton.

Many thanks to fellow chemists Jifan Li, Graham Skelton, and Simon Andrews; also to cell biologist Chris Graham and neurobiologist Laurent Belœil for their friendship.

I thank my parents and brother James; Muriel Goldstein and Fabienne Erivo in Paris; and all my other friends for their continued support.

I would like to acknowledge the financial support of the Engineering and Physical Sciences Research Council (EPSRC) and Aston Biomaterials as part of the CASE award Total Technology programme.

LIST OF CONTENTS

LIST OF TABLES

LIST OF FIGURES

ABBREVIATIONS

AMO	Acryloylmorpholine
AZBN	Azo-bis-isobutyronitrile
Calcein AM	Calcein acetoxy methyl ester
CHN	Carbon, Hydrogen, Nitrogen
DAPI	4',6-diamidino-2-phenylindole
DCA	Dynamic Contact Angle
DEAEMA	Diethylaminoethyl methacrlyate
DMAPAA	*N*,*N*-dimethyl aminopropyl acrylamide
DMEM	Dulbecco's Modified Eagle's Medium
DMSO	Dimethyl sulphoxide
DNA	Deoxyribonucleic acid
DPBS	Dulbecco's Phosphate Buffered Saline
DSC	Differential Scanning Calorimetry
ECM	Extracellular matrix
EDTA	Ethylenediaminetetra-acetic acid
EGDMA	Ethylene glycol dimethacrylate
EMA	Ethyl methacrylate
EthD-1	Ethidium homodimer-1
EWC	Equilibrium water content
FCS (or FBS)	Foetal calf serum
Fn	Fibronectin
HEMA	2-Hydroxyethyl methacrylate
HIV	Human Immunodeficiency Virus
HPLC	High Performance Liquid Chromatography
IPN	Interpenetrating polymer network
ITA	Itaconic acid
KPro	Keratoprosthesis
LMA	Lauryl methacrylate
MAA	Methacrylic acid
MeOH	Methanol

MMA	Methyl methacrylate
MMP	Matrix metalloprotease
MTT	3-(4,5-dimethylthiazol-2-yl)-2,5-diphenyl tetrazolium bromide
NMR	Nuclear Magnetic Resonance
NNDMA	*N*,*N*-dimethylaminoethyl methacrylate
NVI	*N*-vinyl imidazole
NVP	*N*-vinyl-2-pyrrolidone
OOKP	Osteo-odonto-keratoprosthesis
PDL	Population doubling level
PDMS	Poly(dimethylsiloxane)
PEGMA	Poly(ethylene glycol methacrylate)
PEM	Phenoxyethyl methacrylate
PEO	Poly(ethylene oxide)
PK	Penetrating keratoplasty
PTFE	Poly(tetrafluoroethylene)
RGD	arginine-glycine-aspartic acid peptide sequence
SEM	Scanning Electron Microscopy
SPA	(3-sulphopropyl)-acrylate, potassium salt
SPE	*N*,*N*-dimethyl-*N*-(2-methacryloyloxyethyl)-*N*-(3-sulphopropyl) ammonium betaine
SPI	itaconic acid bis-(3-sulphopropyl)-ester, di potassium salt
SPP	*N*,*N*-dimethyl-*N*-(3-methacrylamidopropyl)-*N*-(3-sulphopropyl) ammonium betaine
SPV	1-(3-sulphopropyl)-2-vinylpyridinium betaine
STY	Styrene
Vn	Vitronectin

CHAPTER 1
INTRODUCTION

1.1 Overview

Biomaterials are synthetic or natural materials which can be used for biomedical applications, to replace or assist a natural body part which no longer functions satisfactorily. Examples include artificial hip prostheses, finger joints, contact lenses and keratoprostheses (artificial corneas). To avoid rejection of the implanted material, the material must not adversely affect the body or be adversely affected by the environment. In the case of keratoprostheses and other implants where inertness is not sufficient, a better definition of biocompatibility is one which takes into account the integration necessary for successful implantation. A biocompatible material, therefore, is a material which produces an appropriate host response. There has been great interest in the surface properties of potential biomaterials because it is the surface properties which will govern performance at the tissue/material interface.

A gel is a polymer network that swells when immersed in solvent, but which is prevented from dissolving by the presence of crosslinks which hold the structure intact. Hydrogels are water-swollen polymer networks. Hydrogels have applications in biomaterials, and have seen most commercial success in soft contact lenses, drug delivery systems and wound dressings[1].

Cells which are cultured *in vitro* can be used as sensitive surface probes[2] to better understand the interactions between biological systems and hydrogels, in particular the factors which make cells grow on surfaces. Eventually, it would be desirable to be able to modify the surface of a polymer in order to make it more or less cell adhesive, as required. For example, current designs of keratoprosthesis incorporate a non cell adhesive core and a cell adhesive skirt[3] as the artificial cornea must be optically clear in the centre for light to be transmitted, but able to integrate with the host tissue at the periphery. In addition, cultured cells have advantages over *in vivo* experimentation. The technique avoids the use of costly and time consuming animal trials and the use of defined media enables individual parameters to be studied.

The special place that the eye holds in biomaterials work stems from its ready accessibility.

1.2 Structure of the Cornea

The cornea is a transparent, avascular tissue situated at the front of the eyeball. The anterior corneal surface is covered by the tear film and the posterior surface is directly bathed by the aqueous humour. It is a very tough avascular tissue where the presence of capillaries would otherwise reduce the transparency and it is highly innervated to ensure rapid detection of damage and instigation of repair[4]. Its surface is protected and lubricated by the tear film. Tears are made from a complex mixture of lipid oils, mucus, carbohydrates and cells involved in immunity[5]. Without a tear film the ocular surface dries out, warps or thins leading to blindness. Oxygen is supplied primarily by diffusion from the air via the tear fluid. When the tear film is poorly formed or lacking the passage of pathogens is made easier, while healing is slower and less well defined.

The cornea is the point of entry for light into the eyeball. It transmits and bends incoming light onto the lens, providing about two thirds of the total refractive power of the eye. The cornea also serves as a barrier to the entry of pathogens and to fluid loss.

Three cellular layers of tissue separated by two interfaces make up the cornea (Figure 1.1). Outermost is the epithelium composed of five to seven layers of cells resting on a basement layer (Bowman's layer). Below this layer is a connective tissue stroma. Descemet's membrane separates the stroma and the endothelium.

At the outermost layer of the cornea epithelial cells are regularly shed and renewed and therefore moderate physical damage has no disruptive effect. This process also ensures that bacteria and viruses attempting to penetrate the eyeball are removed from the surface of the cornea.

The stroma, or middle region forms the bulk of the cornea (90%) and is composed of a highly ordered meshwork of collagen fibrils interspersed with keratocytes. The exact orientation of these fibrils is crucial to giving the cornea its transparency. Collagen fibrils are arranged in a manner in which the wave pattern of light passing straight through the cornea and the wave pattern of light scattered by the solid elements making up the cornea become perfectly aligned in what is called constructive interference. It is more likely that light scatter is removed by the scaling of the refractile elements to just below the wavelength of visible light[6].

Very severe diseases of the cornea alter collagen fibril arrangement and while the epithelium is able to properly regenerate, the stroma cannot do the same. The initiators of collagen fibril arrangement are the keratocytes. Cellular components occupy only 2 to 3% of the total volume of the stroma[7]. The rest is occupied by various extracellular matrices, mainly collagen and glycosaminoglycans. The organisation of the stromal extracellular matrix (ECM) is dictated by keratocyte activity. Approximately 2.4 million keratocytes are present within the stroma where they fill only 2 to 3% of the total stromal volume[8]. They are quiescent in the resting cornea and turnover is estimated at approximately 2 to 3 years[9]. However, keratocytes may be quickly activated in response to stromal injury for involvement in the wound healing response. Following wounding the activated keratocyte is stimulated to move into the wound and begin synthesis of products involved in corneal tissue repair.

With any injury to the cornea, corneal stroma keratocytes near the injured sites lose their network connection and behave independently. Activated keratocytes migrate into the wound and are adapted to produce the various structural proteins, enzymes, enzyme inhibitors and growth factors required to remodel the stroma and re-establish corneal transparency[10]. They synthesise collagen molecules (pro-collagen) and glycosaminoglycans. At the same time, the cells synthesise collagen degrading enzymes, such as matrix metalloproteases (MMPs).

Keratocytes act in conjunction with signals from the ECM which means that cell maintenance of ECM integrity is in turn important for cell growth and growth factor responsiveness[11].

Lying posteriorly in the cornea is the endothelium. This layer of tissue has a physiological role in maintaining corneal transparency by actively pumping water from the stroma into the anterior chamber. This maintains the stroma at constant turgidity. If either too much or too little water is pumped posteriorly the fibrils become distorted and clump together causing opacity[12].

Figure 1.1 Structure of the cornea (photograph reproduced from Kaufman et al.[13])

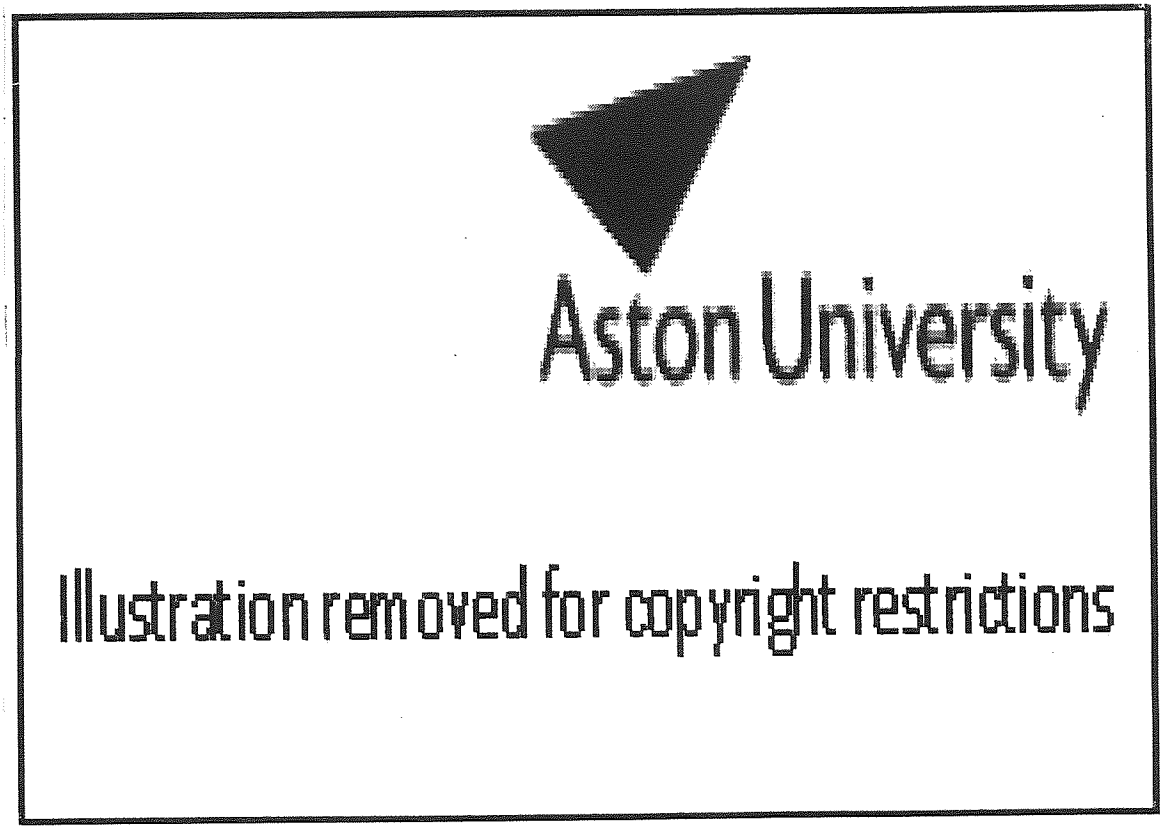

Cell adhesion tests and especially work on keratocytes will give information which may be of great value in the development of an artificial cornea. Adhesion to the ECM is mediated primarily by the integrin family of cell surface receptors[14].

1.3 Contact Lenses

It is interesting to note that early biomaterials research was led by work in the area of contact lenses[1], due to the accessibility of the eye as a site for material implantation. No surgery is required and short term effects can easily be observed.

A contact lens will come into contact with the cornea, the eyelid and the tears. The cornea dictates the range of acceptable transport properties of the contact lens, the eyelid governs comfort and mechanical properties and the tears govern the surface properties of the hydrogel[1].

A contact lens can be seen as an extension of the cornea, and ideally has similar properties such as oxygen permeability, wettability, water content and mechanical strength. If the cornea does not receive sufficient oxygen through the contact lens it will attempt to derive oxygen from surrounding areas, before swelling and becoming opaque. Conventional wisdom would suggest that the contact lens must be non toxic, and its surface properties must not encourage accumulation of protein or lipid deposits on the surface of the lens. The tear fluid must wet the lens sufficiently to enable a continuous tear film to be maintained on the lens.

However, a contact lens which is homogeneous in structure cannot be expected to perfectly mimic the behaviour of the cornea which has a layered structure: bulk properties are determined by the stroma and surface properties are determined by the epithelium.

1.4 Artificial Corneas: Keratoprosthetic Implants

The artificial cornea is a device that replaces severely diseased, damaged and opaque corneas. These keratoprosthetic devices are used when it is not feasible to carry out a corneal transplant e.g. when there is a possible risk of rejection or when the anatomic integrity of the eye has been damaged. For example, severe damage to the corneal stroma such as caused by chemical burns cannot be adequately treated. Stevens-

Johnson syndrome and phemphigoid are serious incurable conditions that cause corneal blistering and scarring. The use of artificial implants also eliminates the risk of transmission of infectious disease such as Human Immunodeficiency Virus (HIV) and Hepatitis B. Typically, the implant consists of a visual optical core supported in the cornea by a haptic peripheral component. Two components are needed to produce a functioning keratoprosthesis, a clear optical core that is non-cell adhesive and a peripheral (haptic) skirt that supports cell adhesion and integration (Figure 1.2).

Figure 1.2 Structure of a modern artificial cornea: the popular core and skirt model[15, 16, 17]

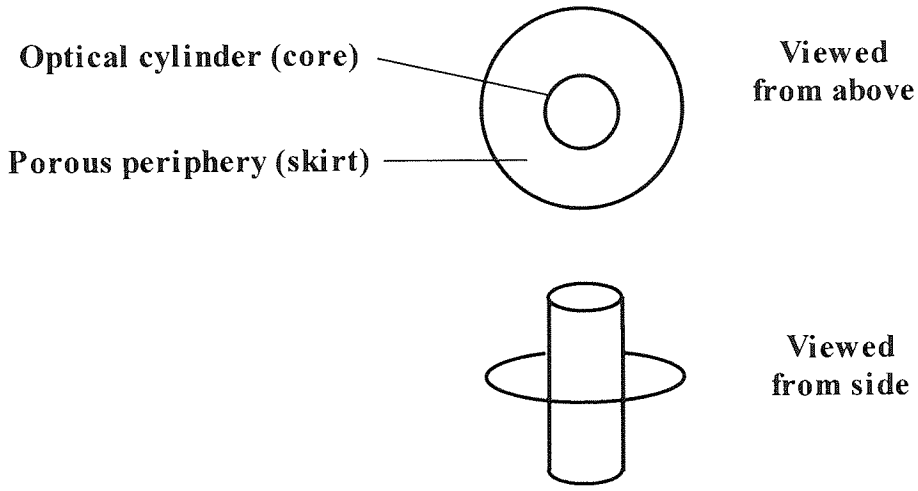

A keratoprosthetic device (KPro) must be securely attached to the surrounding cornea. The KPro also requires the periphery of the device (constructed of a porous material) to be penetrated by stromal fibroblasts which will proliferate and synthesize connective tissue proteins. This allows natural healing and anchorage to take place[18]. The optical core needs to protrude from the front and back of the cornea for vision to be maintained and to avoid the overgrowth of keratocyte cells or the downgrowth of epithelial cells. Long-term success of keratoprosthetic devices requires that the perforating plastic optical core is stabilised within the cornea[19].

Not only does the peripheral portion of a keratoprosthesis need to stabilise the optical cylinder so as to maintain the optical core in a correct position in the cornea, the periphery needs to be flexible and resistant to stresses and also to act as a barrier to epithelial downgrowth. The haptic component, however, is also required to be sufficiently porous to allow keratocyte ingrowth so that adhesion, migration and

replication of host epithelium can take place. The periphery must not interfere with the normal metabolic actions of the cells in the eye and elicit, at the most, only a limited inflammatory response. The periphery must encourage the ingrowth of fibrous tissues from the adjacent rim of the host cornea and maintain continued viability of the tissues.

KPros were considered as early as the eighteenth century. Pellier de Quengsy[20, 21, 22] first suggested using glass to replace an opaque cornea in 1796 but his designs were not developed further due to the success of donor corneal transplants (keratoplasty). The concept of an artificial cornea was revived when it was later observed that keratoplasty was not successful in all cases.

In 1853 Nussbaum[23] implanted a glass stud into a rabbit cornea, and Heusser is thought to be the first to operate on a human patient in 1859; his glass implant lasted for 3 months[24].

During World War II it was noted that poly(methyl methacrylate) (polyMMA) fragments from shattered aeroplane canopies embedded in pilots' corneas were well tolerated. For this reason, most current KPros use a poly(MMA) optic. Familiar models resemble a mushroom shape and include Dohlman's 'collar button' KPro[25] (Figure 1.3), and Cardona's 'nut and bolt' and 'through-and-through' KPros[26, 27]. These designs incorporate an anchoring surround to fix the rigid poly(MMA) optic through the host cornea.

Figure 1.3 Dohlman KPro (photograph reproduced from Hicks et al.[24])

Stone and Herbert[28] initially developed the idea of a peripheral KPro skirt containing holes or pores to allow better host tissue ingrowth. Porous skirt materials have been shown to reduce the rate of expulsion[29]. This is because cells and matrix proteins can infiltrate much deeper into the material. With a sufficiently strong adhesion between tissue and material surface, leakage of aqueous humour to the surface and the potential for infection are minimised.

Modern polymers have been very useful because they can be easily moulded into any desired shape and are resilient to a range of chemical solvents and physical conditions.

Legeais and his coworkers[30] have designed a second generation KPro substituting the poly(MMA) optic with an optic made from poly(dimethylsiloxane) (PDMS) coated with poly(vinyl pyrrolidone) (Figure 1.4). Expanded PTFE with a pore diameter of 80 μm is used for the skirt material. The optic still does not support epithelial cell coverage, a feature considered desirable by Legeais. However, most of the eyes were clinically stable after 7 months follow up and the new material appears to show advantages such as better surface properties compared with poly(MMA).

Figure 1.4 Legeais KPro[30]

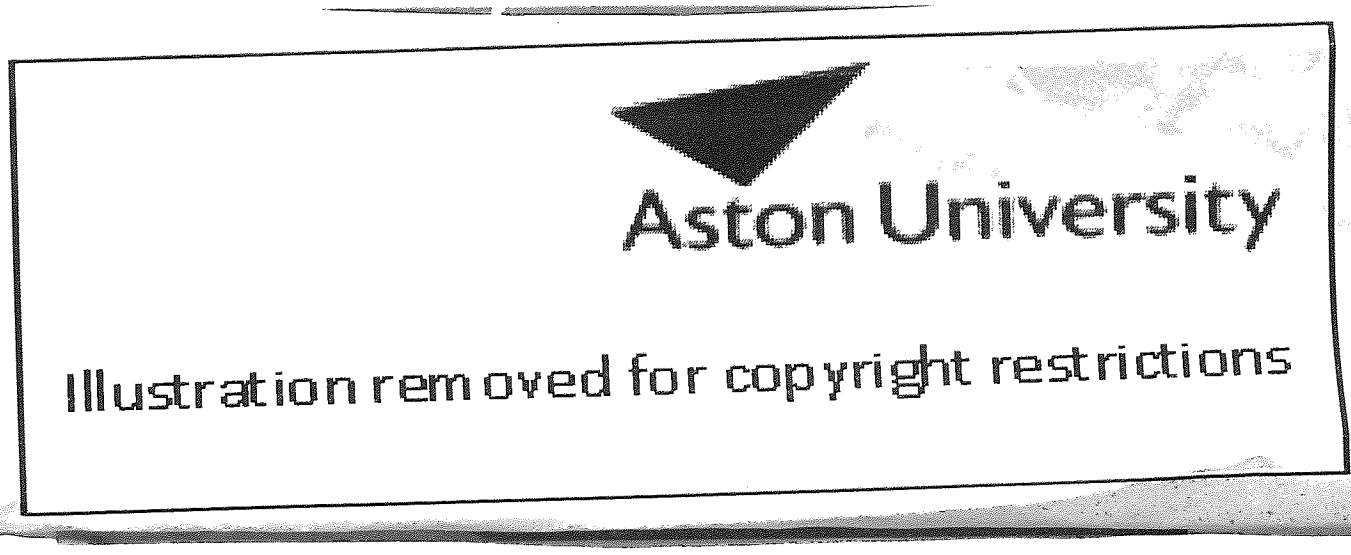

Chirila and his team of researchers have employed simple hydrogel chemistry to manufacture a keratoprosthesis that can biologically integrate with the host cornea[29, 31, 32] (Figures 1.5 to 1.7).

Figure 1.5 Chirila KPro (photograph reproduced from Hicks[33])

Figure 1.6 Chirila KPro before implantation (photograph reproduced from Hicks et al.[24])

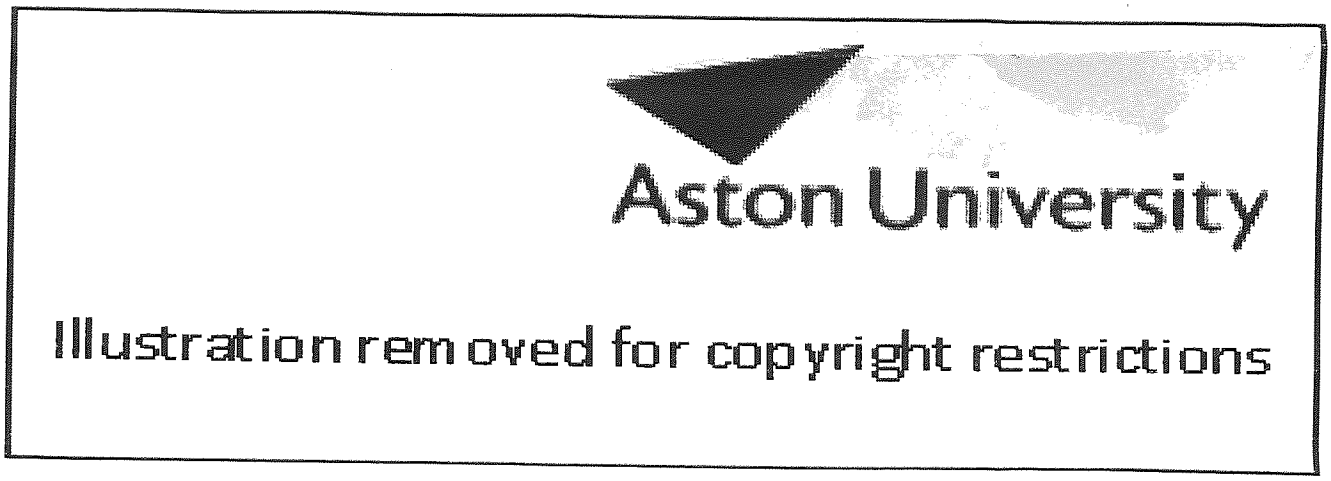

Figure 1.7 Chirla KPro during surgery (photograph reproduced from Hicks[33])

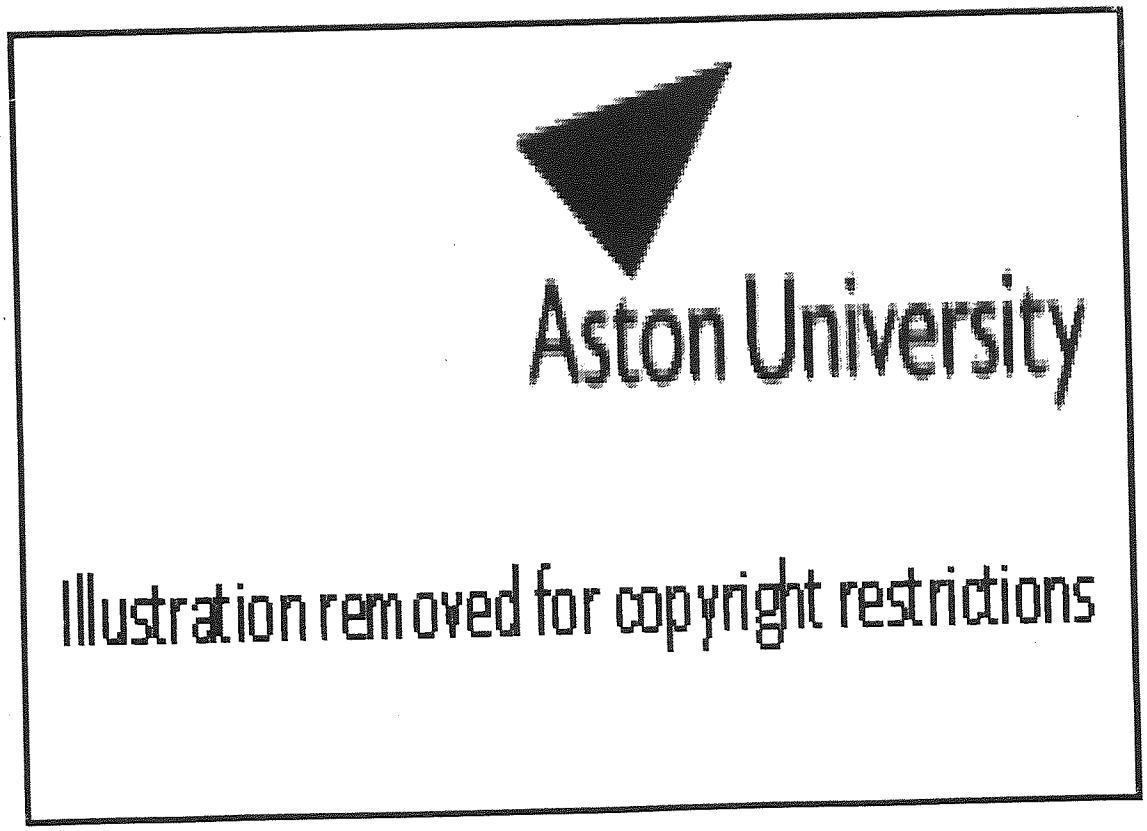

They have been able to overcome the problem of combining a solid transparent element (the optical core) with a spongy, opaque periphery, using interpenetrating polymer network forming (IPN) technology to form a graduated fully interpenetrative bond between the two elements. The spongy periphery encourages rapid fibrovascular inward growth into the pore spaces. Poly(HEMA) is used for both components. Chirila's KPro has been implanted into 11 human patients, 4 of whom have retained the prosthesis for 12 to 18 months so far, all have improved vision[34].

Porous poly(HEMA) sponges have been shown by Chirila's group[35] to support viable cellular colonisation, thereby providing a suitable environment for maintaining cell viability. However, unmodified poly(HEMA) is considered nonadhesive for mammalian cells, so the optic does not support epithelial cell coverage.

The most successful KPro to date is the osteo-odonto-keratoprosthesis (OOKP) which consists of a tooth and bone supporting frame and a poly(MMA) core[36, 37] (see Figure 1.8). Devised by Strampelli in 1963 and improved by Falcinelli, the OOKP is the only prosthesis with more than 20 years follow-up. The OOKP uses an osteo-odontal lamina for the support frame. The lamina is a section of the afflicted patient's canine tooth (including dentine, cementum and peridontal ligament) and a region of surrounding jawbone in which the tooth is supported. The use of autologous tissue avoids rejection by the immune system and the spongy bone integrates well with the host cornea.

Figure 1.8 OOKP. Basal surface of a freshly excavated section of tooth root and alveolar bone with optical cylinder inserted; prior to reattachment of periosteum and insertion into a subcutaneous pocket (photograph provided by Mr Christopher Liu, Sussex Eye Hospital)

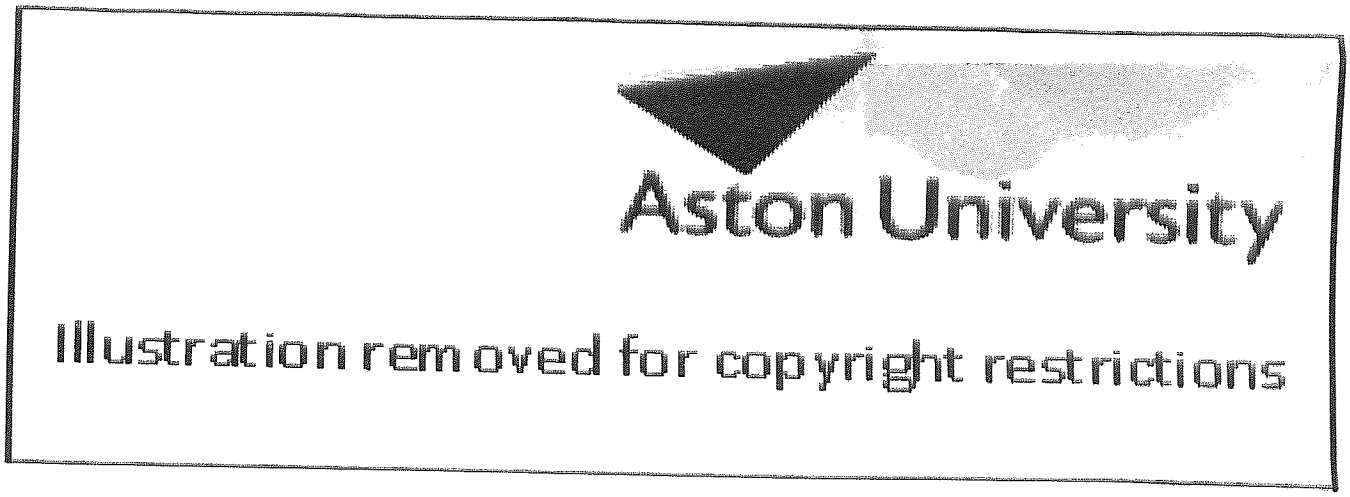

Figure 1.9 Implanted OOKP. Final placement into the anterior eye: the plastic optic is surrounded by soft and moist buccal mucosa bandage removed from the inner cheek of the afflicted patient (photograph provided by Mr Christopher Liu, Sussex Eye Hospital)

Figure 1.10 Implanted OOKP with cosmetic iris (photograph provided by Mr Christopher Liu, Sussex Eye Hospital)

An independent analysis of the work of Falcinelli was made by Liu and Pagliarini[38] and the success rate was confirmed to be very high. 77% of eyes could see 6/12 or better and no KPros had extruded from the eye. The reason for these results is attributed to the function of the cementum in preventing epithelial downward growth and hence expulsion.

The OOKP does have some disadvantages which have made the technique unpopular with some surgeons. Early trials were largely unsuccessful and this may have contributed to the relative lack of interest. Also, the procedure is complex and traumatic for the patient due to the multiple stages of the treatment. Sometimes the patient does not have a suitable tooth available. There are, therefore, good reasons for developing a synthetic version of the OOKP. A synthetic OOKP would reduce the first stage of surgery by half since extraction of tooth and bone would be unnecessary.

KPros currently in clinical use tend to be PMMA based. However, the success of these KPros is constrained by a number of the complications previously described.

Trinkaus-Randall *et al.*[39] has reported that poly(vinyl alcohol) copolymer hydrogels are able to support epithelial cells. The copolymer is claimed to have twice the tensile strength of corneal tissue and be optically transparent. The skirt material is a web made from poly(propylene) and poly(butylene) and allows fibroblastic ingrowth. Trinkaus-Randall demonstrated that stromal keratocytes could penetrate the material, proliferate, and synthesise collagen. The KPro has not yet been tested on human patients.

Kornmehl *et al.*[40] developed the rabbit derived collagen allograft as a material for an artificial cornea. Collagen is the primary structural protein of the cornea and collagen allografts are readily available, disease free and optically clear. Extrusion did not occur but epithelial coverage over the clear central zone was poor, and necrosis occurred. However, Kornmehl believed that these problems could be overcome.

A "Seoul-Type" KPro consisting of a poly(MMA) core together with an expanded PTFE or poly(urethane) skirt and a poly(propylene) haptic has been developed by Lee *et al.*[41]. The skirt is anchored to the cornea, and the haptic is anchored to the sclera to improve its biostability. An amniotic membrane graft also improved stability of the implant. Two human patients have received the KPro and have maintained a good postoperative condition for 18 and 8 months.

Recently Green[42] has developed a keratoprosthesis using biocoral though this has yet to be implanted in an eye (Figure 1.11).

Figure 1.11 Biocoral KPro[42]

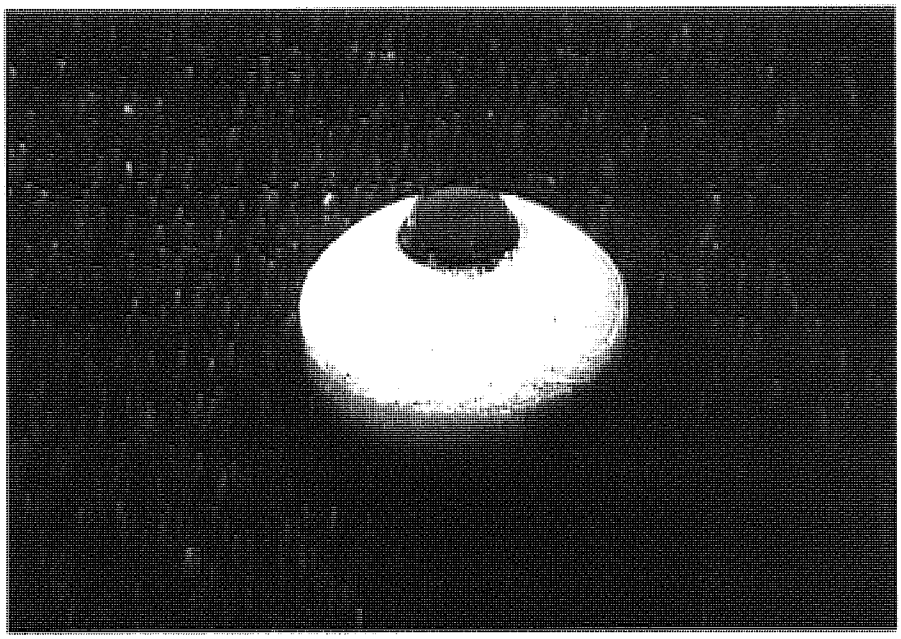

All KPros currently available produce serious complications such as implant extrusion, membrane formation, infection, inflammation and glaucoma[25, 43]. The most common KPro complications include tissue necrosis ("corneal melting") around the perforating impervious plastic optical core, due to enzymatic degradation of stromal collagen[16]. Leakage of aqueous humour around the KPro, and downgrowth of surface epithelium causing extrusion are also frequent complications[44].

Gradual ulceration (melting) is most likely to be the direct result of the local release of proteolytic enzymes such as collagenases and proteases from polymorphonuclear leukocytes[45]. If this inflammation is severe, leukocytes can also pass into the tear film from dilated conjunctival capillaries. If at the same time the inflammation has caused an epithelial defect in the cornea, the leukocytes in the tear film can adhere in large numbers to the naked stromal surface within the defect. The subsequent release of proteolytic enzymes at the site of keratoprosthetic attachment can cause digestion of the basal membrane and lead to keratoprosthetic extrusion and stromal perforation[46].

Complications have commonly arisen because integration of the KPro materials within the host corneal tissue fails to occur. However, keratoprosthetic implants have been shown to have more success when the anterior prosthetic surface is covered by

autologous materials, for example, the conjunctiva or buccal mucosa[47]. Coating with a biological substrate such as collagen also demonstrates less post-operative necrosis in adjacent tissue[44].

The ideal KPro would be an epithelialised "artificial donor button" that could be implanted as in penetrating keratoplasty (PK)[25]. It would comprise a transparent, semi-rigid core of sufficient diameter to allow a reasonable field of view, and providing similar refractive index to that of the natural cornea, together with an ultraviolet radiation filter. A porous skirt of similar chemical composition and flexibility should surround the core, the two components being joined in a manner which prevents loosening or leakage at their interface. The skirt should allow fibroblast ingrowth and collagen deposition sufficient to provide a permanent anchorage, and be strong enough to bear sutures. It should also be permeable to all nutrients and regulatory agents that ensure a return to near normal tissue architecture. The anterior surface should be wettable and should allow epithelialisation but discourage protein or lipid deposition. All the chemical constituents should be free from any tendency to cause inflammation or mutagenesis. The device should be implantable without requiring extensive surgery, thus reducing the risk of glaucoma, retinal detachment, and intraocular inflammation. The posterior surface should inhibit cellular attachment and proliferation to prevent the formation of opaque retroprosthetic membranes.

Hydrogel polymers are good candidates for potential keratoprostheses due to their optical, chemical and physical properties and because of their commercial success as contact lenses.

1.5 Scope and Objectives

The aim of the study undertaken in this thesis is therefore to determine the surface properties of a range of hydrogel polymers, especially those expressing charged groups, in order to gain an understanding of the tissue/material interface so that improved materials for use in ophthalmic applications can be developed. Physical

chemistry techniques have been used in conjunction with cell biology methods so that predictive techniques may be developed for assessing potential biomaterials.

Hydrogel polymers, grouped into 'families' were synthesised by bulk free radical vinyl polymerisation. Families comprised materials of increasing water content, or increasing ionic monomer. A typical contact lens composition was used as a starting point and each hydrogel was assessed for its suitability as a KPro candidate.

Both static and dynamic contact angles were measured. Static contact angles are employed to determine surface free energy parameters, while dynamic contact angles are very useful in determining the wettabilities of the test materials. Cell adhesion studies were carried out in the tissue culture laboratory in order to test the biological compatibility of the hydrogels. It is hoped that a knowledge of the factors involved in cell adhesion will aid in the targeted design of polymers having specific characteristics, removing the need to rely on currently available 'off the shelf' materials for biomedical applications.

CHAPTER 2

HYDROGEL SYNTHESIS AND CHARACTERISATION

2.1 Introduction

2.1.1 Hydrogels

The unique properties of synthetic hydrogels were first described in 1960 by Otto Wichterle[48] who developed poly(2-hydroxyethyl methacrylate), commonly referred to as poly(HEMA). Wichterle showed that poly(HEMA) could be used to manufacture soft contact lenses[49, 50] due to its surface properties, handling characteristics and ease of fabrication. In addition, oxygen transport to the cornea was assured, owing to the water contained in the hydrated polymer.

Hydrogel polymers are analogous in structure to a washing line. A variety of chemical groups (i.e. the washing) can be suspended from the backbone chain (i.e. the washing line. The reaction scheme follows the usual vinyl polymerisation, as shown in Figure 2.1.

Figure 2.1 Outline reaction scheme for vinyl polymerisation

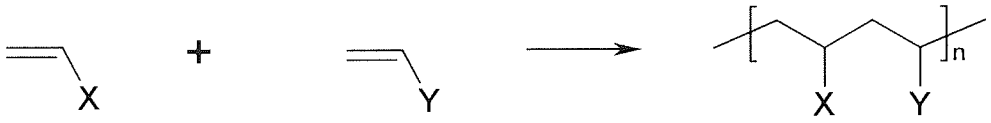

where X and Y refer to the pendent "washing line" groups on each monomer

Figure 2.2 Detailed reaction scheme for vinyl polymerisation

Initiation

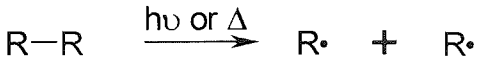

where R is any hydrocarbon group and R• is its radical, and

where hυ is ultraviolet radiation, and Δ is heat energy

Propagation step 1

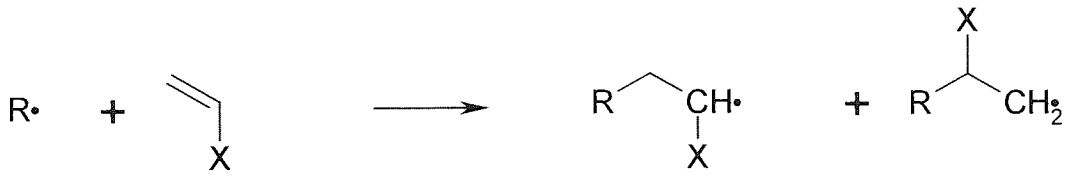

(a) (b)

Product (a) predominates because the methylene carbon is less sterically hindered for attack and yields a more stable product.

Propagation step 2

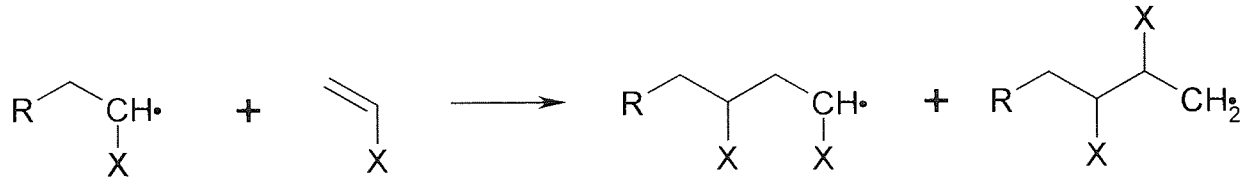

(a) (b)

Product (a) predominates for the same reasons as above.

Termination

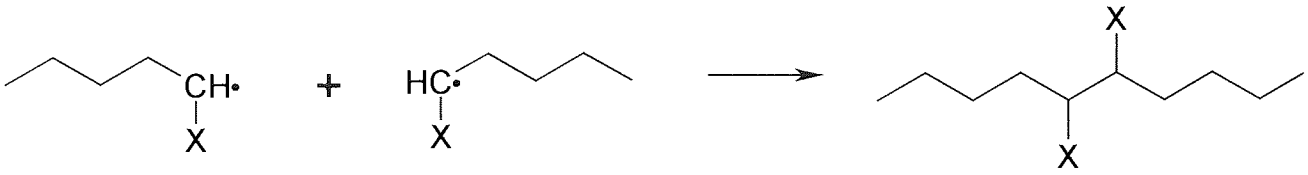

This type of termination step is known as combination

This type of termination step is known as disproportionation

The structure of poly(HEMA) is similar to that of poly(methyl methacrylate), or poly(MMA), the difference being the presence of a hydroxyl group on every repeat unit of the poly(HEMA) polymer chain (Figure 2.3). When dehydrated, poly(HEMA) has similar properties to poly(MMA) in that it is hard, clear and glassy. However, when poly(HEMA) comes in contact with water, the polymer becomes flexible and elastomeric, due to the tendency for the hydrophilic hydroxyl groups to associate with water. The dehydrated xerogel swells to accommodate the water, resulting in a flexible hydrogel. Poly(MMA) remains hard and glassy when in contact with water because it lacks hydrophilic groups.

Figure 2.3 Structure of poly(MMA) and poly(HEMA)

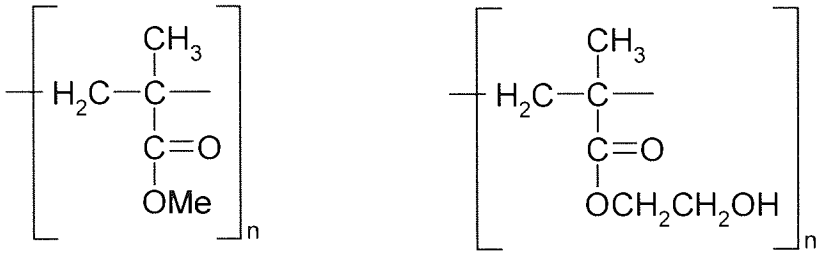

poly(MMA) poly(HEMA)

The degree of swelling exhibited by homogeneous hydrogels depends on the cross-link density, that is the length of backbone chain between cross-links.

2.1.2 Equilibrium Water Content

The equilibrium water content (EWC) is the most important property of a hydrogel as it influences permeability, mechanical, surface and other properties of the polymer. The EWC is expressed as the ratio of the weight of water in the hydrogel to the weight of the hydrogel at equilibrium hydration, converted to a percentage.

The total amount of water in hydrogels is related in part to the balance of hydrophilic and hydrophobic components and the steric and polar contributions of backbone substituents. The EWC is also governed by the nature and density of the crosslinking agent and by external factors such as temperature, tonicity (especially the nature of the constituent ions), and pH of the hydrating medium.

2.1.3 Structure of Water

The water contained in a hydrogel exists as a continuum of states between two extremes. Water strongly associated with the polymer matrix through hydrogen bonding is referred to as bound or non-freezing water. Water which is not hydrogen bonded to the polymer, but hydrogen bonded to both freezing and non-freezing water molecules is referred to as free or freezing water as it has a greater degree of mobility.

The ratio of freezing to non-freezing water influences the properties of the hydrogel. Differential Scanning Calorimetry (DSC) is used to determine the relative amounts[51, 52].

2.1.4 Developments in Hydrogel Chemistry

Poly(HEMA) in the hydrated form contains approximately 40% water; however, more recently there has been considerable interest in hydrogels containing both nitrogen and carboxyl water structuring groups[53]. These groups attract water more strongly than hydroxyl groups and hydrogels containing up to 96% water have been produced[54]. Higher water content hydrogels allow greater oxygen permeability, an important property for application to contact lenses. Such materials include copolymers containing *N*-vinyl-2-pyrrolidone (NVP). The pendent ring structure of poly(NVP) contains nitrogen and oxygen which both contribute polarity and the ability to form hydrogen bonds. The large size of this repeating structure gives free volume in the material, resulting in increased flexibility and space to accommodate water.

Although these newer materials can contain more water than poly(HEMA), they are also much weaker mechanically. To counteract this effect they are copolymerised with more hydrophobic and sterically hindering monomers, such as styrene and MMA to increase their tensile strength. The EWC is lower in such copolymers, and hence these copolymers are more rigid. Another technique for improving the mechanical properties of hydrogels is the use of interpenetrating networks (IPNs). Briefly, an interpenetrating network is a combination of two polymers, each in network form, at least one of which has been synthesised and/or crosslinked in the presence of the other[55]. IPNs give materials that are stiffer and stronger but less elastic than the simple hydrogel copolymers of similar water content.

2.1.5 Copolymer Sequence Distribution

As discussed in Chapter 1, cellular interaction is influenced by the chemical structure of the polymer substrate. The sequence distribution of a polymer is the regularity of the sequence of monomer units in the chain. A well dispersed sequence arises when

monomers with similar reactivity ratios are used. When monomers with differing reactivity ratios are copolymerised a polymer with long blocky sections is formed. The monomer with the highest reactivity ratio tends to constitute the blocks in the polymer at the start of the polymerisation, whereas the monomer with the lowest reactivity ratio tends to form a residual block at the end of the polymerisation. Fitton[56] showed that a random distribution of poly(ethylene oxide) (PEO) along the backbone chain was more effective at reducing cell adhesion than a blocky distribution. A computer simulation program (POLSIM) was developed in order to predict the order of chemical constituents at different compositions in a copolymer or terpolymer, based on the concentration and reactivity ratios of the monomers used.

2.1.6 The Terminal Model of Copolymerisation

The standard kinetic treatment of free radical polymerisation is the terminal model of copolymerisation[57, 58]. In this model the reactivity of an active centre is dependent only on the monomer unit in the copolymer chain on which the radical is located. For two monomers the growth of the polymer chain and the consumption of monomer is illustrated by four propagation steps:

$$\sim\sim\sim M_1\bullet + M_1 \text{ ----}> \sim\sim\sim\sim M_1\bullet \qquad rate_{11} = k_{11}[M_1\bullet][M_1] \qquad (1.1)$$

$$\sim\sim\sim M_1\bullet + M_2 \text{ ----}> \sim\sim\sim\sim M_2\bullet \qquad rate_{12} = k_{12}[M_1\bullet][M_2] \qquad (1.2)$$

$$\sim\sim\sim M_2\bullet + M_1 \text{ ----}> \sim\sim\sim\sim M_1\bullet \qquad rate_{21} = k_{21}[M_2\bullet][M_1] \qquad (1.3)$$

$$\sim\sim\sim M_2\bullet + M_2 \text{ ----}> \sim\sim\sim\sim M_2\bullet \qquad rate_{22} = k_{22}[M_2\bullet][M_2] \qquad (1.4)$$

where

M = monomer

$M\bullet$	=	monomer radical
k	=	rate constant
[ ]	=	concentration of individual species

The rate of consumption of the monomers can be expressed as:-

$$d[M_1] / dt = k_{11} [M_1\bullet] [M_1] + k_{21} [M_2\bullet] [M_1] \qquad (1.5)$$

$$d[M_2] / dt = k_{12} [M_1\bullet] [M_2] + k_{22} [M_2\bullet] [M_2] \qquad (1.6)$$

$\frac{d[M_1] / dt}{d[M_2] / dt}$ is the mole ratio of the monomers in the copolymer. This gives

$$\frac{d[M_1] / dt}{d[M_2] / dt} = \frac{k_{11} [M_1\bullet] [M_1] + k_{21} [M_2\bullet] [M_1]}{k_{12} [M_1\bullet] [M_2] + k_{22} [M_2\bullet] [M_2]} \qquad (1.7)$$

If a steady state is reached instantly after polymerisation is started, the total concentrations of $M_1\bullet$ and $M_2\bullet$ will remain constant and the rate of conversion of $M_1\bullet$ to $M_2\bullet$ will equal the rate of conversion of $M_2\bullet$ to $M_1\bullet$ i.e.:

$$k_{21} [M_2\bullet] [M_1] = k_{12} [M_1\bullet] [M_2] \qquad (1.8)$$

If k_{11} / k_{12} is defined as r_1, the reactivity ratio of monomer M_1 and k_{22} / k_{21} is defined as r_2 the reactivity ratio of monomer M_2 then equation 1.7 reduces to the copolymer equation

$$\frac{d[M_1]}{d[M_2]} = \frac{[M_1] (1 + r_1 [M_1] / [M_2])}{[M_2] (r_2 + [M_1]/M_2])} \qquad (1.9)$$

The monomer reactivity ratios r_1 and r_2 are the ratios of the rate constant for a given radical adding to its own monomer compared with that for the addition to the other monomer. They are a measure of which monomer a particular radical has a preference to react with, thus if $r_1 > 1$ radical $M_1\bullet$ prefers to add to monomer M_1 and

if $r_1 < 1$, radical $M_1\bullet$ prefers to add to monomer M_2. The relative values of r_1 and r_2 will therefore determine the mechanism of polymerisation of the copolymer.

If r1.r2 = 1, the situation is referred to as an ideal copolymerisation in that the radicals have the same preference of addition to each of the monomers. The units of the two monomer types are arranged completely at random along the chain. When $r_1 = r_2 = 0$, each radical shows a strong preference for cross propagation which results in the monomers alternating regularly regardless of the monomer feed ratio until one monomer is completely consumed. In the situation of $r_1 = r_2 = 1$ neither radical centre shows a preference for either monomer and the rates of consumption are determined by the relative concentrations of monomer in the initial feed. If r_1 is much greater than r_2, the polymerisation produces large blocks of M_1 with small clusters of M_2 between the blocks until M_1 is consumed.

2.1.7 Computer Simulation of Sequence Distribution

The terminal model is very useful for explaining the structure of copolymers prepared from various vinyl monomers whose reactivity ratios are known. A computer program based on this model provides an illustration of the sequence distribution of copolymers whilst allowing alterations in key parameters such as monomer type and initial feed concentration. The approximate sequence distributions of various copolymers can be determined easily without the need for producing the polymer and performing detailed structural analysis required for determination of the sequence distribution.

Computer simulation of sequence distributions is carried out using two computer programs. The 'COPOL' program allows the simulation of the sequence distribution for binary systems whilst the 'TERPOL' program allows ternary systems to be studied. Ashraf[59] has provided experimental evidence for the accuracy of the simulations using these two programs.

2.1.8 The Alfrey-Price Q-e Scheme

The reactivity ratios of monomers must be known to allow the computer simulations described previously to be utilised. For many monomers the reactivity ratios have been determined experimentally but there are still a number of monomers for which this process has not been carried out. To overcome this problem without the need to carry out lengthy experimental work, an approximation technique known as the Alfrey-Price Q-e scheme has been employed[60, 61]. This scheme quantifies reactivity by consideration of the polar and resonance stabilisation effects of the monomer and the influence these have on the copolymerisation process.

The two reactants in the copolymerisation were assigned values e_1 and e_2 to represent their charges, identical charges being assumed for a monomer and its radical. The reactivities of the monomers and radicals were then denoted by Q and P respectively. The rate of reaction was considered to be dependent on the four quantities P, Q, e_1 and e_2 as indicated in equation 1.10.

$$k_{12} = P_1 Q_1 \exp(-e_1 e_2) \qquad (1.10)$$

Four of these equations are obtained from the propagation steps outlined previously in equations 1.1 - 1.4, which were then combined and rearranged to give:-

$$r_1 = (Q_1 / Q_2) \exp[-e_1(e_1 - e_2)] \qquad (1.11)$$

and

$$r_2 = (Q_2 / Q_1) \exp[-e_2(e_1 - e_2)] \qquad (1.12)$$

Combination of these equations gives

$$r_1 r_2 = \exp[-(e_1 - e_2)^2] \qquad (1.13)$$

Thus the Q-e scheme enables predictions of the reactivity ratios to be made for a pair of vinyl monomers which have not been studied experimentally.

2.2 Materials and Methods

2.2.1 Reagents

Monomers were purified by reduced pressure distillation before use, as described in the literature[62].

Table 2.1 Molecular weights and suppliers of the monomers used

Monomer	**Abbreviation**	**Molecular weight**	**Supplier**
2-Hydroxyethyl methacrylate	HEMA	130.14	Laporte
Methyl methacrylate	MMA	100.114	Vista Optics
N-vinyl-2-pyrrolidone	NVP	111.142	Vista Optics
Acryloylmorpholine	AMO	141.144	Vista Optics
N-vinyl imidazole	NVI	94.1	Aldrich
Diethylaminoethyl methacrlyate	DEAEMA	157.252	Aldrich
Methacrylic acid	MAA	86.086	Aldrich

2.2.2 Structures of Monomers

Figure 2.4 Structures of reagents listed in Table 2.1

2-hydroxyethyl methacrylate HEMA

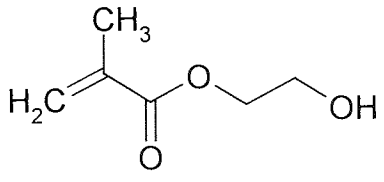

Methyl methacrylate MMA

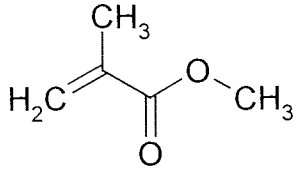

N-vinyl pyrrolid-2-one NVP

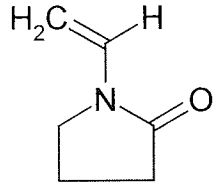

Acryloylmorpholine AMO

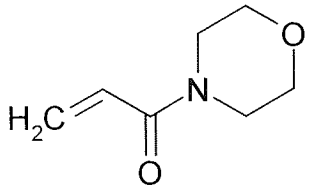

N-vinyl imidazole NVI

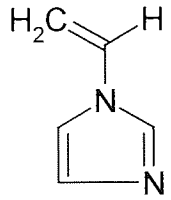

Diethylaminoethyl methacrylate DEAEMA

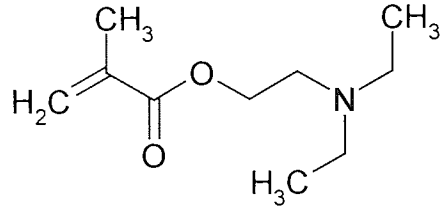

Methacrylic acid MAA

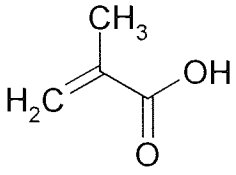

2.2.3 Initiator and Crosslinker

Table 2.2 Molecular weights and suppliers of the initiator and crosslinking agent used

Reagent	Abbreviation	Molecular weight	Supplier
Azo-bis-isobutyronitrile	AZBN	164.21	BDH
Ethylene glycol dimethacrylate	EGDMA	198.2	BDH

2.2.4 Structures of Initiator and Crosslinker

Figure 2.5 Structures of initiator and cross-linker

Azo-bis-isobutyronitrile AZBN

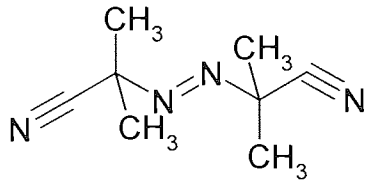

Ethylene glycol dimethacrylate EGDMA

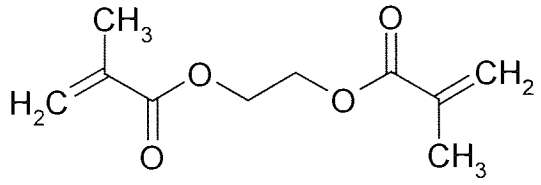

2.2.5 Preparation of Membranes

Polymers were produced in the form of membrane sheets which were produced by free radical polymerisation in a glass mould. To make the mould two glass plates, 15cm x 10cm were covered with melinex sheets, which were secured in place on the glass plates with spray mount. This allowed for easy removal of the finished membrane from the mould. The plates were placed together with two poly(ethylene) gaskets, each 0.2mm thick, separating the melinex sheets. The whole assembly was held together using spring clips. The monomer was injected into the mould cavity using a syringe and size G18 syringe needle, see Figure 2.6.

Figure 2.6 Membrane preparation

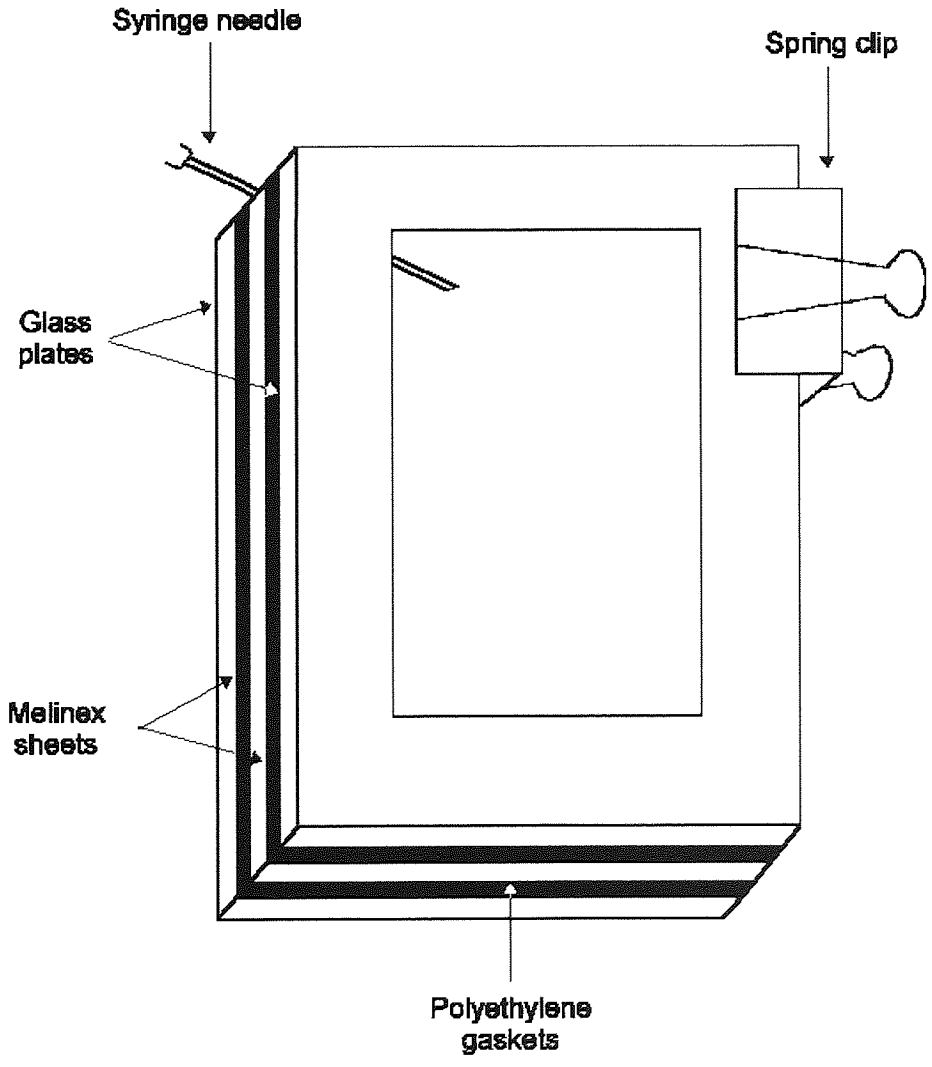

Polymers and copolymers were made using a standard 1% (w/w) cross-linker of ethylene glycol dimethacrylate (EGDMA) and 0.5% (w/w) of initiator, azo-bis-isobutyronitrile (AZBN). Once a homogeneous mixture was obtained the cross-linker and initiator were added. A total of 5 grams of mixture was used. Nitrogen gas was bubbled through the mixture for ten minutes before injection into the mould to ensure that all oxygen was removed from the mixture. The mould was then placed in an oven at 60°C for three days to cure and at 90°C for a further three hours to post cure.

On removal from the oven the clips were removed and the polymer sheet was placed in distilled water and hydrated for at least one week. The water in which the membrane sheets were placed was changed daily in order to remove unreacted monomer and other water soluble contaminants.

2.2.6 Equilibrium Water Content

The equilibrium water content (EWC) was calculated by weight difference of the hydrated and dehydrated samples. Several samples of polymer were cut from a hydrated membrane sheet using a size seven cork borer. Surface water was removed using filter paper; care was taken not to squeeze out water from within the structure. Samples were weighed using a five place electric balance and then dehydrated in a microwave oven to constant weight. The equilibrium water content was calculated using equation 1.1 and the final value reported is an average of the results from at least three determinations.

$$\text{EWC}(\%) = \frac{\text{weight of the water in the gel}}{\text{total weight of hydrated gel}} \times 100 \qquad (1.14)$$

2.2.7 Copolymer Sequence Distribution

The effect of monomer reactivity on sequence distributions was studied using a computer simulation model. The program uses the Monte Carlo method of statistical trials[63], which constructs a random process for the solving of computational mathematical problems. The development of the model on which the computer simulation is based, was constructed using the basic free radical polymerisation

model. The statistical hypothesis for the reaction kinetics of this model is that the reactivity of the radical centre is governed by the monomer unit upon which the active radical centre is located. Four propagation steps for the reaction are possible, as shown in Equations 1.1 – 1.4:

$$\sim\sim M_1\bullet + M_1 \text{ ----}> \sim\sim M_1\bullet \quad rate_{11} = k_{11}\,[M_1\bullet]\,[M_1] \tag{1.1}$$

$$\sim\sim M_1\bullet + M_2 \text{ ----}> \sim\sim\sim M_2\bullet \quad rate_{12} = k_{12}\,[M_1\bullet]\,[M_2] \tag{1.2}$$

$$\sim\sim M_2\bullet + M_1 \text{ ----}> \sim\sim\sim M_1\bullet \quad rate_{21} = k_{21}\,[M_2\bullet]\,[M_1] \tag{1.3}$$

$$\sim\sim M_2\bullet + M_2 \text{ ----}> \sim\sim\sim M_2\bullet \quad rate_{22} = k_{22}\,[M_2\bullet]\,[M_2] \tag{1.4}$$

where:

M	=	monomer
M•	=	monomer radical
k	=	rate constant
[ ]	=	concentration of individual species

Considering the reactions which involve polymer chains ending with a M_1 radical, gives an overall rate for these reactions of:

$$R_1 = rate_{11} + rate_{12} \tag{1.15}$$

and the fraction of these polymer chains that will add a further unit of M_1 at the radical end will be given by:

$$f_{11} = rate_{11} / R_1 \tag{1.16}$$

where f_{11} is the fraction of polymer chains ending in an M_1 radical adding to another unit of M_1. Substitution of the above equations into equation 1.16 gives:

$$f_{11} = k_{11} [A] / (k_{11} [A] + k_{12} [B]) \quad (1.17)$$

where A is monomer 1 and B is monomer 2. This equation simplifies to:

$$f_{11} = 1 / (1 + k_{12} [B] / k_{11} [A]) \quad (1.18)$$

The individual reactivity ratios of M_1 and M_2 are defined as the ratio of the rates of reaction of a polymer chain ending in a radical of one type adding itself to the rate of its reaction with the second monomer in the copolymer system. Therefore:

$$r_1 = k_{11} / k_{12} \quad (1.19)$$

and

$$r_2 = k_{22} / k_{21} \quad (1.20)$$

where r_1 and r_2 are the reactivity ratios of the monomers M_1 and M_2 respectively.

Substitution of equation 1.19 into equation 1.18 gives:

$$f_{11} = 1 / (1 + 1 / r_1 [B] / [A]) \quad (1.21)$$

Similarly it follows that:

$$f_{22} = 1 / (1 + 1/r_2 [A] / [B]) \quad (1.22)$$

Therefore, if the initial concentrations of the monomers and their reactivity ratios are known then the fraction of the polymer chains ending in the radical M_1 that add to unreacted monomer M_1 will be given by f_{11}. Similarly, the fraction of polymer chains ending in M_1 that add to unreacted monomer M_2 will be given by f_{12}.

The computer simulation generates a random number (RN) after each addition step, in the range 0 to 1 and compares this to the value of f_{11} generated from initial concentrations and reactivity ratios. If $f_{11} > RN$ then the simulation adds an M_1 monomer unit onto the growing free radical polymer chain. If $f_{11} < RN$ then to the growing chain an unreacted M_2 monomer unit is added. After the addition of a M_2 monomer unit, the simulation considers addition of the two monomers onto a growing polymer chain ending with an M_2 radical. This procedure continues until there is 100% conversion of the monomers into polymer.

Ashraf[59] studied the viability of using these computer simulation programs. Computer simulations similar to that shown in Figure 2.7, were prepared using a number of methacrylate based comonomer systems together with the experimental preparation of the same copolymers. It was found that the sequence lengths determined using the methods of 13C NMR and elemental analysis were within 3% of the sequence lengths produced by the computer simulation. It is therefore assumed that the computer simulation is accurate enough to simulate the reactivity of comonomers in a free radical polymerisation. An example simulation is shown below in Figure 2.7 and Table 2.3.

Figure 2.7 Example of a sequence simulation for a hydrogel copolymer

80 mole % of monomer A, NVP

20 mole % of monomer B, MMA

r (AB) = 0.01 r (BA) = 4.04

In the simulated copolymer NVP is represented by O and MMA is represented by X

XXOXOXXXOXXOXOXXXOXOXOOXXOXXOXXXOXXOXXOXXXOXOXOXO
XOXOXXXXOXOXXXXXXXOXXXOXOXXXXXXXXOXXXOXXXOXXOXXXO
XXOXOXXOXOXOXOXXXOXXXXXOXXXOXXOXXOXXXOXOXOXOXOXXX
OXOXOXOXXOXXXXOXXOXOXXOXOXOXOOXOXXOXOXXOXOXXXOXOX
OXOXXXXOXOXOXOOOXOXXOXXOXOXOXOXXOXXXXOXOOXOXXXOXO
XOXXOXXOXOXXXOXXOXXXXXXOXOXOXXOXOXXOXOXXOXOXXXOXX
OXXOXXOXOOXXXXXXOXXOXOXXXXOXOXOXOXOXXOXOXOXOXOXOX

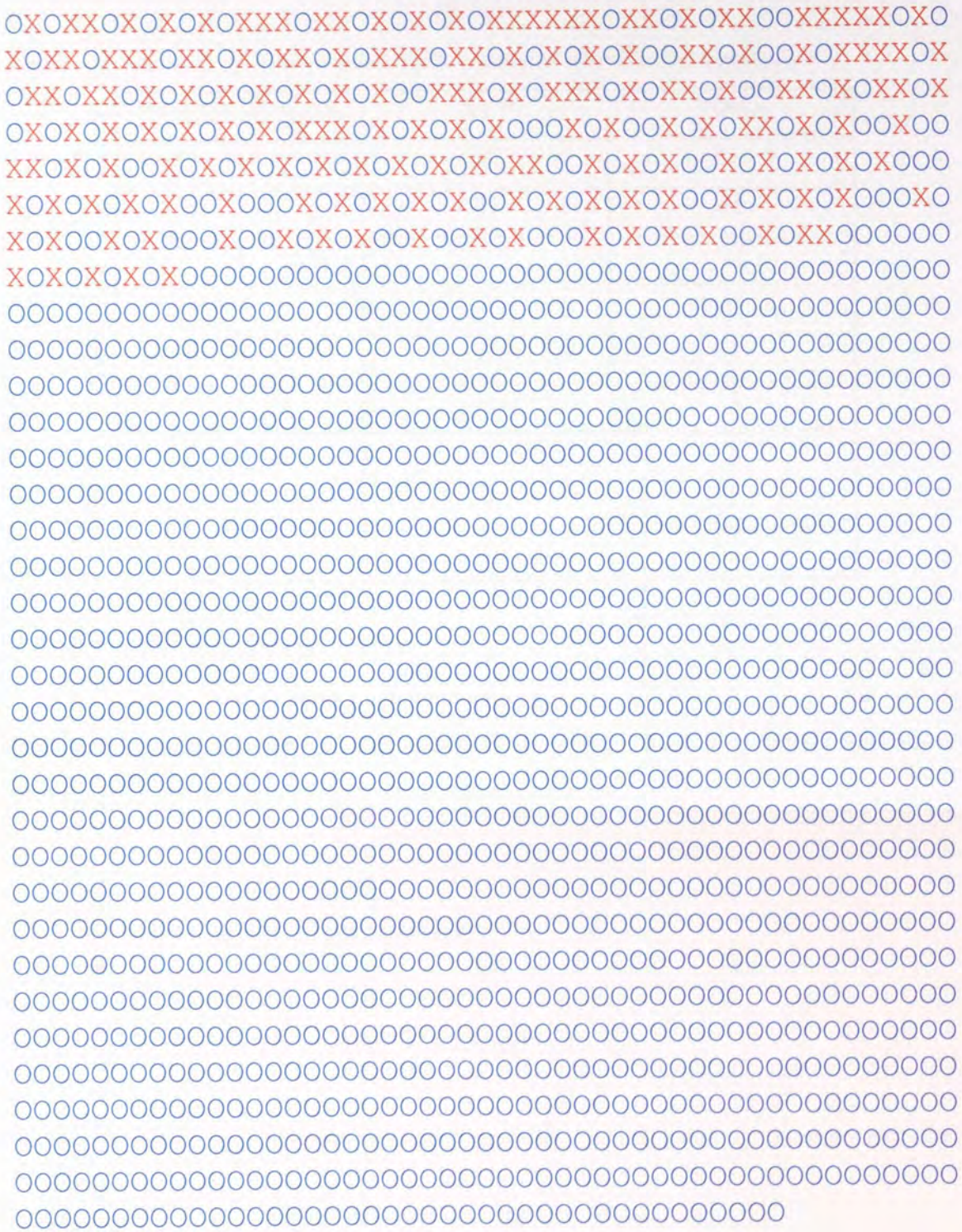

The simulated copolymer contains 1600 NVP units and 400 MMA units

Table 2.3 Example of summary table for sequence distribution simulation

Sequence Length	NVP	MMA
1	222	171
2	23	48
3	7	22
4	0	6
5	0	2
6	1	3
7	0	1
8	0	1
1305	1	0

2.2.8 CHN Analysis

Dehydrated samples were sent to Medac Ltd, Egham, Surrey for CHN analysis to determine the composition of the synthesised polymers.

2.3 Results and Discussion

2.3.1 Equilibrium Water Content

Table 2.4 shows the different hydrogel polymers which were synthesised and their EWC.

Table 2.4 Membranes prepared

Composition (molar parts)	**Equilibrium Water Content**
HEMA	38%
NVP/MMA 60 : 40	56%
NVP/MMA 70 : 30	64%
NVP/MMA 80 : 20	75%
NVP/MMA 90 : 10	84%
NVP/MMA 25:75	14%
AMO/MMA 25:75	18%
NVP/MMA/NVI 79 : 19 : 2	76%
NVP/MMA/NVI 77.5 : 17.5 : 5	78%
NVP/MMA/NVI 76.5 : 16.5 : 7	79%
NVP/MMA/NVI 75 : 15 : 10	81%
NVP/MMA/DEAEMA 79 : 19 : 2	78%
NVP/MMA/DEAEMA 77.5 : 17.5 : 5	78%
NVP/MMA/DEAEMA 76.5 : 16.5 : 7	79%
NVP/MMA/DEAEMA 75 : 15 : 10	79%
NVP/MMA/MAA 79.75:19.75:0.5	78%

As can be expected, water content increases with the addition of hydrophilic monomer. Although a study of mechanical properties is outside the scope of this thesis, a compromise has to be made between high EWC and acceptable tensile properties. Therefore, a high water content gel which could be manipulated easily without tearing was chosen as the base material for the addition of ionic monomers. This was the NVP/MMA membrane containing 80 molar parts NVP to 20 molar parts MMA, with an equilibrium water content of 75%.

To this starting material was added similar amounts of either the cationic *N*-vinyl imidazole (NVI), diethylaminoethyl methacrylate (DEAEMA), or the anionic methacrylic acid (MAA). Increasing the ionic component increased the water contents observed, but not greatly. NVI and DEAEMA have relatively bulky groups

which restrict mobility and limit the accessibility of the hydrophilic groups, so the EWC does not increase significantly. Therefore the effect of increasing the ionic component on surface and cell behaviour can be studied with little corresponding increase in equilibrium water content.

2.3.2 Reactivity and Sequence Distribution

To produce sequence distributions, copolymerisation simulations were performed for each of the copolymers. The reactivity ratios of the monomers were obtained from either experimentally determined literature values[64] or from the Q and e scheme when experimental values have not been determined and are shown in Table 2.5. The reactivity ratios for DEAEMA have been approximated by calculating from Q and e values for dimethylaminoethyl methacrylate[65].

Table 2.5 Reactivity ratios for copolymers of monomers used

Monomer 1	Monomer 2	r_1	r_2
NVP	MMA	0.01	4.04
NVP	NVI	0.174	2.368
MMA	NVI	4.603	0.067
NVP	DEAEMA	0.004	2.82
MMA	DEAEMA	1.184	0.838
NVP	MAA	0.002	2.777
MMA	MAA	0.869	1.096
AMO	MMA	0.512	1.759

Computer simulations for the sequence distribution of the copolymers studied were carried out and can be found in Appendix I. The sequences represent reaction to 100% conversion and the results are summarised in Tables 2.6 - 2.11.

2.3.2.1 NVP/MMA copolymers

Table 2.6 Sequence simulation results for high water content NVP/MMA copolymers

Sequence Length	Number of sequences for 60:40 composition		Number of sequences for 70:30 composition		Number of sequences for 80:20 composition		Number of sequences for 90:10 composition	
	NVP	MMA	NVP	MMA	NVP	MMA	NVP	MMA
1	342	167	300	192	222	171	140	130
2	15	98	24	69	23	48	13	19
3	1	37	4	32	7	22	5	8
4	0	17	0	18	0	6	0	2
5	1	21	0	12	0	2		
6	0	4	0	3	1	3		
7	0	6	0	2	0	1	1	0
8	0	3			0	1		
9	0	3						
10	0	1	0	1				
12	0	1						
14	0	1						
820	1	0						
1040			1	0				
1305					1	0		
1612							1	0

Table 2.6 shows that NVP reacts poorly with MMA because there is an uneven distribution of monomers. Most of the NVP is left over after all the MMA has been used up. The computer simulation of the sequence distribution for the 80:20 composition was shown in Figure 2.7. Table 2.7 below demonstrates that this effect is also apparent at lower concentrations of NVP.

Table 2.7 Sequence simulation results for the low water content NVP/MMA copolymer studied

Sequence Length	NVP	MMA
1	239	56
2	3	42
3	0	23
4	0	23
5	0	12
6	0	12
7	0	14
8	0	8
9	0	2
10	0	5
11	0	6
12	0	4
13	0	4
14	0	3
15	0	4
16	0	5
17	0	3
18	0	3
19	0	1
20	0	1
21	0	1
23	0	2
24	0	1
25	0	2
28	0	1
31	0	1
33	0	1
34	0	1
36	0	1

42	0	1
255	1	0

2.3.2.2 Polymers containing a cationic group

Table 2.8 Sequence simulation results for NVP/MMA/NVI copolymers

Sequence Length	Number of sequences for 79:19:2 composition			Number of sequences for 77.5:17.5:5 composition			Number of sequences for 76.5:16.5:7 composition			Number of sequences for 75:15:10 composition		
	NVP	MMA	NVI	NVP	MMA	NVI	NVP	MMA	NVI	NVP	MMA	NVI
1	223	146	36	241	159	90	228	168	119	288	158	160
2	24	49	2	43	54	5	51	46	9	46	40	20
3	9	22	0	14	12	0	10	15	1	10	13	0
4	1	7	0	7	8	0	4	5	0	4	3	0
5	0	6	0	0	3	0	5	1	0	1	1	0
6	2	2	0	2	0	0	3	0	0	0	1	0
7							1	0	0			
8				1	0	0						
9							3	0	0			
12							1	0	0			
13							1	0	0			
1052							1	0	0			
1069										1	0	0
1133				1	0	0						
1266	1	0	0									

Table 2.9 Sequence simulation results for NVP/MMA/DEAEMA copolymers

Sequence Length	Number of sequences for 79:19:2 composition			Number of sequences for 77.5:17.5:5 composition			Number of sequences for 76.5:16.5:7 composition			Number of sequences for 75:15:10 composition		
	NVP	MMA	DEAEMA	NVP	MMA	DEAEMA	NVP	MMA	DEAEMA	NVP	MMA	DEAEMA
1	243	164	40	267	173	85	277	171	115	297	169	160
2	19	56	0	21	47	6	19	48	11	20	33	17
3	3	18	0	1	14	1	1	18	1	3	14	2
4	0	8	0	1	9	0	1	1	0	0	3	0
5	0	1	0	0	1	0	0	1	0	0	1	0
6	0	1	0							0	1	0
7	0	1	0									
1154										1	0	0
1208							1	0	0			
1234				1	0	0						
1290	1	0	0									

Tables 2.8 and 2.9 show that polymers incorporating either NVI or DEAEMA also contain blocky NVP domains. The NVI or DEAEMA appears to be well incorporated in the polymer because they are present as short sequences. However, from the reactivity ratios it would be expected that DEAEMA is more randomly incorporated than NVI, since $r_1 r_2 = 0.992$ for MMA and DEAEMA but $r_1 r_2 = 3.084$ for MMA and NVI. This situation becomes evident when viewing the simulation of the sequence distribution for the different terpolymers. Figures 2.8 and 2.9 show NVP/MMA polymers containing 10% NVI or DEAEMA.

Figure 2.8 Computer simulated sequence distribution of NVP/MMA/NVI 75:15:10 copolymer

75 mole % of monomer A, NVP

15 mole % of monomer B, MMA

10 mole % of monomer C, NVI

r(AB) = 0.01 r(AC) = 0.174 r(BA) = 4.04

r(BC) = 4.603 r(CA) = 2.368 r(CB) = 0.067

Polymerised to 100% conversion

In the simulated copolymer NVP is represented by O, MMA is represented by X and NVI is represented by *

The simulated copolymer contains 1500 NVP units and 300 MMA units and 200 NVI units

Figure 2.9 Computer simulated sequence distribution of NVP/MMA/DEAEMA 75:15:10 copolymer

75 mole % of monomer A, NVP

15 mole % of monomer B, MMA

10 mole % of monomer C, NVI

r(AB) = 0.01 r(AC) = 0.004 r(BA) = 4.04

r(BC) = 1.184 r(CA) = 2.82 r(CB) = 0.838

Polymerised to 100% conversion

In the simulated copolymer NVP is represented by O, MMA is represented by X and DEAEMA is represented by *

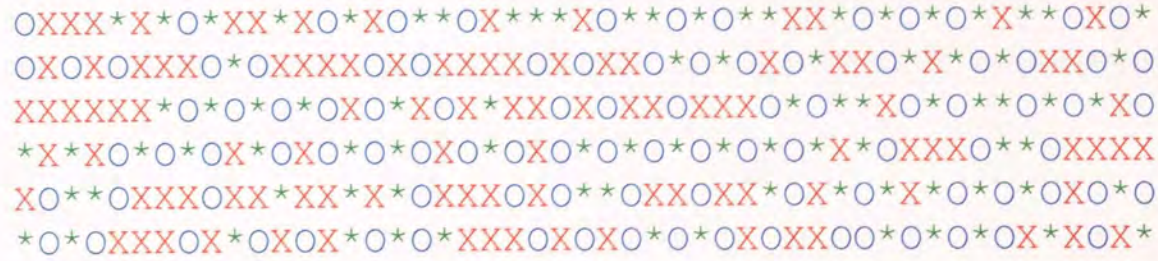

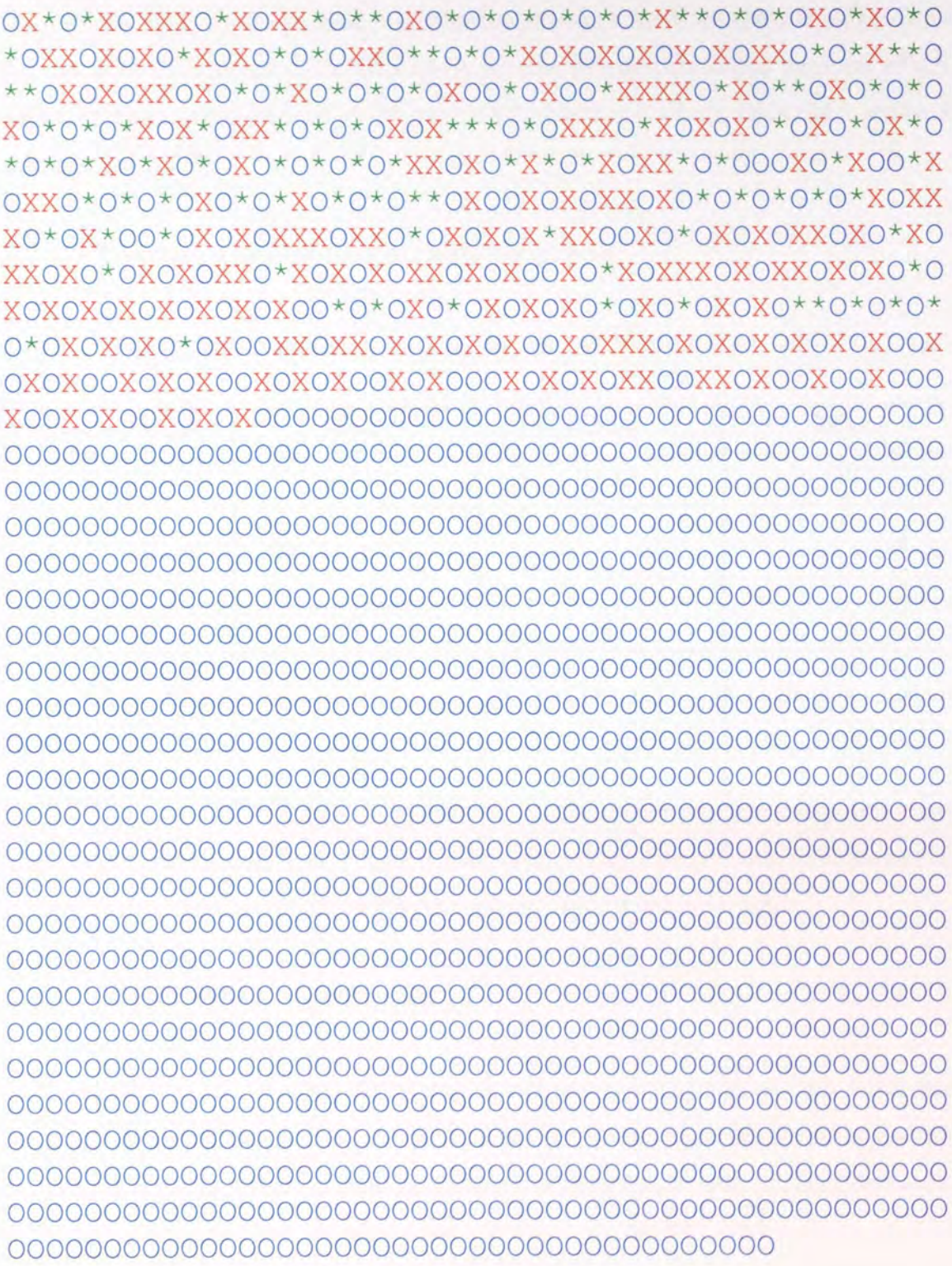

The simulation represents polymerisation to 100% conversion

The simulated copolymer contains 1500 NVP units and 300 MMA units and 200 DEAEMA units

Most of the NVI is incorporated just after the MMA is used up; there is still a large amount of NVP left over. The DEAEMA is more evenly distributed until the MMA runs out, with a large amount of left over NVP. Neither NVI nor DEAEMA are well matched with NVP.

2.3.2.3 Polymers containing an anionic group

Table 2.10 Sequence simulation results for the NVP/MMA/MAA 79.75:19.75:0.5 polymer

Sequence Length	NVP	MMA	MAA
1	251	185	10
2	15	54	0
3	5	15	0
4	0	8	0
6	0	3	0
7	0	1	0
1299	1	0	0

The anionic methacrylic acid appears to be well incorporated in this terpolymer but does not affect the amount of NVP left over at the end of polymerisation.

2.3.2.4 AMO/MMA copolymers

The reactivity of the nitrogen containing monomers is a function of both steric and polar effects as well as resonance stabilisations. Steric and polar effects are important in both the reacting radical and the monomer and must be considered simultaneously. It would be expected that the steric and polar effects for NVP and AMO would be similar as the structures and size of the constituents within their structures are comparable. The resonance stabilisation energy, however, which occurs when monomer is converted to radical is more important than the reactivity of the radical. If a radical has resonance structures it will be more stable than a radical that does not. This causes the activation energy for the reaction to be lower and consequently an increased rate of reaction for the monomer addition to the radical.

The AMO radical has a higher resonance stabilisation energy than the NVP radical, due to the formation of the resonance structure shown in Figure 2.10.

Figure 2.10 The resonance stabilisation structures of the AMO radical

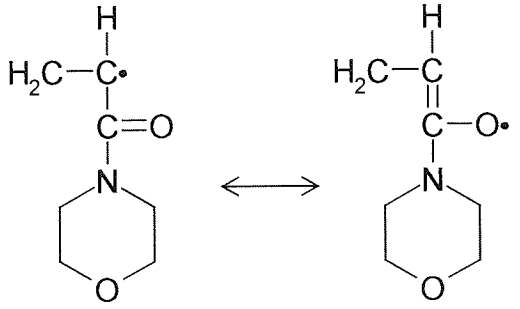

This resonance stabilisation does not occur with the radical of NVP as its structure will not allow the formation of the radical structures. It would therefore be expected that AMO will add to MMA at a greater rate than NVP due to the lower activation energy that results from the formation of the resonance structures. AMO will have a higher reactivity than NVP to vinyl polymerisation with MMA and this is reflected in the results of the simulation of the sequence distribution (see Figure 2.11 and Table 2.11). AMO is consumed at a faster rate in the copolymerisation reaction than NVP which is consumed in the latter stages of the reaction and forms a large terminal block.

Figure 2.11 Computer simulated sequence distribution of the AMO/MMA 25:75 copolymer

25 mole % of monomer A, AMO

75 mole % of monomer B, MMA

r (AB) = 0.512 r (BA) = 1.759

Polymerised to 100% conversion

In the simulated copolymer AMO is represented by O and MMA is represented by X

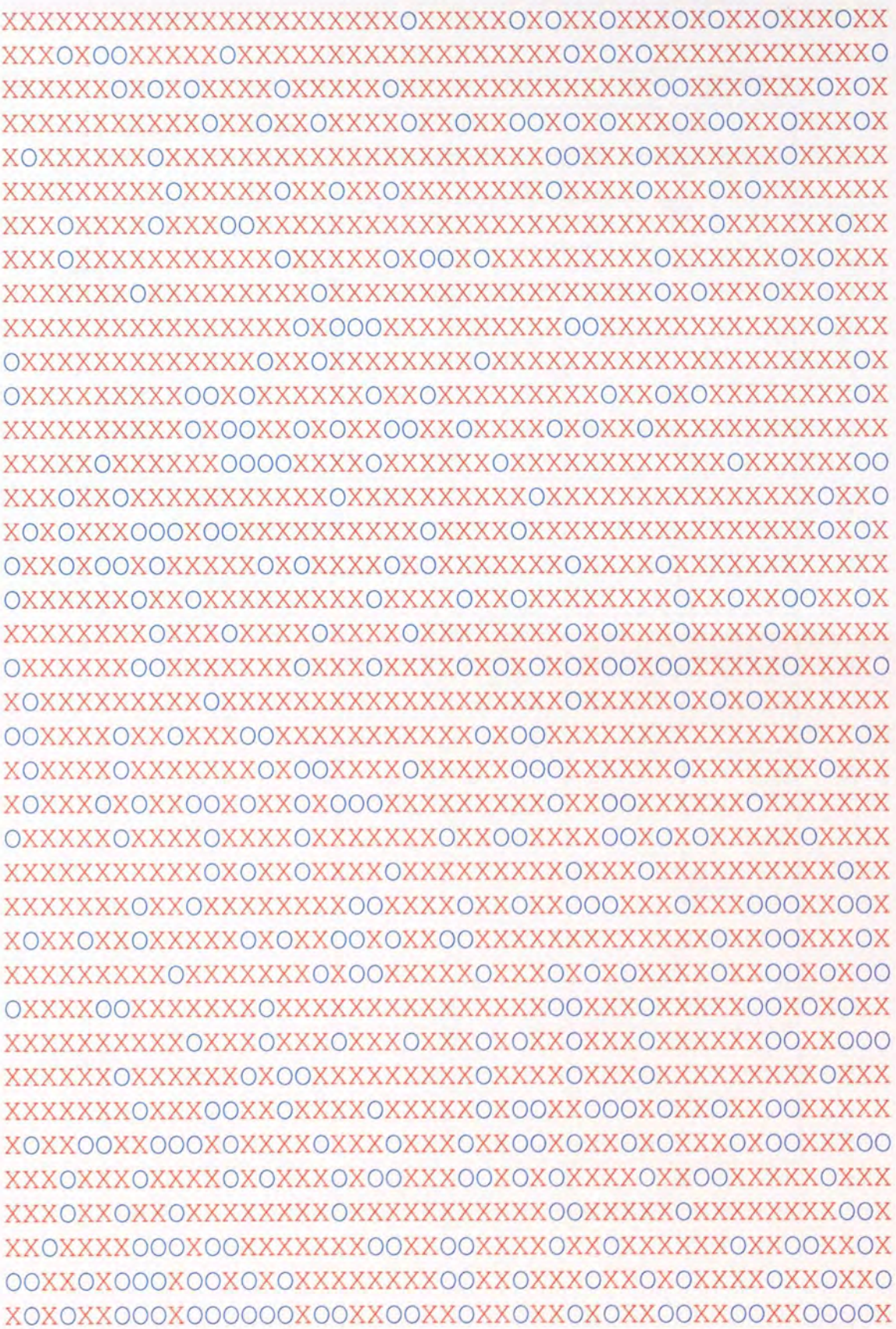

OXOXXOOXOOOXOOOXXXOXOXOOXOXOXXXOOXXOXOOXXXXOOOXXX
XOOOOOOOOOOOOOOOOOOOOOOOOOOOOOOOOOOOOOOOO

The simulated copolymer contains 500 AMO units and 1500 MMA units

Table 2.11 Sequence simulation results for the AMO/MMA 25:75 copolymer

Sequence Length	AMO	MMA
1	269	91
2	65	77
3	16	43
4	2	36
5	0	19
6	1	19
7	0	11
8	0	9
9	0	12
10	0	8
11	0	5
12	0	6
13	0	2
14	0	3
15	0	3
16	0	1
18	0	3
19	0	2
20	0	1
21	0	1
22	0	1
25	0	1
39	1	0

2.3.3 CHN Analysis

A consequence of the reactivity ratios is the difference in composition of the resulting copolymer compared with the initial feed ratio of monomers.

Table 2.12 shows the feed ratios and actual ratios of monomers in NVP/MMA copolymers studied, expressed both as molar percentages and weight percentages.

Table 2.12 The feed ratio and actual ratio of monomers in some copolymers studied

Copolymer composition	Initial feed ratio (molar %)	Initial feed ratio (weight %)	Actual weight ratio (weight %)	Actual molar ratio (molar %)
NVP/MMA	60:40	62.3:37.7	51.6:48.4	49.1:50.9
NVP/MMA	70:30	72:28	57.6:42.4	55.2:44.8
NVP/MMA	80:20	81.5:18.5	67.6:32.4	65.4:34.6
NVP/MMA	90:10	90.8:9.2	81.2:18.8	79.7:20.3

It is evident that much less NVP is incorporated in the polymer than is available from the initial mixture. Any left over NVP which is not crosslinked is eluted out when the membrane is swollen in distilled water. AMO/MMA copolymers are likely to polymerise more precisely according to the initial feed ratios.

2.4 Conclusions

A range of hydrogels were produced by bulk free radical polymerisation: one series of increasing hydrophilic monomer, two series of increasing cationic monomer, one hydrogel incorporating anionic monomer, and two low water content polymers. The hydrogels had an EWC of between 14% and 81%.

Computer simulations for the sequence distributions were performed using the Monte Carlo method of statistical trials[63]. NVP was shown to react poorly with MMA which leads to a blocky structure and could affect surface properties. DEAEMA is more randomly incorporated into these polymers than is NVI due to the favourable

reactivities of DEAEMA and MMA. MAA appears to be well incorporated in the one anionic containing hydrogel studied.

AMO was shown to be capable of producing more random structures than NVP when copolymerised with MMA due to its resonance stabilisation energy.

CHN analysis was carried out on the series of increasing hydrophilic monomer to determine the actual composition of the final NVP/MMA copolymers after polymerisation. Marked differences were observed between the initial feed ratios and the actual weight and molar ratios. It would be expected that AMO/MMA copolymers would polymerise more precisely according to the initial feed ratios.

2.5 Further Work

AMO/MMA copolymers should be sent for CHN analysis to confirm that the actual molar ratio corresponds more precisely to the initial feed ratios than for NVP/MMA copolymers.

CHAPTER 3
STATIC CONTACT ANGLE MEASUREMENTS

3.1 Introduction

Contact angle measurements provide valuable information about the surface properties of a hydrogel. Several workers[1, 53, 56] have suggested that the surface free energy of a polymer is an important parameter in determining the biocompatibility or biotolerance of the material. From the values obtained for the contact angles, the surface free energy of the hydrogel can be determined both in the hydrated and dehydrated states. Contact angle measurements rely on the resolution of the forces at a three phase interface of a drop of wetting liquid or vapour on a solid surface either immersed in liquid or in air. Several techniques have been used for the measurement of contact angles, including captive bubble[66, 67, 68], sessile drop[69], Wilhelmy plate[68, 70] and also by a method utilising laser examination of an adherent liquid[71]. In the work described in this thesis the sessile drop technique was used for dehydrated hydrogels while Hamilton's method[72, 73] and the captive bubble technique were used for hydrated hydrogels. These techniques were used in conjunction with dynamic contact angle measurements (Chapter 4) and with cell adhesion studies (Chapter 5) in an attempt to correlate surface chemistry with biotolerance in the development of predictive techniques.

In this Chapter the measured surface energies of several hydrogel copolymers are presented in an attempt to correlate molecular structure with surface free energy. The results are presented graphically in this Chapter and are listed in Appendices II and III.

Consistent and accurate surface energy measurements of hydrogel materials can be very difficult to obtain particularly in the dehydrated state, where hydrophilic samples readily absorb water, altering the state of the surface and changing true readings. It should also be remembered that due to effects such as sedimentation, evaporation of the liquid and other chemical or physical interactions at the solid surface, the contact angle is time dependent.

3.2 Dehydrated Surfaces

When a drop of liquid is placed on a smooth solid surface, the shape of the drop is determined by the wettability of the solid surface (Figure 3.1). The contact angle θ is the angle between the surface of the solid and the tangent to the liquid surface. A wettable surface will allow the liquid to spread, so the contact angle will be small. Conversely a non wettable surface will give large contact angles and the liquid will form a lens on the surface.

Figure 3.1 Sessile drop method

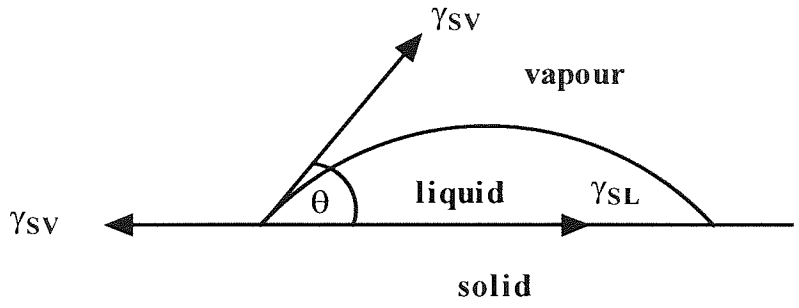

where γ_{SV} is the surface free energy of the solid

γ_{LV} is the surface free energy of the liquid

γ_{SL} is the interfacial free energy of the solid and liquid

Young's equation[74] involves the resolution of the forces at a point of contact of a sessile drop and a solid, as demonstrated in Figure 3.1.

$$\gamma_{SV} = \gamma_{SL} + \gamma_{LV} \cos \theta \qquad (3.1)$$

Continuing from Young, Dupré[75] expressed the reversible work of adhesion of a liquid and a solid as:

$$W_{SL} = \gamma_{SV} + \gamma_{LV} - \gamma_{SL} \qquad (3.2)$$

Combining these two equations gives the Young-Dupré equation:

$$W_{SL} = \gamma_{LV} (1 + \cos \theta) \quad (3.3)$$

The spreading pressure π_e is the reduction of the surface tension of the solid due to vapour adsorption, and can be ignored for solids which give large values of θ.

$$\pi_e = \gamma_S - \gamma_{SV} \quad (3.4)$$

Fowkes[76] and Good and Girifalco[77] took into consideration polar (e.g. H-bonding) and dispersive (e.g. Van der Waals) forces and their equations can be combined to give:

$$W_{SL} = 2 [(\gamma_1^d \gamma_2^d)^{1/2} + (\gamma_1^p \gamma_2^p)^{1/2}] \quad (3.5)$$

where γ_1^d and γ_2^d are the dispersive components and γ_1^p and γ_2^p are the polar components of liquids 1 and 2. For a solid-liquid interface, combining this equation with Young's equation gives the Owens and Wendt equation[78]:

$$1 + \cos \theta = (2 / \gamma_{LV}) [\gamma_{LV}^d \gamma_{SV}^d)^{1/2} + (\gamma_{LV}^p \gamma_{SV}^p)^{1/2}] \quad (3.6)$$

This expression may be used to determine the surface free energies of polymers in the dehydrated state. Two wetting liquids, whose polar and dispersive characteristics are known, are used. By measuring the contact angles of the liquids on the polymer surface and solving the equations simultaneously, γ_S^p and γ_S^d, the polar and dispersive components of the surface free energy of the polymer may be determined. Water and diiodomethane are usually used as wetting liquids because of their high total surface free energies and their balance of polar and dispersive forces.

Rearranging equation (3.6) gives the following equations:

$$(\gamma_S^p)^{0.5} = (36.4 / \sqrt{51.0}) (1 + \cos \theta_w) - (\sqrt{21.8} / \sqrt{51.0}) (\gamma_S^d)^{0.5} \quad (3.7)$$

$$(\gamma_S^p)^{0.5} = (25.4 / \sqrt{2.3}) (1 + \cos \theta_d) - (\sqrt{48.5} / \sqrt{2.3}) (\gamma_S^d)^{0.5} \quad (3.8)$$

$$(\gamma_S^d)^{0.5} = (36.4 / \sqrt{21.8}) (1 + \cos \theta_w) - (\sqrt{51} / \sqrt{21.8}) (\gamma_S^p)^{0.5} \quad (3.9)$$

$$(\gamma_S^d)^{0.5} = (25.4 / \sqrt{48.5})(1 + \cos\theta_d) - (\sqrt{2.3} / \sqrt{48.5})(\gamma_S^p)^{0.5} \quad (3.10)$$

where θ_w is the water contact angle and θ_d is the diiodomethane contact angle.

Solving equations (3.7) and (3.8) leads to an expression for γ_S^d:

$$\gamma_S^d = [4.25(1 + \cos\theta_d) - 1.29(1 + \cos\theta_w)]^2 \quad (3.11)$$

Solving equations (3.9) and (3.10) leads to an expression for γ_S^p:

$$\gamma_S^p = [5.94(1 + \cos\theta_w) - 2.78(1 + \cos\theta_d)]^2 \quad (3.12)$$

Table 3.1 shows the surface free energies and the polar and dispersive components of several liquids that may be used.

Table 3.1 Polar and dispersive components of some wetting liquids commonly used for contact angle studies

Liquid	γ^d **(mN/m)**	γ^p **(mN/m)**	γ^t **(mN/m)**
Water	21.8	51.0	72.8
Glycerol	37.0	26.4	63.4
Formamide	39.5	18.7	58.2
Diiodomethane	48.5	2.3	50.8
n-Hexane	27.6	0.0	27.6
n-Octane	21.8	0.0	21.8

An alternative method for calculating polar and dispersive components consists of rearranging the Owens and Wendt equation into the form y = mx + c (Figure 3.2). Hence simple rearrangement of equation (5.12) leads to:

$$\gamma_{LV}(1 + \cos\theta) / 2(\gamma_{LV}^d)^{0.5} = (\gamma_S^p)^{0.5}(\gamma_{LV}^p / \gamma_{LV}^d)^{0.5} + (\gamma_S^d)^{0.5} \quad (3.13)$$

Plotting $\gamma_{LV}(1 + \cos\theta) / 2(\gamma_{LV}^d)^{0.5}$ against $(\gamma_{LV}^p / \gamma_{LV}^d)^{0.5}$ for at least 2 wetting liquids allows the gradient $(\gamma_S^p)^{0.5}$ and the intercept $(\gamma_S^d)^{0.5}$ to be determined.

Figure 3.2 Owens and Wendt graphical method for poly(HEMA)

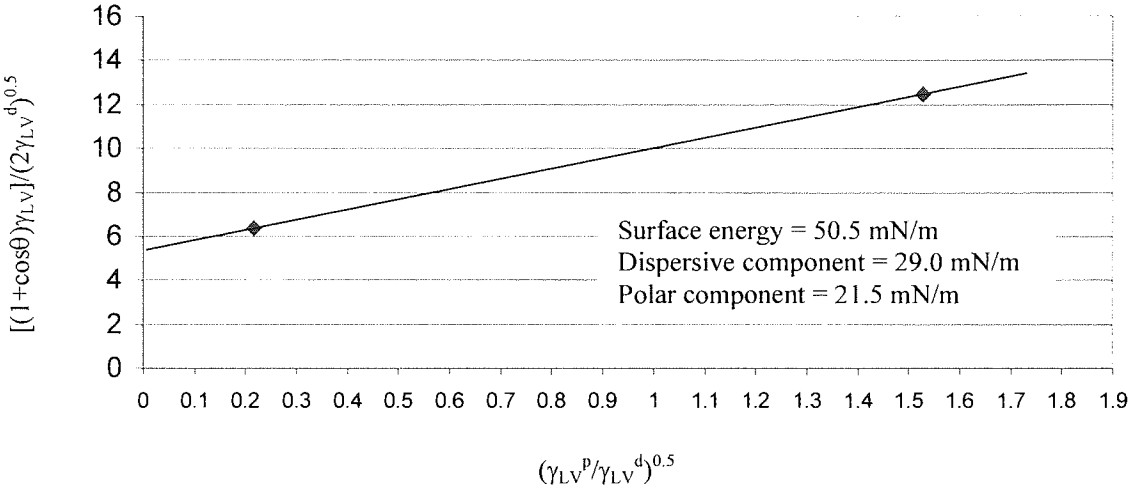

3.3 Hydrated Surfaces

The sessile drop technique is an unsatisfactory method for measuring hydrated surfaces because hydrated hydrogels begin to lose water by evaporation as soon as they are placed in air. It is therefore difficult to measure the contact angle accurately because the angle will change according to the state of dehydration of the sample. In addition, there exists no efficient and reproducible way to remove the surface water from the sample before measurement.

Hamilton's method involves measuring the contact angles of small n-octane droplets on solid surfaces under water[72, 73] (Figure 3.3).

Figure 3.3 Hamilton's method

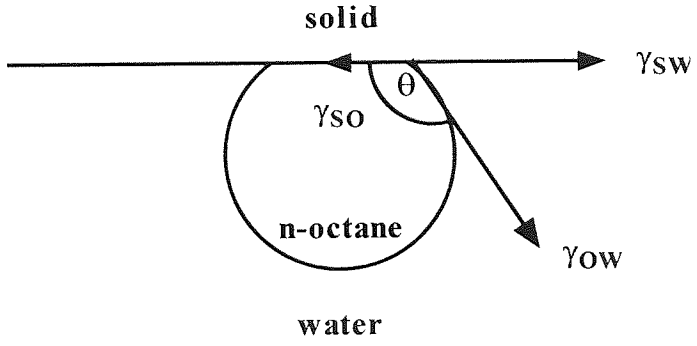

where γ_{SW} = solid - water interfacial free energy

γ_{SO} = solid - octane interfacial free energy

γ_{OW} = octane - water interfacial free energy

Fowkes[76] developed an equation for the work of adhesion at a solid – liquid interface, assuming that there was no polar interaction across the surface.

$$\gamma_{SL} = \gamma_S + \gamma_{LV} - 2\,(\gamma_{LV}^{d}\,\gamma_S^{d})^{0.5} \qquad (3.14)$$

A modified form of this equation was developed by Tamai *et. al.*[79] which accounted for stabilisation by non-dispersive forces.

$$\gamma_{SL} = \gamma_S + \gamma_{LV} - 2(\gamma_{LV}^{d}\,\gamma_S^{d})^{0.5} - I_{SL} \qquad (3.15)$$

where:

$$I_{SL} = 2\,(\gamma_{LV}^{p}\,\gamma_S^{p})^{0.5} \qquad (3.16)$$

n-Octane has no polar component and the dispersive components for n-octane and water are identical, thus it is possible to combine Young's equation with Tamai's equation to give an expression for I_{SW}, the polar stabilisation energy between water and the solid. The subscripts O for n-octane and W for water have been used.

$$I_{SW} = \gamma_{W\cdot V} - \gamma_{OV} - \gamma_{OW}\cos\theta \qquad (3.17)$$

$\gamma_{W'V}$ is the surface tension of n-octane saturated water and γ_{OV} and γ_{OW} can be determined experimentally allowing the equation for I_{SW} to be solved. γ_S^p, the polar component of surface free energy can now be determined from the equation for I_{SL}.

Andrade *et. al.*[66] showed that by using data from Hamilton's method and also the captive air bubble technique[80] (Figure 3.4), it is possible to define values for γ_{SV}, γ_{SV}^p, γ_{SV}^d and γ_{SW} for the hydrogel water interface. Applying Young's equation with water as the liquid phase gives:

$$\gamma_{SV} - \gamma_{SW} = \gamma_{WV} \cos \theta' \qquad (3.18)$$

γ_{WV} is known to be 72.8 mN/m and θ' is the contact angle of the captive air bubble, measured as shown in Figure 3.4. Thus $\gamma_{SV} - \gamma_{SW}$, the adhesion tension can be calculated.

Figure 3.4 Captive air bubble technique

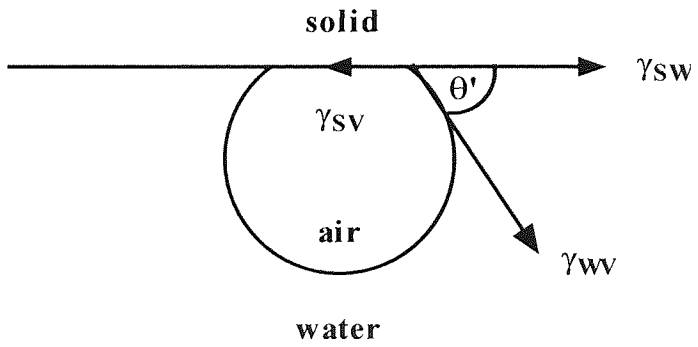

where γ_{SW} = solid – water interfacial free energy

γ_{WV} = water – vapour interfacial free energy (i.e. the surface tension of water)

γ_{SV} = solid – vapour interfacial free energy $\approx \gamma_S$ = solid surface free energy

An equation for the polar stabilisation parameter has already been derived

$$I_{SW} = \gamma_{W'V} - \gamma_{OV} - \gamma_{OW} \cos \theta \qquad (3.17)$$

Knowing that γ_{WV} = 72.8 mN/m, γ_{OV} = 21.8 mN/m and γ_{OW} = 51.0 mN/m, this equation can be rewritten:

$$I_{SW} = 51.0\ (1 - \cos\theta) \qquad (3.19)$$

I_{SW} can now be calculated. Combining Tamai's and Andrade's equations gives:

$$(\gamma_{SV} - \gamma_{SW}) = 2\ (\gamma_{WV}^{d}\ \gamma_{SV}^{d})^{0.5} + I_{SW} - \gamma_{WV} \qquad (3.20)$$

Rearranging this equation gives an expression for the dispersive component, (γ_{SV}^{d}) of the hydrogel:

$$\gamma_{SV}^{d} = [\{(\gamma_{SV} - \gamma_{SW}) - I_{SW} + \gamma_{WV}\} / 2\ (\gamma_{WV}^{d})^{0.5}]^2 \qquad (3.21)$$

The polar component, (γ_{SV}^{p}) can also be derived by rearranging the equation for I_{SL} to give:

$$\gamma_{SV}^{p} = I_{SW}^{2} / (4\ \gamma_{WV}^{p}) \qquad (3.22)$$

The equations used were therefore:

$$\gamma_{SV}-\gamma_{SW} = 72.8 \cos\theta' \qquad (3.23)$$

$$I_{SW} = 51\ (1 - \cos\theta) \qquad (3.19)$$

$$\gamma_{SV}^{d} = [(72.8 \cos\theta') - 51\ (1 - \cos\theta) + 72.8) / 2\ (\sqrt{21.8})]^2 \qquad (3.24)$$

$$\gamma_{SV}^{p} = I_{SW}^{2} / (4 * 51) \qquad (3.25)$$

$$\gamma_{SV} = \gamma_{SV}^{d} + \gamma_{SV}^{p} \qquad (3.26)$$

$$\gamma_{SW} = \gamma_{SV} - 72.8 \cos\theta' \qquad (3.27)$$

where θ is the n-octane contact angle from Hamilton's method and θ' is the air contact angle by the captive bubble technique.

An alternative method of calculating the dispersive component can be used based on the Owens and Wendt equation. The polar component is obtained by using

Hamilton's method and by inserting this value into the Owens and Wendt equation, together with the measured water-air contact angle, the dispersive component can be calculated. Results obtained for the dispersive component using both methods have been shown to be within 0.2 mN/m[81].

3.4 Materials and Methods

Contact angles were measured using a "Digidrop" goniometer manufactured by GBX Instrumentation Scientifique (France), paired with a PC running "Digidrop" software under Microsoft Windows 95.

Past researchers in this laboratory have cleaned samples using "Teepol L" or "Tween 20" detergent to remove any grease on the surface that may affect measurements and then rinsed thoroughly using distilled water. However, there is a high risk of traces of detergent remaining on the surface, and modification of the surface chemical groups by the detergent, especially with materials containing ionic monomers. It was decided, therefore, not to clean samples, but to ensure that fingers did not touch them, and that the risk of contamination was reduced.

3.4.1 Dehydrated Materials

Small samples of the hydrogel membrane were cut using a scalpel and dehydrated to constant weight between two blocks of PTFE in a microwave oven. Samples were then stored in a dessicator until they had cooled down before testing. One at a time materials were placed on the "Digidrop" stage in front of the camera and a drop of liquid was placed on the sample using the software. A drop size of 1.0 μl was selected. A photograph was taken automatically as soon as the drop was placed on the material (Figure 3.5). At least three drops were examined on each sample, and at least two different samples of each material was used, in order to obtain consistent and accurate results. The experiments were carried out using water and diiodomethane (methylene diiodide) which allow the polar, dispersive and total surface free energies in the dehydrated state to be determined. Measurements were

carried out quite quickly because dehydrated hydrogels readily absorb water from the air, thus reducing the contact angle.

Figure 3.5 Example image produced by GBX goniometer (sessile drop)

3.4.2 Hydrated Materials

Hydrated materials were cut using a size 7 cork borer and superglued to an electron microscope stub which was placed inside the hole of a rubber bung which was itself glued to a microscope slide. An optically perfect cell was filled with HPLC grade water and the slide was laid across the top of the cell in an inverted position so that the sample was immersed in the water. An air bubble (Figure 3.6) or a drop of n-octane (Figure 3.7) was carefully placed on the exposed surface of the sample manually using a specially curved syringe needle. A photo was taken which allowed the determination of the contact angle. At least three bubbles and drops were examined on each material. By the use of both air and n-octane the polar, dispersive and total surface energies in the hydrated state were determined.

Figure 3.6 Example image produced by GBX goniometer (captive air bubble)

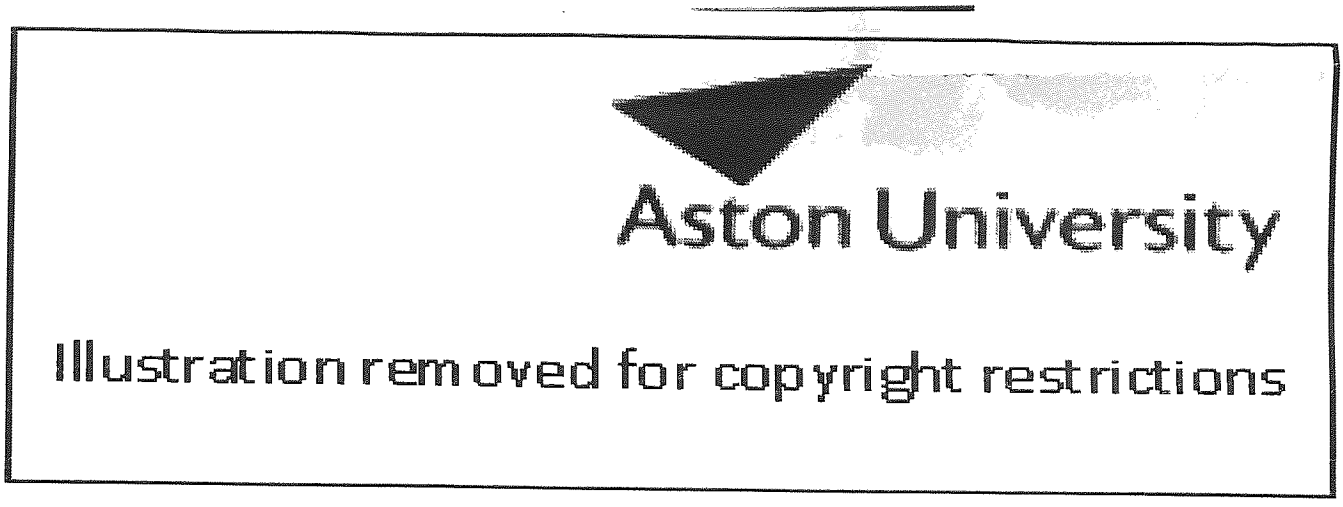

Figure 3.7 Example image produced by GBX goniometer (Hamilton's method)

3.4.3 Statistical Analysis

Results were tested for statistical significance using analysis of variance (ANOVA), heteroscedastic t-tests and paired t-tests for means. Tests assume unequal variances and normal distributions.

3.5 Results

3.5.1 Surface Properties of Dehydrated Hydrogels

3.5.1.1 The effect of increasing hydrophilic monomer

Figure 3.8 The surface free energy of dehydrated NVP/MMA copolymers of increasing EWC (error bars too small to be shown)

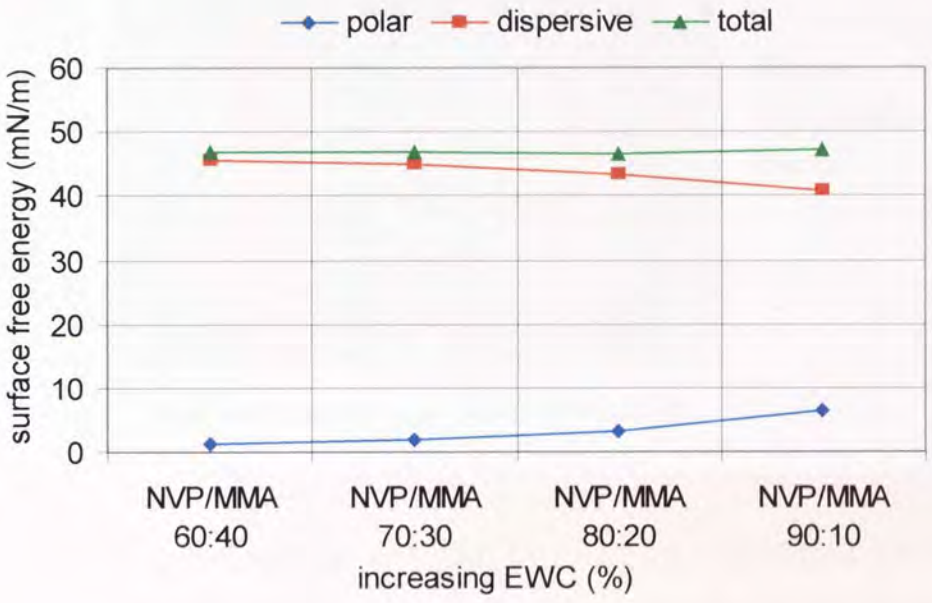

Figure 3.8 shows that with the increase in EWC the polar component of the surface free energy increases slightly (ANOVA $p<0.01$, $n=3$). A corresponding decrease is observed in the dispersive component of the surface free energy (ANOVA $p<0.05$, $n=3$). This is a direct result of the change in composition towards polymers containing increasing amounts of hydrophilic monomer and decreasing amounts of hydrophobic monomer. In the dehydrated state, the values for the dispersive component are much higher than those for the polar component of surface free energy. This observation is consistent with the effect of hydrophobic group expression at the air interface and the orientation of the hydrophilic groups towards the polymer bulk. Such effects result in the surface of the polymer being dominated by hydrophobic groups and the value of the surface energy being dominated by the dispersive component.

Overall, the effect of incorporation of the hydrophilic monomer has little effect on the total surface free energy (ANOVA $p=0.62$, $n=3$). In comparison, poly(HEMA) has a polar component of 8.5 mN/m and a dispersive component of 35 mN/m.

Figure 3.9 The surface free energy of the dehydrated NVP/MMA 25:75 and the AMO/MMA 25:75 copolymers (error bars too small to be shown)

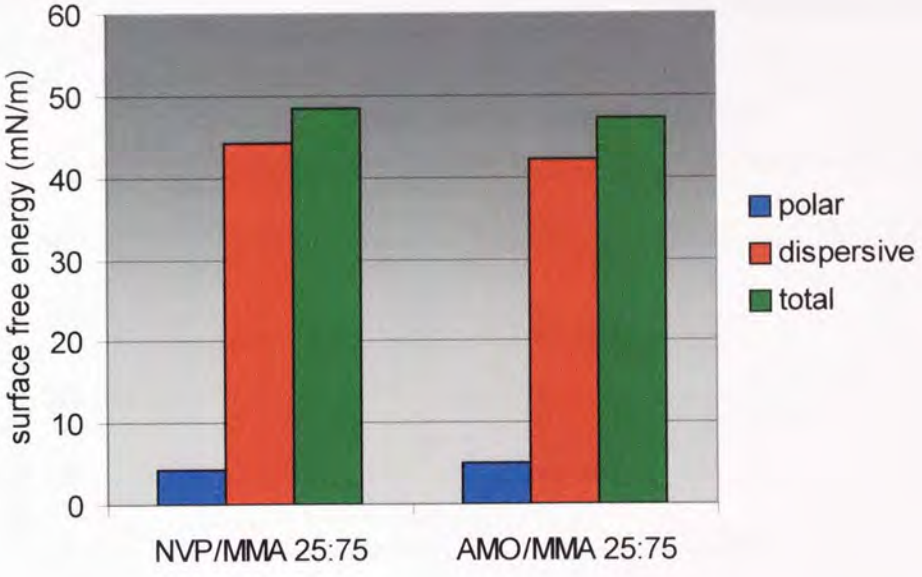

The two low EWC materials tested (NVP/MMA 25:75 and AMO/MMA 25:75) have slightly higher polar components of surface free energy than the lowest of the higher water content neutral hydrogels (NVP/MMA 60:40) (heteroscedastic t-test $p<0.05$ and $p<0.01$, $n=3$ respectively); their dispersive components of surface free energy are slightly lower though only the AMO/MMA result is statistically significant (heteroscedastic t-test $p=0.23$ and $p<0.05$, $n=3$ respectively). In comparison, the hydrogels of higher EWC, when in the dehydrated state exhibited a surface free energy that is dominated by the dispersive component, though it is unclear why a higher polar component was observed in these polymers with small amounts of hydrophilic monomer. The AMO copolymer appears to have a slightly higher polar component and slightly lower dispersive component than the NVP copolymer due to it having more polar chemical groups though the differences are not statistically significant (heteroscedastic t-test $p=0.38$ and $p=0.15$, $n=3$ respectively).

3.5.1.2 The effect of increasing cationic monomer

To enable the effect of ionic monomer to be studied, the NVP/MMA copolymer at 80:20 composition was used as the base material. NVI or DEAEMA was added at concentrations of 2, 5, 7 and 10%.

Figure 3.10 The surface free energy of dehydrated NVP/MMA copolymers containing increasing amounts of NVI (error bars too small to be shown)

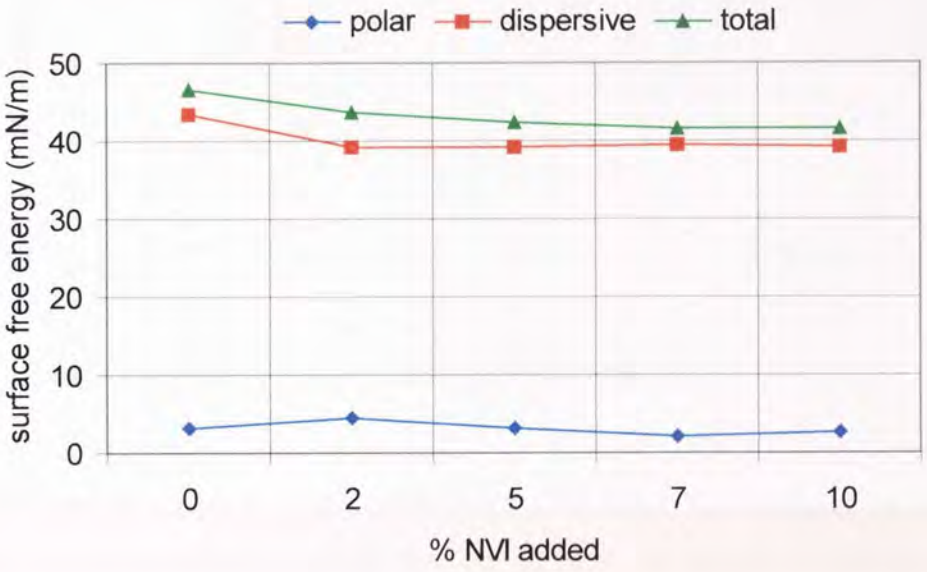

The effect of incorporating increasing proportions of NVI on the surface free energy in the dehydrated state is shown in Figure 3.10. As the amount of NVI is increased from 0% to 10% there is a slight reduction in the total surface free energy (ANOVA $p<0.05$, $n=3$). However, both the polar and dispersive components of surface free energy remain around the same values across the series of dehydrated materials tested (ANOVA $p=0.11$ and $p=0.99$, $n=3$ respectively). NVI contains both hydrophobic and hydrophilic regions, and the amount of NVI was increased at the expense of the hydrophilic NVP and the hydrophobic MMA, so this may partly explain the similarity in the values for surface free energy. Furthermore, there is very little variation in the EWC of the hydrated polymers, so it is expected that the surface free energies would remain approximately the same although there appears to be no effect from the cationic groups.

Across this series the surface free energy is dominated by the dispersive component due to the polymer being in the dehydrated state.

Figure 3.11 The surface free energy of dehydrated NVP/MMA copolymers containing increasing amounts of DEAEMA (error bars too small to be shown)

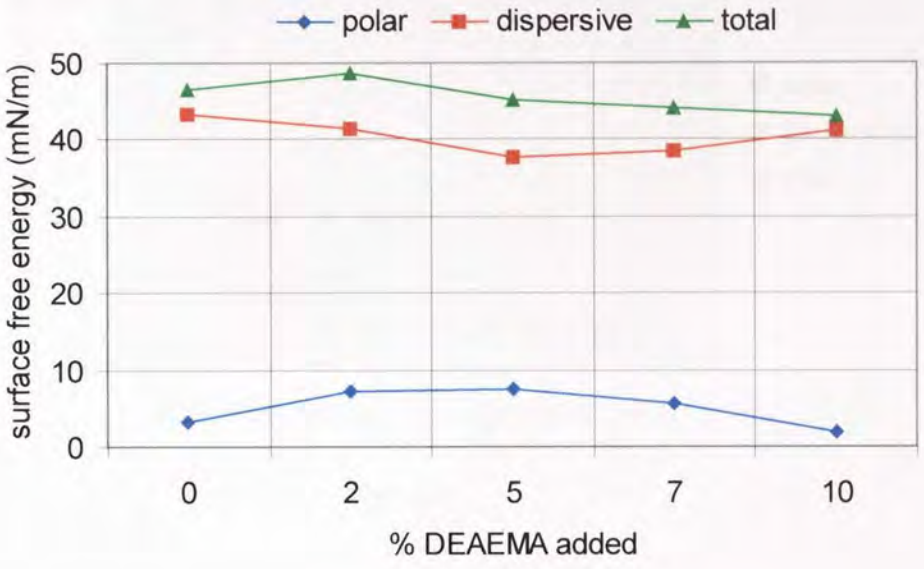

As can be seen in Figure 3.11, the addition of DEAEMA has an effect on the polar and dispersive components of surface free energy with the greatest difference seen at 5% incorporation (ANOVA $p<0.01$ and $p<0.05$, $n=3$ respectively). The total surface free energy remains is reduced slightly with increasing DEAEMA (ANOVA $p<0.01$, $n=3$). This behaviour is likely to be the result of similar factors to those outlined for the NVI containing gels.

3.5.1.3 The effect of anionic monomer

Figure 3.12 shows that the addition of 0.5% methacrylic acid reduces the polar component of surface free energy and increases the dispersive component in the dehydrated state; the total surface free energy is increased slightly (ANOVA $p<0.05$, $p<0.01$ and $p<0.05$, $n=3$ respectively). This is a consequence of the rotation that occurs along the carbon main chain to expose the hydrophobic groups at the interface between the polymer and air. This orientation results in the hydrophilic groups burying themselves within the bulk of the polymer which is the most thermodynamically favourable position.

Figure 3.12 The surface free energy of the dehydrated NVP/MMA/MAA 79.75:19.75:0.5 copolymer (error bars too small to be shown)

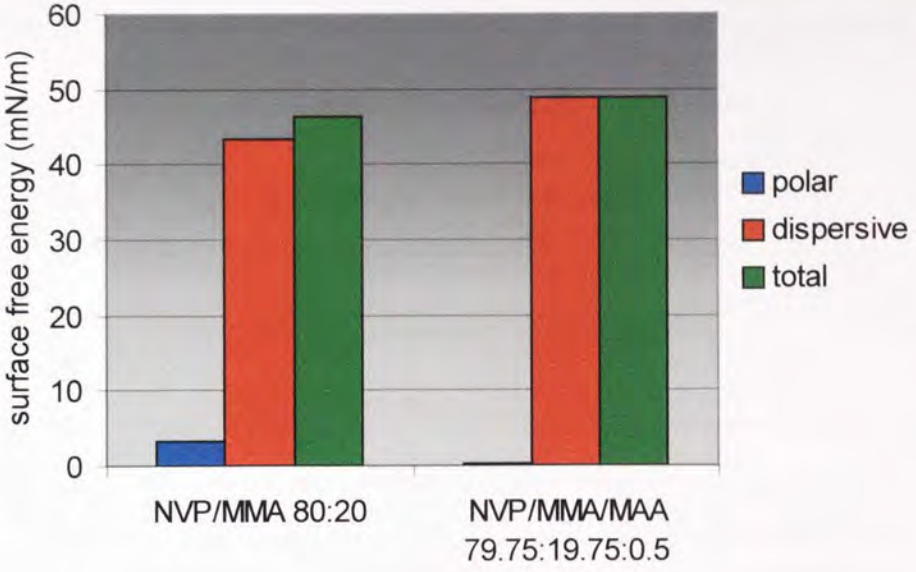

3.5.2 Surface Properties of Hydrated Hydrogels

3.5.2.1 The effect of increasing hydrophilic monomer

The determination of surface energies in the dehydrated state provides useful information about the surface of the polymer. However when hydrogel materials are swollen as they are in biomedical applications, the surface energies change dramatically. The determination of contact angles of hydrated hydrogels is a difficult process due to dehydration of the polymer surface during measurement. However the use of inverted droplet methods has overcome to a large extent many of these problems.

The effect of increasing EWC on the polar and dispersive components of the surface free energy of the NVP/MMA copolymers is shown in Figure 3.13. When the results are compared with the dehydrated state it can be seen that a large polar component has arisen while the dispersive component is greatly reduced. The increase in the total surface free energy with increasing EWC is significant (ANOVA $p<0.01$, $n=3$). As these materials have high water contents, the values of the two components are similar

to those of pure water. In comparison, poly(HEMA) has a polar component of 36.7 mN/m and a dispersive component of 22.1 mN/m.

Figure 3.13 The components of the surface free energy for NVP/MMA copolymers with increasing EWC in the hydrated state (error bars too small to be shown)

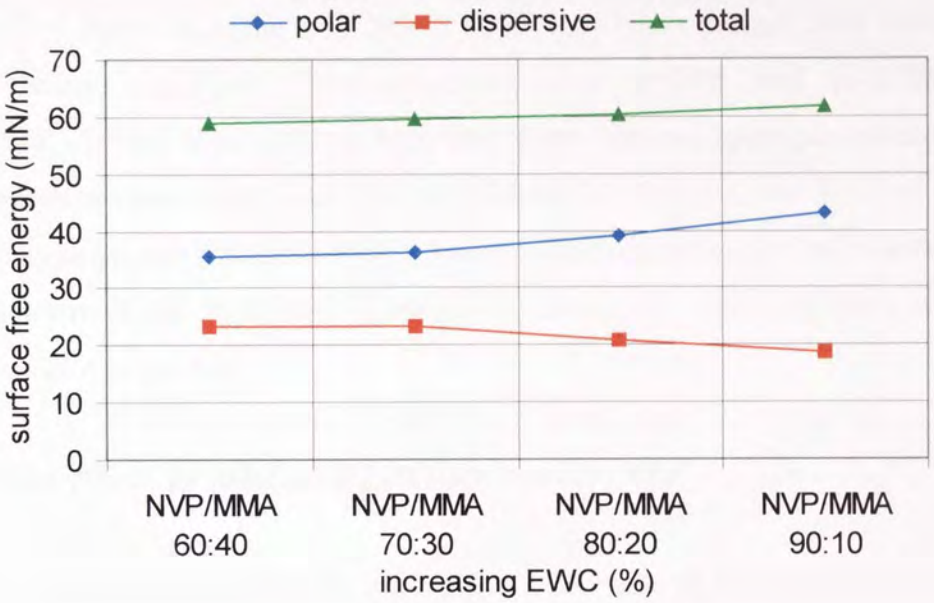

Figure 3.14 The surface free energy of the hydrated NVP/MMA 25:75 and the AMO/MMA 25:75 copolymers (error bars too small to be shown)

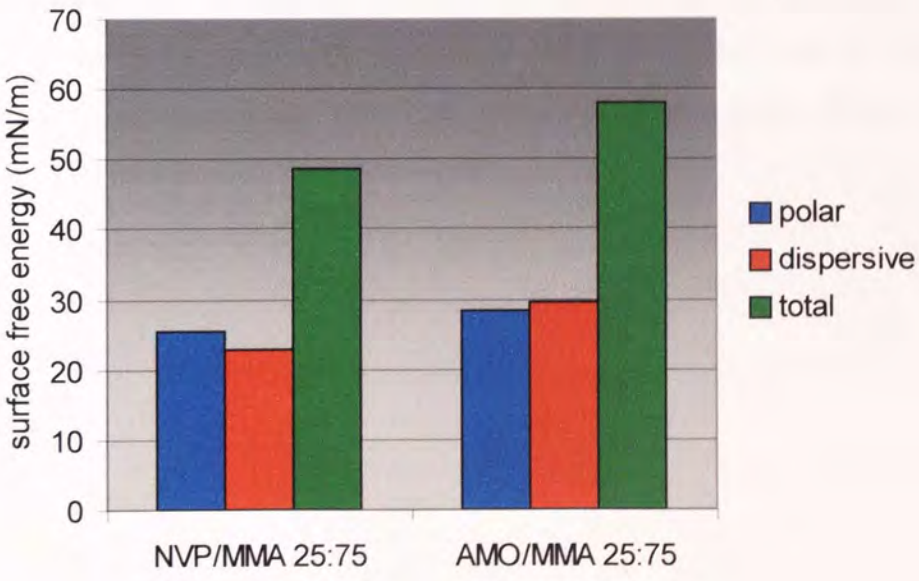

The two low EWC materials tested (NVP/MMA 25:75 and AMO/MMA 25:75) have lower polar components of surface free energy than the lowest of the higher water content neutral hydrogels (NVP/MMA 60:40) (heteroscedastic t-test $p<0.01$ and $p<0.01$, $n=3$ respectively). The NVP/MMA 25:75 copolymer has a lower dispersive component and the AMO/MMA 25:75 copolymer has a higher dispersive component of surface free energy than the NVP/MMA 60:40 copolymer though these results are not statistically significant (heteroscedastic t-test $p=0.86$ and $p<0.08$, $n=3$ respectively). It was expected that both low water content hydrogels would have higher dispersive components than the NVP/MMA 60:40 copolymer because of the amount of hydrophobic monomer they contain. One explanation for the results is the blocky structure of the NVP copolymer which causes the surface to have areas of differing surface properties.

3.5.2.2 The effect of increasing cationic monomer

As for the dehydrated materials, the NVP/MMA copolymer at 80:20 composition was used as the base material and either NVI or DEAEMA was added at concentrations of 2, 5, 7 or 10%. The surface free energy is dominated by the polar component when the materials are in the hydrated state. With increasing NVI or DEAEMA the dispersive component of surface free energy remains stable, but the polar component of surface free energy is raised slightly due to the charged NVI or DEAEMA though only the NVI result is statistically significant (ANOVA $p<0.01$ and $p=0.74$, $n=3$ resepctively). Correspondingly the total surface free energy is raised slightly (ANOVA $p<0.01$ and $p=0.38$, $n=3$ resepctively).

Figure 3.15 The surface free energy of hydrated NVP/MMA copolymers containing increasing amounts of NVI (error bars too small to be shown)

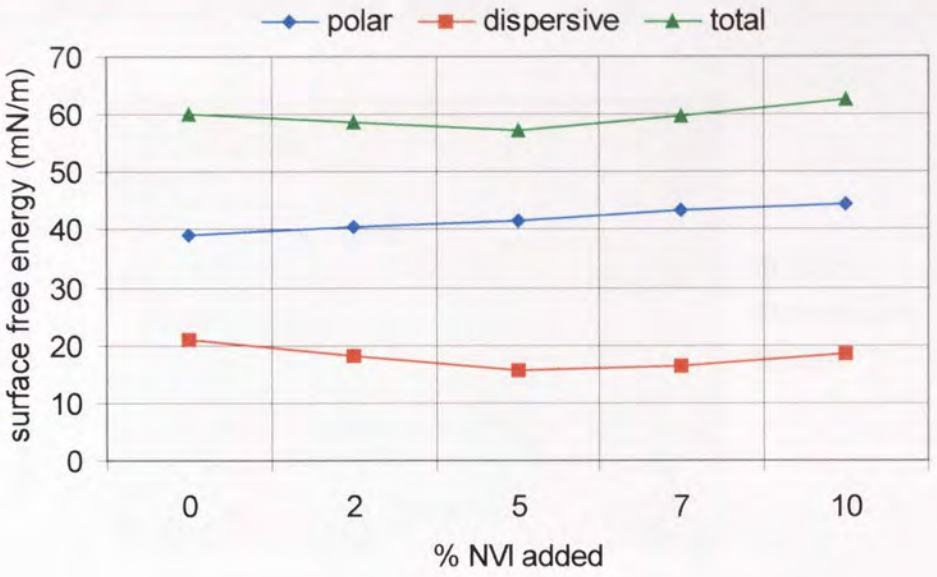

Figure 3.16 The surface free energy of hydrated NVP/MMA copolymers containing increasing amounts of DEAEMA (error bars too small to be shown)

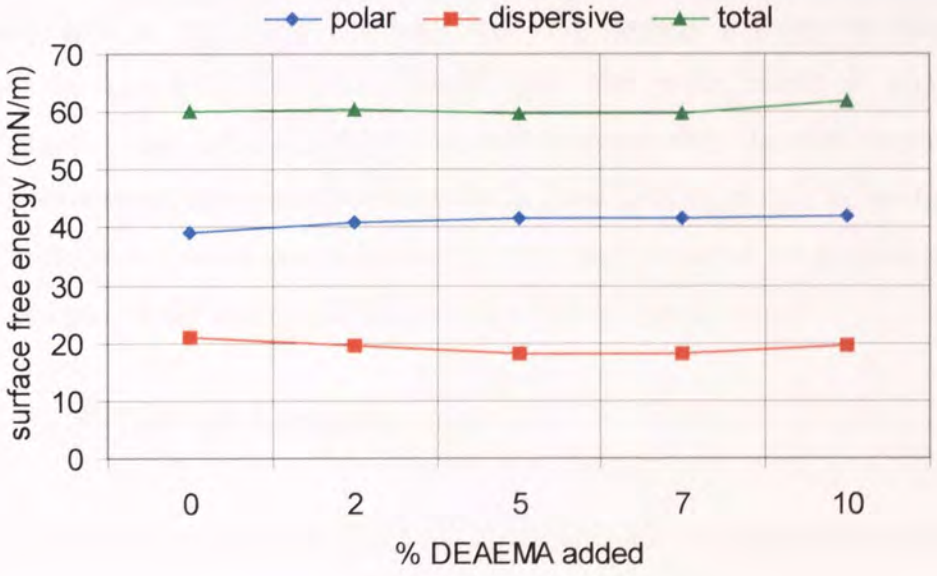

3.5.2.3 The effect of anionic monomer

Figure 3.17 The surface free energy of the hydrated NVP/MMA/MAA 79.75:19.75:0.5 copolymer (error bars too small to be shown)

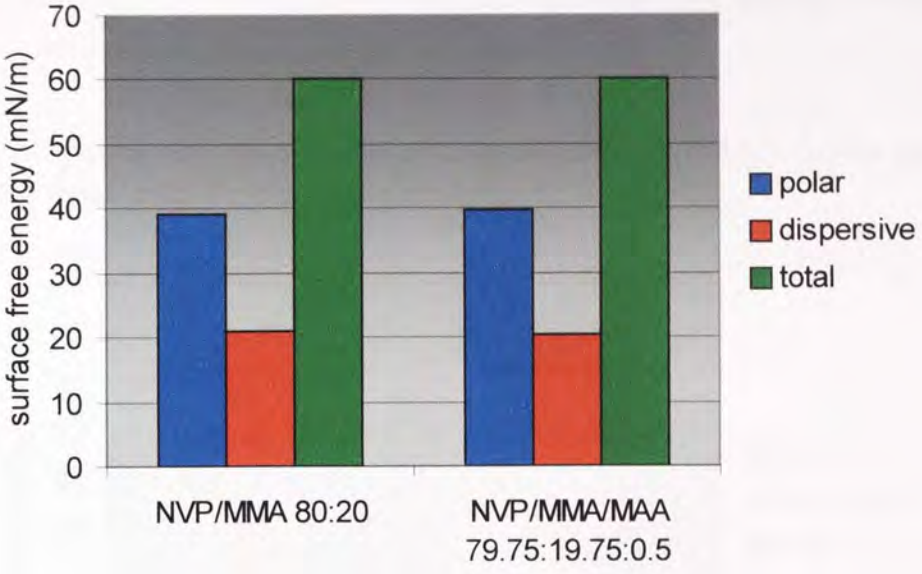

Figure 3.17 shows that the addition of 0.5% methacrylic acid slightly increases the polar component of surface free energy and very slightly reduces the dispersive component in the hydrated state though only the polar result is significant (heteroscedastic t-test $p<0.01$ and $p=0.75$, $n=3$ respectively); the total surface free energy remains about the same (heteroscedastic t-test $p<0.95$, $n=3$). In the hydrated state the hydrophilic groups are positioned towards the exterior of the polymer and the hydrophobic groups are buried within the bulk of the polymer.

3.5.3 The Effect of Autoclaving

It is obvious that any biomaterial has to be sterilised before it is implanted in the body so as not to spread infection. Autoclaving is the simplest method of sterilisation but this involves subjecting the materials to a very high temperature and pressure. It was thought that this treatment could perhaps modify the polymers in some way, thereby changing the surface properties of the materials. Preliminary results indicated that autoclaving did modify the samples since a marked increase in polar component along with a similar decrease in dispersive component was observed in the dehydrated state,

and a marked increase in dispersive component was observed in the hydrated state. The experiment was therefore repeated with poly(HEMA).

Hydrogel samples were sterilised for 15 minutes at 115°C and 3 bar in an Astelle Scientific Swiftlock autoclave and were tested using the dipping balance and compared with a control which had not been autoclaved.

Figure 3.18 The surface free energy of dehydrated poly(HEMA), before and after autoclaving (error bars too small to be shown)

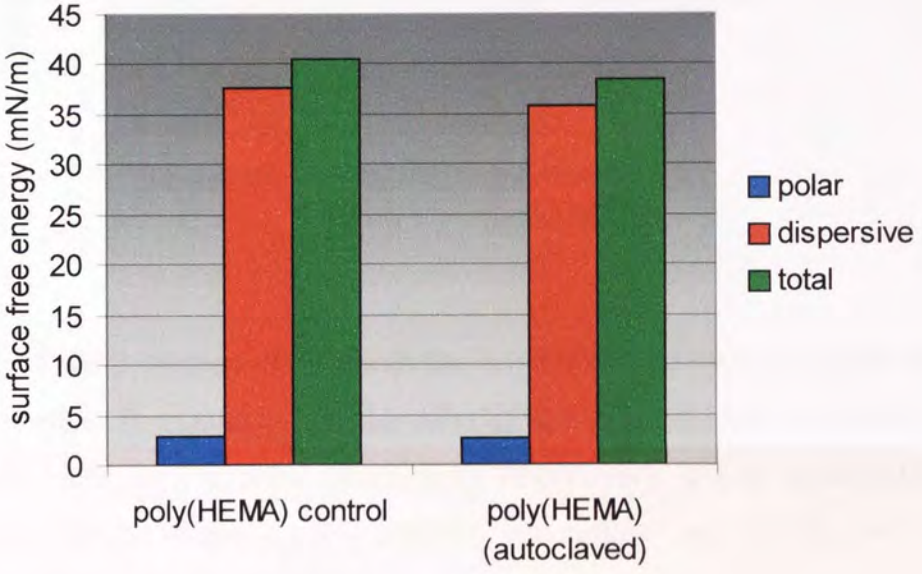

Figure 3.19 The surface free energy of hydrated poly(HEMA), before and after autoclaving (error bars too small to be shown)

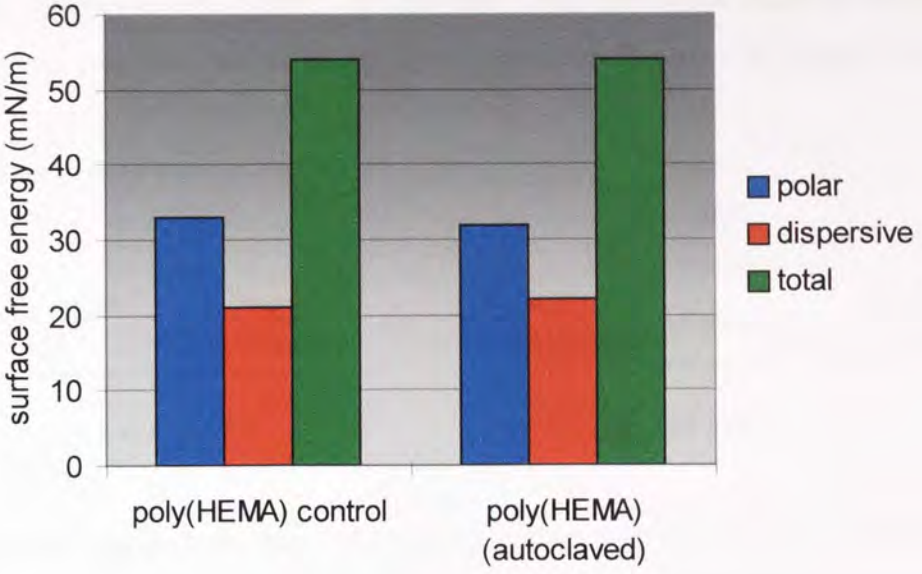

Figures 3.18 and 3.19 show that in both the dehydrated and hydrated states there is a significant effect from autoclaving the poly(HEMA) (paired t-test for means $p<0.01$ and $p<0.01$, $n=3$ for the polar components respectively, $p<0.01$ and $p<0.01$, $n=3$ respectively for the dispersive components, and $p<0.05$ and $p=0.21$, $n=3$ for the respective total surface free energies).

3.6 Discussion

The results for the dehydrated hydrogels of increasing hydrophilic monomer are in good agreement with those of Corkhill[81] who noted similar trends with comparable materials. However, it should be noted that the actual values for each component of surface free energy can vary quite considerably when experiments are carried out by different operators. One reason for this is that there may be a delay between the positioning of the drop and the reading of the contact angles. A goniometer can be a difficult instrument to use, so that several seconds may elapse before the contact angle is determined. When the drop of liquid is placed on the dehydrated gel the contact angle is high, due to the hydrophobic groups being present on the surface.

Hydrophobic liquids begin to be absorbed almost immediately which reduces the contact angle. In the case of hydrophilic liquids, there is rapid rotation of the hydrophilic groups in the gel towards the surface and the liquid begins to be absorbed, resulting in lower contact angles. At the same time the liquid starts to evaporate, reducing the amount of liquid on the surface. This effect is shown in Figure 3.20.

Fig 3.20 Time dependence of contact angles

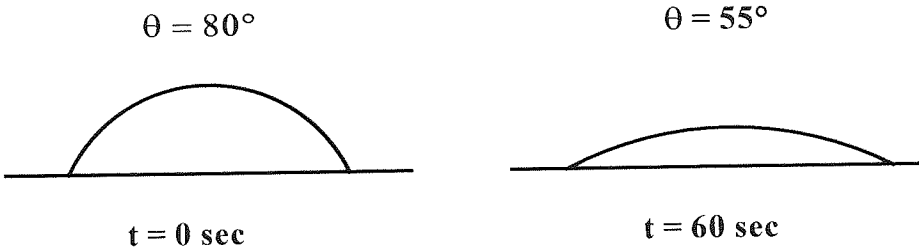

The "Digidrop" goniometer now used in this laboratory reduces this variation by automatically taking a photograph instantaneously the moment the drop is placed.

A second reason for variation in results is that the dehydrated gel quickly rehydrates due to the absorption of water from the air. Therefore, hydrophilic groups may have already rotated towards the surface before the drop of liquid is placed on the material and the contact angle is lower than would be expected with a fully dehydrated gel. Placing the material in a dessicator before testing can reduce this effect, though the time taken to do this may vary between operator. A third cause of error is the variation in drop size between operator. Larger drops produce higher contact angles. An automated system such as the "Digidrop" automatically produces drops of constant size, but there could be evaporation from the drop before it is placed on the material.

Therefore, this technique is useful to make comparisons between materials where trends may be seen, but actual values for contact angles may vary considerably with the operator.

In the hydrated state results for hydrogels of increasing hydrophilic monomer are also in good agreement with those of Corkhill[81], with less variation noted than found for those tested in the dehydrated state. The measured surface energies of the hydrated

materials are higher than those for the dehydrated materials and the contribution of the polar component is greater. In addition to the effect of surface group rotation, this effect is also due to the presence of water with a high polar component of surface free energy (51.0 mN/m) and a higher total surface free energy, (72.8 mN/m).

In this Chapter it was shown that NVI nor DEAEMA reduced the total surface free energy in the dehydrated state, though in the hydrated state the polar component was raised slightly. This was explained by the presence of the cationic groups which would be dissociated in the hydrated state but not in the dehydrated state. However, French[82] found that neither NVI nor DEAEMA made any difference in either the hydrated or dehydrated states and explained that the freedom of rotation around the backbone of the polymer was restricted due to the ring structure in NVI and the α-methyl group in DEAEMA. The view, therefore, was that even in the hydrated state the material remained dominated by the hydrophobic groups as opposed to any polar groups being expressed at the surface. In the light of the present work it appears that the surface groups are not completely restricted, though there may be some restriction because of the fact that the charged groups only show a mild increase in polar component when in the hydrated state.

The incorporation of a small amount of the anionic monomer methacrylic acid reinforces the belief that an α-methyl group does not affect rotation around the carbon backbone. In the dehydrated state the polar groups are buried within the polymer bulk but in the hydrated state they are oriented towards the surface. The decreased polar component noted in the dehydrated state, along with the increased polar component in the hydrated state in such polymers, as compared with a similar hydrogel not containing any methacrylic acid proves that the rotation does occur.

A small change in surface properties was observed when poly(HEMA) was autoclaved, though it is possible that other materials may behave differently.

3.6 Conclusions

Static contact angle measurements were carried out on a series of hydrogel polymers with increasing or decreasing hydrophilic monomer content, or increasing ionic monomer content. In the dehydrated state the surface free energy is dominated by the dispersive component whereas in the hydrated state the polar component is dominant due to the presence of water and the effect of rotation of the surface groups around the carbon backbone.

An increase in hydrophilic monomer causes an increase in the polar component and a decrease in the dispersive component of surface free energy both in the dehydrated and hydrated states. Although only one hydrogel containing AMO was tested it had a higher polar component and lower dispersive component than the corresponding NVP copolymer with the same composition ratio due to the presence of more polar chemical groups in the dehydrated state. In the hydrated state the AMO copolymer showed increased polar and dispersive components compared with the NVP copolymer though the results were not statistically significant.

An increase in cationic monomer (either NVI or DEAEMA) had the effect of reducing total surface free energy in the dehydrated state, but increased the polar component in the hydrated state. In the dehydrated state these polar groups are held within the polymer bulk but rotate when the polymer is hydrated.

The incorporation of MAA into one of the copolymers reduces the polar component and increases the dispersive component in the dehydrated state, but the opposite is true in the hydrated state. Again, the reason for this is the rotation of the surface groups.

Autoclaving the poly(HEMA) samples had a small effect on the surface free energy of the polymer, though further work should be carried out on a wider range of materials.

3.7 Further Work

Further work needs to be carried out on a range of hydrogels in order to confirm that autoclaving samples affects surface properties since the preliminary results were not reproduced.

Previous work in this laboratory has shown that the monomer acryloyl morpholine (AMO) produces polymers with more even sequence distributions when MMA is used as the comonomer, therefore a continuation of the present study using a wider range of AMO copolymers would be of interest.

CHAPTER 4
DYNAMIC CONTACT ANGLE MEASUREMENTS

4.1 Introduction

Dynamic contact angle measurement (DCA) enables advancing and receding contact angles to be measured by dipping the test material into the probe solution. This method is based on the Wilhelmy plate technique and is shown diagrammatically in Figure 4.1. The solid test sample is attached to an electrobalance and the test solution is raised or lowered on a scissor jack with a motorised micropositioner in order to immerse and then remove the sample.

In vitro techniques enable direct measurement of contact or wetting angles, which is one of the most sensitive methods of investigating the outer surfaces of a polymer[66]. As mentioned in Chapter 3, hydrogel contact angles have been studied using a variety of techniques, including captive bubble[66, 67, 68], sessile drop[69], Wilhelmy plate[68, 70] and also by a method utilising laser examination of an adherent liquid[71].

Using the sessile drop and captive bubble methods it is often difficult to estimate the angle between a bubble or drop and the lens surface, resulting in poor reproducibility of the measurements. However, the Wilhelmy plate technique is a more objective method of assessing contact angle and operates by alternately immersing and withdrawing the sample from a test liquid. The advancing contact angle is measured as the solution is moved over a previously unwetted surface (during immersion) and the receding angle when the sample is withdrawn from the liquid (during emmersion). A microbalance is used to measure the weight of the sample as it is moved into and out of the fluid. Measurements such as these, which are based upon force, result in greater accuracy and remove the subjective bias characteristic of other methods[83, 84] such as sessile drop and captive bubble techniques. To date, the constraints of sample configuration have limited the applicability of this method.

Previous studies in the contact lens arena have applied both the captive bubble[85] and the Wilhelmy technique to investigate wetting of rigid lens materials[83, 84] but have not extended these studies to soft lenses. This has been principally due to the poor dimensional stability of intact hydrogel lenses upon immersion into a probe fluid.

However, investigators in other fields have overcome these constraints and studied hydrogel materials using the Wilhelmy plate technique by attaching a small weight to the hydrogel prior to immersion[86, 87, 88] and this has been extended to soft contact lenses[89].

The force exerted by the test sample is proportional to the apparent weight of the sample, and this in turn, is defined by the height of the meniscus of liquid adhered to the sample (a product of wetting) and the buoyancy. The contact angle at the instant of insertion and removal from the test liquid, when there are no buoyancy effects, can be calculated using the following formula:

$$\cos\theta = \frac{F}{\sigma \times P} \qquad (4.1)$$

where: θ = advancing or receding contact angle

F = measured force (dynes)

σ = surface tension of probe solution (dynes/cm) (or mN/m)

P = perimeter of test sample (cm)

Results are presented graphically in this chapter and are listed in Appendices IV and IV.

Figure 4.1 DCA measurement using the Wilhelmy plate technique

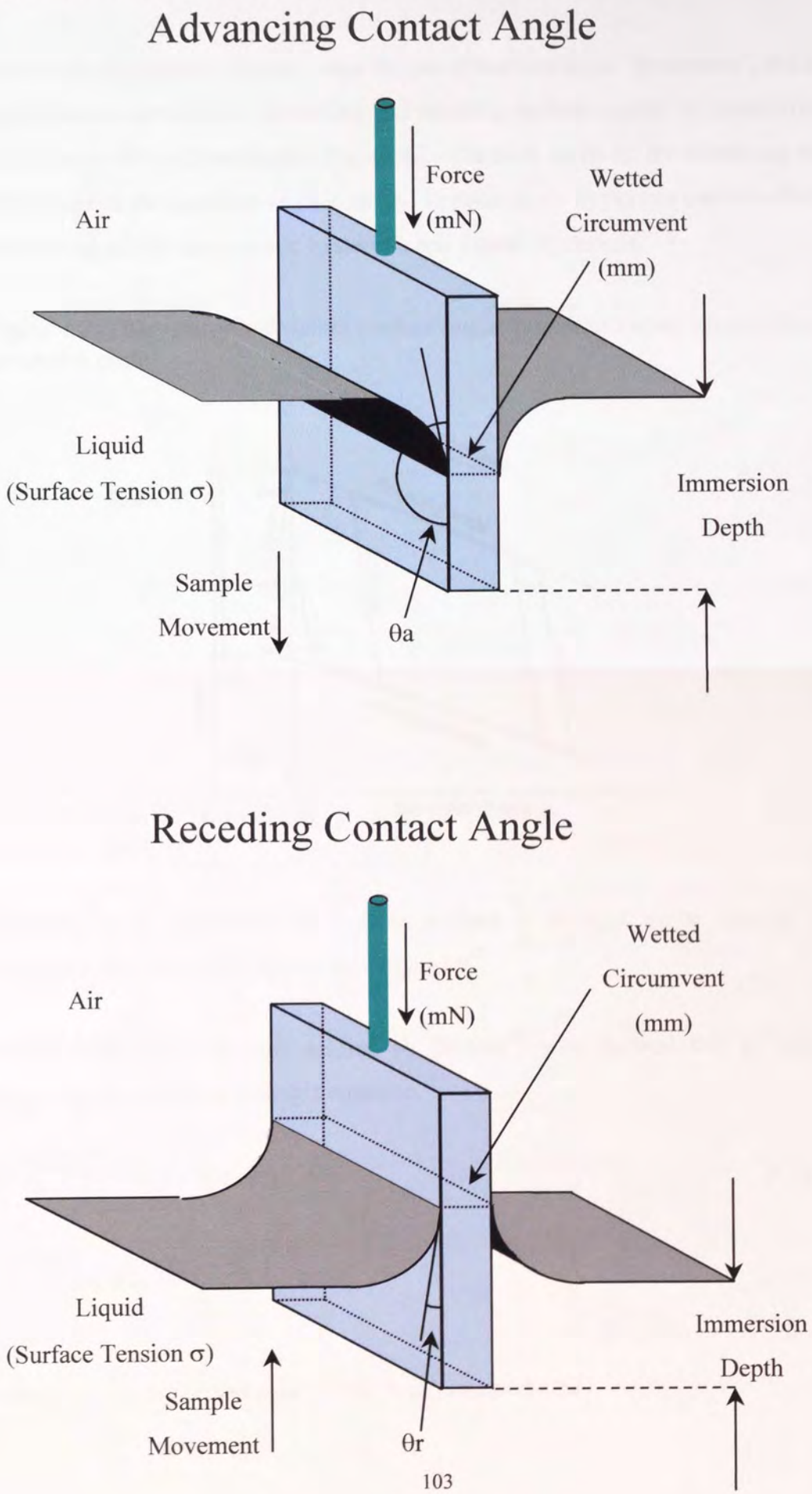

4.1.1 Hysteresis

Many polymer systems display some degree of contact angle "hysteresis", defined as the difference between the advancing and receding contact angles. A typical dynamic hysteresis profile is illustrated in Figure 4.2. On most surfaces, the advancing contact angle exceeds the receding contact angle. Contact angle hysteresis can be subdivided into two types: thermodynamic hysteresis and kinetic hysteresis.

Figure 4.2 Diagram of a dynamic contact angle hysteresis curve, illustrating a two immersion cycle

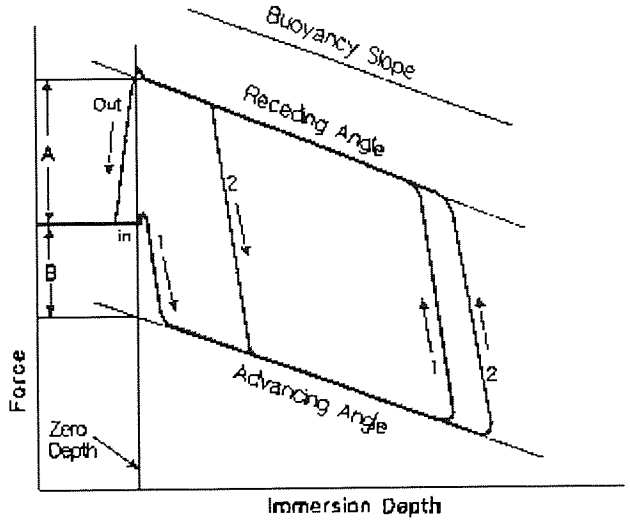

Thermodynamic hysteresis on a clean surface is thought to be due to surface roughness (rugosity) and surface heterogeneity[86].

Surface roughness has been studied by Wenzel[90] who showed that a "roughness factor" can be added to Young's equation.

$$r\,(\gamma_S - \gamma_{SL}) = \gamma_L \cos\theta \qquad (4.2)$$

$$\cos\theta = \frac{r\,(\gamma_S - \gamma_{SL})}{\gamma_L} \qquad (4.3)$$

where: r = "surface roughness" = true area/projected area

Therefore,

$$\cos \theta_{apparent} = r \cos \theta_{true} \qquad (4.4)$$

Thus the sign of cos θ is unchanged by the roughness, but its magnitude, whether positive or negative, is increased, since r is necessarily greater than unity. Hence roughness decreases $\theta_{apparent}$ if θ_{true} is less than 90° and roughness increases $\theta_{apparent}$ if θ_{true} is greater than 90°.

Surface heterogeneity is a second cause of thermodynamic hysteresis. Patches of different surface energies produce metastable differences when the contact line moves.

Kinetic hysteresis is usually accounted for by time or rate dependent processes, such as swelling, liquid penetration into the surface region and surface reorientation of functional groups[86] (such that the conformation of the polymer changes to minimise the interfacial energy between itself and the adjacent phase). The large hysteresis observed for polymers containing hydrophilic functional groups is mainly due to the high rotational mobility of macromolecules at the surface[70]. The rate of reorientation is likely to be particularly fast within hydrogel materials, where flexibility of the polymer network enables free motion of such functional groups. A hydrogel polymer in air will tend to orientate its polar groups into the structure of the hydrogel, towards the imbibed water, and the hydrophobic groups will tend to be at the surface. However, when the polymer is placed in water, the hydrophilic groups will reorient towards the surface where there is more water, and the hydrophobic groups will orient towards the hydrophobic polymer backbone.

In this work the test was conducted on fully hydrated samples and the hysteresis observed between the advancing (θ_A) and receding (θ_R) contact angles was taken as an indication of the change in the level of wettability of the sample between the dry and wet states. This, in turn, is a consequence of the mobility of the groups present at the surface. The phenomenon of surface mobility is related to the mobility of the hydrophilic and hydrophobic groups on the backbone of the polymer. If a sample is unwettable this suggests that the hydrophobic groups prefer the phase (air) on the

surface of the gel and the hydrophilic groups prefer to be away from the surface and associate with water molecules already trapped within the polymer bulk.

Incomplete wetting is characterised by the contact angle θ of the liquid on the solid surface. If an initially unwettable sample is dipped into an aqueous solution, the advancing angle is high. The hydrophilic groups will tend to associate with the water molecules and rotate around the backbone of the carbon to orientate themselves at the surface of the gel, while the hydrophobic groups move into the gel. The sample at this point will be wettable and the receding angle will be low, hence the hysteresis will be large. In this case there is a high surface mobility. On the other hand, if the sample is already wettable, the hydrophilic groups will already be present on the surface of the gel, so there is little mobility of the surface.

A low advancing angle combined with negligible hysteresis can therefore be considered to be an indication of excellent wettability.

Polymers containing anionic groups will tend to be wettable at high pH, and polymers containing cationic groups will be wettable at low pH. This is due to the repulsion of the ionic groups, which results in large pores in the matrix of the polymer. Water molecules in solution can then flood into the matrix and form a hydration shell around the charged groups, thus giving a wettable gel.

4.1.2 Static Surface Tension

To determine the final hysteresis angle the surface tension of the probe solution used solution must be measured. The static surface tension is the simplest method of defining surface activity and was measured in this study by use of the du Noüy ring technique[91, 92, 93]. Some of the other techniques for measuring surface tension are oscillating jet[94], hanging drop[95, 96], spinning drop, sessile drop, capillary rise[97] and maximum bubble pressure[98, 99, 100].

Surface (interfacial) tension σ is the isothermal, reversible work of forming unit area of interface.

Figure 4.3 Static surface tension measurement using the du Noüy ring

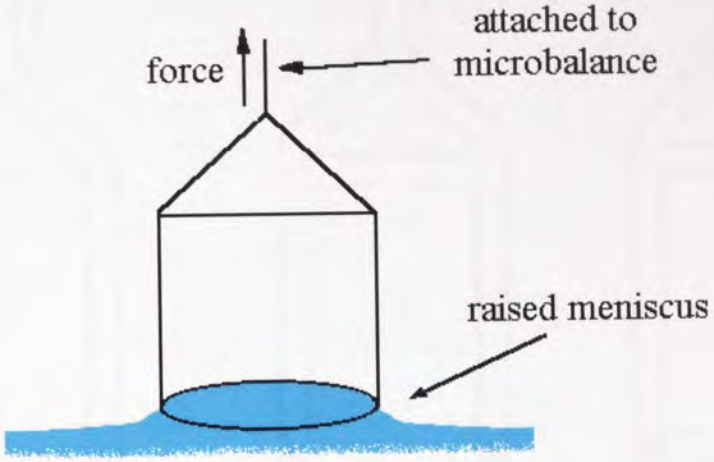

Platinum is used to ensure wetting of the ring by the liquid by forming a contact angle of zero between the liquid and ring. During measurement, the ring is first dipped below the surface. Then, since it is more convenient to move the liquid than the force measuring system, the liquid container is slowly lowered while measuring the force exerted on the ring. When the ring reaches the surface, it does not break through but instead stretches the surface producing lamella which have an area larger than the initial surface. Surface tension is a vector with magnitude and direction. It acts against both the outside and the inside of the ring. At maximum pull, the tension acts vertically. If we continue lowering the liquid, the force will decrease slightly before the lamella break because the lamella continue to stretch so that the tension no longer acts vertically (see Figure 4.4).

Figure 4.4 Tension acts vertically at maximum pull on the du Noüy ring

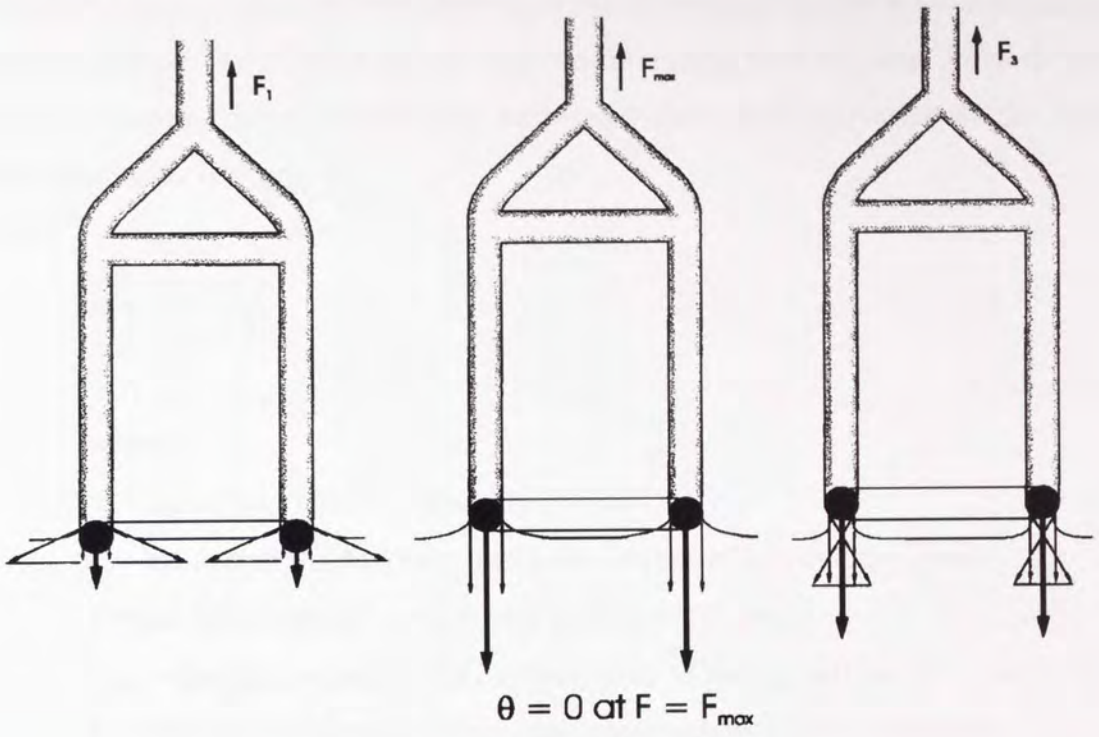

Figure 4.5 Determining maximum pull on the du Noüy ring

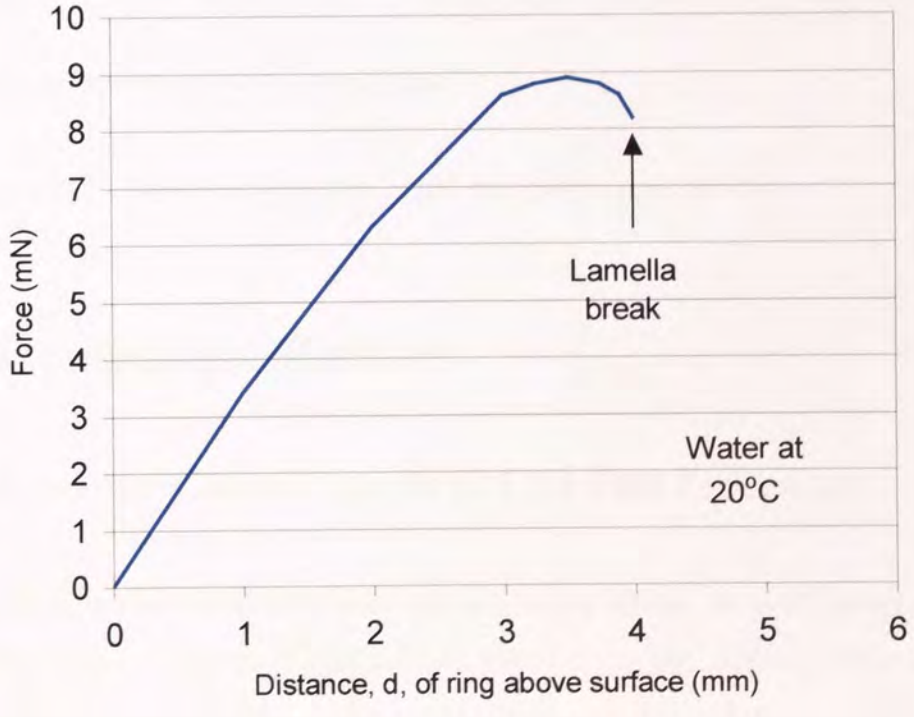

$\theta = 0$ at $F = F_{max}$

At the maximum pull, a volume element of liquid hanging directly beneath the ring is being weighed. This liquid weight must be subtracted from the total force to yield surface tension. Some error is also introduced from slight curvature of the liquid interface inside the ring.

$$\sigma = \frac{F_{max} - F_V}{L \cos \theta} \qquad (4.5)$$

where:

σ = the surface tension (dynes/cm) (or mN/m)

L = the wetted length (outer plus inner circumference of ring) (mm)

θ = the contact angle between ring and liquid (degrees)

F_{max} = the maximum force at the ring detected during pull out of liquid (mN)

F_V = the force of liquid volume withdrawn underneath the wire (mN)

and

$$F_V = gV (\rho_L - \rho_A) \qquad (4.6)$$

g = acceleration due to gravity (ms^{-2})

ρ_L and ρ_A are densities of the liquid and gas phases (gm^{-3})

4.2 Materials and Methods

4.2.1 Dynamic Contact Angle (DCA) Test Procedure

Samples of hydrated membrane were cut into strips 3.3mm in width using a sample cutter (Ray Ran, Nuneaton, England) and tested using the dipping surface balance (White Electrical Instrument Company Ltd, Worcestershire, England. Model No. DB 2kS) equipped with a micropositioner (Ealing Electro-Optics, Watford, England).

One end of the gel was secured to a teflon coated crocodile clip and suspended from the electrobalance. A fishing hook (size 22) and lead shot (No 6) were attached to the other end of the gel in order to maintain the strip in a straightened condition. The weight was tared and the gel was slowly lowered into 20 ml of HPLC grade water (Fisher Chemicals), or other test solution. The test strip was then lowered and raised five times to a depth of 7 mm and at a rate of 0.1 mm s^{-1}. A computer program developed in-house (Dipsurf) was used to plot immersion depth against the force which by use of equation 4.1 gives the advancing angle (θ_A) when the gel is immersed and the receding angle (θ_R) when the gel is removed from the water. The difference between the advancing and receding angles (the hysteresis) gives an approximation of the wettability of the gel.

Figure 4.6 Schematic diagram of the dynamic contact angle analyser

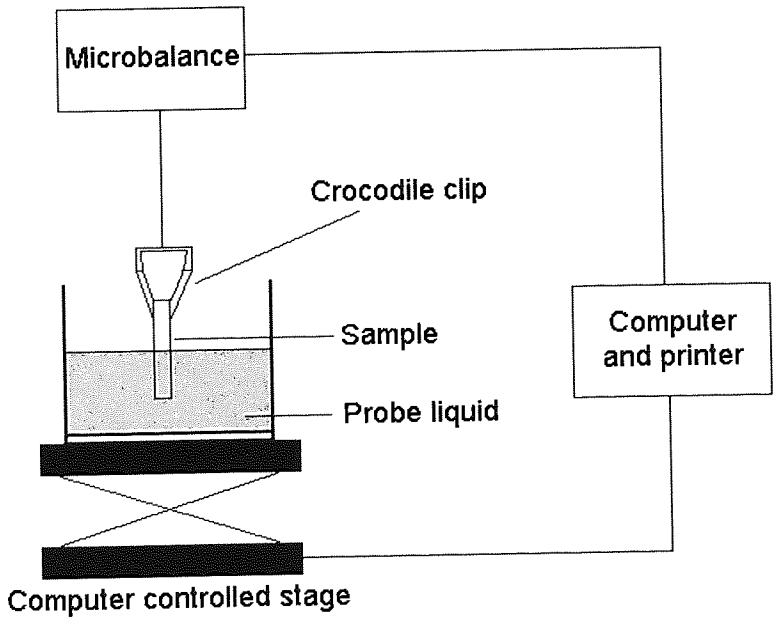

4.2.2 Static Surface Tension – The du Noüy Ring Technique

All surface tension measurements were carried out with a digital tensiometer (White Electrical Instrument Company Ltd, Worcestershire, England. Model No. DB 2kS) using approximately 20ml of sample liquid for each determination.

The platinum/iridium du Noüy ring was cleaned with a gas flame prior to each measurement to remove contaminants. The ring was then suspended horizontally from the balance about 5mm into the solution and the reading was tared. Finally, the solution was lowered slowly so that the du Noüy ring reached and went beyond the normal surface level of the solution. Care was taken to record only the maximum value displayed by the instrument; further movement of the du Noüy ring was then stopped in order to prevent the ring from breaking through the air/liquid surface. This procedure was carried out to minimise disturbance to any lamellar structures formed at the surface of the solution, and hence, to increase the accuracy of the experiment. An average of 5 consistent measurements was recorded for each test material.

Figure 4.7 Example of chart produced by Dipsurf program

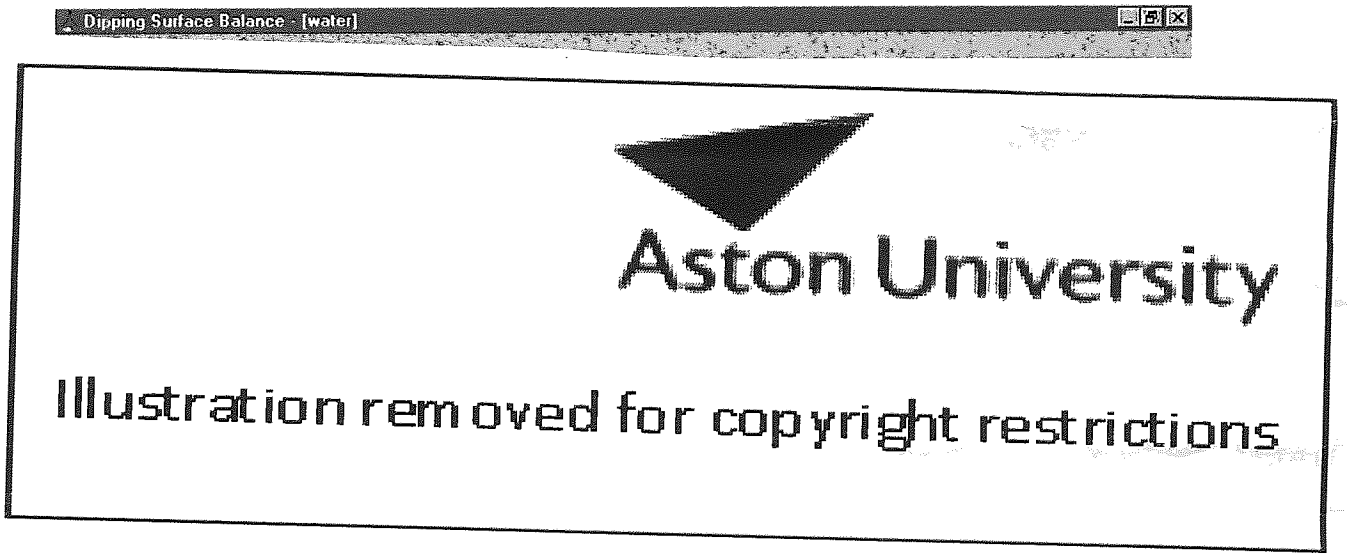

4.2.3 Tensile Testing

Tensile testing was carried out on a small number of hydrogel samples in order to substantiate the theory that hydrogen bonds are present in the hydrogels described in this thesis. A Hounsfield HK10KN universal testing machine in conjunction with an

IBM 55SX computer was used to test the mechanical properties of samples. This equipment calculated the Young's modulus (E), tensile strength at break (σ_b), and elongation to break (ε_b), after the dimensional values of polymer length (8.0mm), width (3.3mm), and thickness were entered into the computer program.

Figure 4.8 Dimensions of a hydrogel sample for mechanical testing

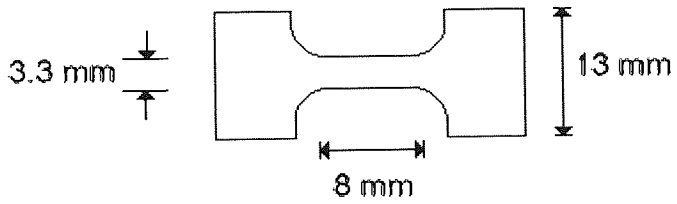

Samples of polymer from a membrane sheet were cut using a 'dog bone' cutting jig giving constant length and width, as shown in Figure 4.8. The thickness of each sample was measured using a micrometer. For hydrogel samples a moderate pressure was sufficient to cut a polymer sample. A test speed of 20mm/min was selected for testing the hydrogels. Throughout the testing procedure the hydrogel samples were sprayed with water, which enabled 100% humidity to be maintained throughout the test. All samples were tested at room temperature and atmospheric pressure. An average from at least five sets of results was obtained for each sample.

The following equations are used to calculate mechanical properties:-

$$E = \sigma/\varepsilon \qquad (4.7)$$

where: Stress (σ) = load / cross-sectional area

Strain (ε) = extension of gauge length / original gauge length

Stress at break (σ_b) = load at break / cross-sectional area

Elongation at break (ε_b) (%) = extension of gauge length / original gauge length x 100

Figure 4.9 An example of a stress-strain curve obtained from the tensometer

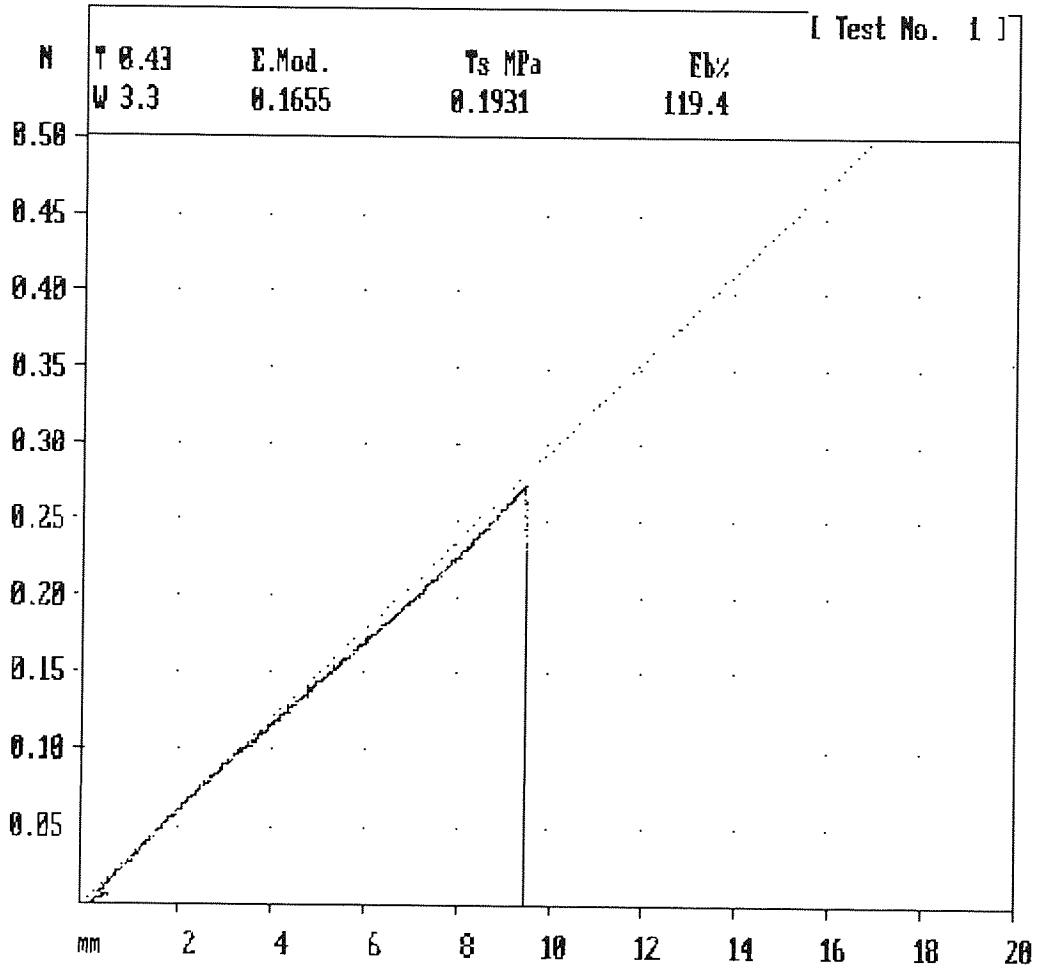

4.3 Results

4.3.1 Water

The liquid normally used as the test solution is HPLC grade water. The high surface tension of pure water (72.8 mN/m) allows impurities to be easily detected. For example, if the test material were to contain unreacted monomer, it would leach out of the sample into the water and significantly reduce the surface tension of the test solution. This is because the surface tension of pure water is readily reduced by the presence of contaminants.

The HPLC grade water was found to have a pH of 6.0 and a surface tension of 72.2 mN/m. This value was unaffected by the hydrogels during testing. Recently single distilled water was found to have a pH of 4.6 and a surface tension of 71.6 mN/m.

4.3.1.1 The effect of increasing or decreasing hydrophilic monomer

Figure 4.10 The advancing and receding angles and hysteresis of NVP/MMA copolymers of increasing water content, with water as the test solution

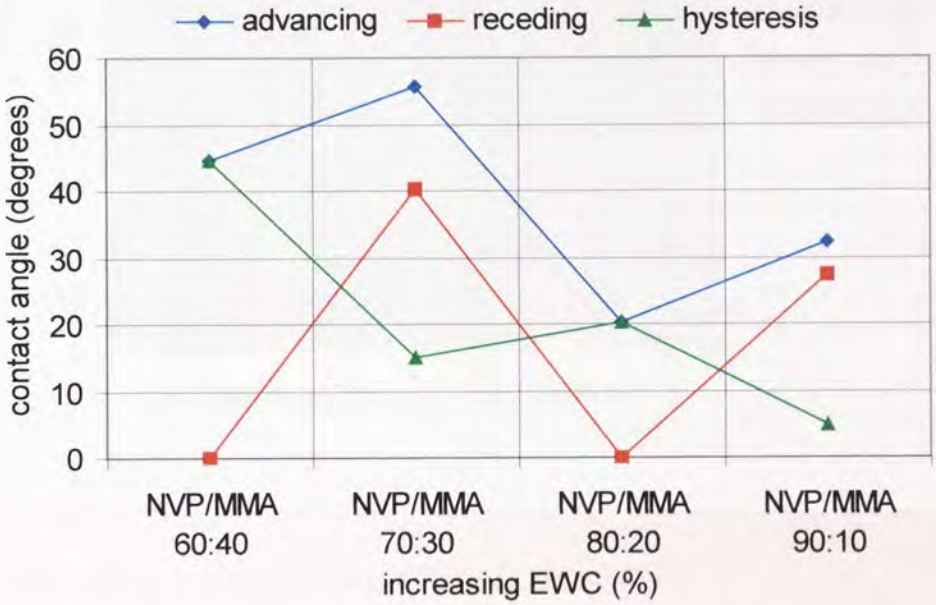

Figure 4.10 shows that with increasing EWC there is a reduction in the hysteresis recorded for this series of materials. This indicates that as EWC increases the materials become more wettable. However, when the advancing and receding angles are considered there is no clearly visible trend. This may be due to the fact that NVP/MMA copolymers are blocky in structure due to the contrasting reactivity ratios of their monomer constituents, as discussed in Chapter 2. Therefore, the surface of the sample is not completely homogeneous, resulting in variations in the contact angles measured. This observation on the consistency of results is studied in more detail in section 4.3.7

The two low EWC materials tested (NVP/MMA 25:75 and AMO/MMA 25:75) have much higher advancing contact angles than the higher water content materials (see Figure 4.11). Hysteresis values are also higher indicating more mobile surface groups. The AMO copolymer is less wettable than the NVP copolymer despite

having a higher water content (18% instead of 14%). This is an unexpected result because AMO contains more polar groups than does NVP.

Figure 4.11 The advancing and receding angles and hysteresis of the NVP/MMA 25:75 and the AMO/MMA 25:75 copolymers, with water as the test solution

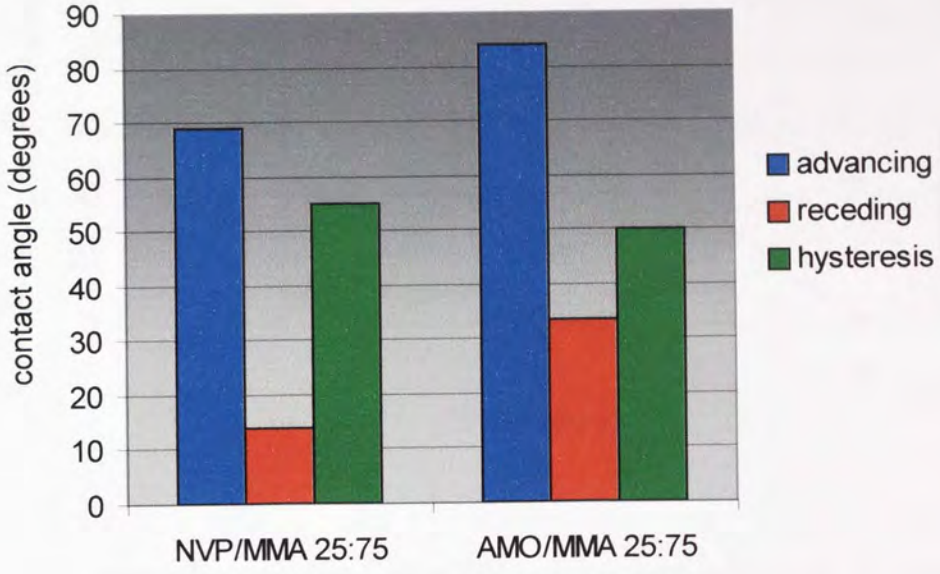

4.3.1.2 The effect of increasing cationic monomer

To enable the effect of ionic monomer to be studied, the NVP/MMA copolymer at 80:20 composition was used as the base material. NVI or DEAEMA was added at concentrations of 2, 5, 7 and 10%.

Figure 4.12 The advancing and receding angles and hysteresis of NVP/MMA copolymers containing increasing amounts of NVI, with water as the test solution

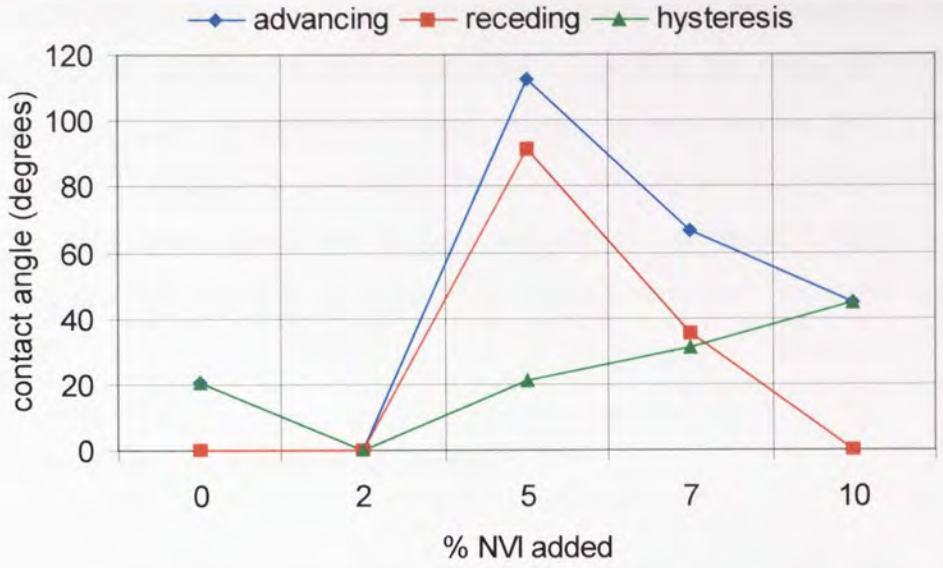

Figure 4.13 The advancing and receding angles and hysteresis of NVP/MMA copolymers containing increasing amounts of DEAEMA, with water as the test solution

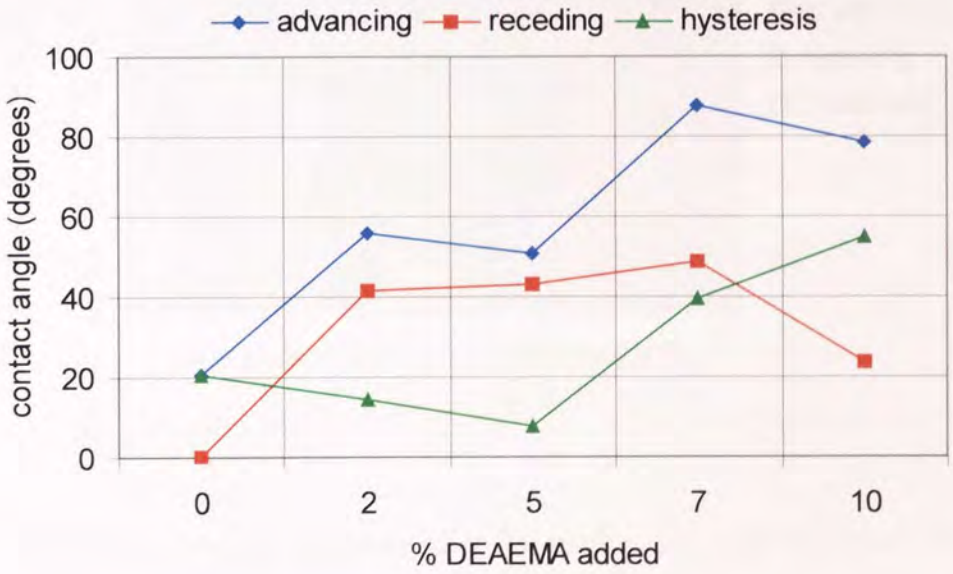

It can be seen in Figures 4.12 and 4.13 that there is no specific change in the hysteresis values when NVI or DEAEMA is incorporated into the NVP/MMA copolymer, though there seems to be an increase at high concentrations of NVI. Both

NVI and DEAEMA contain bulky side groups but these groups do not seem to affect the mobility around the backbone chain, as shown by the increasing hysteresis values.

Again, the blocky structure of these copolymers leads to a heterogeneous surface, accounting for the variation in values observed. However, the range of variation is much greater for these polymers containing cationic groups than for the NVP/MMA polymer alone. This can be explained by the patchy distribution of NVI or DEAEMA moieties in the polymer chain seen in the computer simulations in Chapter 2. From Chapter 3 it can be seen that an increase in cationic monomer increases the water contact angle.

4.3.1.3 The effect of anionic monomer

Figure 4.14 The advancing and receding angles and hysteresis of the NVP/MMA/MAA 79.75:19.75:0.5 copolymer, with water as the test solution

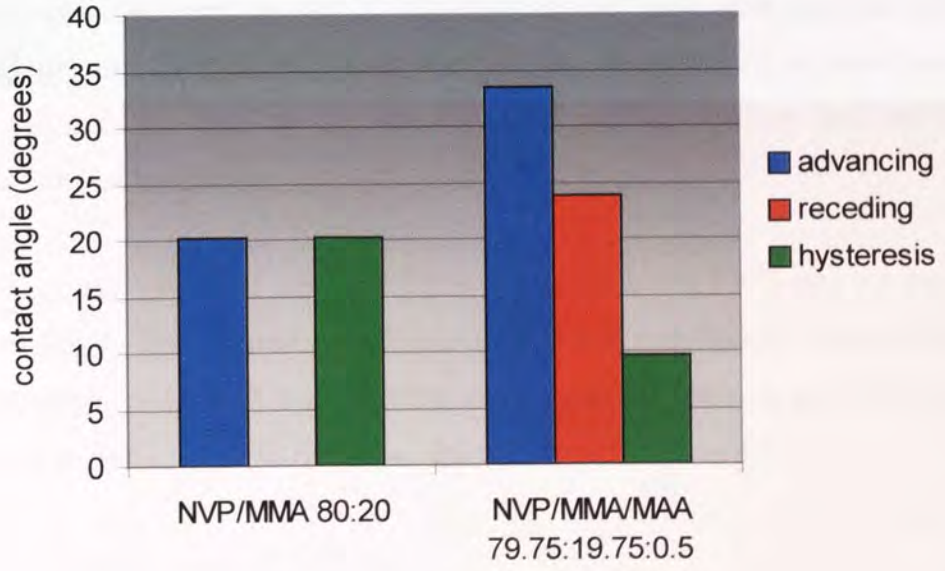

Figure 4.14 shows that the addition of 0.5% methacrylic acid increases both the advancing and receding contact angles and reduces the hysteresis, implying that the hydrogel is less wettable with less mobile surface groups. The introduction of the acidic monomer was expected to increase wettability. A possible explanation is the heterogeneous surface due to the blocky structure of these copolymers, as mentioned previously.

4.3.2 Foetal Calf Serum

To model more closely the interactions between hydrogel biomaterials and the environments in which they are placed, it was decided to experiment with foetal calf serum (FCS) as the probe liquid. It was hoped that such a biological fluid would modify the surface of the polymers in a similar way to the cells and extracellular materials in a biological environment. In this way, a predictive technique for assessing cell adhesiveness may be developed.

In addition, small changes in the surface properties of these materials may not be detectable when the hydrogels are tested in water, but may be visible when FCS is employed.

The FCS behaves as a surfactant (surface active agent) because it contains adhesive proteins, thus adsorbing readily onto the surface of a hydrogel providing the surface is not too mobile. Any surface with an adsorbed layer of surfactant material, where the surfactant possesses a shell of water molecules associated with its exposed polar head groups will not be subject to the same levels of surface mobility and will thereby exhibit a reduced hysteresis.

FCS was added to water at concentrations of 1%, 10% and 100% and the results are discussed below. The addition of FCS had the effect of reducing the surface tension of the test solution. At 1% FCS the surface tension was 63.2 mN/m, at 10% it was 58.6 mN/m and at 100% it was 53.6 mN/m., the pH of the FCS was 7.5

4.3.2.1 1% FCS

4.3.2.1.1 The effect of increasing or decreasing hydrophilic monomer

Figure 4.15 The advancing and receding angles and hysteresis of NVP/MMA copolymers of increasing water content, with 1% FCS as the test solution

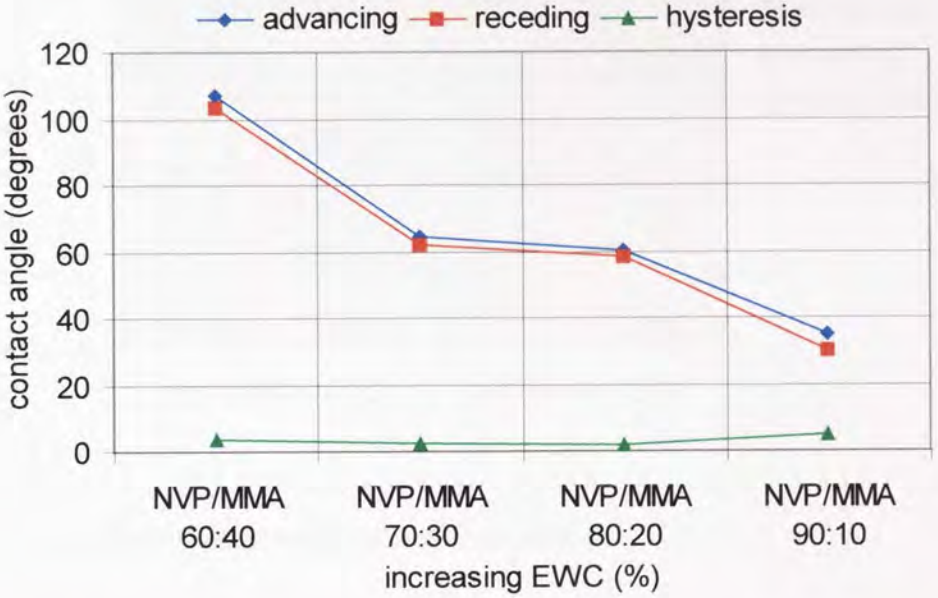

Figure 4.15 shows that when the materials were dipped into 1% FCS, the hysteresis remains around the same value and is not affected by equilibrium water content. This implies that the mobility of the side groups is neither increased nor decreased as EWC increases. The very low values for the hysteresis suggest that when the hydrogels come into contact with the serum, the side groups rotate very rapidly so that the materials are wetted by the serum. However, there is a more consistent fall in values of advancing and receding contact angles than for dipping into pure water. This suggests that the higher water content hydrogels are initially more wettable than the lower water content materials, as would be expected. Higher water content materials have a higher degree of swelling thus the adhesion sites are more easily accessible to biological proteins, in this case, the proteins found in the foetal calf serum.

The low water content polymers have much lower dynamic contact angles than the higher water content hydrogels when 1% FCS is used as the test solution (Figure 4.16). This is most likely due to a higher rate of protein deposition on the materials with lower EWC since they are more hydrophobic

Figure 4.16 The advancing and receding angles and hysteresis of the NVP/MMA 25:75 and the AMO/MMA 25:75 copolymers, with 1% FCS as the test solution

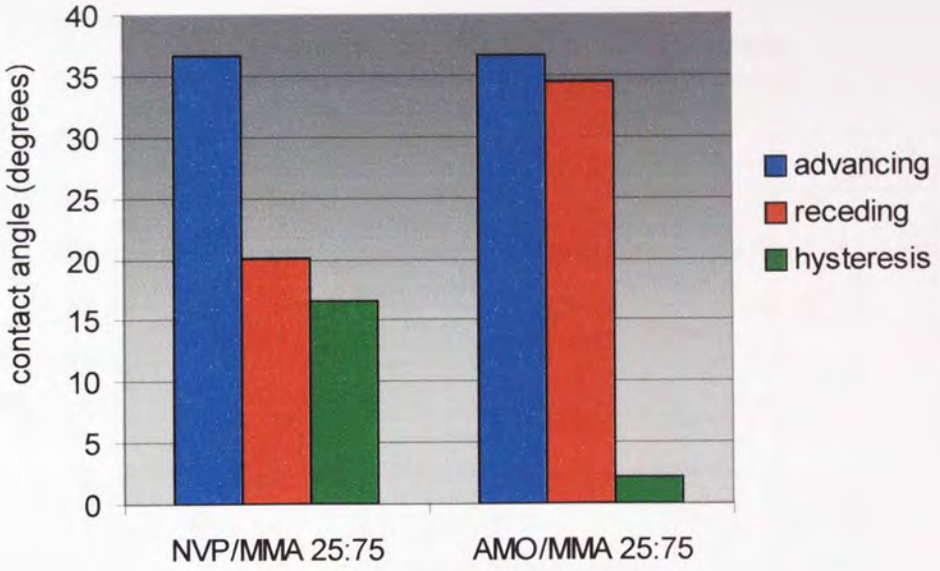

4.3.2.1.2 The effect of increasing cationic monomer

Figure 4.17 The advancing and receding angles and hysteresis of NVP/MMA copolymers containing increasing amounts of NVI, with 1% FCS as the test solution

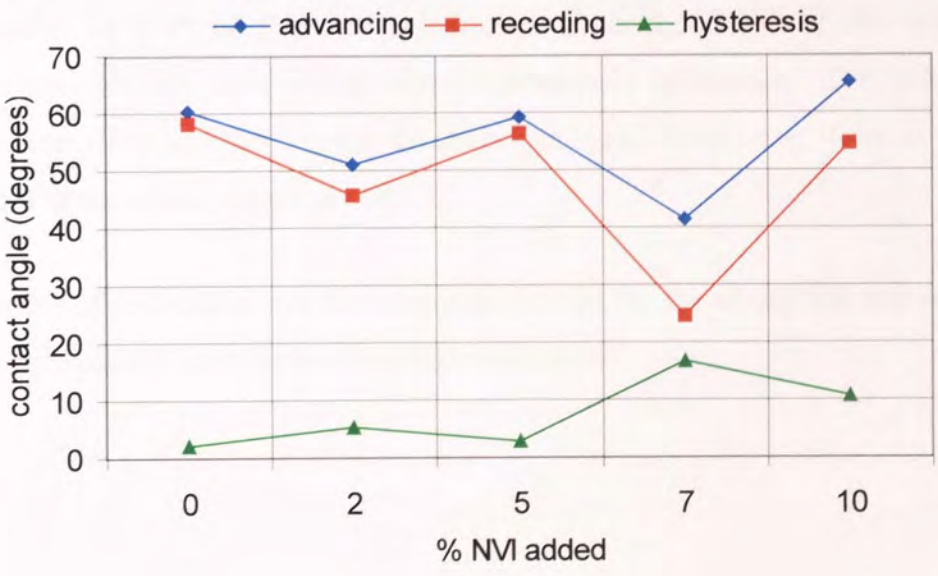

Figure 4.18 The advancing and receding angles and hysteresis of NVP/MMA copolymers containing increasing amounts of DEAEMA, with 1% FCS as the test solution

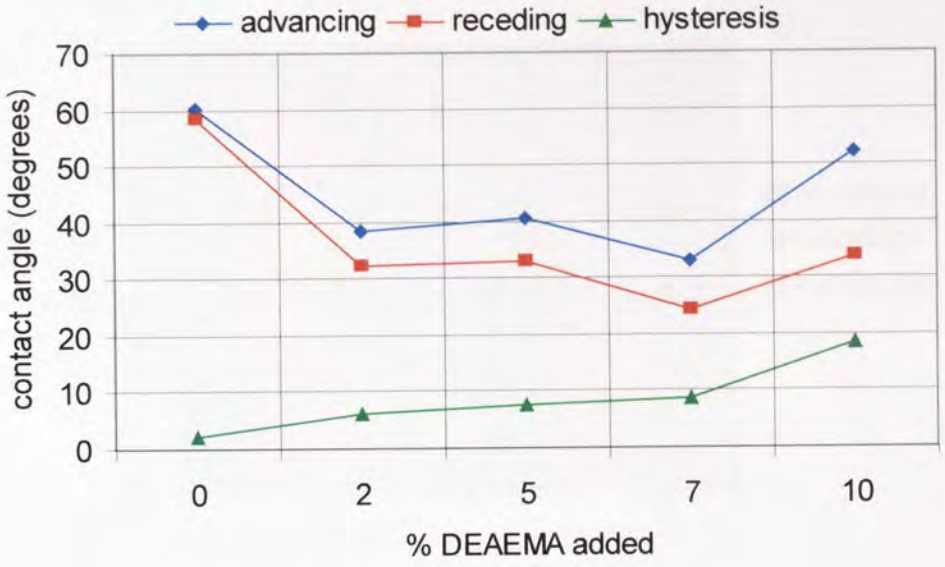

From Figures 4.17 and 4.18 it can be seen that when using 1% FCS as the test liquid, as the proportion of cationic monomer is increased in the test sample the dynamic contact angle hysteresis increases with a clearer trend than when water is used as the test liquid. This implies that the side groups become more mobile as the concentration of NVI or DEAEMA increases since the EWC of the polymers increases very slightly; this would tend to reduce the hysteresis. The bulky side groups do not affect mobility around the chains, as found when using water as the test solution. There could also be a pH effect.

In this series of increasing cationic monomer, values for the advancing and receding contact angles do not show a clearly recognisable trend.

4.3.2.1.3 The effect of anionic monomer

Figure 4.19 The advancing and receding angles and hysteresis of the NVP/MMA/MAA 79.75:19.75:0.5 copolymer, with 1% FCS as the test solution

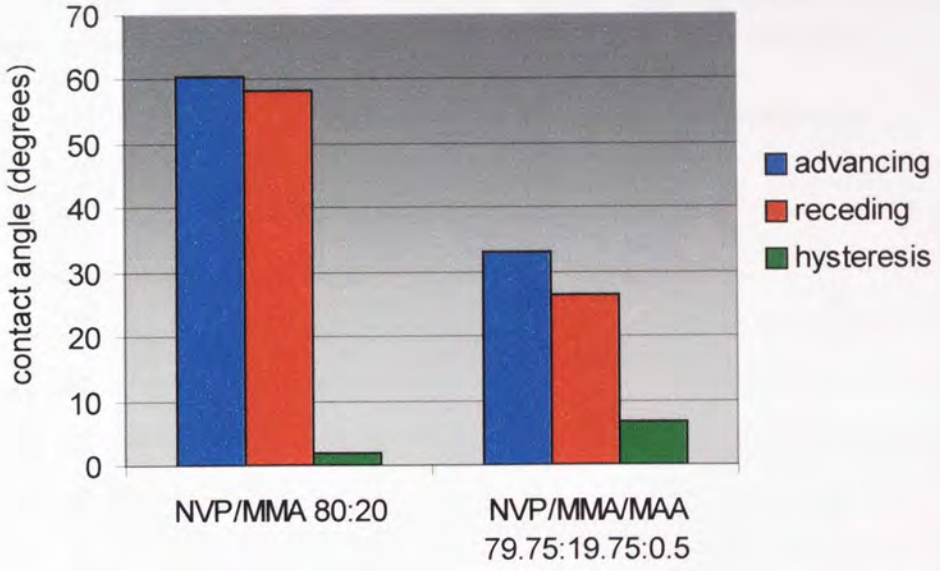

The addition of 0.5% methacrylic acid reduces the advancing and receding contact angles and increases the hysteresis when 1% FCS is used as the test solution. The negatively charged components of the foetal calf serum do not adsorb rapidly to the acidic groups and there may be a repulsion effect, thereby increasing mobility. A slightly higher EWC may also contribute to the increased wettability, and the network will be more expanded at the higher EWC accounting for the increased mobility.

4.3.2.2 10% FCS

4.3.2.2.1 The effect of increasing or decreasing hydrophilic monomer

Figure 4.20 The advancing and receding angles and hysteresis of NVP/MMA copolymers of increasing water content, with 10% FCS as the test solution

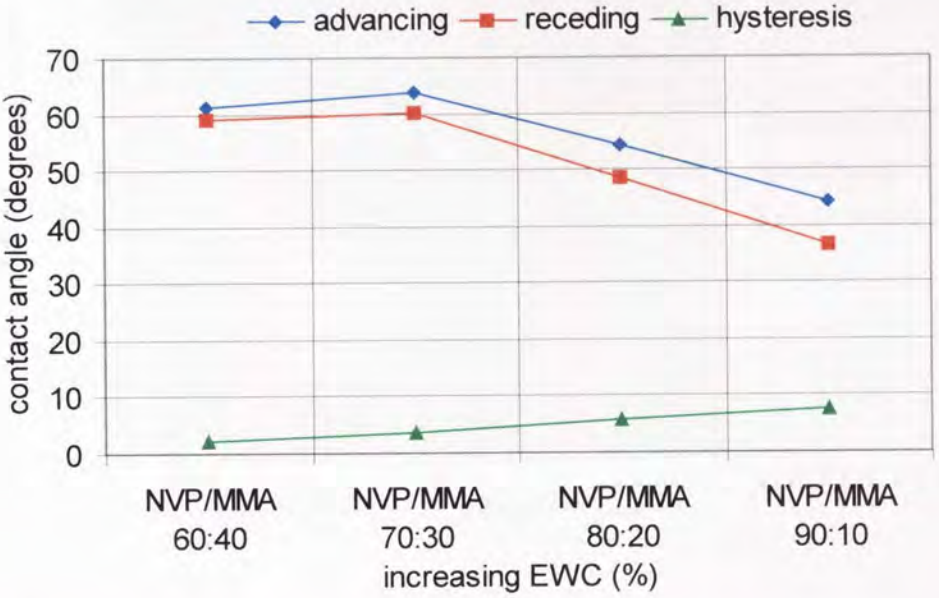

Figure 4.20 shows that when the materials were dipped into 10% FCS, the hysteresis increases slightly with increasing EWC. This could be due to an excess of FCS which cannot attach strongly to the polymer and falls back into the solution on emmersion. Higher water content hydrogels may not be so able to hold on to adsorbed protein due to the mobility of the surface caused by the amount of water present rather than rotation about the backbone chain. There was little change in the surface tension of the dipping solution from the start to the end of each test. This means that only a small proportion of the serum constituents had adhered to the hydrogel sample during the test. The advancing and receding contact angles are lower at the higher water contents, following the trend seen earlier with 1% FCS as the dipping solution: the higher water contents produce more swollen networks which are more easily accessible to serum proteins.

The low water content materials have lower advancing and receding contact angles, but higher hysteresis (Figure 4.21) than the hydrogels of higher EWC. As is the case

for the 1% FCS test solution, this is most likely due to a higher rate of protein deposition on the materials with lower EWC since they are more hydrophobic.

Figure 4.21 The advancing and receding angles and hysteresis of the NVP/MMA 25:75 and the AMO/MMA 25:75 copolymers, with 10% FCS as the test solution

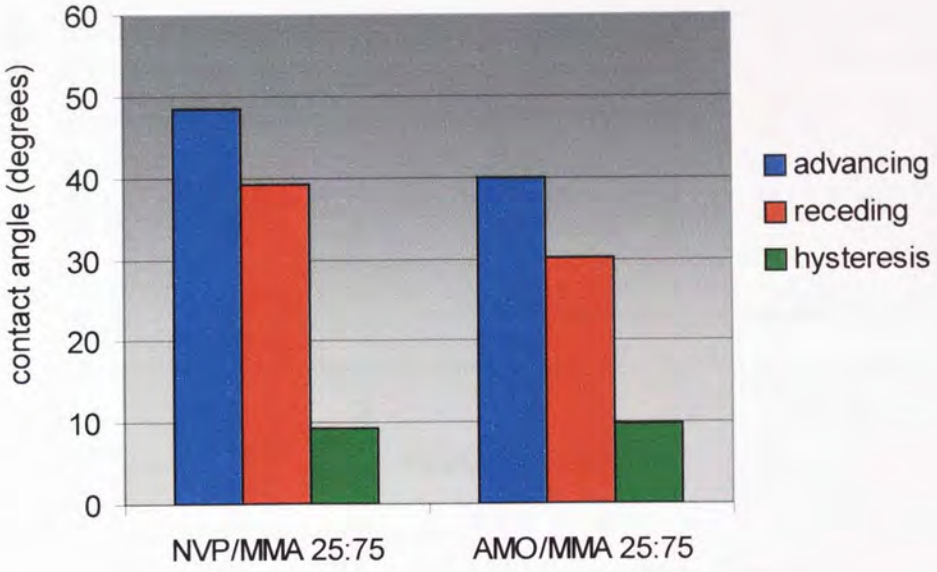

4.3.2.2.2 The effect of increasing cationic monomer

Figure 4.22 The advancing and receding angles and hysteresis of NVP/MMA copolymers containing increasing amounts of NVI, with 10% FCS as the test solution

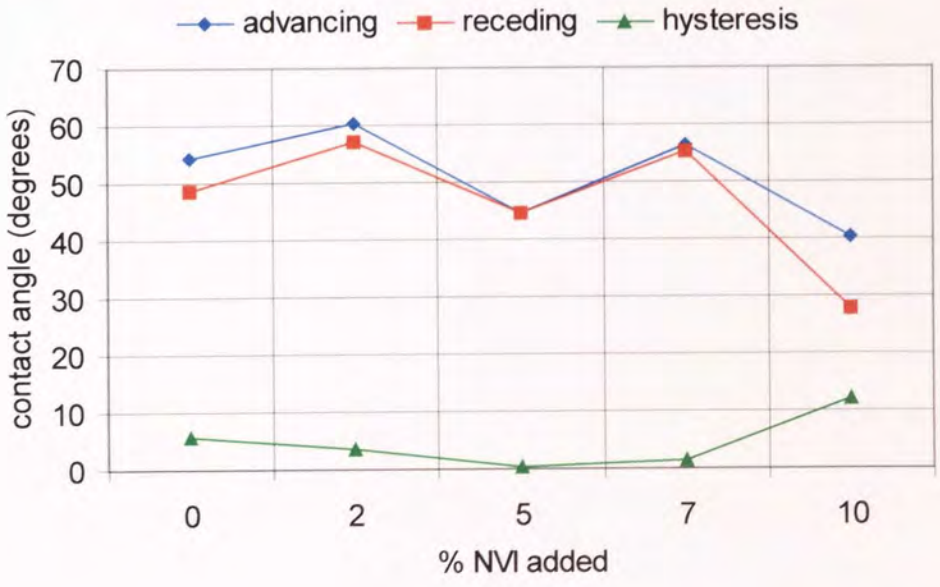

Figure 4.23 The advancing and receding angles and hysteresis of NVP/MMA copolymers containing increasing amounts of DEAEMA, with 10% FCS as the test solution

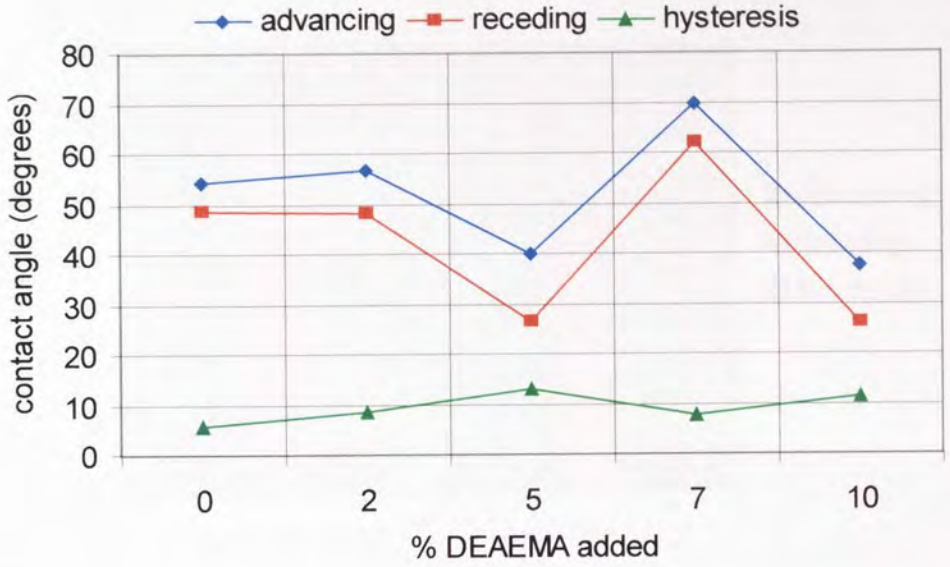

From Figures 4.22 and 4.23 it can be seen that for 10% FCS as the test liquid, there is no clearly identifiable trend as the proportion of cationic monomer is increased. This could be due to an excess of FCS, the uneven sequence distribution within the polymer, or a combination of factors.

4.3.2.2.3 The effect of anionic monomer

Figure 4.24 The advancing and receding angles and hysteresis of the NVP/MMA/MAA 79.75:19.75:0.5 copolymer, with 10% FCS as the test solution

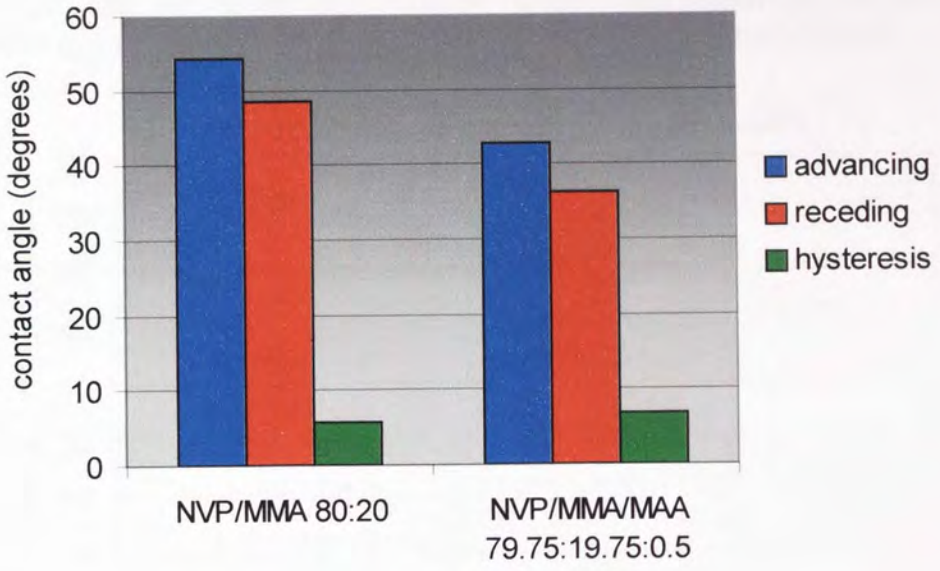

The addition of 0.5% methacrylic acid reduces the advancing and receding contact angles and increases the hysteresis when 10% FCS is used as the test solution, though the effect is smaller than for 1% FCS, probably due to an excess of FCS.

4.3.2.3 100% FCS

4.3.2.3.1 The effect of increasing or decreasing hydrophilic monomer

Figure 4.25 The advancing and receding angles and hysteresis of NVP/MMA copolymers of increasing water content, with 100% FCS as the test solution

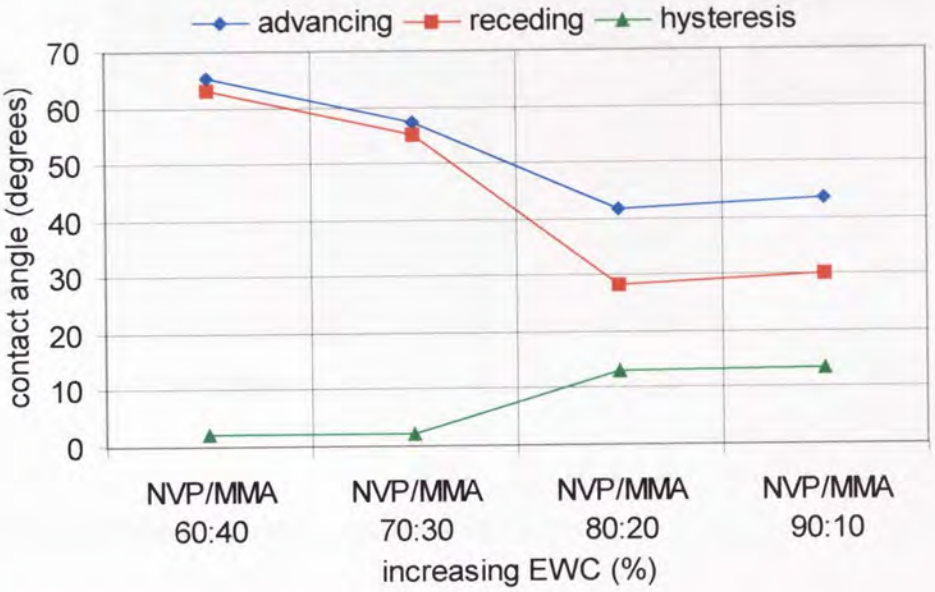

Figure 4.25 shows that when the materials were dipped into 100% FCS, the hysteresis increases with increasing EWC, implying increased mobility. As in the case of 10% FCS, this could be due to an excess of FCS which cannot attach strongly to the polymer and falls back into solution on emmersion. The advancing and receding contact angles appear to fall with increasing water content, except from 75% to 84% when there is a slight increase. The fall in values can be explained by increased mobility of the surface, which reaches a maximum at 75% EWC.

The low water content materials have lower advancing and receding contact angles, but higher hysteresis (Figure 4.26) than the hydrogels of higher EWC when 100% FCS is used as the test solution. This is the same trend as that seen with the 1% and 10% FCS test solutions.

Figure 4.26 The advancing and receding angles and hysteresis of the NVP/MMA 25:75 and the AMO/MMA 25:75 copolymers, with 100% FCS as the test solution

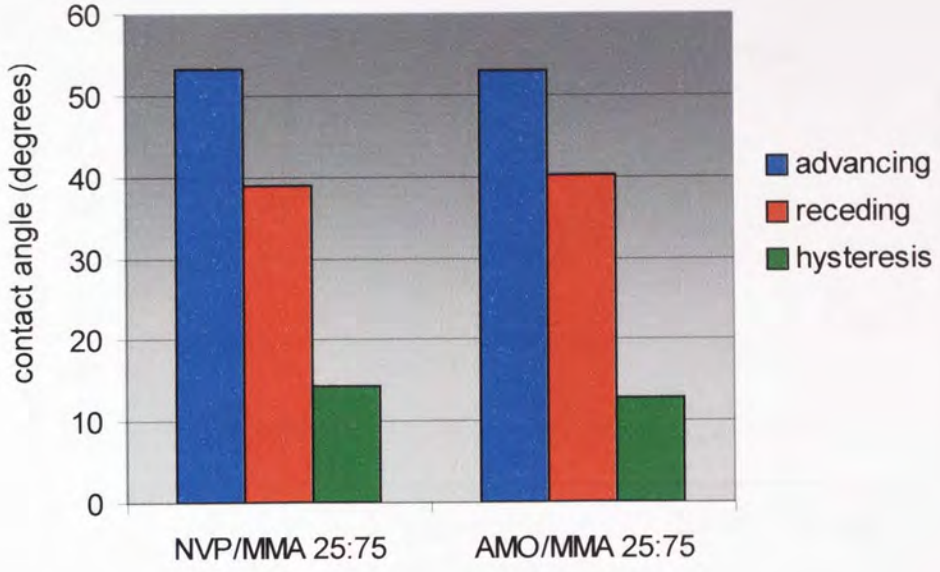

4.3.2.3.2 The effect of increasing cationic monomer

Figure 4.27 The advancing and receding angles and hysteresis of NVP/MMA copolymers containing increasing amounts of NVI, with 100% FCS as the test solution

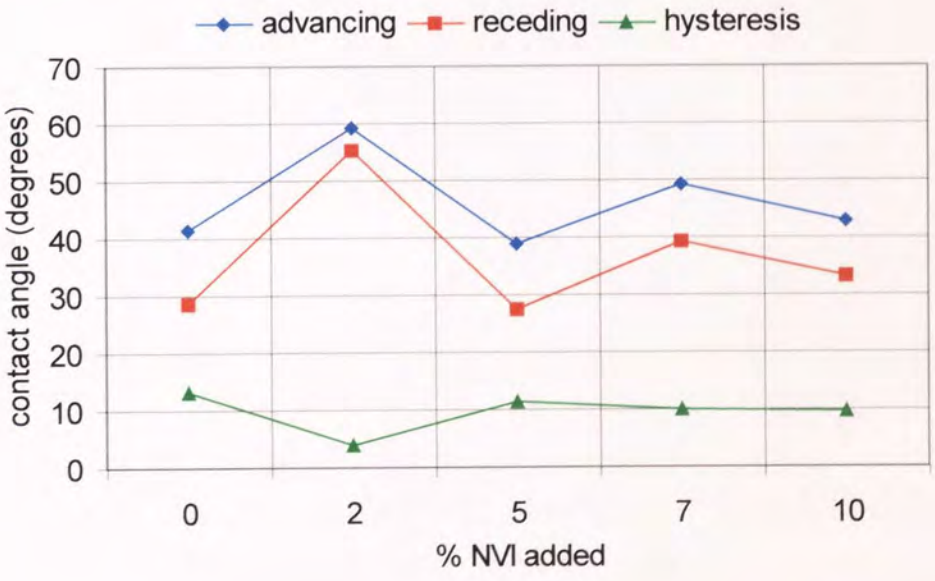

Figure 4.28 The advancing and receding angles and hysteresis of NVP/MMA copolymers containing increasing amounts of DEAEMA, with 100% FCS as the test solution

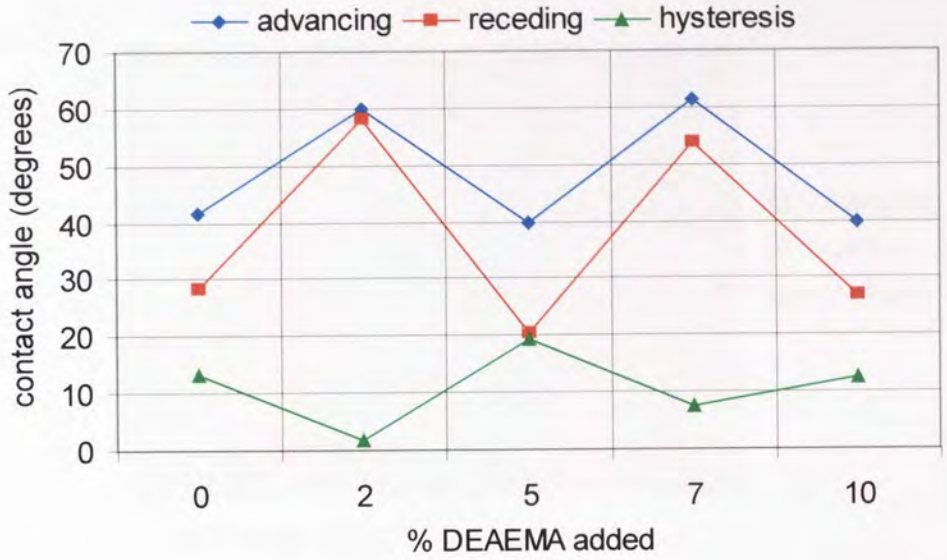

Figures 4.27 and 4.28 show no clearly identifiable trends for increasing cationic component when 100% FCS is used as the test liquid. This could be due to an excess of FCS, the uneven sequence distribution within the polymer, or a combination of factors.

4.3.2.3.3 The effect of anionic monomer

Figure 4.29 The advancing and receding angles and hysteresis of the NVP/MMA/MAA 79.75:19.75:0.5 copolymer, with 100% FCS as the test solution

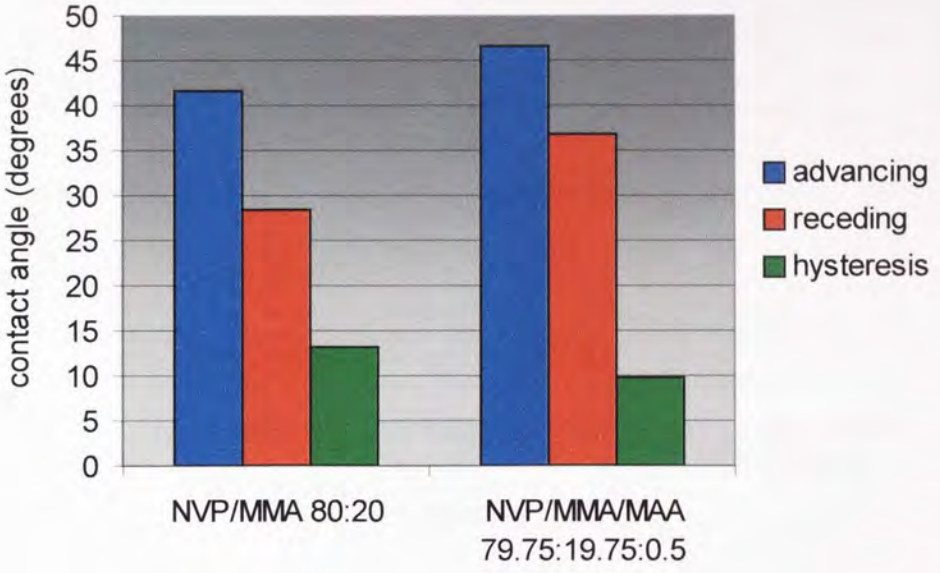

Figure 4.29 shows that the addition of 0.5% methacrylic acid increases the advancing and receding contact angles and reduces the hysteresis when 100% FCS is used as the test solution. This apparent difference compared with the 1% and 10% FCS solutions may be due to the blocky structure of these polymers or an excess of FCS which could mask the effect of the acidic group.

4.3.3 n-Octane

NVP/MMA copolymers of increasing water content were also tested using n-octane as the probe solution. It would be expected that when dipped into a hydrophobic liquid the surface groups reorientate so that the hydrophilic groups are positioned towards the polymer bulk and the hydrophobic groups are positioned towards the surface of the hydrogel. It was hoped that this would show a clearer trend than when dipping into water. Dehydrated material samples were soaked in n-octane for 3 days prior to testing to equilibrate.

Figure 4.30 The advancing and receding angles and hysteresis of NVP/MMA copolymers of increasing EWC, with n-octane as the test solution

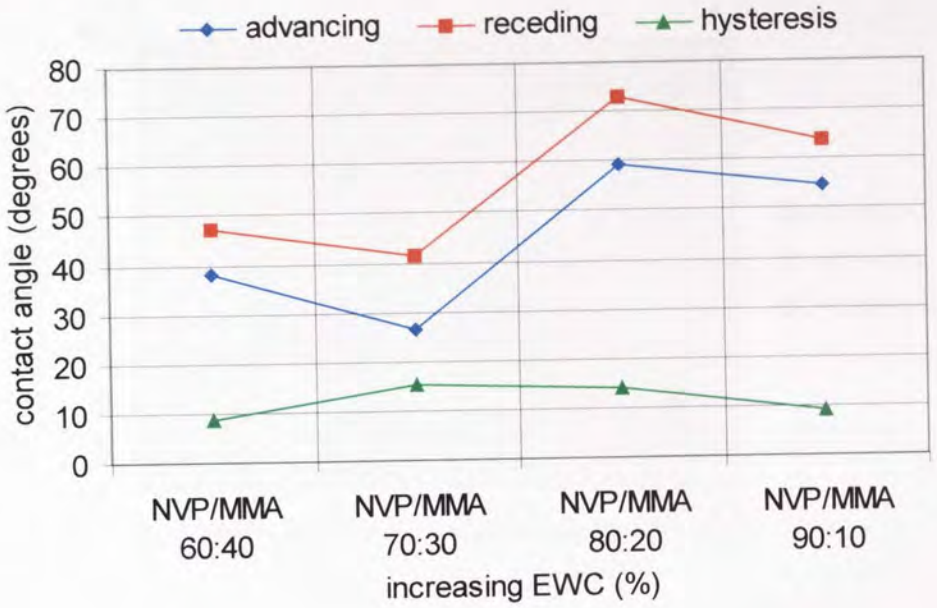

Figure 4.30 shows that there is no recognisable trend when the materials are dipped into n-octane.

4.3.4 Methanol

Hydrogels swell when placed in alcohols due to the high affinity of alcohol for the polar groups in the polymer. The NVP/MMA 60:40 material was the only hydrogel studied which was sufficiently strong, after soaking in methanol for 3 days, to be tested.

The advancing and receding angles were found to be 42.5 and 31.8 respectively, thus giving a hysteresis of 10.7. This compares with an advancing angle of 45° and a receding angle of 0°, giving a hysteresis of 45° when dipped into water.

Figure 4.31 The advancing and receding angles and hysteresis of the NVP/MMA 60:40 copolymer, with methanol as the test solution

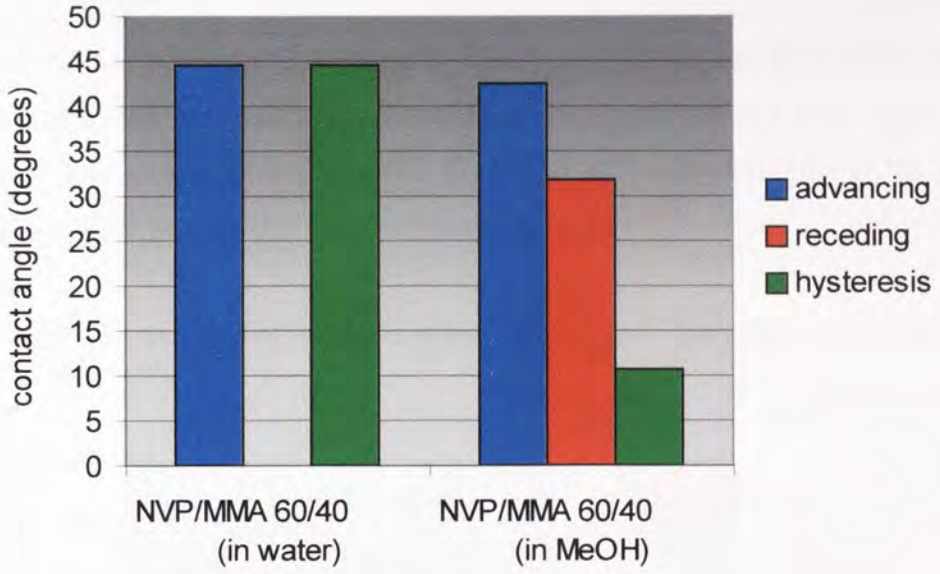

Figure 4.31 shows that when soaked in methanol, the advancing angle is about the same but the receding angle is much increased giving a lower hysteresis, compared with dipping in water. The surface groups are less mobile, possibly due to the deswelling effect when the sample is raised from the methanol.

4.3.5 The Effect of Autoclaving

It is obvious that any biomaterial has to be sterilised before it is implanted in the body so as not to spread infection. Autoclaving is the simplest method of sterilisation but this involves subjecting the materials to a high temperature and pressure. It was thought that this treatment could perhaps modify the polymers in some way, thereby changing the surface properties of the materials.

Hydrogel samples were sterilised for 15 minutes at 115°C and 3 bar in an Astelle Scientific Swiftlock autoclave and were tested using the dipping balance and compared with a control hydrogel which had not been autoclaved.

Preliminary results appeared to indicate that autoclaving the hydrogels rendered the surfaces of these materials much more wettable. It seemed that the surface groups

were being hydrolysed to leave charged species on the surface. If this was correct then it may have been a reversible effect. Also, the EWC would have been increased, though this was not checked at the time.

On repeating the experiment with poly(HEMA) no difference was found between samples which had been autoclaved and samples which had not (see Figure 4.32). Advancing and receding angles were 117° and 40° respectively for the control material, and 119° and 40° for the autoclaved material.

Figure 4.32 The advancing and receding angles and hysteresis of poly(HEMA), before and after autoclaving

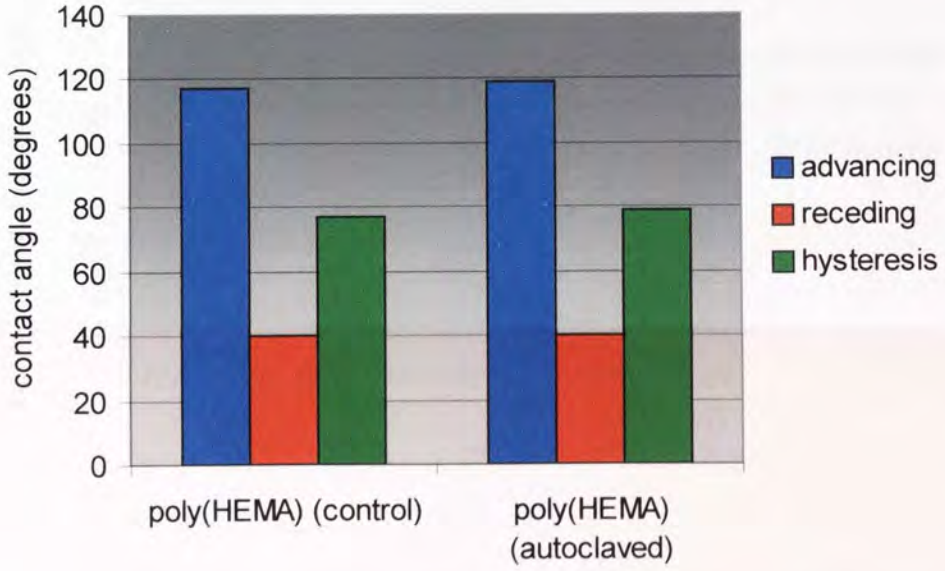

4.3.6 Lithium Bromide

Lithium bromide solutions are known to break hydrogen bonds due to the high charge density of the lithium cation. By using a 10% solution of LiBr as the test solution it should be possible to determine the extent of hydrogen bonding in these materials.

Four materials were tested using the dipping balance; the other available materials were not strong enough to withstand testing. Samples were soaked in lithium bromide for 3 days before testing to reach equilibrium. The surface tension of the test liquid was found to be 64.5 mN/m, which is lower than expected since a salt usually

increases the surface tension of water. The ionic bonds that are formed when salt is dissolved in water create stronger attraction among the water and salt molecules than is present among water molecules in pure water, thereby increasing the surface tension.

Results are shown in Figure 4.33.

Figure 4.33 The advancing and receding angles and hysteresis of NVP copolymers, with lithium bromide as the test solution

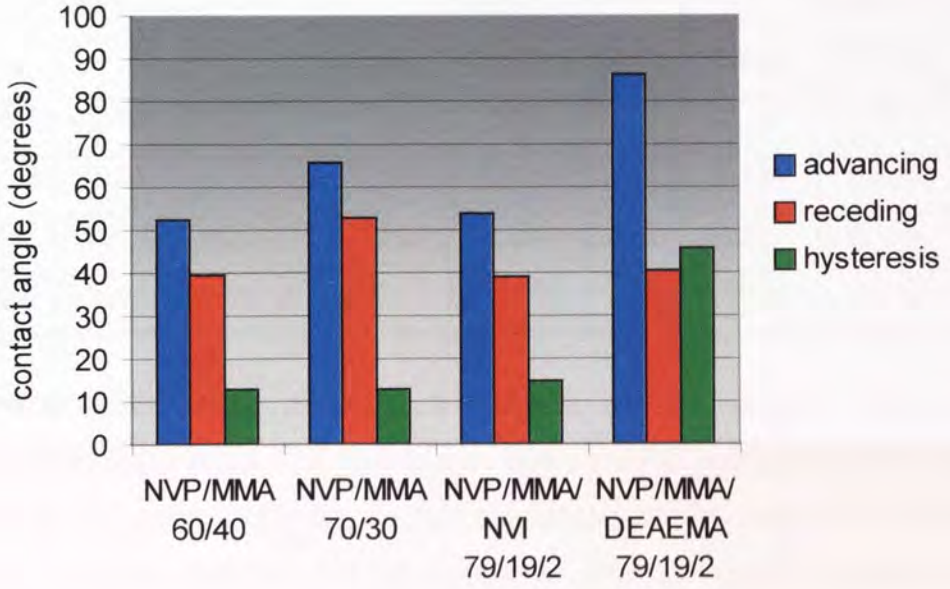

If hydrogen bonding were present in the untreated hydrogels the surface properties would be expected to change when the hydrogen bonds are broken by the lithium bromide. Polar groups would be more accessible and free to interact with the test solution. Surface group mobility would be expected to increase, since hydrogen bonded atoms would have a relatively fixed arrangement, whereas non hydrogen bonded atoms would not.

Hysteresis values obtained for NVP/MMA 60:40, NVP/MMA 70:30 and NVP/MMA/NVI 79:19:2 show that surface mobility has not increased in a solution of lithium bromide. In these 3 materials, therefore, the extent of hydrogen bonding is low. The hysteresis for NVP/MMA/DEAEMA 79:19:2, however, is larger in LiBr than in water, due to a much higher advancing angle and a lower receding angle. This material is initially unwettable with the hydrophilic groups held in the polymer

matrix; the surface groups then rotate so that the hydrophilic groups are positioned towards the surface of the hydrogel.

In order to confirm these findings it was decided to test the mechanical properties of these hydrogels when soaked in either water or lithium bromide. Results are shown below in Table 4.1.

Table 4.1 Table showing the Young's modulus, the tensile strength and the elongation to break of NVP copolymers, soaked in either water or lithium bromide

	water			**LiBr**		
	Emod	Ts Mpa	Eb%	Emod	Ts Mpa	Eb%
NVP/MMA 60/40	3.68	3.30	213	4.86	1.714	88.8
NVP/MMA 70/30	0.569	0.817	169	0.533	0.876	171
NVP/MMA/NVI 79/19/2	0.216	0.200	113	0.329	0.166	68.1
NVP/MMA/DEAEMA 79/19/2	0.0397	0.0892	225	0.00589	0.0163	24.4

The tensile results show that lithium bromide has the greatest effect on the NVP/MMA/DEAEMA 79:19:2 copolymer with an 85% reduction in the Young's modulus, an 82% reduction in the tensile strength, and an 89% reduction in elongation to break. Lithium bromide does not appear to alter the Young's modulus or the tensile strength of the materials with the compositions NVP/MMA 60:40, NVP/MMA 70:30 or NVP/MMA/NVI 79:19:2. Elongation to break is reduced for the NVP/MMA 60:40 and NVP/MMA/NVI 79:19:2 copolymers, though not as considerably as for the NVP/MMA/DEAEMA 79:19:2 copolymer. The latter polymer therefore contains a large number of hydrogen bonds, which is probably due to the strong basic nature of the diethylaminoethyl methacrylate. Even in water, this material is the weakest of the hydrogels tested, due mainly to its higher water content. Although the NVP/MMA/NVI 79:19:2 material has an EWC only slightly below that of the NVP/MMA/DEAEMA 79:19:2 copolymer, it contains a ring structure which adds strength since bulky groups restrict movement of the polymer chains.

4.3.7 Consistency of Results

In section 4.3.1.1 it was suggested that the blocky sequence distribution of NVP/MMA copolymers accounts for the large variation in the results obtained. This section describes the advancing and receding contact angles of 5 samples cut from the same membrane. Poly(HEMA) is used as a comparison and tests were conducted both using water and using 1% FCS as the test solution.

Figure 4.34 The advancing and receding angles and hysteresis of poly(HEMA) with water as the test solution

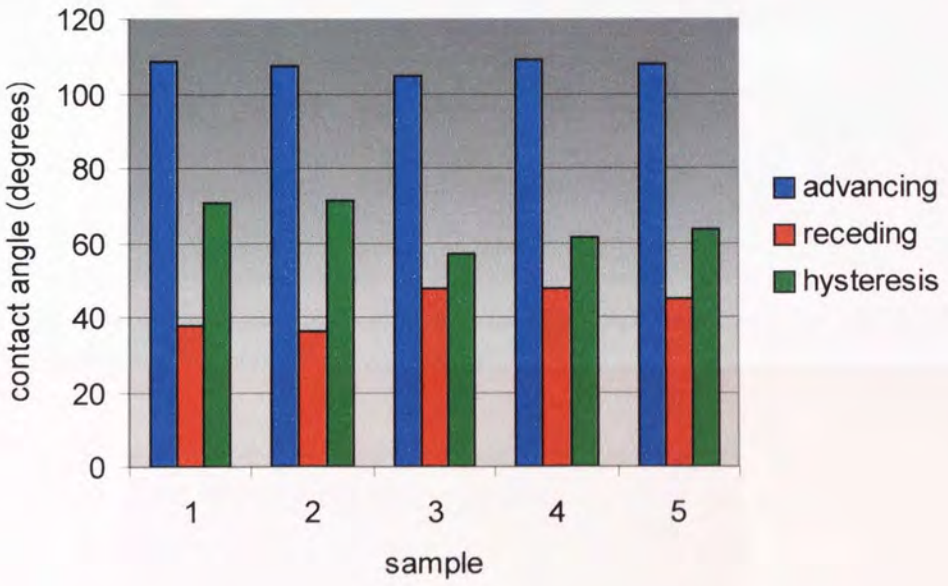

Figure 4.35 The advancing and receding angles and hysteresis of poly(HEMA) with 1% FCS as the test solution

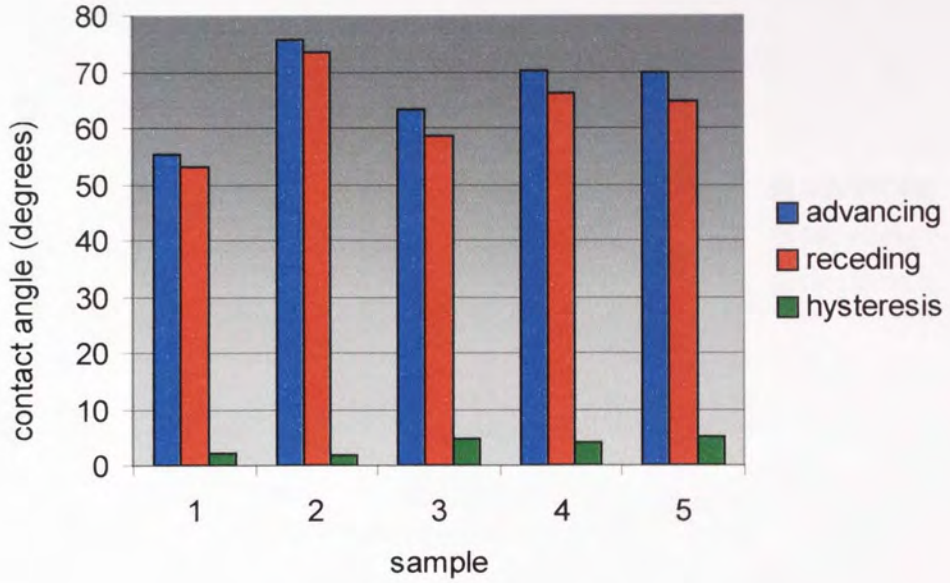

Figure 4.36 The advancing and receding angles and hysteresis of the NVP/MMA 70:30 copolymer with water as the test solution

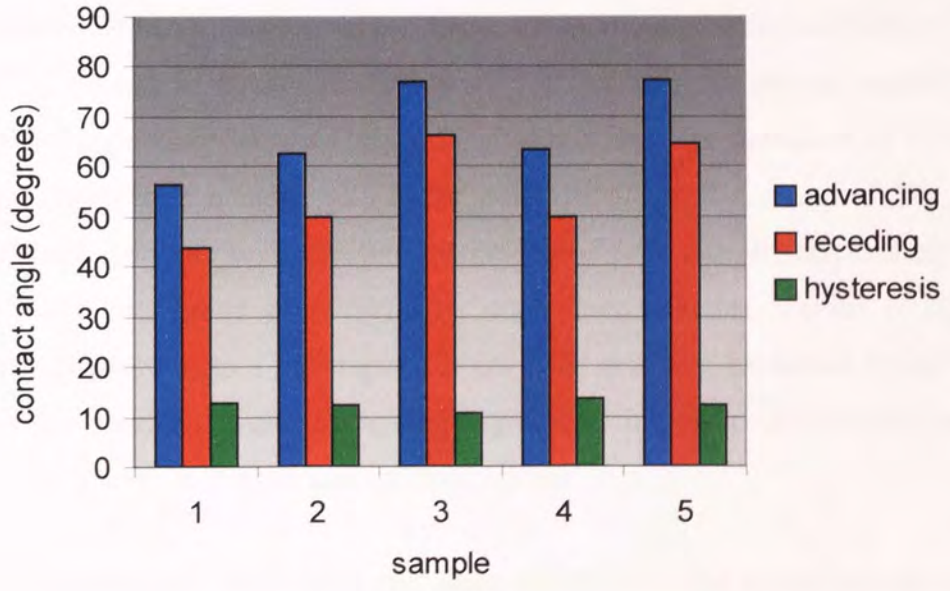

Figure 4.37 The advancing and receding angles and hysteresis of the NVP/MMA 70:30 copolymer with 1% FCS as the test solution

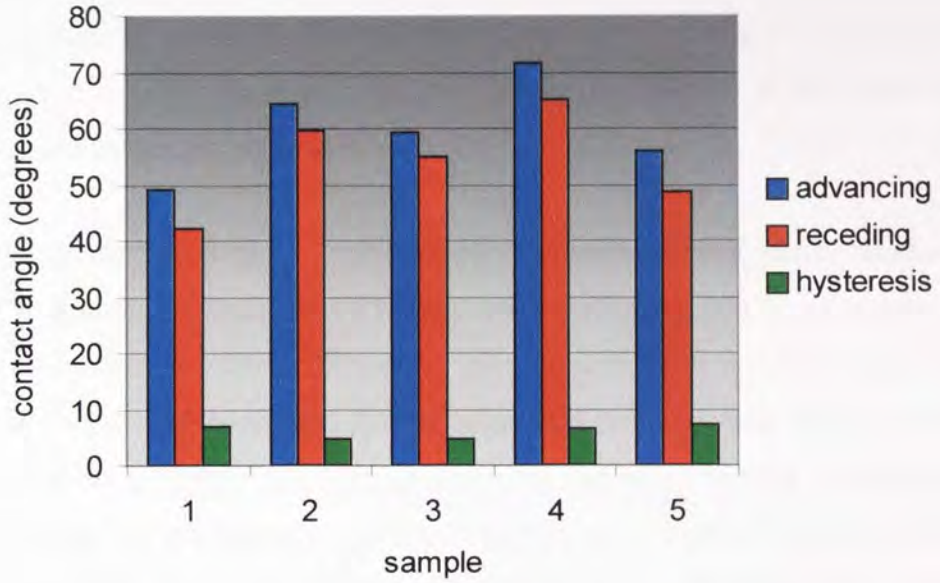

It can be seen from Figure 4.34 and Figure 4.36 that when water is used as the test solution there is more variation in the results for the NVP/MMA 70:30 copolymer than for poly(HEMA). In these experiments advancing angles for poly(HEMA) have a range of 5° and a standard deviation of 1.8° whereas advancing angles for the NVP/MMA copolymer have a range of 21° and a standard deviation of 9.4°. The receding angles have a range of 12° for poly(HEMA) and a range of 23° for the NVP/MMA copolymer with standard deviations of 5.6° and 10° respectively. This means that a membrane of NVP/MMA copolymer contains regions of differing surface properties due to a heterogeneous polymer structure, explained by an uneven sequence distribution. Higher advancing angles tend to correspond to higher receding angles, giving a low variation in hysteresis values.

Figure 4.35 and Figure 4.37 show that when 1% FCS is used as the test solution the variability in advancing and receding angles is high for both poly(HEMA) and the NVP/MMA copolymer. This could be due either to adsorption of foetal calf serum onto the surface of the polymers or fluctuations in the composition of FCS from one test to another despite thorough mixing. Less variation may be observed if the concentration of FCS was achieved by weight rather than volume.

4.4 Discussion

Surface tension measurements using water as the test solution confirmed that all hydrogels studied contained no unreacted monomers or other contaminants which could otherwise affect the results because the surface tension of the probe solution was unaltered by the test sample.

When water was used as the test solution dynamic contact angle measurements showed a general increase in wettability with increasing EWC, as shown by the decreasing hysteresis values. However, the advancing and receding angles did not appear to follow any trend and it was suggested that this was due to the blocky structures of the NVP/MMA copolymers causing regions of varying wettability on the same hydrogel. A non homogeneous surface may also explain the apparently higher wettability of the low water content NVP copolymer than that of the low water content AMO copolymer tested.

In order to evaluate this theory 5 samples of hydrogel were cut from the same membrane, comparing an NVP copolymer with poly(HEMA). Far more variation was noted in the results for the NVP/MMA copolymer than for poly(HEMA). In the light of this finding, dynamic contact angle measurements should be repeated on several samples especially when testing hydrogels with blocky structures. High levels of variation were observed for both poly(HEMA) and NVP/MMA when 1% FCS was used as the test solution, though perhaps measuring FCS by weight instead of volume would have shown a difference due to the accuracy of the balance over the graduated pipette.

There was no specific difference in hysteresis values when NVI or DEAEMA containing polymers were tested. The bulky side groups are not thought to affect the mobility around the backbone chain. More variation in values was observed for these hydrogels containing cationic monomers than for the neutral hydrogels. This is due to a patchy distribution of NVI or DEAEMA in addition to a blocky structure.

Polymers containing anionic methacrylic acid exhibited greater advancing and receding angles and less hysteresis than the neutral hydrogel. A blocky structure is

likely to be masking the real effect of MAA which was expected to increase mobility around the chain.

Foetal calf serum was used as the test solution in order to mimic more closely a biological environment so that a predictive technique for the effects on cell adhesion can be developed.

The higher water content neutral hydrogels exhibited a more consistent fall in advancing and receding contact angles with increasing EWC when FCS was the test solution. This was true at 1%, 10% and 100% concentrations. A very low hysteresis was seen at 1%, but increased at 10% and 100% FCS, possibly due to excess FCS.

An increase in cationic monomer produced an increased hysteresis at 1% FCS, showing increased mobility, though no trend was seen at 10% or 100% FCS. These effects may be due to an uneven sequence distribution or excess of FCS or a combination of these factors.

At 1% and 10% FCS polymers containing acidic monomer showed reduced dynamic contact angles with an increased hysteresis, compared with the neutral NVP/MMA copolymer. This effect was greatest when 1% FCS was used as the test solution, probably because at higher concentrations there is an excess of FCS. At 100% FCS the opposite was true. The negatively charged components of the foetal calf serum do not adsorb rapidly to the acidic groups and there may be a repulsion effect, thereby increasing mobility. A slightly higher EWC may also contribute to the increased wettability.

Four neutral hydrogels were tested using n-octane as the test solution and one neutral hydrogel was tested using methanol. A promising effect was seen with methanol but not with n-octane, though most of the materials were too weak to be tested with methanol so further work must be done in order to see any differences within a series of materials. The dipping balance proved to be a useful instrument in determining the level of hydrogen bonding in the hydrogels when used in conjunction with tensile testing.

No difference in surface properties was observed when poly(HEMA) was autoclaved, though it is possible that other materials may have responded in a different manner.

One of the difficulties of studying the surfaces of hydrogels is that their properties are largely governed by water, which makes any differences between individual materials less obvious, especially when the test liquid is also water, since any polymer effect is minimised in the hydrated state. For example, many of the dynamic contact angles on samples were found to be zero, making comparison impossible. A possible improvement to the approaches employed would be to use a test liquid that will give higher contact angles.

In a series of papers on the spreading of liquids on solid surfaces Zisman and his coworkers[101, 102, 103, 104, 105] plotted the cosine of the contact angle (θ) of the wetting liquid on the solid, against the surface tension of the wetting liquid. This relationship was then extrapolated back to $\cos \theta = 1$ to give the value for the surface tension of a hypothetical liquid which would completely wet the solid surface. This value is called the critical surface tension γ_C, and in calculating this value it is assumed that the equilibrium spreading pressure, $\pi_e = 0$. The value of the critical surface tension will depend, to some extent, on the wetting liquid used. Using non polar wetting liquids yields the maximum value of γ_C while polar liquids give the minimum γ_C value.

This approach could be used for the hydrogels tested in this thesis. A straight line graph could be extrapolated to a value for the surface tension which would least wet the surface of the materials. It may be that a higher surface tension is necessary to show any differences between the materials which gave contact angles of zero in water. An example would be a salt solution such as sodium chloride. Differences were observed when lithium bromide was used as the dipping solution, although the surface tension was unexpectedly lower in this case and so a surface tension higher than water was not investigated.

The exchange of proteins adsorbed at solid-liquid interfaces with proteins in solution as a function of time is known as the Vroman effect[106, 107, 108]. Briefly, when a surface comes into contact with proteins in solution, an adsorbed protein may be displaced by another due to interaction between the proteins. In mixtures, proteins compete and it

has been shown, for example, that vitronectin reduces adsorption of albumin more than of fibronectin[109]. In addition, proteins can alter their conformation in order to adhere to surfaces. Therefore, the usefulness of single protein solutions for quantifying adsorption is questionable, especially when comparing different materials. Hence, using foetal calf serum is preferable to a solution of vitronectin in order to predict cell adhesion behaviour but highlights the fact that protein adhesion is a very complex effect. In this chapter it has been shown how an excess of FCS reduces any advantage, over HPLC grade water, seen at lower concentrations, and this may hold true in the case of cell adhesion. A small amount of protein encourages more protein to attach, but too much protein creates a Vroman effect that may discourage cell adhesion.

Problems encountered during testing included the persistent curling of some of the higher water content samples, making accurate measurement difficult. The materials with the highest EWCs were very prone to tearing so increasing the cross link density may be useful for future experimentation, though the water content would decrease with the same monomer compositions.

It is of my opinion that contact lenses should, in water, have an advancing angle of 80 to 100° with a low hysteresis for the best tolerance in the eye. The results obtained during this study suggest that none of the materials tested consistently meet this requirement, probably in part due to the blocky sequence distributions of the polymers. However, some of these materials are better than certain contact lenses on the market such as Medalist 66 from Bausch & Lomb which has a hysteresis of 71° [110].

4.5 Conclusions

Dynamic contact angle measurements based on the Wilhelmy plate technique yield more objective information about surface properties than do static contact angle measurements. Static surface tension measurements using the du Noüy ring are useful for determining the level of contaminants in a solution, and for ensuring that no unreacted monomers are left within the polymer matrix after polymerisation.

Measurements were made on a series of hydrogels so that comparisons could be made between hydrogels of increasing water content, and with increasing ionic monomer.

With increasing EWC the hydrogels become more wettable and their surface groups are less mobile. NVI or DEAEMA incorporated into the hydrogels does not affect the mobility of the surface groups. MAA is expected to increase mobility around the backbone chain due to a higher advancing angle and lower receding angle, though the results obtained were unclear perhaps due to a higher water content of the MAA containing hydrogel.

The blocky structure of NVP/MMA copolymers was confirmed by testing several areas of one membrane. Results were more varied with NVP/MMA copolymers than with poly(HEMA).

For the first time the dipping procedure was carried out using foetal calf serum as the test solution in an effort to mimic more closely a biological environment and develop predictive techniques for cell adhesion. FCS was useful in comparing different materials, especially at 1% concentration.

There was no apparent difference between the wettability of NVI or DEAEMA when either water or FCS was used as the test solution.

Octane and methanol were also used as the test solution with a smaller number of hydrogels, though no clear conclusions could be drawn from this work.

Lithium bromide solution allowed the level of hydrogen bonding to be determined, which was confirmed by measuring the mechanical properties of the materials tested, with the polymer containing DEAEMA having the highest level of hydrogen bonding.

No differences in surface properties were observed before and after autoclaving poly(HEMA), though other materials may be affected differently.

Using the theory of Zisman and coworkers[101, 102, 103, 104, 105] it may be possible to improve the technique even further by using salt solutions as the test liquid.

There may be a Vroman effect[106, 107, 108] causing different proteins to be adsorbed to different materials.

No material consistently meets the requirements for clinical use, though some of the materials tested have better surface properties than some contact lenses in current use.

4.6 Further Work

Because a higher EWC may have contributed to the increased wettability of the MAA containing hydrogels, a series could be synthesised at constant EWC so that the pure effect of acidic monomer could be determined.

The experiment using methanol as the probe solution could be repeated using hydrogels with lower EWCs which would be much stronger, thereby possibly giving a more comprehensive view. A higher cross link density would also enable stronger samples to be tested, using the dipping balance, using lithium bromide as the probe solution.

Further work needs to be carried out on a range of hydrogels in order to confirm that autoclaving samples affects surface properties since the preliminary results were not reproduced.

Tests should be carried out using a probe liquid with a higher surface tension, such as sodium chloride solution.

Consistency experiments using several samples of one membrane could be reproduced for AMO/MMA copolymers which are known to have a more even sequence distribution than the corresponding NVP copolymers.

As stated in the previous chapter, a continuation of the present study using a wider range of AMO copolymers would be of interest due to the favourable sequence distributions produced when copolymerised with MMA.

CHAPTER 5
CELLULAR RESPONSE TO HYDROGEL MATERIALS

5.1 Introduction

A hydrogel used as a biomaterial must be well tolerated when placed in the biological environment, to avoid rejection of the implant. The material must not be recognised as foreign by the host if the material is to be retained.

A simple elegant means of elucidating the ways in which biomaterials interact with the host system is by the use of *in vitro* cell culture techniques. Cell biology provides a powerful tool which can be used to study the interface between a synthetic material and the biological system. Cells can differentiate small changes in surface characteristics that cannot be detected by other means[81]. Single cell culture models also have the advantage that the effects of single factors can be isolated and studied far more easily than is the case with *in vivo* experimentation. In addition, *in vitro* cell culture techniques enable the study of biomaterials so avoiding the costs and ethical issues of animal experimentation, especially in the initial stages of material evaluation.

The eye is an accessible body site. It therefore provides an opportunity for testing aspects of material biocompatibility with relative ease and without the need for invasive surgery. Therefore, the extensive use of hydrogels as contact lenses enables the ocular compatibility of new polymer materials to be evaluated quickly. However, the range of materials that may be investigated for ophthalmic applications is relatively limited, as there is a need for specific mechanical, surface and permeability properties as dictated by the ocular environment.

5.1.1 Hydrogels used in Keratoprosthetic Implants

The artificial cornea (keratoprosthesis or KPro) is a device that replaces severely diseased, damaged and opaque corneas when a corneal transplant is not possible. Two components are needed to produce a functioning keratoprosthesis, a clear optical core that is non-cell adhesive and a peripheral (haptic) skirt that supports cell adhesion and integration. Non porous hydrogels are impervious to the ingrowth of stromal

keratocytes and epithelial cells[111] and do not encourage integration with the host tissue. Porous hydrogels do allow ingrowth of cells. The lack of adequate integration between the optic and its surrounding skirt, and between the skirt and the host tissue, underlies most of the complications associated with KPros[24]. The aim of this chapter is, therefore, to investigate the cell adhesion, cell proliferation properties and cytotoxicity of a number of hydrogels, in the continued development of predictive techniques, and for the advancement of the artificial cornea.

Poly(HEMA) has been used as the central core of keratoprosthetic devices because of its acceptance as a contact lens and intraocular lens material[18, 112]. Poly(HEMA) is a non-ionic hydrophilic polymer with optimal physical properties and low cytotoxicity. Poly(HEMA) has the advantages of excellent transmission of light, elasticity, moderate hydrophilic properties and can be made into porous sponges[113]. In addition, Lydon *et al.* reports that certain fibroblastic cells (Chinese Hamster Ovary) are non cell adhesive to poly(HEMA)[114]. However, long term studies with poly(HEMA) implanted subcutaneously in rats, hamsters and guinea pigs appear to show the material to be tumourgenic and susceptible to calcification[115]. There is also the problem of limited mechanical strength, and hence the need to study alternative hydrogel materials to find a material that exhibits improved properties for inclusion into a keratoprosthetic device[113].

5.2 Cell Adhesion

5.2.1 Cell Factors

The majority of mammalian cells, including fibroblasts, require a suitable substratum in order to grow. Such cells are called anchorage-dependent cells because they must adhere to the substrate before they will grow[116]. Complex molecular interactions that determine and regulate cell behaviour are established when the cells come into contact with the substrate.

Four major classes of adhesion receptors on the cell surface have been identified: cadherins, immunoglobulin superfamily receptors, selectins, and integrins. Cadherins

are Ca^{2+} dependent, homophilic cell-cell adhesion molecules. Immunoglobulin (Ig) superfamily receptors are a large group of receptors, including antibodies and T cell receptors, which bind to integrin type receptors on other cells and homophilic receptors. Selectins are calcium dependent receptors involved in the regulation of leucocyte binding to endothelium at sites of inflammation. Integrins are heterodimeric receptors with ligand specificities controlled by divalent cations, binding to extracellular matrix proteins and Ig and some integrin receptors on other cells.

The integrins mediate adhesion to proteins such as fibronectin (Fn), vitronectin (Vn) and laminin which can be absorbed to material surfaces from tissue fluids and serum.

There are two theories of cell adhesion. The first is the colloid stability theory which describes a balance between electrostatic repulsion, due to negative charges on the cell surface, and electromagnetic attraction, due to varying dipole moments in the surface layers and intervening medium[117]. No contact is involved in these interactions. This theory does not explain the preferred adhesion to more negatively charged surfaces such as modified poly(styrene).

An alternative theory claims that close range intermolecular forces such as hydrogen bonds are necessary for cell adhesion[118, 119]. This theory predicts that cells will adhere more strongly to hydrophilic surfaces than hydrophobic surfaces, and in general this is found to be the case experimentally[120, 121].

5.2.2 Role of Extracellular Materials

In addition to cell and substrate factors, cell adhesion is also regulated by extracellular factors. A surface must adsorb adhesive proteins, such as fibronectin and vitronectin, so that a cell will adhere to it. It is now believed that under most common tissue culture conditions, it is vitronectin that is the effective molecule for cell adhesion[122, 123].

Vitronectin is an adhesion glycoprotein synthesised primarily in the liver[124] and can be isolated from the liver as a single chain of 73kDa and from serum as a two chain

sequence of 65kDa and 10kDa. It is found in the circulation at a concentration of 0.25-0.45 mg/ml and is deposited at various sites in the body. Vitronectin is found in the closed-eye tear fluid, but is virtually absent in the reflex tear fluid[125], and is thought to be involved in the immune system as it has binding sites for bacteria[126, 127].

This protein is important in regulating cell adhesion and contains an RGD tripeptide sequence which is recognised by a family of integrin receptors on the cell membrane[126]. This arg-gly-asp sequence is found near the amino terminus of the molecule. The presence of vitronectin in focal adhesions of cultured cells has been shown by immunofluorescence techniques[128].

Vitronectin exists in two conformations: folded and extended[129]. It is thought that it becomes activated when adsorbed on surfaces, and the RGD peptide sequence is exposed[109].

5.2.3 Substrate Factors

Early research on different substrates claimed that hydrophobic surfaces such as poly(MMA) and poly(EMA) were more cell adhesive than hydrophilic surfaces such as poly(HEMA)[130, 131, 132], see Figure 5.1.

Figure 5.1 Structures of poly(HEMA), poly(MMA) and poly(EMA)

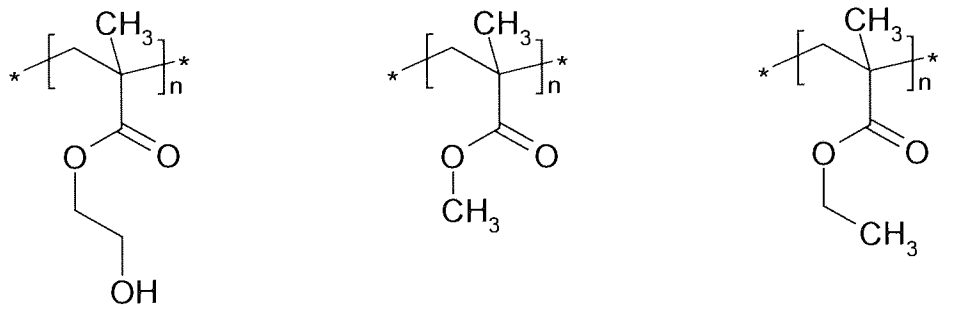

poly(HEMA) poly(MMA) poly(EMA)

However, untreated poly(styrene) does not support cell growth despite being hydrophobic, see Figure 5.2.

Figure 5.2 Structure of poly(styrene)

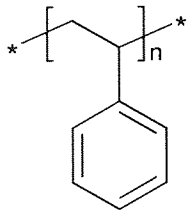

poly(STY)

Surface group expression experiments carried out by Thomas[133] showed that sulphuric acid treatment of poly(styrene) hydroxylates the ring and renders it cell adhesive. Although the addition of the hydroxyl group promotes cell adhesion, surface group exposure cannot be the only factor because poly(HEMA) contains the hydroxyl group but is generally considered to be non cell adhesive.

Anchorage dependent cells have traditionally been grown on glass substrates, however, commercial tissue-culture plastics are now commonly used for convenience. Poly(styrene) is non cell adhesive, however, surface treatment by glow discharge in oxygen plasma increases the wettability of the surface and renders it cell adhesive[133]. Surface group expression is one of several factors which influence cell adhesion. Thomas[133] demonstrated that cold sulphuric acid treatment of poly(styrene) caused the surface to become hydroxylated and cell adhesive while hot sulphuric acid produced sulphonated surfaces which did not promote cell adhesion. Davies[54] suggested that the more negatively charged sulphonate groups caused electrostatic repulsion as a result of the cell surface also being negatively charged.

Surface polarity, which can be calculated from the contact angle using the method of Owens and Wendt[78], affects adhesion because a high surface energy promotes the adsorption of proteins which in turn promotes the adsorption of cells (see later). Fitton[56] determined that some copolymers with well dispersed sequence distributions gave reduced cell adhesion, and hypothesised that such polymers do not benefit from 'islands' of specific chemical functionality possessed by polymers with blocky

sequence distributions. However, some copolymers with well dispersed sequence distributions showed enhanced cell adhesion over blocky polymers. This could be because the hydrophobic comonomer was unable to block hydrophilic adhesion sites perhaps for steric reasons. Surface morphology and surface charge have also been shown to affect adhesion[134, 54, 56, 121, 135]. Thus both the chemical and physical structure play a part in cell adhesion and it is highly likely that all these factors have an effect, but their relative importance is not well understood.

Minett[2, 114] studied hydrogel surfaces by employing cells as "probes" and studied cell response to a range of hydrogels, mostly based on poly(HEMA). By incorporating differing amounts of methyl methacrylate (MMA) or ethyl methacrylate (EMA) into the gel, materials with a range of water contents were obtained. He found that the EWC is an important factor in determining cell behaviour and that none of the materials containing 35-60% water supported cell attachment, see Figure 5.3.

Pettit *et al.*[136] observed a similar pattern, where corneal epithelial outgrowth was greatest onto copolymers of poly(HEMA)/(ethylene methacrylate) with equilibrium water contents below 40%.

Figure 5.3 HEMA curve. Cell count expressed as a percentage of the tissue culture plastic control values for poly(HEMA) based hydrogels of increasing EWC[2, 114]

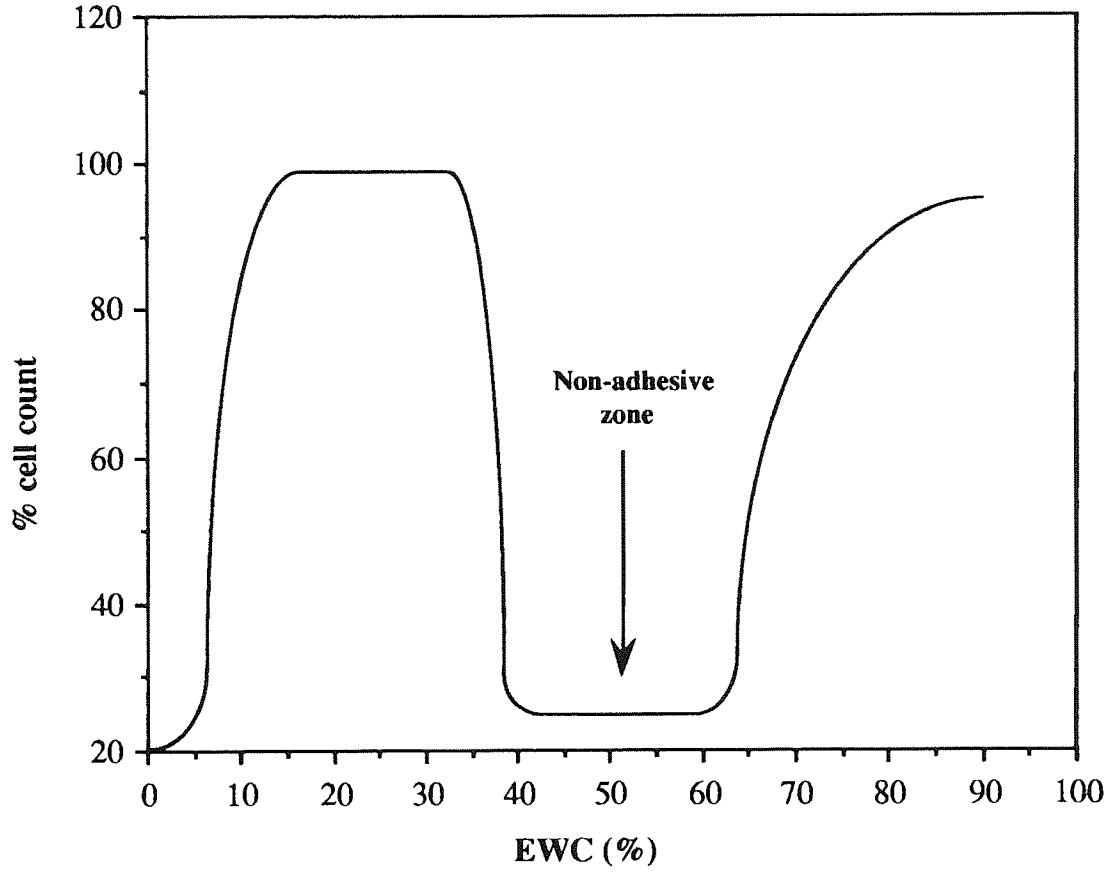

Thomas focussed on high water content hydrogels and found that the nature of the water structuring group can override the effects of EWC alone[133]; Minett's work[2, 114] concentrated on the effect of water content on cell adhesion when hydroxyl was the water structuring group. Thomas[133] observed and speculated the effects of CONRR and CONHR water structuring groups. She mainly studied hydrogels containing NVP and NNDMA (Figure 5.4) water structuring groups and found that Minett's HEMA curve was shifted to the right for these nitrogen containing groups (see Figure 5.5).

Figure 5.4 Structure of N,N-dimethyl acrylamide

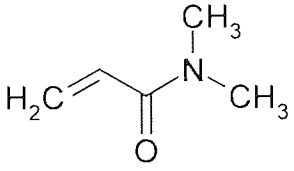

Davies[54] then took this study a stage further by observing an extended range of low and high water content hydrogels containing the same water structuring groups in an attempt to determine the relative effects of water content and functional groups on cellular response. He produced broadly similar results to those of Minett[2, 114] and Thomas[133] and concluded that cell attachment is influenced by comonomer ratio and comonomer composition.

Figure 5.5 Thomas curve Cell count expressed as a percentage of the tissue culture plastic control values for hydrogels containing different water structuring groups of increasing EWC[133]

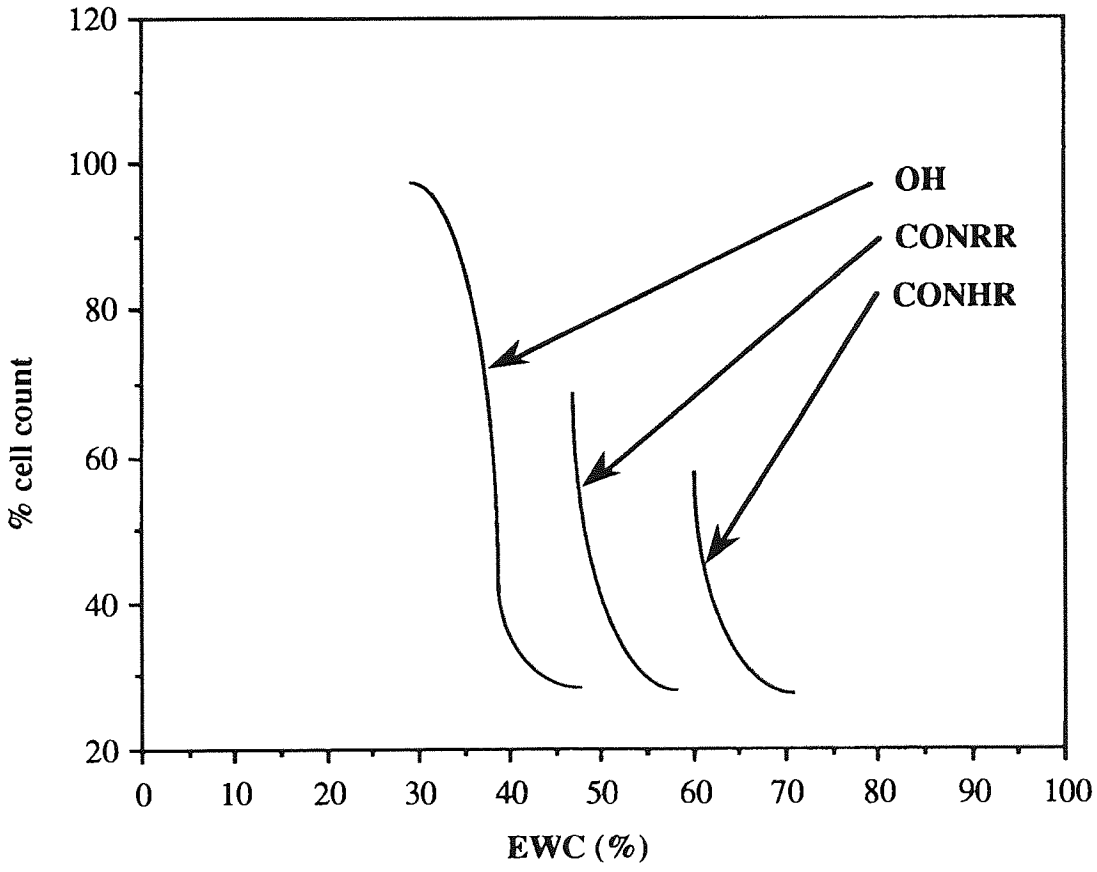

As comonomer was increased, cell attachment increased, and replacement of Lauryl methacrylate (LMA), shown in Figure 5.6, with MMA produced a shift to the right in the 'Minett' curve.

Figure 5.6 Structure of lauryl methacrylate

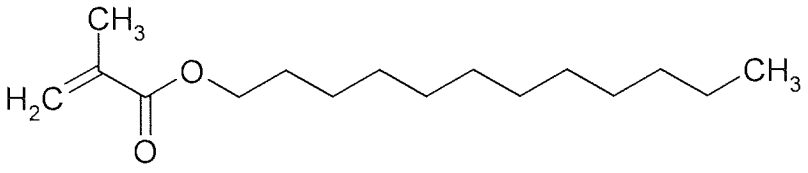

Combining the results of Davies[54] and Thomas[133] shows very clearly the effect of substituting the water structuring groups NVP and NNDMA (Figures 5.7 and 5.8). This shift to the right in the curve is seen for both comonomers studied. The effect is also seen when the comonomers LMA and MMA are substituted (Figures 5.9 and 5.10), and is true for both water structuring groups.

Figure 5.7 Combined Davies[54] and Thomas[133] results for BHK-21 cell count against Equilibrium Water Content (EWC) for 2 different water structuring groups with MMA as the comonomer

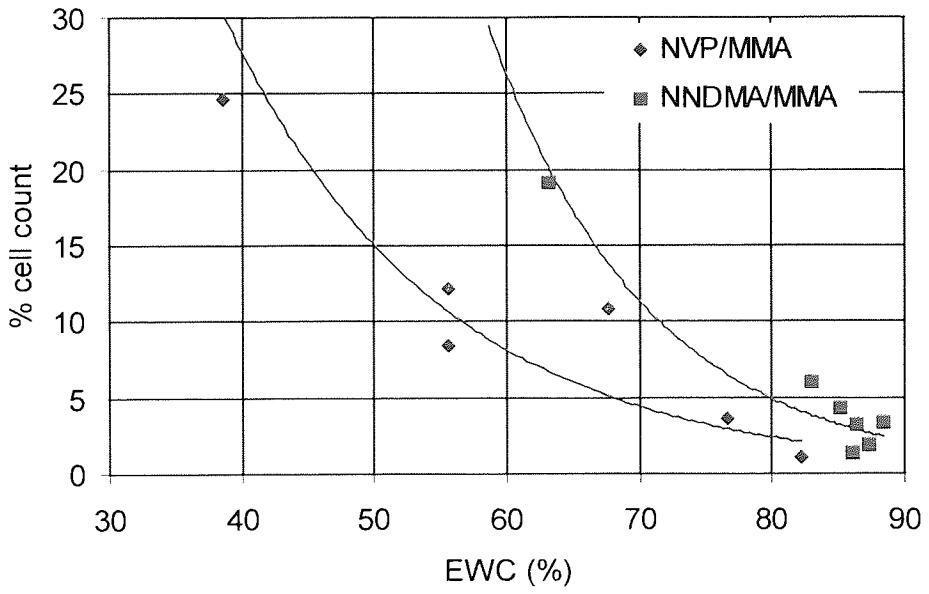

Figure 5.8 Combined Davies[54] and Thomas[133] results for BHK-21 cell count against Equilibrium Water Content (EWC) for 2 different water structuring groups with LMA as the comonomer

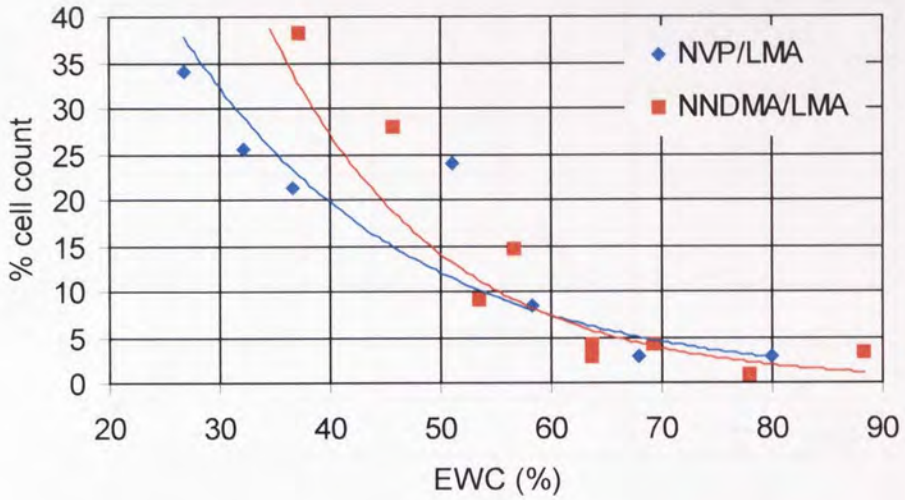

Figure 5.9 Combined Davies[54] and Thomas[133] results for BHK-21 cell count against Equilibrium Water Content (EWC) for NVP copolymers with 2 different comonomers

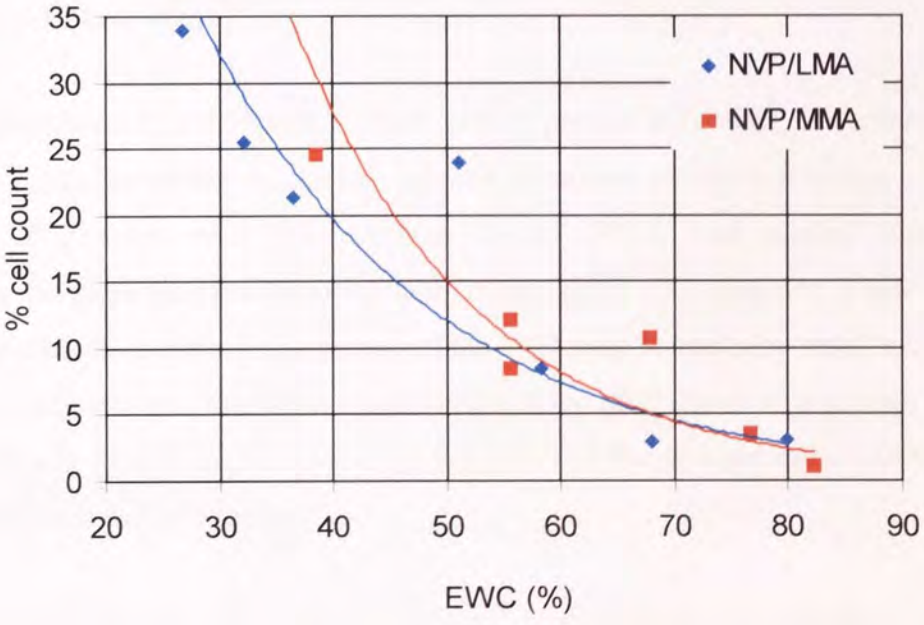

Figure 5.10 Combined Davies[54] and Thomas[133] results for BHK-21 cell count against Equilibrium Water Content (EWC) for NNDMA copolymers with 2 different comonomers

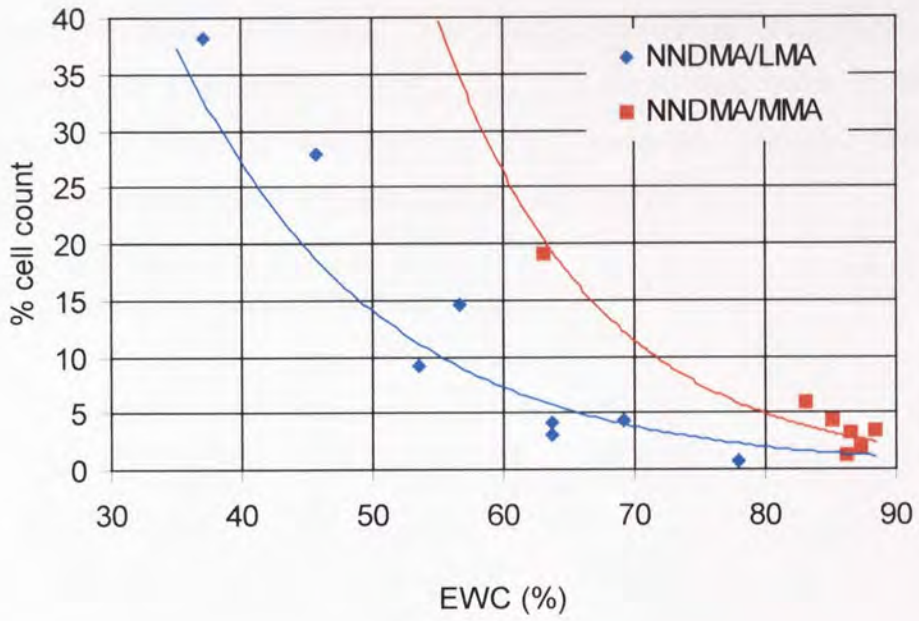

The surface becomes mechanically unstable at extremely high water contents (greater than 95%). A surface which is too mobile begins to behave as a layer of water and does not allow cells to attach[54].

In some applications it is desirable to limit cell or protein adhesion. For example, protein and lipid deposition is one of the complications of contact lenses. The interaction of proteins with poly(ethylene oxide) (PEO) end grafted onto a hydrophobic substrate has been theoretically modelled[137, 138]. Van der Waals and hydrophobic attractions between proteins and the PEO were found to be small relative to the steric repulsion resulting from compression of the PEO chains as a protein was adsorbed. Closely spaced, higher molecular weight PEO chains were suggested to be most effective at reducing adhesion.

In support of this argument is the work of Fitton[56] who studied poly(ethylene oxides) in polyHEMA hydrogels in order to decrease cell adhesion. A range of HEMA

polymers containing 20% poly(ethylene oxide methacrylates) (see Figure 5.11) at molecular weights of 200, 400 and 1000 were synthesised. The trend in cell adhesion was pronounced, with cell adhesion decreasing as the chain length increased. Because the EWC is known to play an important role in cell adhesion, a range of copolymers were produced at 40% EWC. The effect of increasing chain length was still apparent even with a decreased density of chains at the surface, while at similar water contents. Cell adhesion was tested both on untreated hydrogels and on hydrogels with preadsorbed foetal calf serum (FCS), see Figure 5.12.

Figure 5.11 Structure of methoxyPEGmethacrylate

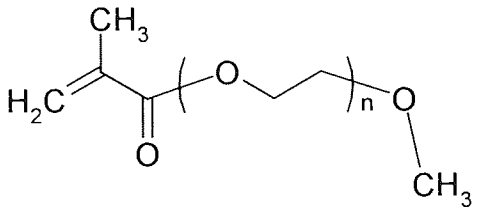

Figure 5.12 3T3 cell adhesion to PEGMA substituted gels at 40% EWC[56]

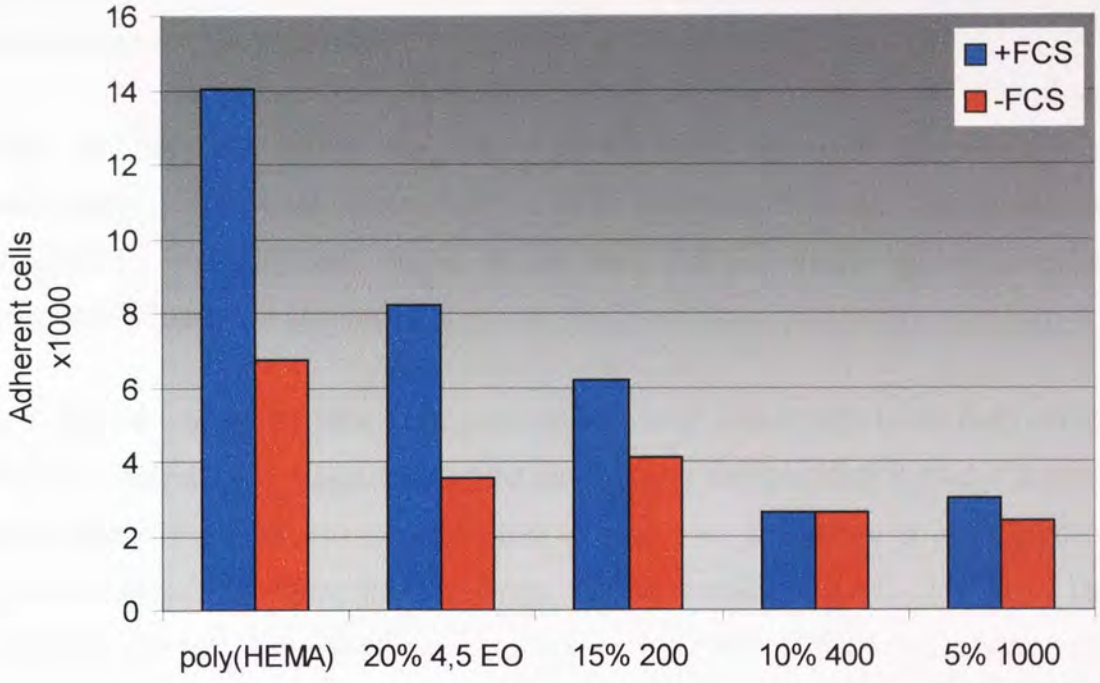

Fitton[56] concluded that the long PEO chains increase the EWC and also offer an unsuitable surface for cell adhesion: the long chains act as a 'carpet' of molecular cilia, preventing the adsorption of adhesion proteins. She also found that the methoxy terminated PEO chains were more effective at inhibiting adhesion than the hydroxy terminated chains. This may be due to the -OH terminated chains looping back to hydrogen bond with ethereal groups within the PEO chains and therefore becoming less mobile. A random sequence distribution was thought to inhibit adhesion better than a blocky distribution of PEO chains. This is because adhesion is mainly inhibited due to the mobility of the long chains which can be thought of as a seaweed effect. Polymers with a random sequence distribution will contain adhesion limiting long chains over the entire surface, whereas polymers with a blocky sequence distribution will contain specific sites on the surface which do not have long PEO chains to discourage cell adhesion.

It has been suggested by Bergethon *et al.* that the functional groups leading to adhesion of cells differ from those responsible for spreading[139]. This idea is also supported by Brandley *et al.*[140] whose results imply that short-term adhesion is most strongly mediated by hydroxyl groups, whereas the presence of carboxyl moieties is preferred for long-term growth.

Other workers have shown that 100% poly(HEMA) hydrogels discourage cell attachment[141, 142], though Bergethon *et al.*[139] reported that cells did attach to poly(HEMA) and remained viable, though they did not spread unless ionisable functional groups were also present.

There has been relatively little work conducted on ionic copolymers in the field of cell adhesion. Maroudas[121] suggested that the requirement for spreading is charge density rather than whether the charge is positive or negative. Bergethon *et al.*[139] studied hydrogels containing either the negatively charged methacrylic acid (MAA) or the positively charged *N,N*-dimethylaminoethyl methacrylate (DMAEMA) (structures shown in Figures 5.13 and 5.14 respectively) and concluded that with both functional groups, spreading was optimal with a concentration of between 0.01% and 0.1%.

Figure 5.13 Structure of methacrylic acid

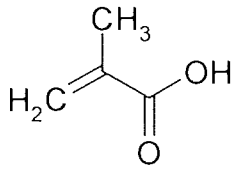

Figure 5.14 Structure of N,N-dimethylaminoethyl methacrylate

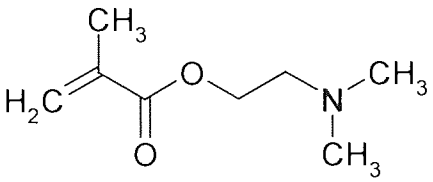

However, Kishida and coworkers[135] found that negatively charged surfaces tend to prohibit adhesion, and that cells adhere readily to positively charged surfaces.

Adhesion increased with increasing positive charge but a high concentration of polycations was found to be toxic to cells. Smetana *et al.*[143, 144] studied the adhesion of monocytes to hydrogels and found that adhesion to poly(HEMA) grafted with *N,N*-dimethylaminoethyl methacrylate (10 mol %) was significantly higher than to poly(HEMA) and poly(HEMA) grafted with methacrylic acid (3 mol %). Lee *et al.*[145] observed that negatively charged acrylic acid (Figure 5.15) grafted surfaces show poor cell attachment, while positively charged *N,N*-dimethyl aminopropyl acrylamide (DMAPAA) (Figure 5.16) grafted surfaces encouraged cell attachment. Surfaces grafted with the negatively charged sodium ρ-styrene sulphonate (Figure 5.17) did show a large amount of cell attachment, though it has been suggested that the existence of an aromatic ring close to the ionisable group may be responsible for this[135]. Sandeman *et al.*[142] measured keratoctye adhesion to a range of hydrogels based on poly(HEMA) incorporating varying amounts of methacrylic acid, *N,N*-dimethylaminoethyl methacrylate, or phenoxyethyl methacrylate (PEM) (Figure 5.18). The incorporation of 15 mol % of PEM or of 20 mol % DMAEMA increased cell adhesion to poly(HEMA) by at least four times, however addition of the negatively charged methacrylic acid did not improve the cell adhesion characteristics of the hydrogels.

Figure 5.15 Structure of acrylic acid

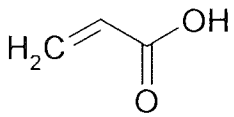

Figure 5.16 Structure of N,N-dimethyl aminopropyl acrylamide

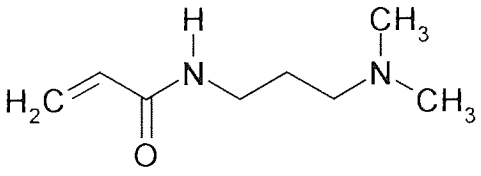

Figure 5.17 Structure of sodium p-styrene sulphonate

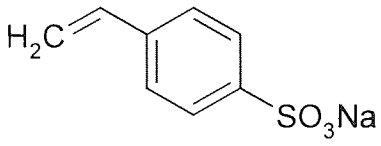

Figure 5.18 Structure of phenoxyethyl methacrylate

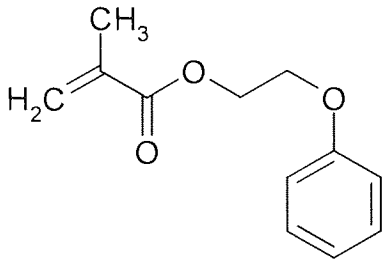

Since serum proteins tend to be negatively charged it is possible that protein adsorption, which is required for cell adhesion, occurs more readily onto surfaces incorporating positive charge[145]. In serum containing medium, this may be due to either, or both, of two effects: the direct interaction of positive charge with the cell membrane, and the increase in adsorption of adhesion proteins from the serum.

It is evident, therefore, that confusion exists, and further work is necessary to evaluate the effect of surface charge. Also, ionic polymers will only be charged if they are dissociated so that an anion or cation is present on the chain. It is often unclear whether surfaces described in the literature are truly charged, or if they have ionic groups which may not be dissociated.

An aim of the studies presented in this thesis is therefore to continue the work of Minett[114, 2], Thomas[133] and Davies[54] by researching the effect of ionic and charged water structuring groups on cell adhesion. Minett studied the effect of water content on cell adhesion when hydroxyl is the water structuring group, and Thomas and Davies looked at cell adhesion with neutral hydrophiles as water structuring groups. The effect of water content on cell adhesion with charged hydrophile are described

here and will constitute the next stage of the work. It would also be interesting to know what constitutes an adhesive and non-adhesive substrate.

Recently, interest has focussed on new monomers such as acryloylmorpholine (AMO) (Figure 5.19) which may give improved surface properties due to a more alternating sequence distribution when copolymerised with alkyl methacrylates[146]. As a result the effect of such monomers and consequently sequence distributions on cell adhesion have been investigated.

Figure 5.19 Structure of acryloylmorpholine

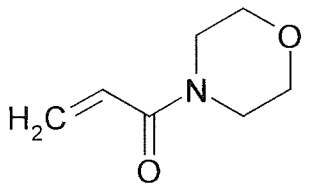

Alternative approaches to manipulate cell adhesion include surface modification with plasmas, grafting with pharmacologically active molecules, and grafting with biomimicking molecules such as those containing the arginyl-glycyl-aspartyl-serine (RGDS) peptide sequence[147].

5.2.4 Keratocytes

In addition to swiss albino mouse 3T3 cells, human keratocytes were used to investigate the cellular response. Keratocytes are cells found in the cornea, thus will be more appropriate for studying the likely ocular response.

Keratocytes have been found to adhere to hydrogel contact lens materials with EWCs ranging from 38% to 80%[148, 149]. No hydrogel in the study was found to be toxic to the keratocytes. Attachment was thought to be influenced by EWC and/or surface charge although no relationship has been observed, however, the relative contributions of each of these was not quantified.

Although keratocytes attach to the hydrogels, they do not grow into the structure matrix. Therefore, it will be necessary to investigate the effect of pore size on keratocyte invasion of the hydrogel. Keratocytes have not to date been used in our laboratory so initial studies attempted to define the procedures required to maintain the cells in culture.

5.2.5 Cell Adhesion Techniques

5.2.5.1 Trypan Blue

Previous work carried out in this laboratory[114, 2, 133, 54, 56, 150] employed the use of the trypan blue dye exclusion test (Figure 5.20) to determine cell viability and cell counts. However, the trypan blue test is prone to overestimates of the viability of the cell population, for a number of reasons detailed below.

Figure 5.20 Structure of Trypan Blue

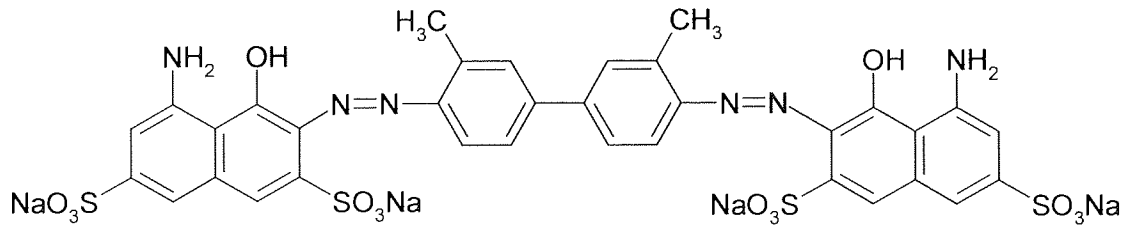

Dye uptake marks cells that have grossly disrupted membranes and may not detect other forms of injury that affect cell attachment or may progress to cell death[151]. Where the cell membrane is still intact the trypan blue dye will not differentiate between viable and non viable cells. It is therefore only valid as a short term assay. In addition, short term tests only demonstrate whether cells are dead at the time of the assay. Also, this method does not account for cells that have fully lysed (i.e. those which are no longer identifiable as cells). It is known that the number of blue staining cells increases with time after addition of the dye[152] so the assay must be completed within 3 to 5 minutes. Furthermore, trypan blue has a greater binding affinity for

protein in solution that for injured cells, and should only be used in protein free solution. Serum used in cell culture contains proteins, mostly albumin, which could therefore interfere with the results of the trypan blue test.

Cells stained with trypan blue are usually counted using an improved Neubauer haemocytometer. This method of counting introduces large errors when counting less than 10^6 cells/ml[153]. Trypsin is used to remove the cells from the materials in order to count them, thus the trypsin will to some extent disrupt cell membranes.

This work was therefore carried out using more reliable techniques of cell counting. Two methods requiring fluorescence microscopy were used. Fluorescence is a type of luminescence where light is emitted from molecules for a short period of time following the absorption of light. When the delay between absorption and emission is of the order 10^{-8} seconds or less, the emitted light is termed fluorescence[154].

5.2.5.2 Calcein AM

It has been suggested that calcein AM (calcein acetoxy methyl ester) best satisfies the criteria for assaying cell adhesion[155, 156, 157], with the least effect on cell viability and other cell funtions. Calcein AM (Figure 5.21) also avoids the use of radioactive material[158], [159]; it is better retained by viable cells than are fluorescein, carboxyfluorescein and BCECF (2',7'-bis-(2-carboxyethyl)-5-(and-6)-carboxy fluorescein) and tends to have brighter fluorescence in a number of mammalian cell types[160].

Figure 5.21 Structure of Calcein AM

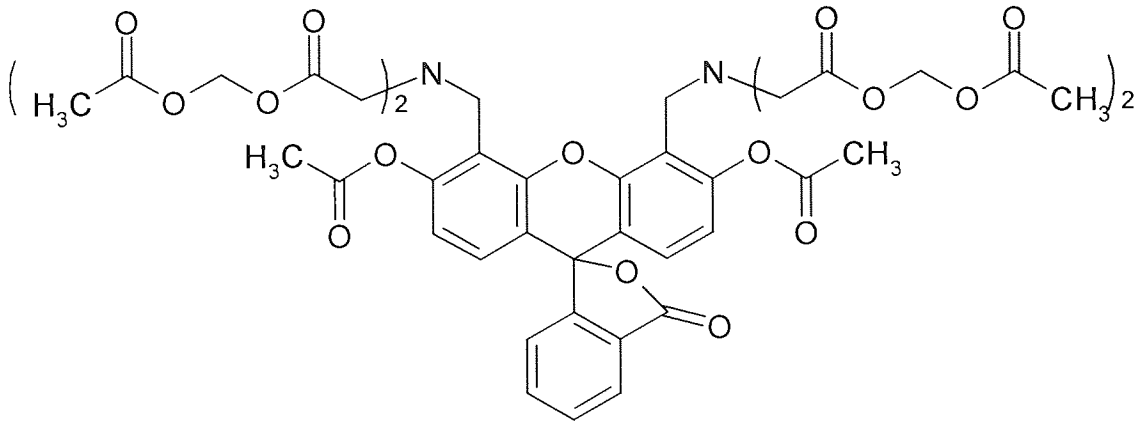

Calcein AM is a fluorogenic esterase substrate that is hydrolysed to a green fluorescent product (calcein); thus, green fluorescence is an indicator of cells that have esterase activity as well as an intact membrane to retain the esterase products.

5.2.5.3 Ethidium homodimer-1

Ethidium homodimer-1 (EthD-1) (Figure 5.22) is a high-affinity, red fluorescent nucleic acid stain that is only able to pass through the compromised membranes of dead cells[161]. Ethidium bromide, propidium iodide and EthD-1 have large stokes shifts and may be used in combination with fluorescein derivatives (such as calcein AM) for two colour applications. Propidium iodide and ethidium bromide have been extensively used to detect dead or dying cells[162, 163, 164, 165, 166] but ethidium bromide may be less reliable because it is not as highly charged.

Figure 5.22 Structure of Ethidium homodimer-1

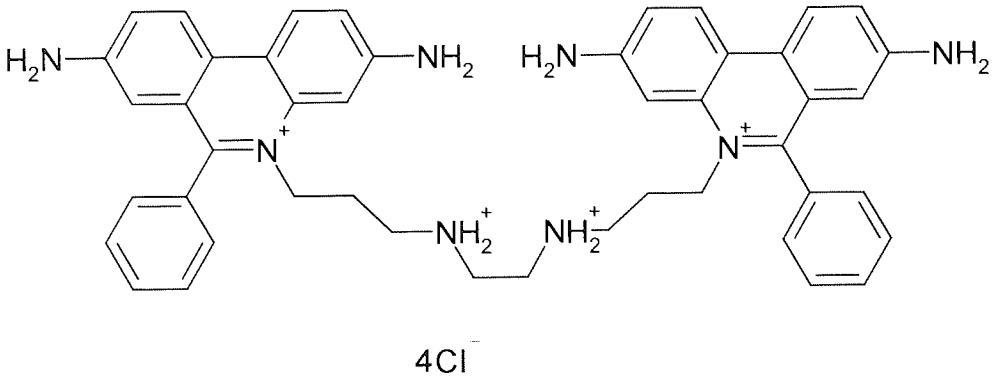

With its high affinity for DNA and low permeability[167, 168, 169, 170] EthD-1 is often the preferred red fluorescent dead cell indicator. EthD-1 binds to nucleic acids 1000 times more tightly than does ethidium bromide and undergoes about a 40-fold enhancement of fluorescence upon binding[169, 171]. Low concentrations are therefore sufficient to stain dead cells.

The LIVE/DEAD viability/cytotoxicity assay from Molecular Probes Inc. offers a simple and reliable test combining calcein AM and ethidium homodimer-1.

5.2.5.4 Neutral Red

Neutral Red (3-amino-7-dimethyl-2-methylphenazine hydrochloride) (Figure 5.23) is a supravital dye. The Neutral Red assay is based on the incorporation of Neutral Red into the lysosomes of viable cells after their incubation with test agents. It is an *in vitro* cell viability test that was developed and extensively studied for *in vitro* cytotoxicity determinations[172].

Figure 5.23 Structure of Neutral Red

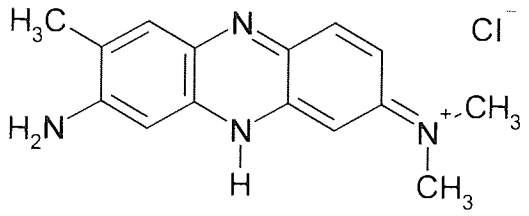

Neutral Red is weakly basic and diffuses through cell membranes, and accumulates in lysosomes, where it either binds with anionic sites, such as those of poly(saccharides), in the lysosomal matrix or the protonated form of neutral red is trapped within the acid milieu of the lysosomes. In damaged or dead cells neutral red is no longer retained in the cytoplasmic vacuoles and the plasma membrane does not act as a barrier to retain the Neutral Red within the cells[173].

The Neutral Red is extracted from the intact, viable cells and quantitated spectrophotometrically.

5.2.5.5 Kenacid Blue R

The cytotoxic effect of chemicals on cells in culture can also be measured by the change in total cell protein arising from the inhibition of cell proliferation (Kenacid Blue R dye binding method), see Figure 5.24.

Figure 5.24 Structure of Kenacid Blue R

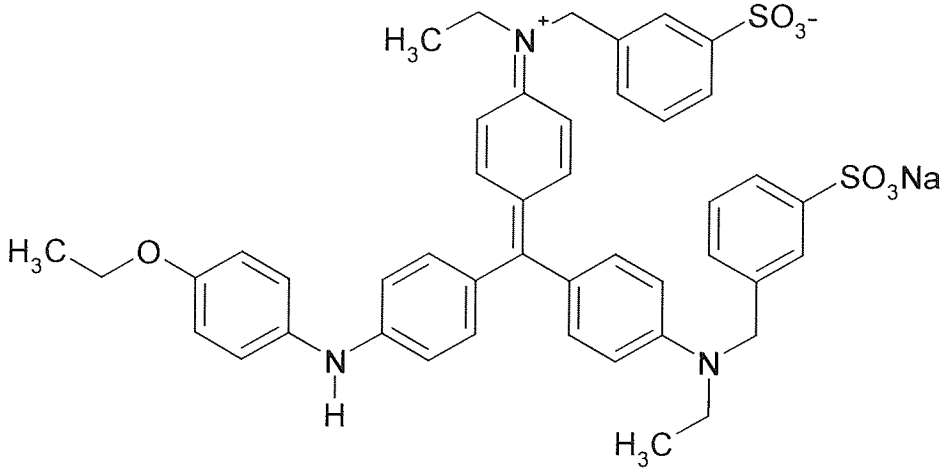

Healthy cells, when maintained in culture continuously divide and multiply over time. The basis of this test is that a cytotoxic chemical will interfere with this process and so result in a reduction of the growth rate and therefore in reduced cell numbers compared with control cultures[174, 175, 176]. This difference is reflected in the total protein content of the culture. Cells in continuous culture proliferate at a known optimal rate, and this can be reduced by chemicals which affect one or more essential functions, such as mitochondrial activity, DNA synthesis, maintenance of membrane integrity, or protein synthesis. The degree of inhibition of growth, related to the concentration of the test compound, provides an indication of toxicity. The continuous cell line 3T3-L1 is usually used in this test.

5.2.5.6 MTT

MTT measures metabolic activity of the cell. The 3-(4,5-dimethylthiazol-2-yl)-2,5-diphenyl tetrazolium bromide (MTT) assay[177] is a sensitive and reliable test that measures cell viability. The yellow water soluble MTT (Figure 5.25) is converted by mitochondrial dehydrogenase enzymes in living cells to give a dark blue water insoluble formazan product. The amount of formazan produced is directly proportional to the cell number in a range of cell lines.

Figure 5.25 Structure of MTT

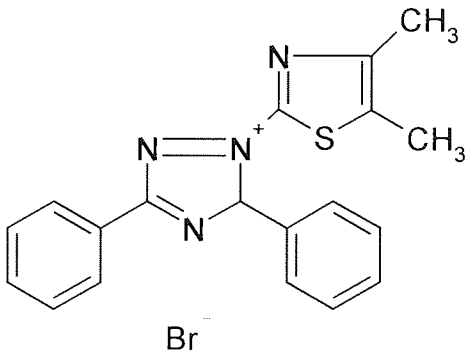

5.2.5.7 DAPI

DAPI (4',6-diamidino-2-phenylindole) (Figure 5.26) is a DNA specific probe which shows blue fluorescence on binding DNA[178, 179]. DAPI does not penetrate the membranes of viable cells, so the cells are fixed prior to staining. The nuclei are visible under the fluorescence microscope equipped with a blue filter and are counted directly by the observer.

Figure 5.26 Structure of DAPI

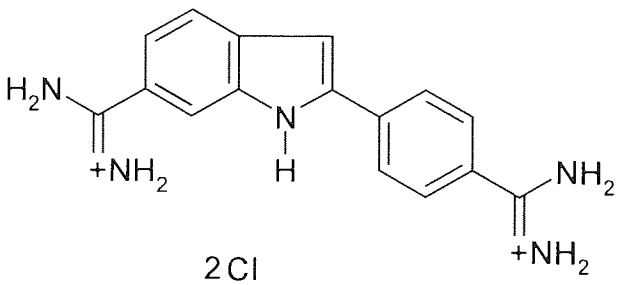

5.2.6 ISO 10993 Guidelines

ISO 10993[180] requires that a number of strict conditions be applied to validate assessments made and to ensure that the control conditions are maintained. Materials have to have at least one flat surface to allow cells to settle evenly over a material and

sterile materials must be handled aseptically. Negative controls which do not produce a cytotoxic response and a positive control material which provides a reproducible response should be incorporated into the assay.

Membrane damage can be used to measure cell viability, estimated by colorimetric measures, such as by the use of Exclusion Dye (dead cells stain) techniques, for example Trypan Blue. Cell populations that display a viability of lower than 70% after contact with a substrate may indicate cytotoxicity.

5.3 Materials and Methods

5.3.1 Cell Culture

Two methods of testing cell adhesion were chosen: the calcein AM/ethidium homodimer-1 assay and the DAPI assay. Calcein AM and ethidium homodimer-1 assays were carried out in our laboratory using 3T3 Swiss Albino Mouse cells supplied by the ECACC (European Collection of Cell Cultures). DAPI assays were carried out in the Department of Pharmacy and Biomolecular Sciences at the University of Brighton using 3T3 Swiss Albino Mouse cells and EK1.BR human foetal keratocytes established in the department[181].

3T3 Swiss Albino Mouse cells were maintained in Dulbecco's Modified Eagle's Medium (DMEM) with 2mM glutamine (GIBCO) and 10% Foetal Bovine Serum (FBS) (Selborne Biological Services Ltd). EK1.BR human foetal keratocytes were maintained in Dulbecco's Modified Eagle's Medium (DMEM) with 2mM glutamine and 10% Foetal Bovine Serum (FBS) with 100 IU/ml penicillin and 100 μg/ml streptomycin (Sigma).

All cell lines were incubated at 37°C in a 5% CO_2/95% air atmosphere in a Gallenkamp Plus Incubator. When the cells reached confluence they were passaged in the usual way. Cells were detached from the flask (IWAKI) using a 2.5% trypsin/EDTA solution (Sigma). The action of trypsin was neutralised by the addition of a 3-fold dilution of fresh working medium, and then cells were centrifuged in 15ml

tubes (Scientific Laboratory Supplies) for 3 minutes at 3000 rpm. The supernatant was pipetted off, and the cells were resuspended in fresh medium. Cells were counted using a haemocytometer. Fresh flasks were seeded with medium and cell suspension to give the required cell density. 3T3 cells and EK1.BR cells were sub-cultured at 5 x 10^3 cells/ml and 1.33 x 10^4 cells/ml respectively.

Population doubling level (PDL) was calculated using the following formula:

$$PD = \frac{\log_{10}(\text{number cells harvested}) - \log_{10}(\text{number cells seeded})}{\log_{10} 2} \qquad (5.1)$$

To freeze cells the following procedure was followed. Cells were sub-cultured using the standard protocol except that after centrifugation they were resuspended in FBS and after calculation of cell concentration FBS and 10% dimethyl sulphoxide (DMSO) were added to give a concentration of 1 x 10^6 cells/ml. Plastic screw-capped ampoules containing the cell suspension were placed in an ampoule cage which was then placed in the neck of the cryostorage dewar for one hour. Finally, ampoules were placed in a cryocane and placed in the vapour phase of liquid nitrogen inside the dewar.

To thaw cells one ampoule was removed from the cryostore dewar and placed in a petri dish at room temperature for one minute, and then placed in a water bath at 37°C until the cell suspension had completely thawed. Working medium was pipetted into a centrifuge tube and the cell suspension was added before spinning down the cells for 3 minutes at 3000 rpm. The supernatant was replaced with fresh working medium and the cells were resuspended and placed in a cell culture flask. Cells were sub-cultured twice before use.

5.3.2 Fluorescence Microscopy

Fluorescence studies were carried out with a Leitz Dialux 20 microscope fitted with a Ploempak 2.4 Fluorescence Vertical illuminator. A 50 watt ultra high pressure mercury lamp was employed as the light source. A H3 filter cube (BP 490 excitation filter and LP 515 suppression filter) was used for the calcein AM and ethidium

homodimer-1 assays and a E3 filter cube (BP 436/7 excitation filter and LP 490 suppression filter) was used for the DAPI assays.

5.3.3 Viability/Cytotoxicity Testing

5.3.3.1 Calcein AM/Ethidium homodimer-1 assay

The Molecular Probes LIVE/DEAD Viability/Cytotoxicity Kit was purchased from Bioscience and used as recommended.

Hydrated hydrogels were cut into 13 mm diameter discs using a size 10 cork borer. 13 mm glass coverslips were used as a positive control and poly(HEMA) was used as the negative control. Discs were sterilised for 15 minutes at 115°C and 3 bar in an Astelle Scientific Swiftlock autoclave and then incubated in wells of a 24 well plate (IWAKI) in Dulbecco's Phosphate Buffered Saline (DPBS) (Sigma) for at least 24 hours. Cells were passaged and resuspended to give a concentration of 1 to 4 x 10^4 cells/ml in working media. 1 ml of the cell suspension was added to each well and the materials were incubated for 72 hours.

A 2 μM calcein AM and 4 μM EthD-1 solution in DPBS was then made up. Media was removed from the materials which were then washed in DPBS to remove serum esterase activity. 100-150 μl of the calcein AM and EthD-1 solution was then added to each well and incubated for 30 to 45 minutes at room temperature. Each disc was transferred to a microscope slide and viewed under the fluorescent microscope at a magnification of x400, counting the number of cells present in each of 20 fields on each disc; 6 discs of each material were used.

The calcein AM count indicated the number of live cells present on each material, while the EthD-1 count indicated the number of dead cells present. The dyes fluoresced at a peak wavelength of 500 nm and 625 nm respectively.

5.3.3.2 DAPI assay

Hydrated hydrogels were cut into 13 mm discs using a size 10 cork borer. 13 mm glass coverslips were used as a positive control and poly(HEMA) was used as the negative control. Discs were sterilised for 15 minutes at 115°C and 3 bar in an Astelle Scientific Swiftlock autoclave and then incubated in wells of a 24 well plate (IWAKI) in Dulbecco's Phosphate Buffered Saline (DPBS) (Sigma) for at least 24 hours.

Cells were passaged according to the standard procedure and seeded onto the sterile materials at a density of 2×10^4 cells/well (1.51×10^4 cells/cm^2). After 72 hours the materials were rinsed 3 times with sterile PBS, fixed with a 1:1 mixture of methanol and actetone for 4 minutes and washed twice, leaving 1 ml sterile PBS in each well. DAPI was added to wells at a concentration of 1×10^{-6} g/ml. Materials were then viewed under epifluorescence using the fluorescence microscope at a magnification of x400. Cell adhesion was counted in 20 fields on each disc, and 6 discs of each material were used.

5.3.4 Scanning Electron Microscopy (SEM)

Cells were fixed using a 1:1 mixture of methanol and acetone for four minutes and washed twice with PBS. After fixation the samples were dehydrated in a microwave oven. The samples were then mounted on aluminium SEM stubs (Biorad) and gold coated in a Polaron splutter coating unit at 1 kV and 20 mA. Samples were then observed with a Cambridge Stereoscan electron microscope at accelerating voltages of 15-25 kV.

5.3.5 Statistical Analysis

Results were tested for statistical significance using analysis of variance (ANOVA), and heteroscedastic t-tests. Tests assume unequal variances and normal distributions.

5.4 Results

5.4.1 Cell Viability

The glass coverslips used for the positive control material exhibited the highest degree of cell adhesion, and the extent of spreading and proliferation of the cells followed classical fibroblastic morphology. Poly(HEMA), the negative control, exhibited a lower level of cell adhesion and proliferation. Hardly any cells attached to the NVP/MMA copolymers under investigation in this thesis. During the calcein AM/ethidium homodimer-1 assay cells became more rounded, see Figures 5.27 to 5.29.

5.4.1.1 Calcein AM and Ethidium homodimer-1

Figure 5.27 Calcein AM/Ethidium homodimer-1 fluorescent staining showing 3T3 adhesion to a glass coverslip (positive control) (x400 magnification)

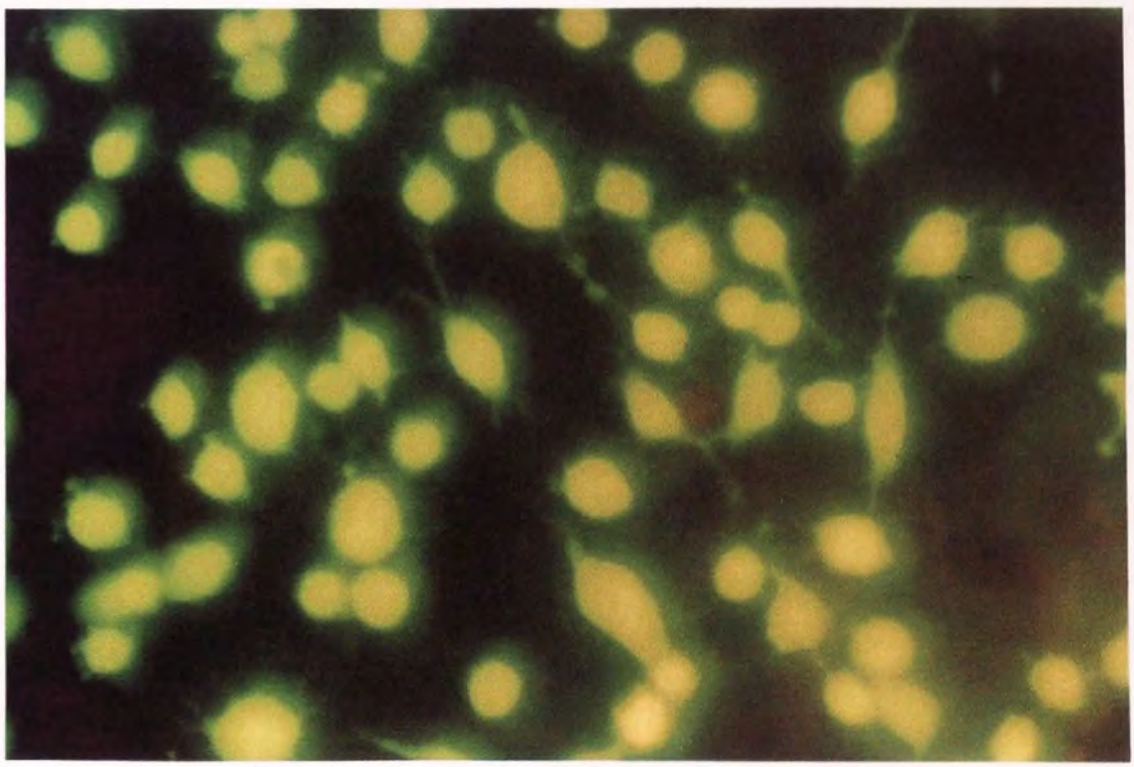

Figure 5.28 Calcein AM/Ethidium homodimer-1 fluorescent staining showing 3T3 adhesion to poly(HEMA) (negative control) (x400 magnification)

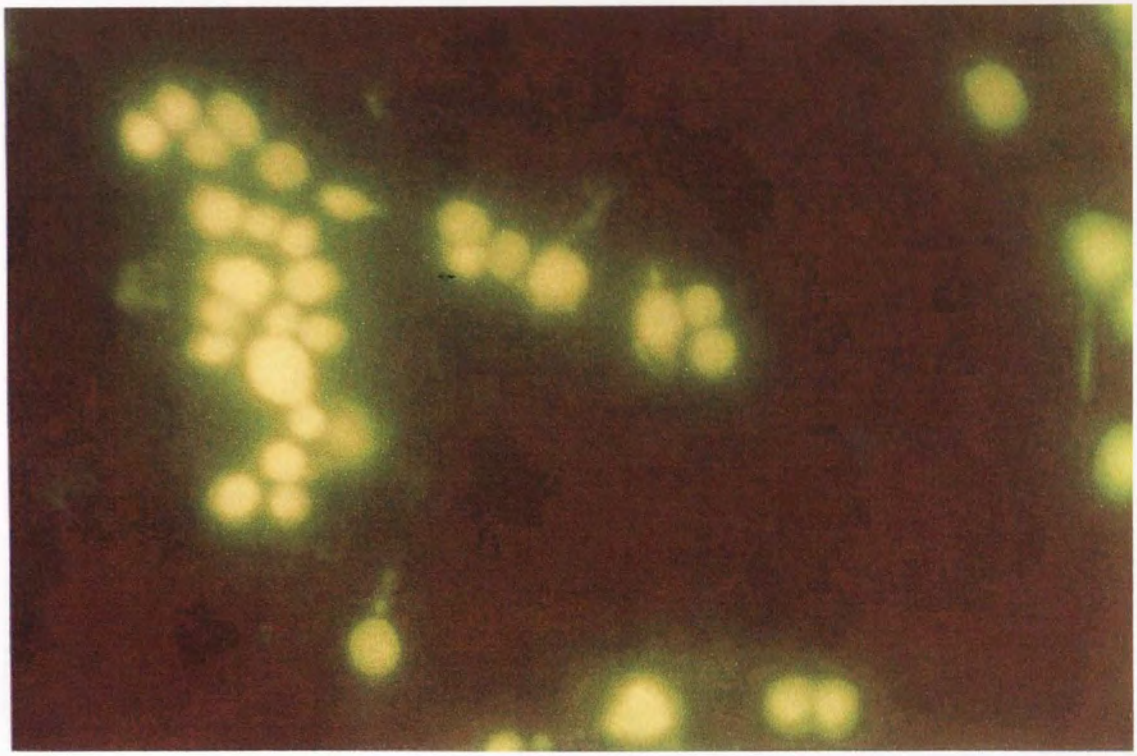

Figure 5.29 Calcein AM/Ethidium homodimer-1 fluorescent staining showing 3T3 adhesion to a NVP/MMA 70:30 (x400 magnification)

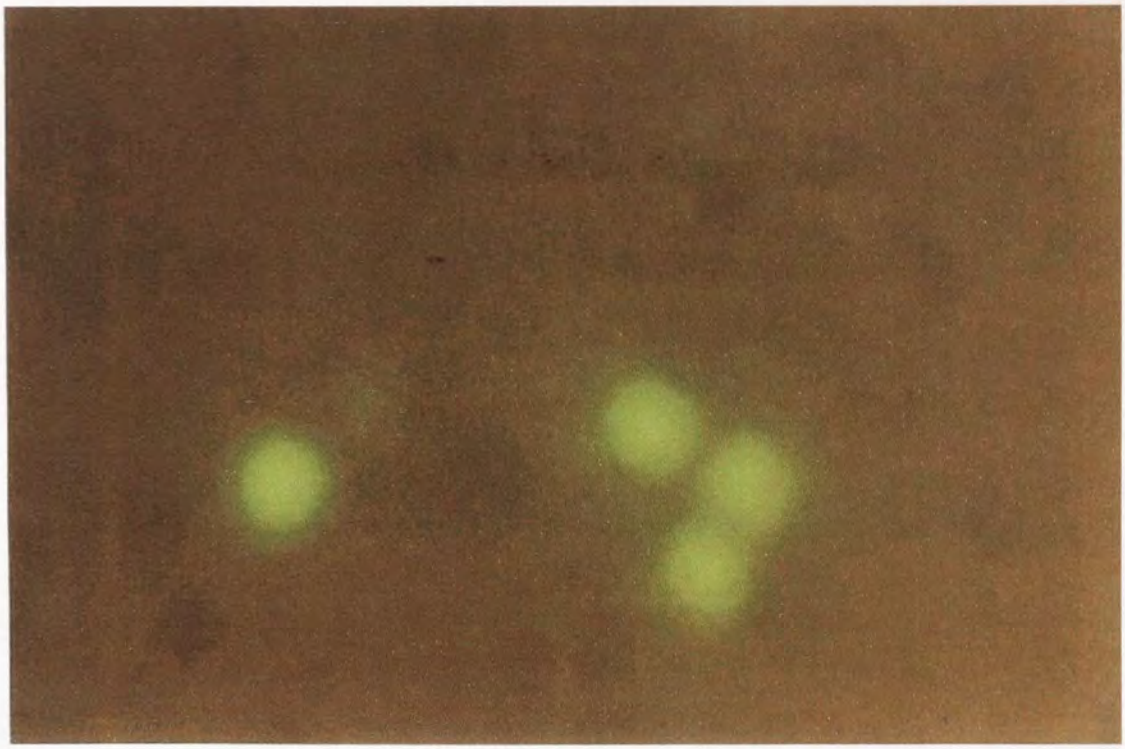

Cells did not adhere very well to the test hydrogels although they seemed to grow well on poly(HEMA). The apparent lack of dead cells is most likely due to the fact that cells with compromised membranes do not adhere and so were washed off before the assay. Although many cells were growing on poly(HEMA) during the 72 hour incubation period, some detatched during staining with calcein AM and ethidium homodimer-1, leaving a patchy coverage on the disc when viewed under the microscope. Cell counts were therefore deemed unreliable. The addition of calcein AM and ethidium homodimer-1 may be expected to weaken the adhesion and this would also account for the rounding of the cells. In view of the rapid observation after staining, it is also possible that some of the cells were less strongly attached on poly(HEMA) than on the glass coverslips. A reduced concentration of calcein AM and EthD-1 would perhaps alleviate the problem of detatching cells.

5.4.1.2 DAPI

Figure 5.30 Typical image obtained using the DAPI fluorescent stain (x400 magnification)

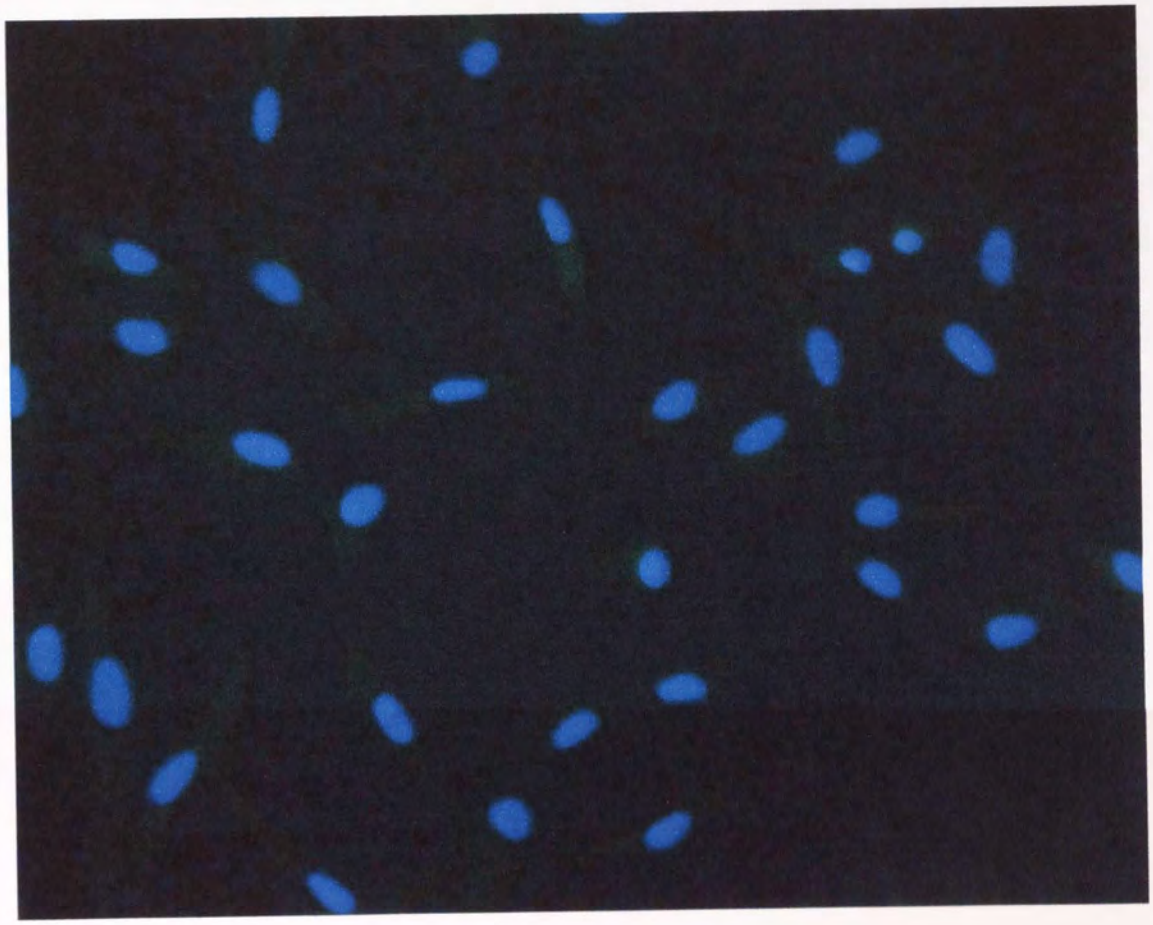

Cell counts obtained using the DAPI fluorescent stain are shown graphically below in Figure 5.31 (3T3 cells) and Figure 5.32 (EK1.BR cells). Actual values can be found in Appendix VI.

Figure 5.31 DAPI viability assay of hydrogels, glass (positive control) and poly(HEMA) (negative control), using 3T3 cells (mean (+/- SEM), n=6). Adherent cells were counted in 20 fields on each disc

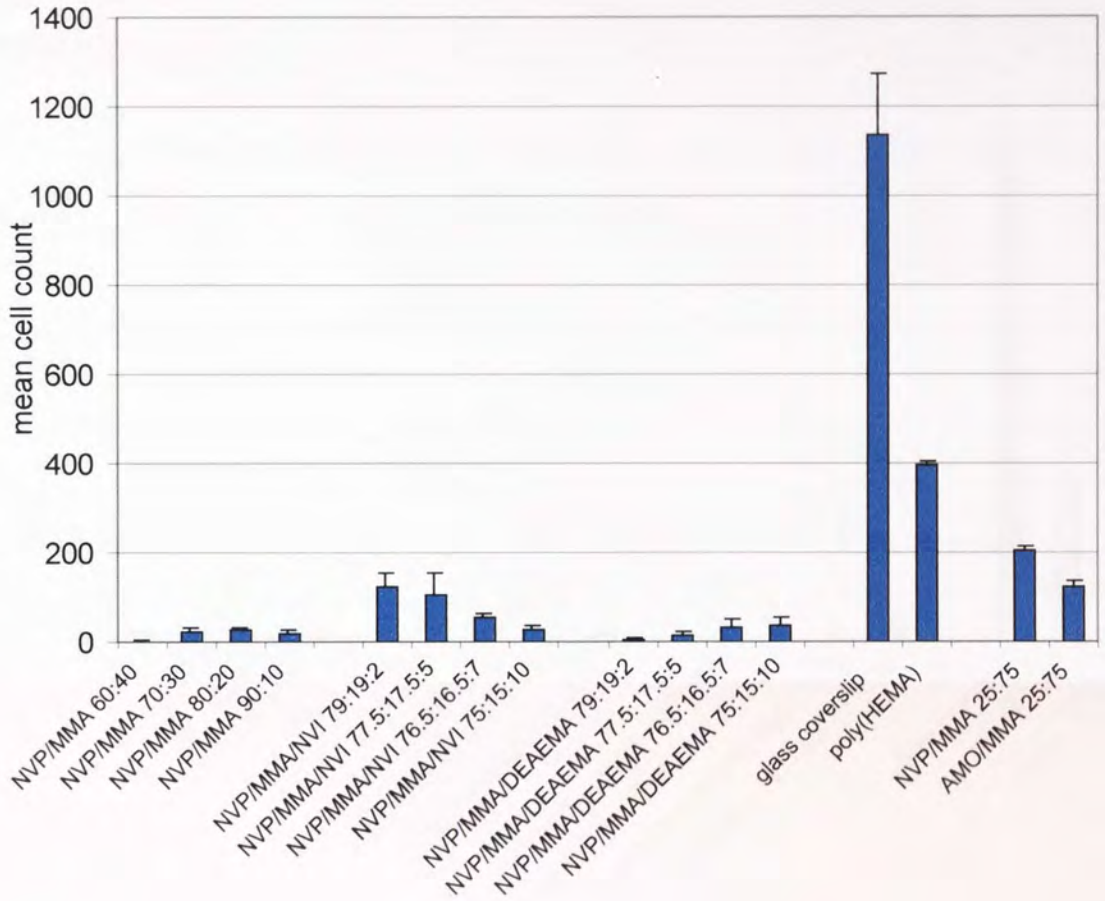

Figure 5.32 DAPI viability assay of hydrogels, glass (positive control) and poly(HEMA) (negative control), using EK1.BR cells (mean (+/- SEM), n=6) Adherent cells were counted in 20 fields on each disc

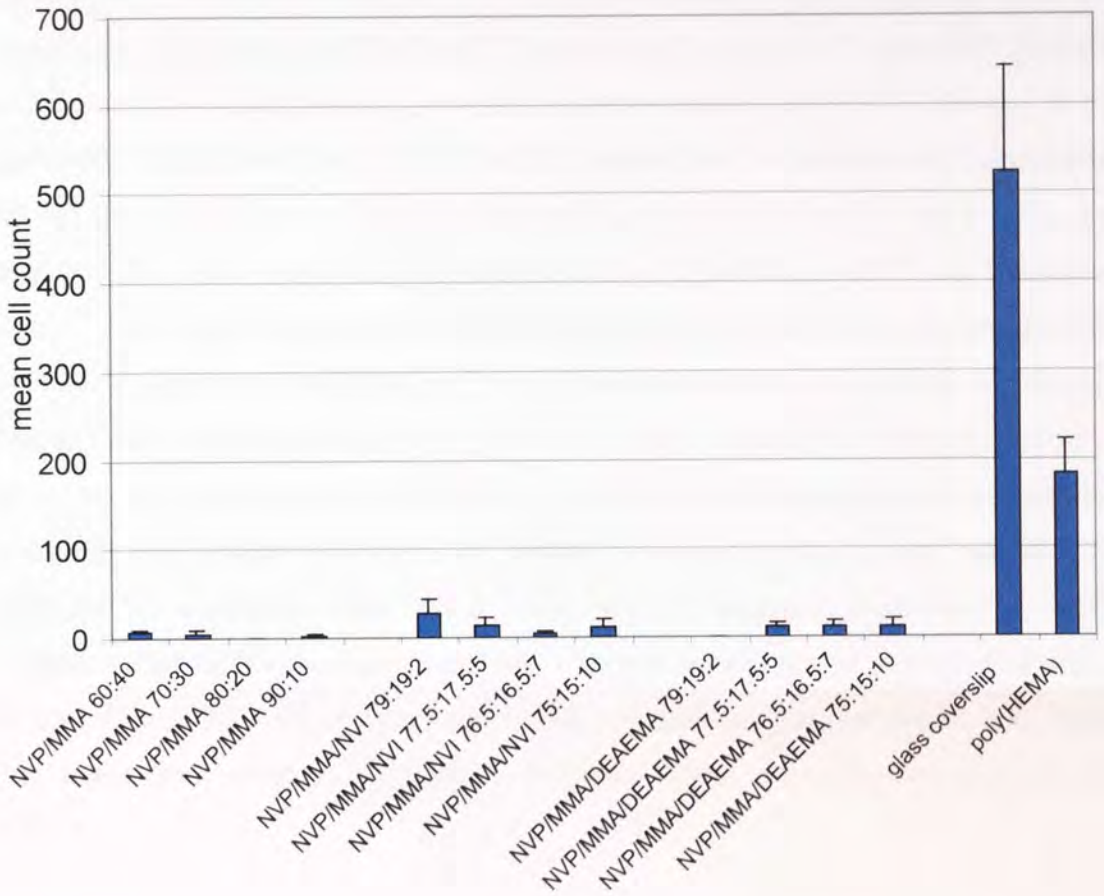

Results are similar for both 3T3 cells and EK1.BR cells, with glass coverslips exhibiting approximately 3 times the number of adhered cells than poly(HEMA), and with NVP/MMA copolymers showing very low cell counts. It is clear that 3T3 cells grow about twice as quickly as EK1.BR cells, this was noted during the routine maintenance of the cell lines. In view of the lack of cell adhesion on the NVP/MMA copolymers seen when carrying out the calcein AM assay, 3T3 cells were grown on two low water content copolymers for these DAPI assays. These copolymers had the compositions NVP/MMA 25:75 with an EWC of 14.1% and AMO/MMA 25:75 with an EWC of 17.7 %. Although cell adhesion was improved on these copolymers, it was still considerbly lower than the negative control poly(HEMA) (ANOVA $p<0.01$,

n=6). There appear to be no clearly identifiable trends from these results. An increase in hydrophilic monomer has no significant effect (ANOVA p=0.07 and p=0.41, n=6 for 3T3 and EK1.BR cells respectively) and the increase in one of two chargeable functional groups is inconclusive. It appears from these data that an increase in NVI causes a decrease in cell attachment, though the results were not statistically significant (ANOVA p=0.21 and p=0.45, n=6 for 3T3 and EK1.BR cells respectively); a small amount gives higher counts than if no NVI is present in the hydrogel, while an increase in DEAEMA causes an increase in cell attachment, though the results were not statistically significant (ANOVA p=0.51 and p=0.42, n=6 respectively). This may seem to contradict the results of Lee *et al.*[145] and Sandeman *et al.*[142] who found an increase in cell attachment when an aromatic ring was present, but NVI is positively charged at pH 7.4 so does not behave as an aromatic substituent. Nearly twice as many cells adhered to the low water content NVP/MMA copolymer as to the low water content AMO/MMA copolymer (heteroscedastic t-test $p<0.01$, n=6), this may be due to the small difference in water contents. It is of note that the AMO/MMA copolymer also has a more random sequence distribution. Ma[146] explained that AMO copolymers contain a greater proportion of non-freezing water compared with NVP copolymers and because of the stronger interaction with water this fact would account for AMO copolymers being less adhesive to cells and proteins.

Previous work[114, 2, 54, 56, 133] focused on the effect of equilibrium water content (EWC) on cell adhesion because the EWC is likely to have the biggest influence on material properties. Shown below in Figures 5.33 to 5.38 are the results obtained in the present work, for those polymers with similar EWCs to the materials studied by Minett[114, 2] Thomas[133] and Davies[54].

Figure 5.33 3T3 Cell count against Equilibrium Water Content (EWC) for NVP/MMA copolymers (mean (+/- SEM), n=6)

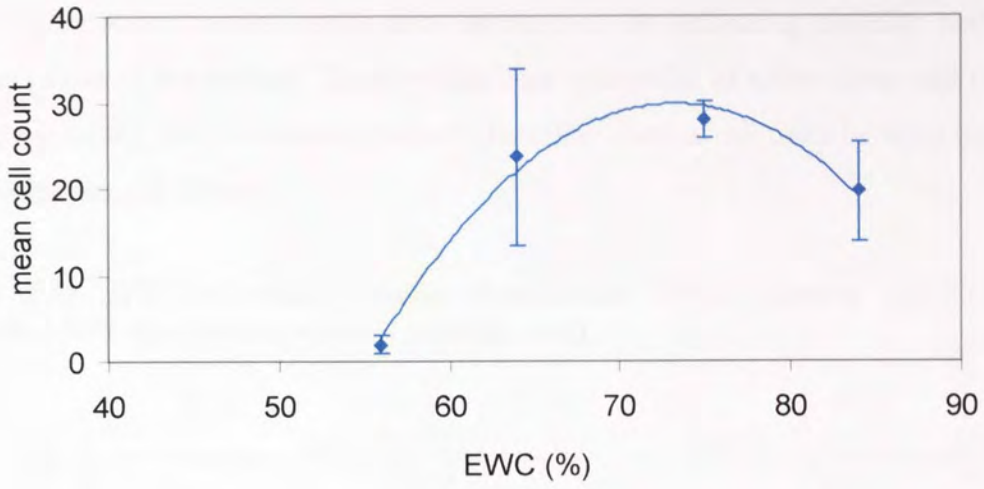

Figure 5.34 EK1.BR Cell count against Equilibrium Water Content (EWC) for NVP/MMA copolymers (mean (+/- SEM), n=6)

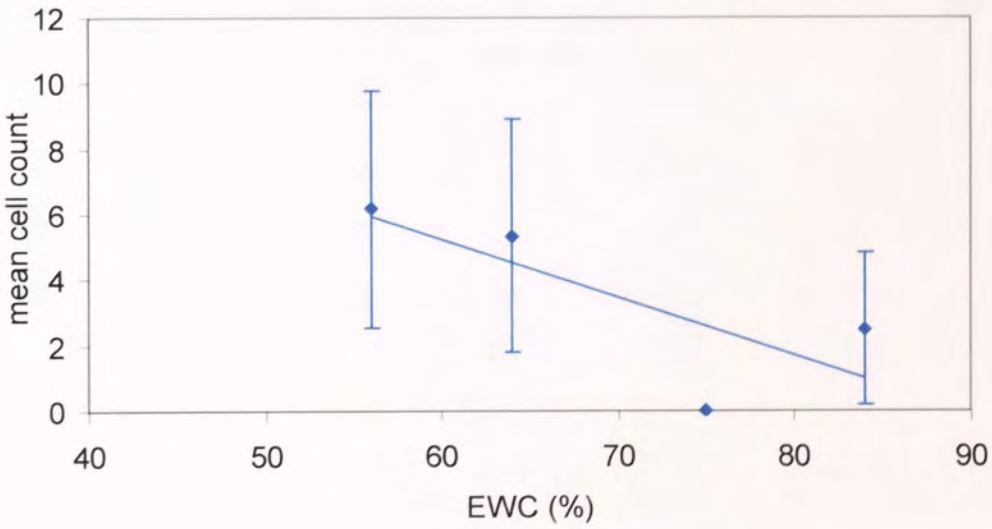

Cell adhesion on hydrogels of increasing hydrophilic monomer, and hence, water content, exhibited an increase in 3T3 cell attachment but a decrease in EK1.BR cell attachment though the results were not significant (ANOVA p=0.07 and p=0.41, n=6 respectively). It had been expected that both cell lines would show reduced adhesion on the higher water content copolymers because of the increasing mobility and the unstable nature of the surface. Usually fibroblast type cells, of which these cell types are two examples, tend to behave similarly therefore more work must be done before any conclusions are drawn.

Figure 5.35 3T3 Cell count against Equilibrium Water Content (EWC) for NVP/MMA/NVI copolymers (mean (+/- SEM), n=6)

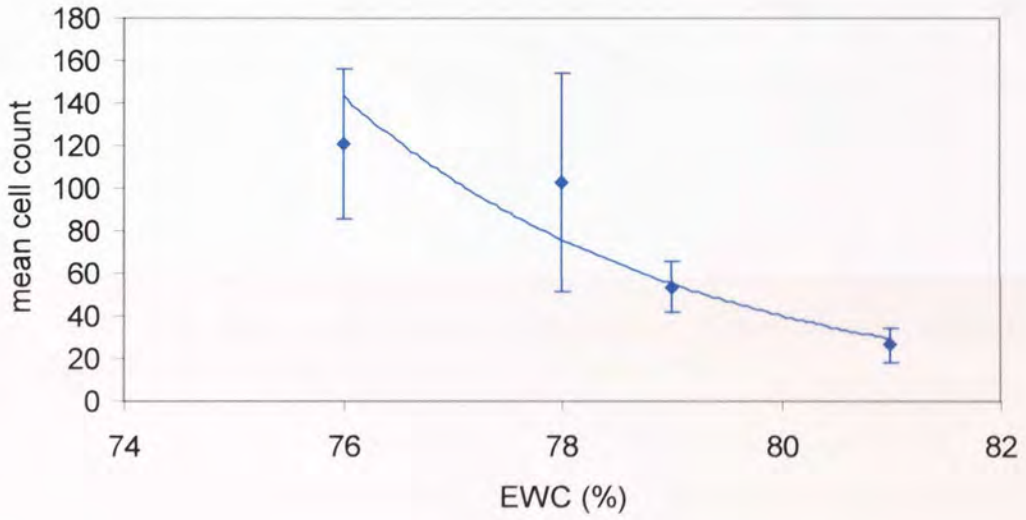

Figure 5.36 EK1.BR Cell count against Equilibrium Water Content (EWC) for NVP/MMA/NVI copolymers (mean (+/- SEM), n=6)

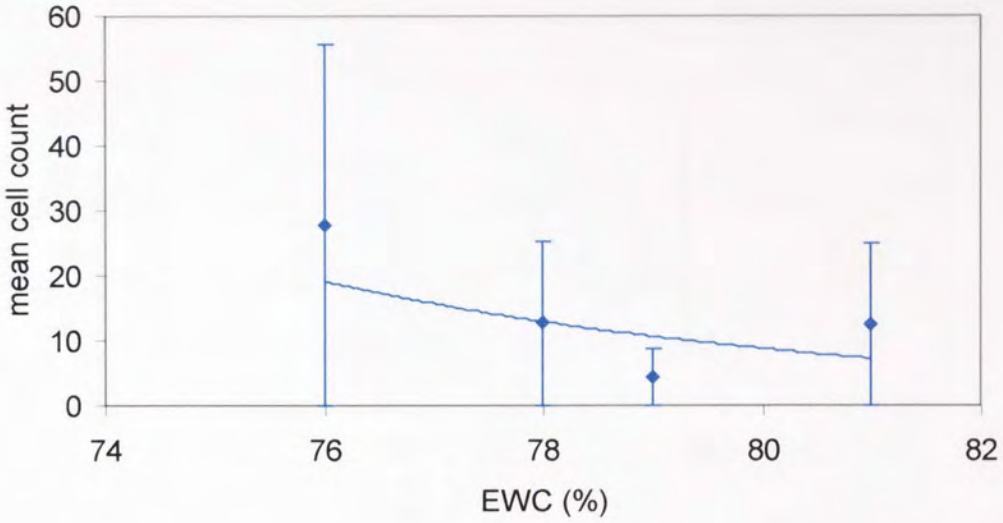

Figure 5.37 3T3 Cell count against Equilibrium Water Content (EWC) for NVP/MMA/DEAEMA copolymers (mean (+/- SEM), n=6)

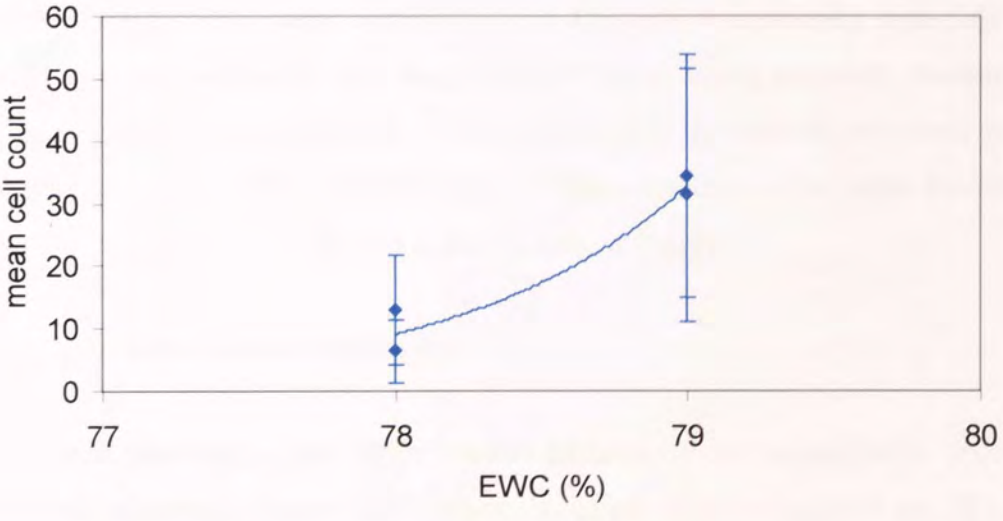

Figure 5.38 EK1.BR Cell count against Equilibrium Water Content (EWC) for NVP/MMA/DEAEMA copolymers (mean (+/- SEM), n=6)

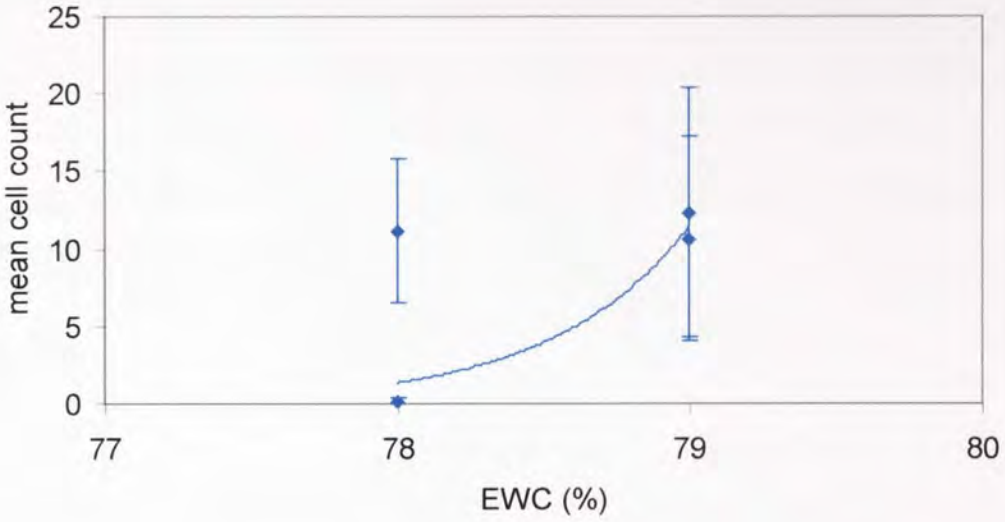

NVI containing copolymers appear to show a reduction in cell adhesion with increasing EWC for both cell lines studied (ANOVA p=0.21 and p=0.45, n=6 for 3T3 and EK1.BR cells respectively), while DEAEMA containing copolymers seem to show an increase in cell numbers with increasing EWC (ANOVA p=0.51 and p=0.42, n=6 respectively). The water contents of the DEAEMA containing materials are contained in a narrower range than those of the NVI containing materials, therefore it is difficult to draw any conclusions. The material with the highest cell count is the NVP/MMA copolymer with 2% NVI added. Higher amounts of ionisable functional groups may be toxic to cells due to a higher degree of charge.

5.4.1.2.1 Low water content hydrogels

As mentioned previously, low water content materials were sythesised in order to increase cell adhesion. Figure 5.39 shows the effect of water content on 3T3 cell count for these low water NVP/MMA and AMO/MMA copolymers. The hydrogel with the lowest EWC has the highest cell count, as would be expected. It should be remembered, however, that only two low water content materials were tested, and that

EWC is only one of a number of factors likely to affect cell adhesion, the others include surface chemical groups, surface energy and surface topology.

Figure 5.39 3T3 Cell count against Equilibrium Water Content (EWC) for low water content NVP/MMA and AMO/MMA copolymers (mean (+/- SEM), n=6)

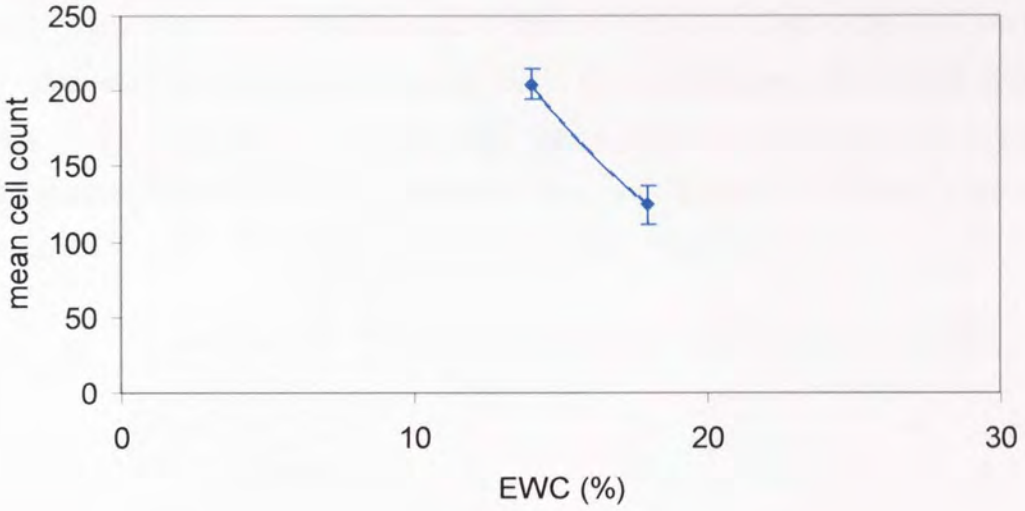

Figure 5.40 3T3 Cell count against Equilibrium Water Content (EWC) for both high and low EWC NVP/MMA copolymers (mean (+/- SEM), n=6)

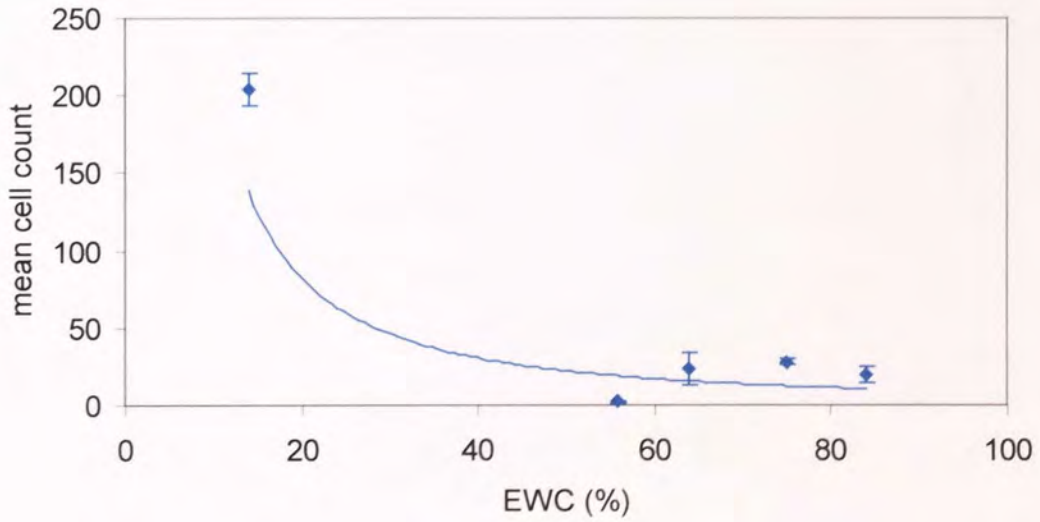

Figure 5.40 shows 3T3 cell adhesion onto all the neutral NVP/MMA copolymers studied. The curve is completely changed by the addition of the low EWC hydrogel result. The 'Minett' curve has not been reproduced, however. Moreover, the differences between the higher water content NVP/MMA copolymers are now seen to be insignificant. The low water content NVP/MMA copolymer, although having an increased cell count, is still only half as cell adhesive as the poly(HEMA) negative control. Such low cell counts observed on these NVP/MMA copolymers indicate that NVP containing polymers may be cytotoxic in the present state. This could also be true for AMO. If there is any unreacted monomer present in these materials then this would certainly make them toxic, though as shown in Chapter 4 the materials are well extracted.

5.4.2 SEM Micrographs

Figure 5.41 SEM micrograph of poly(HEMA) showing 3T3 attachment (x124 magnification)

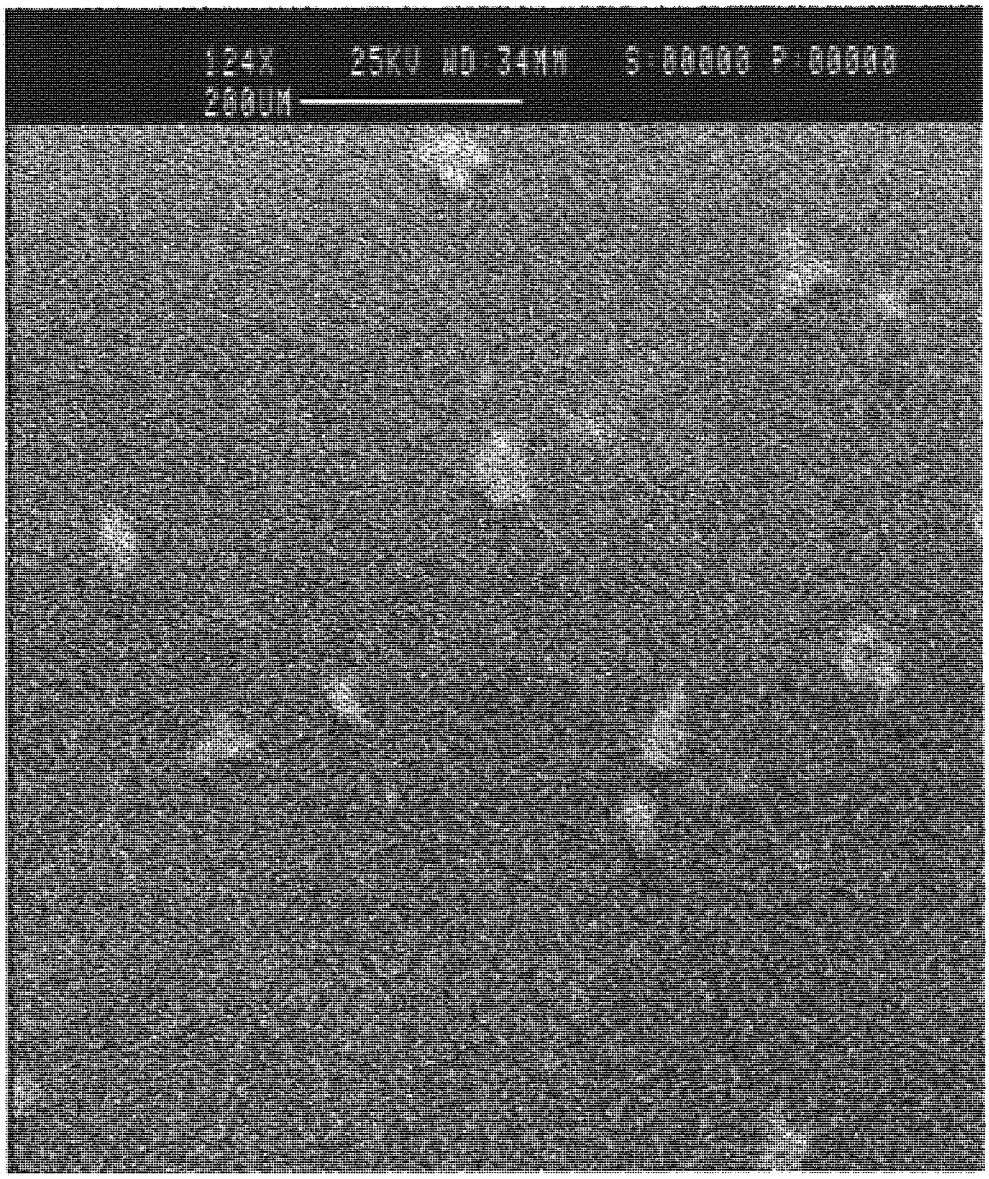

Figure 5.42 SEM micrograph of poly(HEMA) showing 3T3 attachment (x124 magnification)

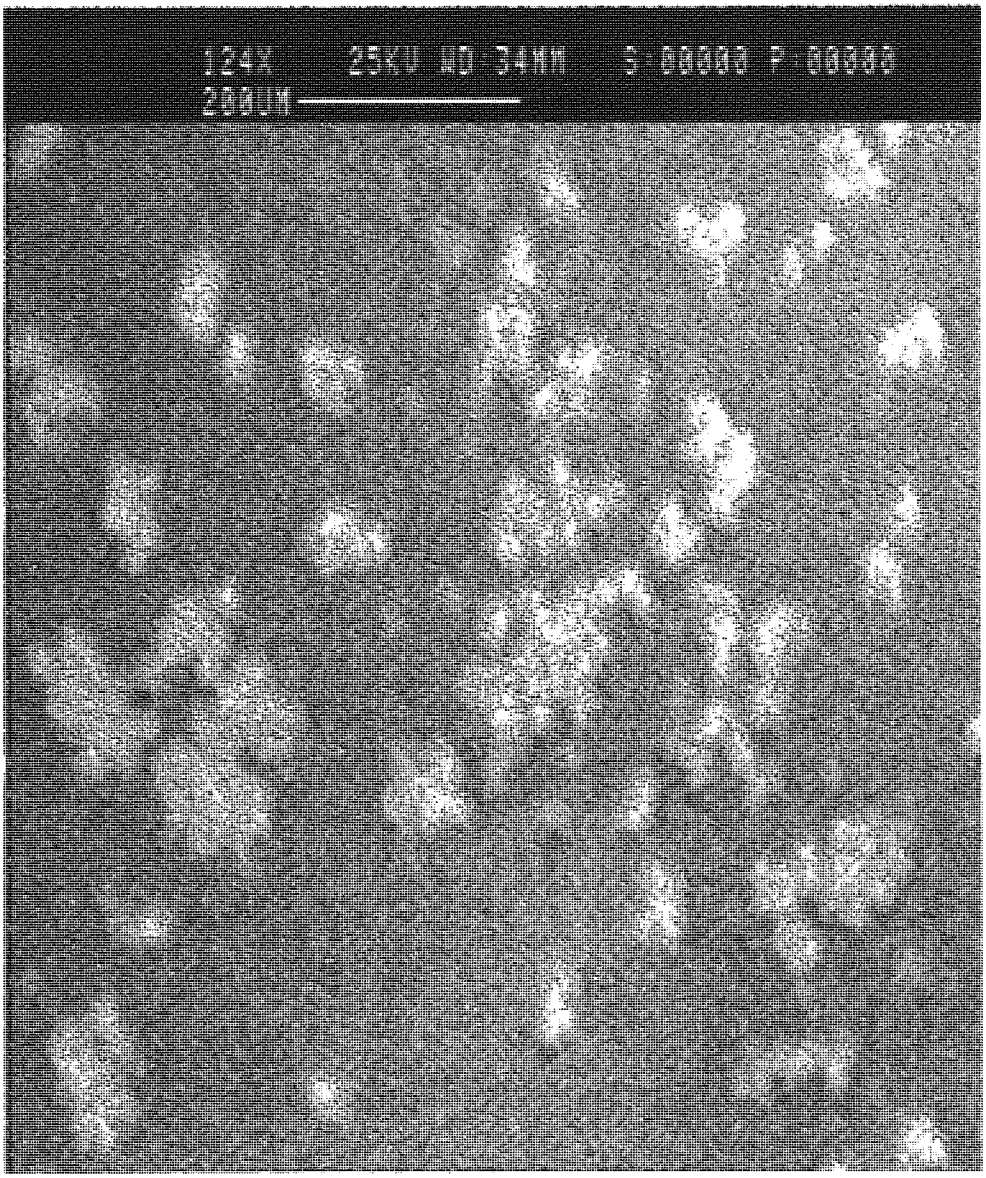

Figure 5.43 SEM micrograph of NVP/MMA/NVI copolymer at 79:19:2 composition showing 3T3 attachment (x198 magnification)

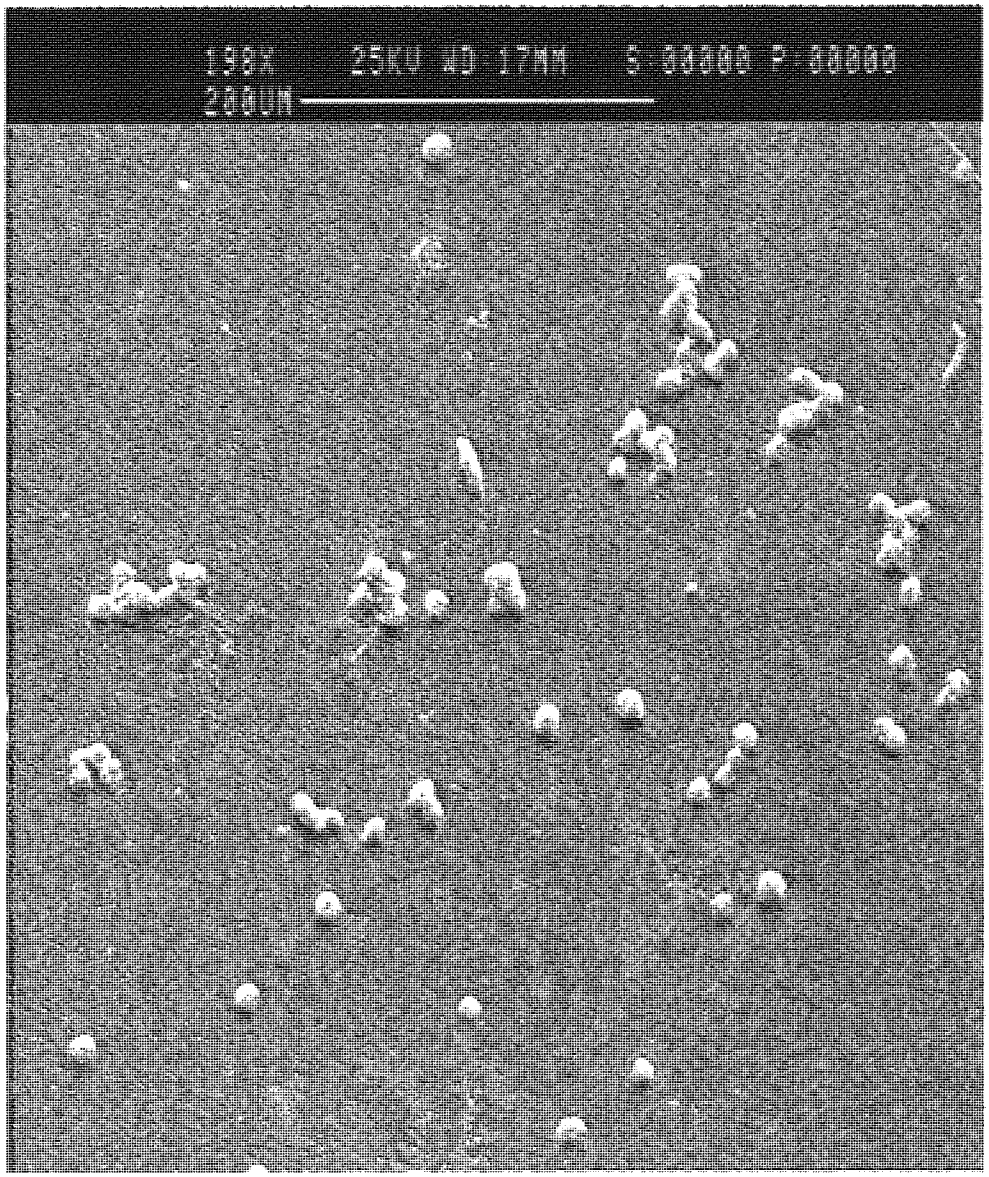

Figure 5.44 SEM micrograph of NVP/MMA/NVI copolymer at 77.5:17.5:5 composition showing 3T3 attachment (x192 magnification)

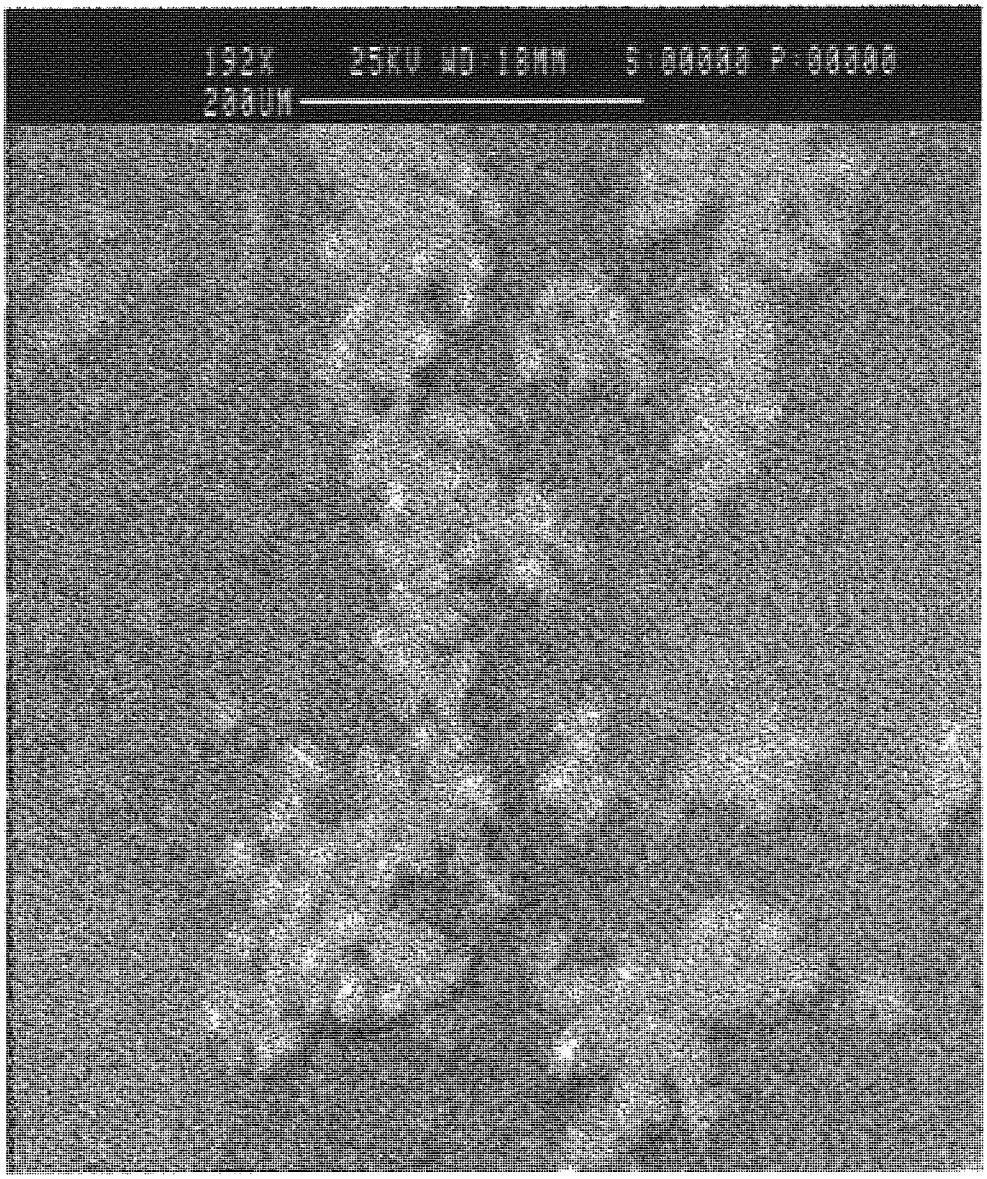

Figures 5.41 to 5.44 show fixed cells adhered to hydrogels as viewed under the scanning electron microscope. Cells tended to be rounded and clustered together, and the observed cell density was very low. Critical point drying is a method of dehydration which may have caused less sample distortion than the microwave technique used.

5.5 Discussion

Cell adhesion results indicate much lower cell counts on hydrogels than previously achieved by Minett[114, 2], Thomas[133], and Davies[54]. This can be explained by the fact that more accurate methods of counting cells were employed. The trypan blue exclusion test used by these authors is known to overestimate the number of viable cells, the results presented here are more reliable due to the fluorescent techniques used.

In addition, past researchers in this laboratory[114, 133, 54, 56, 2, 150] washed hydrogel samples in Tween or Teepol detergents prior to testing. This was carried out to remove contaminants such as skin lipids from the surface of the hydrogels. Skin lipids would undoubtedly affect the surface properties and hence cell adhesion. However, it is also well known among surface chemists that detergents are very difficult to remove from surfaces, even with prolonged rinsing. Most detergents contain ionic groups that may also interact with chargeable groups on the polymer. Since any detergent would have the effect of reducing surface energy, it could be expected that cell adhesion would be reduced, but this does not account for the higher counts of previous workers. It was therefore decided to manipulate the hydrogels only with tweezers, eliminating the need for washing with surfactants.

The poly(HEMA) negative control was found to be significantly more cell adhesive than any of the hydrogels under investigation. Although poly(HEMA) is generally considered to be non cell adhesive commercial supplies of the monomer contain small amounts of impurities such as ethylene glycol dimethacrylate (EGDMA) and methacrylic acid (MAA). This is because HEMA readily disproportionates leaving appreciable amounts of these chemicals which have an effect on cell adhesion. As discussed earlier Bergethon *et al.*[139] reported the cell adhesive properties of methacrylic acid when incorporated in hydrogels at levels of between 0.01% and 0.1%. The HEMA monomer supplied by Laporte for this study was a high purity batch and contained 0.015% methacrylic acid. The EWC of poly(HEMA) samples was tested before and after boiling in sodium carbonate solution; the presence of MAA was confirmed by the increase in EWC after this treatment. Therefore, this

may account for the cell counts obtained on poly(HEMA). It is impossible to stop the disproportionation of HEMA though Hydron Z6 contact lenses manufactured by Biocompatibles are known to contain very low levels of MAA and could be tested for cell adhesiveness. One NVP copolymer was synthesised containing 0.5% methacrylic acid in order to substantiate this theory though has not yet been tested.

Also, ionic polymers will only be charged if they are dissociated so that an anion or cation is present on the chain. It is often unclear whether surfaces described in the literature are truly charged, or if their ionic groups are fully dissociated.

Cell counts on the NVP/MMA and AMO/MMA copolymers were very low indeed. This raises the question of cytotoxicity. Increased numbers of cells were counted on the lower water content NVP/MMA and AMO/MMA copolymers, but this may be due to the fact that only 25% of each polymer was composed of NVP or AMO respectively. The calcein AM/ethidium homodimer-1 assay is a suitable cytotoxicity test because EthD-1 stains dead cells red. However, very few dead cells were seen under the microscope with the hydrogels under study and this is probably due to the fact that dead cells usually have compromised membranes and therefore will detach from the surface of the hydrogel. By using an inverted fluorescence microscope it would be possible to examine the contents of the well plates after removal of the sample disc; this was not available in our laboratory. This may reveal dead cells and a cytotoxic effect. Unpolymerised monomer may be expected to cause cytotoxicity though this is most unlikely because of the lengthy extraction process with distilled water. Surface tension results in Chapter 4 confirm that no surface active monomers were leachable from the polymers.

NVP containing copolymers have been used successfully for many years as contact lenses. However, these polymers may still be slightly cytotoxic. In a similar manner, it was recently shown that certain sun lotions containing the UVB filter octyl methoxycinnamate (OMC) or the UVA filter butyl methoxydibenzoylmethane are, in fact, cytotoxic, especially when placed under ultraviolet light[182]. Sun lotions are very useful for preventing sunburn though the compounds they contain are toxic to skin cells.

If NVP and AMO copolymers are cytotoxic then one may ask how Thomas[133], and Davies[54] observed higher cell counts on NVP containing copolymers. Thomas and Davies tested hydrogels synthesised by Baker[183] and Corkhill[81] and consequently these materials may have been made 10 years before the cell adhesion testing. Hydrogels are commonly stored in unsterilised distilled water; after a few months standing algae can be seen growing on the samples. Cells will probably attach to almost any material if given a long enough contact time as they will begin to construct their own adhesive matrix. The algae and algal matter may not have been fully removed during the cleaning stage. Once protein deposition has occurred on a surface, cells will attach much more readily as the adsorbed protein at the surface, rather than the underlying polymer, regulates cell adhesion.

Fitton[56] mentioned that densely charged surfaces, such as can be achieved by coating with poly(L-lysine), can override the effects of protein mediated adhesion. This may be a useful technique to encourage initial cell attachment to materials which would otherwise be non cell adhesive, provided that integration into the polymer matrix was not necessary. Also, the fact that protein mediated adhesion can be overridden possibly accounts for the decrease in cell numbers seen with increasing NVI concentration.

During the calcein AM/ethidium homodimer-1 assay it was noted that cells became rounded and tended to detatch from the substrate. Cells fluoresced very brightly under the microscope so a reduced concentration of calcein AM and ethidium homodimer-1 would not adversely affect visibility of stained cells. A reduced concentration would probably also be less damaging to the cells, resulting in a reduction in detachment. The concentration could reasonably be halved to 1 μM calcein AM and 2 μM EthD-1.

5.6 Conclusions

Cell adhesion is induced by cell factors, extracellular materials and substrate factors. Substrate factors controlling cell adhesion include hydrophilicity/hydrophobicity,

surface group expression, surface energy, surface morphology, surface charge, sequence, distribution, and equilibrium water content (EWC).

The work described in this thesis was carried out in order to continue the work of Minett[114, 2], Thomas[133] and Davies[54] and to investigate cell adhesion on hydrogels containing ionic functional groups. The work was carried out using reliable fluorescent techniques and scanning electron microscopy (SEM) for assessing cell adhesion. Both 3T3 and EK1.BR cells were used, with results being similar for both cell lines.

A poly(HEMA) negative control exhibited a lower level of cell adhesion than the glass positive control, but a much higher level than the NVP and AMO copolymers under investigation. Low water content hydrogels were synthesised which exhibited higher cell counts, though still much lower than poly(HEMA). The 'Minett' shape curve was not reproduced and no apparent trends were visible as regards equilibrium water content, with differences in cell counts at the higher water contents negligible. This may be due to the more dependable techniques used, the fact that hydrogels were not washed with detergents, and the fact that hydrogels were tested rapidly after synthesis. The possibility that the NVP and AMO copolymers tested may be cytotoxic has been discussed.

Improvements to the techniques employed in the continued development of the keratoprosthesis have been suggested.

5.7 Further Work

The long term goal of tissue engineering is to be able to control cell adhesion with precision. The artificial cornea is one example where both a cell adhesive material and a non cell adhesive material are required. There may be potential applications where it would be desirable to be able to switch cell adhesion on or off, depending on the specific requirements. Hypercoiling polymers[184] are environment sensitive 'smart' hydrogels that transform their structure and surface properties with chemical

or physical changes such as pH. These rapidly changing polymers may be of great importance in the future.

One MAA containing gel needs to be tested in order to prove or disprove the hypothesis that poly(HEMA) was the most cell adhesive hydrogel tested due to the presence of methacrylic acid caused by disproportionation of HEMA monomer.

Direct charge effects, which can override the effects of protein mediated adhesion, remain to be investigated. Samples could be coated with poly(L-lysine) in order to encourage cell attachment.

Further work needs to be done on the copolymers tested in this work, other ionic monomers available include the acidic itaconic acid (ITA), (3-sulphopropyl)-acrylate potassium salt (SPA), itaconic acid bis-(3-sulphopropyl)-ester, di potassium salt (SPI), and the zwitterionic *N*,*N*-dimethyl-*N*-(2-methacryloyloxyethyl)-*N*-(3-sulphopropyl) ammonium betaine (SPE), *N*,*N*-dimethyl-*N*-(3-methacrylamidopropyl)–*N*-(3-sulphopropyl) ammonium betaine (SPP), and 1-(3-sulphopropyl)-2-vinylpyridinium betaine (SPV).

CHAPTER 6
DISCUSSION

6.1 Discussion

This chapter serves to bring together the results from the experimental chapters of this thesis (Chapters 2, 3, 4 and 5), and discuss the links between them so that a coherent picture may be seen. One aim of this work was to develop predictive techniques for cell adhesion. In this chapter results from the most cell adhesive materials are compared with results from the least cell adhesive materials.

Table 6.1 A small selection of materials tested and their cell counts for both 3T3 and EK1.BR cells compared with the glass positive control. (Cell counts are expressed as a percentage of the positive control values)

	3T3 Cell number	**Percentage of cell count on glass %**	**EK1.BR Cell number**	**Percentage of cell count on glass %**
Most cell adhesive:				
Glass	1136.67	100	524.6	100
poly(HEMA)	393.5	34.6	182.4	34.8
NVP/MMA/NVI 79:19:2	121.0	10.6	27.83	5.3
NVP/MMA 25:75	204.67	18.0	N/A	N/A
Least cell adhesive:				
NVP/MMA 60:40	2.0	0.0	6.17	1.2
NVP/MMA/DEAEMA 79:19:2	6.33	0.6	0.17	0.0

Table 6.2 A small selection of materials tested with their results from static contact angle measurements

	Water θ°	CH_2I_2 θ°	Polar mN/m (dehydrated)	Dispersive mN/m (dehydrated)	Octane θ°	air θ'°	polar mN/m (hydrated)	dispersive mN/m (hydrated)
Most cell adhesive:								
poly(HEMA)	70.7	37.2	8.5	35	134.2	37.6	36.7	22.1
NVP/MMA/NVI 79:19:2	77.6	32.5	4.4	39.3	141.5	37.3	40.5	18.2
NVP/MMA 25:75	75.1	19.2	4.3	44.1	114.65	52.7	25.6	22.9
Least cell adhesive:								
NVP/MMA 60:40	85.6	23.7	1.2	45.6	131.9	37.9	35.5	23.4
NVP/MMA/DEAEMA 79:19:2	69.2	22.3	7.3	41.4	142	35	40.8	19.5

Although it was hoped that the surface chemistry would predict cell behaviour this has not been the case. Cell adhesion was measured using the Calcein AM and Ethidium homodimer-1 (EthD-1) assay, the DAPI assay, and by Scanning Electron Microscopy (SEM). Of all the hydrogels tested in this study, poly(HEMA) was found to be the most cell adhesive (see Table 6.1), with a cell count of 35% compared with the count on glass (the cell number for glass was assigned a value of 100%), with both 3T3 and EK1.BR cells.

Table 6.2 shows contact angles together with the polar and dispersive component of surface free energy for some of the materials under investigation, both in the dehydrated and hydrated states.

In the dehydrated state, poly(HEMA) was found to have a total surface free energy of 43.5 mN/m, the polar component being 8.5 mN/m and the dispersive component being 35 mN/m. However, these figures for the surface properties are not sufficient or even necessary for cell adhesion. The NVP/MMA 25:75 composition achieved a cell count of 18% compared with glass and had a slightly higher surface free energy of 48.4 mN/m, though the polar component was only 4.3 mN/m and the dispersive component was 44.1 mN/m. The material having the third highest cell count was the

NVP/MMA/NVI 79:19:2 composition with 11% coverage compared with glass using 3T3 cells and 5% using EK1.BR cells. The polar and dispersive components of surface free energy were determined as 4.4 mN/m and 39.3 mN/m respectively, giving a total surface free energy of 43.7 mN/m. The best of these poorly cell adhesive materials therefore showed varying surface free energy values.

Likewise, the worst materials with respect to cell adhesion also produced varying surface free energy values. For example, the NVP/MMA 60:40 copolymer demonstrated a cell count of 0% compared with glass for 3T3 cells and 1% for EK1.BR cells. The polar and dispersive components of surface free energy were measured as 1.2 mN/m and 45.6 mN/m respectively, giving a total surface free energy of 46.8 mN/m (only slightly higher than the value for poly(HEMA) and lower than the value for the NVP/MMA 25:75 composition). Another poor hydrogel was the NVP/MMA/DEAEMA 79:19:2 composition which showed a cell count of 1% compared with glass for 3T3 cells and 0% for EK1.BR cells. However, this material had a polar component of surface free energy of 7.3 mN/m (close to the value for poly(HEMA)) and a dispersive component of 41.4 mN/m (close to the value for the NVP/MMA/NVI 79:19:2 composition) giving a total surface free energy of 48.7 mN/m.

A similar lack of correlation was observed in the hydrated state. poly(HEMA) was found to have a total surface free energy of 58.8 mN/m, the polar component being 36.7 mN/m and the dispersive component being 22.1 mN/m. The NVP/MMA 25:75 composition had a lower surface free energy of 48.5 mN/m, though the polar component was only 25.6 mN/m and the dispersive component was 22.9 mN/m. The NVP/MMA/NVI 79:19:2 composition gave polar and dispersive components of 40.5 mN/m and 18.2 mN/m respectively, giving a total surface free energy of 58.7 mN/m.

The worst materials with respect to cell adhesion also produced varying surface free energy values in the hydrated state. For example, the polar and dispersive components of surface free energy for the NVP/MMA 60:40 copolymer were measured as 35.5 mN/m and 23.4 mN/m respectively, giving a total surface free energy of 58.9 mN/m (almost identical to poly(HEMA)). The NVP/MMA/DEAEMA 79:19:2 terpolymer had a polar component of surface free energy of 40.8 mN/m

(almost identical to the NVP/MMA/NVI 79:19:2 composition) and a dispersive component of 19.5 mN/m giving a total surface free energy of 60.3 mN/m.

Therefore, in both the dehydrated and hydrated states, it is not possible to expect a certain cell count for a given surface free energy value. High values can lead to both high and low cell counts and the same is true for low values. Cell adhesion appears to be determined neither by the polar component nor the dispersive component of surface free energy, it is therefore likely that other factors are involved.

Table 6.3 A small selection of materials tested with their advancing, receding and hysteresis angles from dynamic contact angle measurements

	Water			**1% FCS**			**10% FCS**			**100% FCS**		
	θ_A^o	θ_R^o	θ_H^o	θ_A^o	θ_R^o	θ_H^o	θ_A^o	θ_R^o	θ_H^o	θ_A^o	θ_R^o	θ_H^o
Most cell adhesive:												
poly(HEMA)	92.9	26.6	66.2	50.1	47.9	2.2	68.2	64.5	3.7	61.0	54.9	6.1
NVP/MMA/NVI 79:19:2	0	0	0	51.1	45.6	5.5	60.5	57.0	3.5	59.3	55.3	4.0
NVP/MMA 25:75	68.8	14.0	54.8	36.6	20.1	16.5	48.4	39.2	9.2	53.2	38.8	14.4
Least cell adhesive:												
NVP/MMA 60:40	44.6	0	44.6	107.3	103.3	4.0	61.3	59.1	2.2	65.2	63.2	2.0
NVP/MMA/DEAEMA 79:19:2	55.8	41.4	14.5	38.4	32.4	6.0	56.8	48.1	8.7	60.0	58.2	1.8

Dynamic contact angle measurements were made using different test solutions so that the materials tested could be distinguished from each other more easily and, in the case of foetal calf serum, that a biological environment could be mimicked thereby aiding the pre-selection of potential biomaterials. However, advancing and receding angles and hysteresis values were not found to correlate with cell adhesion results.

In water, the most cell adhesive hydrogel tested, poly(HEMA) (with a cell count of 35% compared with glass) had advancing and receding angles of 92.9° and 26.6° respectively, giving a hysteresis of 66.2°. The NVP/MMA 25:75 copolymer (with a cell count of 18% compared with glass) produced a hysteresis of 54.8° from

advancing and receding angles of 68.8° and 14.0° respectively. However, the NVP/MMA/NVI 79:19:2 terpolymer gave values of 0.0° for both the advancing and receding angles and the hysteresis yet a few cells had attached (11% coverage compared with glass for 3T3 cells and 5% for EK1.BR cells).

The least cell adhesive hydrogels also gave varying results. The NVP/MMA 60:40 copolymer (0% compared with glass for 3T3 cells and 1% for EK1.BR cells) displayed an advancing angle of 44.6°, a receding angle of 0.0°, producing a hysteresis of 44.6°. The NVP/MMA/DEAEMA 79:19:2 terpolymer (which showed a cell count of 1% compared with glass for 3T3 cells and 0% for EK1.BR cells) had advancing and receding angles of 55.8° and 41.4° respectively, giving a hysteresis of 14.5°. Therefore, a cell adhesive gel cannot necessarily be characterised by having a high hysteresis value, though poly(HEMA) did have the highest value, along with the highest advancing angle, that is to say the least wettable and most mobile surface.

When 1% FCS was used as the dipping solution poly(HEMA) gave a hysteresis value of 2.2° from advancing and receding angles of 50.1° and 47.9° respectively. The NVP/MMA 25:75 copolymer produced a hysteresis of 16.5° from advancing and receding angles of 36.6° and 20.1° respectively. The NVP/MMA/NVI 79:19:2 terpolymer gave values of 51.1° for the advancing angle and 45.6° for the receding angles giving a hysteresis of 5.5°. Again, the difficulty in interpreting these results is that the NVP/MMA 25:75 composition has lower advancing and receding angles and a higher hysteresis than the other two hydrogels (whose values are more closely related) yet exhibited a higher cell count than the NVP/MMA/NVI 79:19:2 terpolymer.

When looking at the least cell adhesive hydrogels under study, the NVP/MMA 60:40 material had advancing and receding angles of 107.3° and 103.3° respectively, giving a hysteresis of 4.0° and the NVP/MMA/DEAEMA 79:19:2 material had advancing and receding angles of 38.4° and 32.4° respectively, giving a hysteresis of 6.0°. Unfortunately, it is clear that in 1% FCS dynamic contact angle measurements do not predict cell behaviour, although in Chapter 4 it was observed that a 1% concentration was the most promising level of FCS because it appeared to allow differences between materials to be observed.

Using 10% FCS does not improve the ability to determine cell adhesion from dynamic contact angle results. Poly(HEMA) was found to have advancing and receding angles of 68.2° and 64.5° respectively, giving a hysteresis of 3.7°. The NVP/MMA 25:75 polymer had much lower advancing and receding angles of 48.4° and 39.2° respectively, but a higher hysteresis of 9.2°. The NVP/MMA/NVI 79:19:2 polymer had advancing and receding angles of 60.5° and 57.0° respectively, producing a hysteresis of 3.5°.

The least adhesive gels, however, produced similar results. The NVP/MMA 60:40 material had advancing and receding angles of 61.3° and 59.1° respectively, giving a hysteresis of 2.2° and the NVP/MMA/DEAEMA 79:19:2 material had advancing and receding angles of 56.8° and 48.1° respectively, giving a hysteresis of 8.7°.

When 100% FCS was used as the dipping solution poly(HEMA) gave a hysteresis of 6.1° from an advancing angle of 61.0° and a receding angle of 54.9°. The NVP/MMA 25:75 hydrogel showed a lower advancing angle of 53.2° and a lower receding angle of 38.8°; the hysteresis being 14.4°. The NVP/MMA/NVI 79:19:2 hydrogel produced a hysteresis of 4.0° from an advancing angle of 59.3° and a receding angle of 55.3°.

When looking at the least cell adhesive hydrogels under study, the NVP/MMA 60:40 material had advancing and receding angles of 65.2° and 63.2° respectively, giving a hysteresis of 2.0° and the NVP/MMA/DEAEMA 79:19:2 material had advancing and receding angles of 60.0° and 58.2° respectively, giving a hysteresis of 1.8°. It was observed in Chapter 4 that 10% and 100% FCS solutions led to an excess of serum when the sample was removed from the dipping solution because the hydrogels were only able to adsorb a limited amount of the serum constituents. By this it is meant that the surface area of the test sample is completely covered by adsorbed components of serum and hence further adsorption does not occur with an increase in concentration of serum.

Therefore the surface chemistry is not an indicator of cell adhesion. It is likely that these techniques are not sensitive enough to distinguish between the materials. As emphasized previously in Chapter 5, cell adhesion is probably determined by several different factors, explaining the difficulty of isolating single causative properties.

However, it would be interesting to test, using surface chemistry, a hydrogel having much higher cell counts if one can be found.

One factor which influences the surface properties is sequence distribution of the polymer. In Chapter 4 it was shown how samples from one NVP/MMA copolymer membrane produced more varied wettability results than samples from one poly(HEMA) membrane. The variation arises from a non homogeneous surface. Sequence distribution simulations and CHN results shown in Chapter 2 demonstrate the uneven distribution of monomers in the NVP/MMA copolymer. It would be interesting to see how the wettability varies on samples of an AMO/MMA membrane which, according to the simulations shown in Chapter 2, has a more even sequence distribution. However, the AMO/MMA copolymer still achieved very low cell counts compared with poly(HEMA), inspite of its more even sequence distribution.

According to the 'Minett' curve, reducing the EWC of a hydrogel can improve the cell count. Whilst it is obvious that cells will not be able to adhere to a material of very high water content due to the mobility of water at the surface, there has been no visible trend in this study from low to high water content hydrogels. The NVP/MMA and AMO/MMA materials at 25:75 composition had equilibrium water contents of 14% and 18% respectively, yet achieved much lower cell counts than poly(HEMA) having an EWC of 38%. In addition, the AMO/MMA copolymer produced achieved a lower cell count than the corresponding low water content NVP/MMA hydrogel despite a more even theoretical sequence distribution.

In the case of hydrogels containing ionic monomer, NVI containing hydrogels generally gave higher cell counts than did DEAEMA containing hydrogels. In Chapter 2 it was found that DEAEMA was more randomly incorporated in the polymers than NVI, producing a more even sequence distribution. Fitton[56] suggested that densely charged surfaces can override the effects of protein mediated adhesion. Accordingly, there may be more than one mechanism of cell adhesion. Although one protein may displace another already attached to a surface (Vroman effect, as discussed in Chapter 4), this effect may not be seen on all surfaces, or there could be different proteins involved in the displacement. Cell death has previously been noted on highly charged polymer surfaces[135], though Fitton[56] did not observe cell death on

polymers containing NVI. However, Fitton assessed cell growth only up to one hour, whereas a 72 hour assay was used in the study described in this thesis. Another possible reason for the differences between these results and those found in the literature is that previous workers have usually grafted ionic monomers to poly(HEMA) rather than to an NVP/MMA copolymer.

NVP is a heterocyclic amide (also known as a lactam) and so is completely non basic, in contrast to amines, for two reasons. Firstly, the ground state of an amide is stabilised by delocalisation of the nitrogen lone pair electrons through orbital overlap with the carbonyl group. In resonance terms it is possible to draw two contributing forms, as shown in Figure 6.4.

Figure 6.1 Resonance stabilisation of NVP in polymer

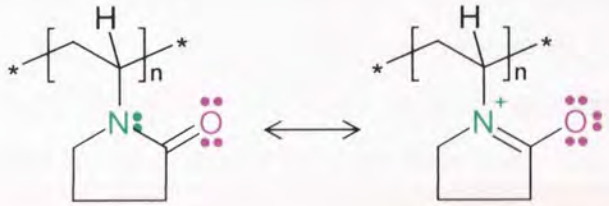

Since this amide resonance stabilisation is lost in the protonated product, protonation is disfavoured. Secondly, a protonated amide is higher in energy than a protonated amine because the electron withdrawing carbonyl group inductively destabilises the neighbouring positive charge (Figure 6.5). A protonated amide has no resonance stabilisation and has inductive destabilisation of the positive charge.

Figure 6.2 Diagram of a protonated NVP unit in polymer

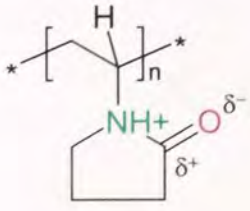

However, NVP units may undergo hydrolysis since the lactam ring is strained, mainly due to torsional strain. Pyrrolidone units can be hydrolysed to 4-aminobutyric acid (GABA) units, as shown in Figure 6.3.

Figure 6.3 Hydrolysis of a NVP unit in polymer

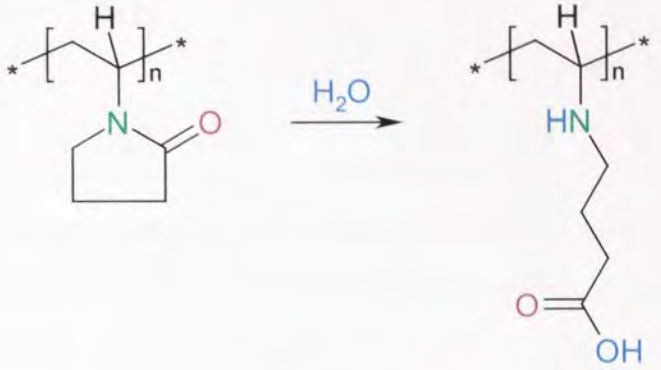

This reaction is irreversible due to the high energy of the ring structure of pyrrolidone units. Thus, the presence of a carboxylic acid may explain the very low cell counts obtained on the NVP/MMA copolymers. Hydrolysis of amides is usually carried out using either a strong acid or base catalyst together with heat. So it is perhaps unlikely that hydrolysis of NVP units occurs, though with the strained ring system and the rinsing of the hydrogel samples in weakly acidic (carbonic acid containing) distilled water it remains a possibility.

Morpholine is a heterocyclic amine and is weakly basic, the pK_a of its conjugate acid being 8.49[185].

Figure 6.4 Basicity of morpholine

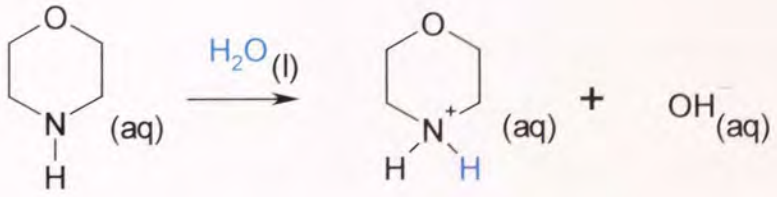

The magnitude of dissociation of acids and protonation of bases is described by the Henderson-Hasselbach equation.

$$\mathrm{pH} = \mathrm{p}K_a + \lg\frac{[\mathrm{A}^-]}{[\mathrm{HA}]} \qquad (6.1)$$

for acids, and

$$\mathrm{pOH} = \mathrm{p}K_b + \lg\frac{[\mathrm{BH}^+]}{[\mathrm{HA}]} \qquad (6.2)$$

for bases

where A^- is the conjugate base of acid A, and BH^+ is the conjugate acid of base B. Figure 6.5 shows the ionisation of acids and bases according to the Brønsted-Lowry classification.

Figure 6.5 Ionisation of acids and bases

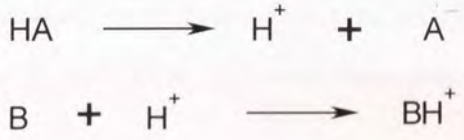

For a weak acid the more acidic the environment, the less ionised the acid. At 50% ionization, pH = pK_a. If the pH is raised by 2 units (making the solution more alkaline) the acid becomes 90% ionised. If the pH is reduced by 2 units, the acid becomes 10% ionised. Weak bases have the opposite effect.

The exact degree of ionisation can be determined by rearranging the Henderson-Hasselbach equation.

$$\%\ \text{ionisation} = \frac{100}{1+10^{(\mathrm{p}K_a - \mathrm{pH})}} \qquad (6.3)$$

for acids, and

$$\%\ \text{ionisation} = \frac{100}{1+10^{(\mathrm{pH} - \mathrm{p}K_a)}} \qquad (6.4)$$

for bases,

since the pK_a of a conjugate acid is 14.0 - pK_b of the base. The autoprotolysis constant at 25°C is

$$pK_w = pH + pOH = 14.0 \qquad (6.5)$$

So at pH 7.4 morpholine is 92.5% ionised; the polymerised acryloyl morpholine is likely to be a little less dissociated at this pH since cation-cation repulsion in the polymer makes it progressively more difficult to protonate as the mole fraction of protonated amine groups increases.

Therefore, the presence of protonated groups due to the cationic nature of AMO may explain the very low cell counts obtained on the AMO/MMA copolymers. As mentioned earlier, high densities of cations are toxic to cells.

Alternatively, it is possible that live cells remain in the well plates which would imply that these surfaces are not cytotoxic but that they are still unsuitable for cell attachment.

The ionic comonomers used (NVI, DEAEMA and MAA) may also be cytotoxic due to charge density. The conjugate acid of NVI monomer has a pK_a of 6.99 according to Dean[185] (28.0% ionised) and 6.95 according to McMurry[186] (26.2% ionised) at pH7.4, the polymerised form being less ionised than this. The pK_a of the conjugate acid of DEAEMA monomer has been reported to be 9.5[187] (99.2% ionised), and the homopolymer 6.9[188] (24.0% ionised) or 7.5[189] (55.7% ionised). DEAEMA is therefore much more cationic than NVI. Methacrylic acid has a pK_a of 4.66 in the monomer and 5.65 in the polymer[190]. So the polymerised form will be 98.3% ionised. Methacrylic acid is therefore more charged at pH 7.4 than DEAEMA or NVI, making comparison between anionic and cationic polymers more complicated.

It is often unclear in the literature if the surfaces described are truly charged since ionic groups may not be dissociated at biological pH depending on their pK_a values of

their constituent monomer units. In addition, pK_a values are related to the Gibbs function and are temperature dependent, as shown in Equation 6.6.

$$\Delta G^{\ominus} = - RT \ln K_a = 2.303\ RT\ .\ pK_a \qquad (6.6)$$

where $\Delta G^{\ominus}$ is the standard Gibbs free energy change (free energy of products - free energy of reactants)

R is the gas constant, 8.314 J K^{-1} mol^{-1}

T is the temperature in Kelvin

K_a is the dissociation constant

For a favourable reaction, $\Delta G^{\ominus}$ has a negative value, meaning that the reaction is exothermic; for an unfavourable reaction, $\Delta G^{\ominus}$ has a positive value, indicating that the reaction is endothermic. For weak acids and bases, $\Delta G^{\ominus}$ is positive because the ionised products have higher free energies than the initial acid or base. Le Chatelier's principle predicts that for endothermic reactions, increased temperature favours the products.

So for acids,

$$pK_a = \Delta G^{\ominus} / 2.303\ RT \qquad (6.7)$$

and for bases,

$$pK_b = \Delta G^{\ominus} / 2.303\ RT \qquad (6.8)$$

Therefore, morpholine has a $\Delta G^{\ominus}$ of 48.443 kJ mol^{-1} giving a pK_a for its conjugate acid at 37°C of 8.16. At 37°C and pH 7.4 morpholine is 85.2% dissociated, the polymerised form being less dissociated than this. Similarly, NVI monomer has a pK_a of 6.72 (17.3% ionised) or 6.68 (16.0% ionised), DEAEMA has a pK_a of 9.13 in the monomer (98.2% ionised) and 6.63 (14.5% ionised) or 7.21 (39.2% ionised) in the polymer, and the polymerised form of MAA has a pK_a of 5.43 (98.9% ionised).

Therefore, at 37°C AMO, NVI and DEAEMA are less ionised than at 25°C but MAA is more ionised at 37°C than at 25°C. The protonation of a base is an associative process while the ionisation of an acid is a dissociative process.

The van't Hoff equation can be used to more accurately predict the change in the equilibrium constants with respect to temperature and is shown below.

$$\frac{\mathrm{d}\ \ln K}{\mathrm{d}T} = \frac{-\Delta H^{\ominus}}{RT_2} \tag{6.8}$$

In order to find the value of the dissociation constant at a temperature T_2 in terms of its value K_1 at another temperature T_1, it is necessary to integrate Equation 6.8.

$$\int_{\ln K_1}^{\ln K_2} \mathrm{d}\ln K = \frac{-1}{R}\int_{/T_1}^{/T_2} \Delta H^{\ominus}\,\mathrm{d}\left(\frac{1}{T_1}\right) \tag{6.9}$$

The integral on the left evaluates to $\ln K_2 - \ln K_1$. Assuming $\Delta H^{\ominus}$ varies only slightly with temperature over the temperature range of interest, it can be taken out of the integral. Then

$$\ln K_2 - \ln K_1 = \frac{-\Delta H^{\ominus}}{R}\left(\frac{1}{T_2} - \frac{1}{T_1}\right) \tag{6.10}$$

The Gibbs free energy ($\Delta G^{\ominus}$) is made up of the enthalpy ($\Delta H^{\ominus}$) and the entropy ($\Delta S^{\ominus}$) as shown in Equation 6.11.

$$\Delta G^{\ominus} = \Delta H^{\ominus} - T\Delta S^{\ominus} \tag{6.11}$$

The enthalpy term is usually larger and more important than the entropy term and so the entropy contribution is often ignored, as $\Delta G^{\ominus} \approx \Delta H^{\ominus}$.

This would mean that, at 37°C the conjugate acid of morpholine has a pK_a 18.10 which is impossible. It is clear that the entropy term $\Delta S^{\ominus}$ becomes significant in these systems due to an increase in the number of components after ionisation. It would be possible to calculate $\Delta H^{\ominus}$ and hence the pK_a corrected for temperature if the $\Delta S^{\ominus}$ term

was known. However, this analysis shows that charge density, and acidity or basicity is dependent on the chemical nature of monomer units and is affected by temperature.

It is therefore not enough to claim that a cationic surface encourages cell adhesion more than an anionic surface or vice versa, since one is likely to be more ionised than the other even at the same concentration. This almost certainly accounts for the confusion in previous research as noted in Chapter 5.

As highlighted in Chapter 4, the fact that DEAEMA is the most cationic of the monomers tested explains the high level of hydrogen bonding seen in NVP/MMA copolymers incorporating DEAEMA. Water molecules will arrange themselves around the protonated nitrogen atoms, holding the structure together strongly.

Thus it has been difficult to assess any structure/property relationship concerning cell adhesion. The suggestion of cytotoxicity has been evaluated and shown to be a likely consequence of the potentially acidic or basic constituents of the polymers. An acid has more of an effect than a base at the same concentration due to it being more ionised.

6.2 Further Work

It was suggested in Chapter 5 that the NVP/MMA and AMO/MMA copolymers may be cytotoxic because of the very low cell counts obtained on these materials compared with poly(HEMA). Dead cells usually have compromised membranes and therefore will detach from the surface of the hydrogel. By using an inverted fluorescence microscope it would be possible to examine the contents of the well plates after removal of the sample disc. This may reveal dead cells and a cytotoxic effect. A possible cause of cytotoxicity would be the presence of acidic or basic groups on the polymer chain.

CHAPTER 7

CONCLUSIONS AND SUGGESTIONS FOR FURTHER WORK

7.1 Conclusions

The work in this thesis has demonstrated the nature of the behaviour of mammalian cells in contact with potential biomaterial substrates. It is clear that cell adhesion is a complex process which is affected by many different properties of the surface.

Although the surface chemistry results show trends these techniques do not accurately predict cellular behaviour. Both 3T3 and EK1.BR cells produced the same pattern of results when grown on all the materials under investigation. This shows that the cell adhesion studies are reliable. However, it is not possible to identify particular surface characteristics which induce cell adhesion.

The negative control, poly(HEMA), was found to be the most adhesive hydrogel tested. This appears to contradict previous work within our research group and opinion in the published literature. However, the work in this thesis was carried out with dependable techniques, and care was taken to avoid contamination. Low EWC is not necessarily important. With respect to cationic monomers, an increase in DEAEMA concentration gave an increase in cell count, whereas the opposite was true for NVI. A detailed analysis of the electrochemistry and thermodynamics involved in these systems has shown that one ionic monomer may be more charged than another at the same concentration. The degree of ionisation is also dependent on temperature. Protein mediated adhesion may be overridden by densely charged surfaces, meaning that alternative mechanisms of protein displacement are likely.

Although cell counts were seen to vary amongst the NVP/MMA copolymers, their values remain very low and insignificant compared with those obtained on the glass used as a positive control and poly(HEMA) used as a negative control.

Surface chemistry techniques have been shown to be insufficiently sensitive to detect changes in surface properties capable of increasing or decreasing cell adhesion. However, this may in part be due to the blocky structure of the NVP/MMA copolymers having regions of varying surface free energies and wettabilities even on

the same membrane. This heterogeneity was confirmed and compared with the situation found with homogeneous poly(HEMA).

In this study it was concluded that hydrogel copolymers having uneven sequence distributions supported cell adhesion better than hydrogels having even distributions, benefiting from 'islands' of specific chemical functionality.

Although surface chemistry testing proved unsuccessful in predicting cell behaviour, the use of foetal calf serum in dynamic contact angle experiments allowed materials to be distinguished more easily.

NVP/MMA and AMO/MMA copolymers may be cytotoxic possibly because of an ability to hydrolyse and ionise respectively. Alternatively, oligomers may leach out of the hydrogels and into the cellular growth medium. This may account for the low cell counts, though further work will be needed to establish whether or not this is the case.

The hydrogel materials tested are unsuitable for use as a keratoprosthesis skirt due to their inability to support cell growth but may be useful for the non adhesive core providing that they are proved to be non cytotoxic.

7.2 Suggestions for Further Work

On the basis of the results presented here there is a clear requirement for hydrogels with greater cell adhesiveness, if these materials are to be considered suitable for use as a potential keratoprosthesis skirt material. Results presented here would indicate it better to incorporate ionic monomers into poly(HEMA) rather than into NVP/MMA copolymers since poly(HEMA) was found to be much more adhesive than NVP/MMA hydrogels. More research needs to be done regarding the incorporation of neutral monomers and ionic monomers and it would be especially interesting to identify the properties of polymers containing both anionic and cationic monomers or zwitterionic monomers. Contact angle techniques proved to be too insensitive to predict cellular behaviour. A more accurate method of measuring surface charge is to

measure the zeta potential ζ also known as the electrokinetic potential and the use of this could be considered.

A small number of liquids were used as the test solution for dynamic contact angle measurements but it would be interesting to investigate liquids having a higher surface tension, in line with the theory of Zisman and coworkers[101, 102, 103, 104, 105]. One suggestion would be saline.

The contents of the well plates should also be examined after removal of the sample discs in order to establish whether or not the materials are cytotoxic. Inflammatory cells may also be employed in place of fibroblast like cells because they may serve as an alternative indicator to cellular response.

The effect of autoclaving samples should in addition be studied with a wide range of materials to ensure that properties are not altered in any way.

A functional KPro requires a clear, non cell adhesive optical core and a peripheral cell adhesive skirt. Once a suitable cell adhesive hydrogel has been designed the next stage would be to make it porous in order for keratocytes to grow into the structure and integrate with the material. Work has previously been carried out in this laboratory on porous hydrogels. Fitton[56] reported that the porous grain modulates the direction of cellular growth. There are two techniques for creating porous hydrogels. The first method of increasing pore size in polymers employs a "freeze-thaw" technique. Monomers are polymerised around a crystalline matrix, such as ice crystals, that are subsequently dispersed or dissolved to leave an interconnected meshwork. Pore size can also be increased by a porosigen technique where a water-soluble porosigen such as dextrin is incorporated into the monomer mixture before polymerisation, and dissolved out after polymerisation[191, 134].

REFERENCES

1 Corkhill PH, Hamilton CJ, and Tighe BJ, (1990) "The design of hydrogels for medical applications" *Critical Reviews in Biocompatibility* **5**(4), 363-436

2 Minett WT, (1986) *Cell Adhesion on Synthetic Polymer Substrates*, PhD Thesis, Aston University

3 Chirila TV, Hicks CR, Dalton PD, Vijayasekaren S, Lou X, Hong Y, Clayton AB, Ziegelaar BW, Fitton JH, Platten S, Crawford GJ, and Constable IJ, (1998) "Artificial cornea" *Progress in Polymer Science* **23**(3), 447-473

4 Gipson IK, and Sugrue SP, (1992) "Corneal surfaces: Cell biology of the corneal epithelium" in *Principles and Practice of Ophthalmology* DM Albert et al (eds) WB Saunders Co, Philadelphia

5 Tighe BJ, (1990) "Blood, sweat and tears – some problems in the design of biomaterials" Nissel memorial lecture, Royal Society of Medicine, Reprinted in *Journal of the British Contact Lens Association* **13**(1), 13-19

6 Benedek GB, (1971) "Theory of transparency of the eye" *Applied Optics* **10**, 459-473

7 Otori T, (1967) "Electrolyte content of the rabbit corneal stroma" *Experimental Eye Research* **6**, 356-367

8 Møller-Pedersen T, Ledet T, and Ehlers N, (1994) "The keratocyte density of human donor corneas" *Current Eye Research* **13**, 163-169

9 Nishida T, (1997) "Cornea" in *Cornea – Fundamentals of Cornea and External Disease* Volume 1, Krachmer, Mannis and Holland (eds) Mosby Year Book Inc, St Louis 3-27

10 Tuft S, Garty D, Rave I, and Meek K, (1993), "Photorefractive keratectomy: implications of corneal wound healing" *British Journal of Ophthalmology* **77**, 243-247

11 Nakagawa S, Pawelek P, and Grinnel F, (1989) "Extracellular matrix organization modulates fibroblast growth and growth factor responsiveness" *Experimental Cell Research* **182**, 572-582

12 Trinkaus-Randall V, (1993) "Cornea Chapter 26 pages 383-401 in *Principles of Tissue Engineering* RP Lanza, R Langer and WL Chick (eds) Landes Bioscience

13 Kaufman HE, Barron BA, and McDonald MB, (1999) *The Cornea* 2nd Edition, Butterworth-Heinemann, Boston, Oxford

14 Rouslahti E, (1991) "Integrins" *Journal of Clinical Investigation* **87**, 1-5

15 Singh D, (1984) "Keratoprosthesis" *Indian Journal of Ophthalmology* **932**(5), 405-407

16 Van Andel J, (1993) "Results of champagne cork keratoprosthesis in 127 corneal blind eyes" KPro Abstracts, *Refractive and Corneal Surgery* **9**, 189-190

17 Wintermantel E, Mayer J, Blum J, Eckert K-L, Luscher P, and Mathey M, (1996) "Tissue engineering scaffolds using superstructures" *Biomaterials* **17**(2), 83-91

18 Leibowitz HM, Trinkaus-Randall V, Tsuk AG, and Fransblau C, (1994) "Progress in the development of a synthetic cornea" *Progress in Retinal and Eye Research* **13**(2), 605-621

19 Trinkaus-Randall V, Capecchi J, Sammon L, Gibbons D, Leibowitz HM, and Franzblau C, (1990) "*In vitro* evaluation of fibroplasia in a porous polymer" *Investigative Ophthalmology and Vision Science* **31**, 1321-1326

20 Pellier de Quensgy G, (1789-90) Precis ou Cours d'Opérations sur la Chirurgie des Yeux. Paris Didot & Mequignon, Paris, Vol **1**(XV), 96-1031

21 Cardona H, (1962) "Keratoprosthesis" *American Journal of Ophthalmology* **54**, 284-294

22 Parel J-M, (1990) "200 years of KPro: Pellier de Quengsy and the artificial cornea" *An Instr Barraquer* **28**(suppl), 33-41

23 Nussbaum I, (1856) *Die Behandlung der Hornhauttrubungen mit besonderer Berucksichtigung der kunstlicher Hornhaut (cornea artificialis)*, Munchen

24 Hicks C, Fitton H, Chirila T, Crawford G, and Constable I, (1997) "Keratoprostheses: advancing toward a true artificial cornea" *Survey of Ophthalmology* **42**(2), 175-189

25 Dohlman CH, Schneider HA, and Doane MG, (1974) "Prosthokeratoplasty" *American Journal of Ophthalmology* **77**, 694-700

26 Cardona H, (1969) "Mushroom transcorneal keratoprosthesis" *American Journal of Ophthalmology* **68**, 604-612

27 Cardona H, (1991) "The Cardona keratoprosthesis: 40 years experience" *Refractive Corneal Surgery* **7**, 468-471

28 Stone W, and Herbert E, (1953) "Experimental study of plastic material as replacement for the cornea" *American Journal of Ophthalmology* **36**, 168-173

29 Chirila TV, (1994) "Interpenetrating polymer network (IPN) as a permanent joint between the elements of a new type of artificial cornea" *Journal of Biomedical Materials Research* **28**, 745-753

30 Legeais J-M, and Renard G, (1998) "A second generation of artificial cornea (Biokpro II)" *Biomaterials* **19**, 1517-1522

31 Chirila TV, (1997) "Artificial cornea with a porous polymeric skirt" *Trends in Polymer Science* **5**(11), 346-348

32 Hicks CR, Chirila TV, Clayton AB, Fitton JH, Dalton PD, Vijaysekaran S, Lou X, Hatten S, Ziegelaar S, Hong Y, Crawford GJ, and Constable IJ, (1998) "Clinical results of implantation of the Chirila keratoprosthesis in rabbits" *British Journal of Ophthalmology* **82**, 18-25

33 Hicks C, (1998) "Artificial cornea update" *Optician* **216**(5668), 28-29

34 Lion's Eye Institute, (2000) *Annual Report*, Nedlands, Australia

35 Vijayasekaran S, Fitton JH, Hicks CR, Chirila TV, Crawford GJ, and Constable IJ, (1998) "Cell viability and inflammatory response in hydrogel sponges implanted in the rabbit cornea" *Biomaterials* **19**(24), 2255-2267

36 Ricci R, Pecorella I, Ciardi A, Rocca C, Tondo U, and Marchi V, (1992) "Strampelli's osteo-odonto-keratoprosthesis. Clinical and histological long-term features of these prostheses" *British Journal of Ophthalmology* **76**, 232-234

37 Falcinelli G, Barogi G, and Taloni M, (1993) "Osteo-odonto-keratoprosthesis: Present experience and future prospects" *Refractive and Corneal Surgery* **9**, 193-194

38 Liu C, and Pagliarini S, (1996) "Long-term results of the Falcinelli osteo-odonto keratoprosthesis (OOKP)" (abstract) *Fourth World Congress on the Cornea Abstracts*, The Castroviejo Society, 91

39 Trinkaus-Randall V, Cappechi J, Banwatt R, Sammon L, Leibowitz HM, Franzblau C (1987) "Development of biopolymeric kerathoprosthesis: epithelial adhesion *in vitro* and *in vivo*" ARVO Abstracts *Investigative Ophthalmology and Visual Science* **28** (suppl) 54

40 Kornmehl EW, Bredvik BK, Kelman CD, Raizman MB, and DeVore DP, (1995) "*In vivo* evaluation of a collagen corneal allograft derived from rabbit dermis" *Journal of Refractive Surgery* **11**, 502-507

41 Lee JH, Wee WR, Chung ES, Kim HY, Park SH, and Kim YH, (2000) "Development of a newly designed double-fixed Seoul-type keratoprosthesis" *Archives of Ophthalmology* **118**, 1673-1678

42 Green DW, (2000) *A Biological-Inspired Support Frame for an Artificial Cornea*, PhD Thesis, Aston University

43 Barber JC, (1988) "Keratoprostheses: Past and present" *International Ophthalmology Clinics* **28**(2), 103-110

44 Kirkham SM., and Dangel ME, (1991) "The keratoprosthesis: Improved biocompatibility through design and surface modification" *Ophthalmic Surgery* **22**, 8, 455-461

45 Kenyon KR, Berman M, Rose J, and Gage J, (1979) "Prevention of stromal ulceration in the alkali burned rabbit cornea by glued on contact lens. Evidence for the role of PMN leukocytes in collagen degradation" *Investigative Ophthalmology and Visual Science* **18**, 570-587

46 Dohlman CH, (1983) "Biology of complications following keratoprosthesis" *Cornea* **2**, 175-176

47 Chirila TV, (1994) "Modern artificial corneas: the use of porous polymers" *Trends in Polymer Science* **2**(9), 296-300

48 Wichterle O and lim D, (1960) "Hydrophilic gels for biological use" *Nature* **185**, 117-118

49 Wichterle O, and Lim D, (1965) "Cross-linked hydrophilic polymers and articles made therefrom" US Patent 3,220,960

50 Wichterle O, (1970) "Method of preparing shape retaining bodies of organic polymer Hydrogels" US Patent 3,499,862

51 Corkhill PH, Jolly AM, Chiong O, Ng CO, and Tighe BJ, (1987) "Synthetic hydrogels: 1. Hydroxyalkyl acrylate and methacrylate copolymers – water binding studies" *Polymer* **28**, 1758-1766

52 Taniguchi Y, and Horigome S, (1975) "The states of water in cellulose acetate membranes" *Journal of Applied Polymer Science* **19**, 2743-2748

53 Baker DA, Corkhill PH, Ng CO, Skelly PJ, and Tighe BJ, (1988) "Synthetic hydrogels. 2. Copolymers of carboxyl-containing, lactam containing and amide-containing monomers structure property relationships" *Polymer* **29**(4), 691-700

54 Davies SM, (1991) *Cellular Responses to Potential Biomaterials*, PhD Thesis, Aston University

55 Sperling LH, (1981) *Interpenetrating Polymer Networks and Related Materials* Plenum press, New York

56 Fitton JH, (1993) *Cells, Surfaces and Adhesion*, PhD Thesis, Aston University

57 Alfrey T, and Goldfinger G, (1944) "The mechanism of copolymerisation" *Journal of Chemical Physics* **12**, 205-209

58 Mayo FR, and Lewis FM, (1944) "Copolymerisation I. A basis for comparing the behaviour of monomers in copolymerisation; the copolymerisation of styrene and methyl methacrylate" *Journal of the American Chemical Society* **66**, 1594-1601

59 Ashraf N, (1993) *Sequence Distributions in Free-Radical Polymers*, PhD Thesis, Aston University

60 Alfrey T, and Price CC, (1947) "Relative reactivities in vinyl copolymerisation" *Journal of Polymer Science* **2**, 101-106

61 Varma IK, and Patnaik S, (1976) "Copolymerisation of 2-hydroxyethyl methacrylate with alkyl acrylate" *European Polymer Journal* **12**, 259-261

62 Yocum RH, and Nyquist EB (eds) *Functional Monomers*, Volumes 1 and 2, Marcel Dekker, New York, 1973

63 Rubenstein RY, (1981) *Simulation and the Monte Carlo Method* John Wiley & Sons, New York

64 Brandrup J, (1989) *Polymer Handbook* 3rd Edition John Wiley and Sons Inc, New York

65 Nagai K, Fujii I, and Kuramoto N, (1992) "Polymerization of surface-active monomers: 4. Copolymerization of long-chain alkyl salts of 2-dimethylaminoethyl methacrylate or styrene" *Polymer* **33**(14), 3060-3065

66 Andrade JD, King RN, Gregonis DE, and Coleman DL, (1979) "Surface characterisation of poly(hydroxyethyl methacrylate) and related polymers. I. Contact angle methods in water" *Journal of Polymer Science, Polymer Symposia* **66,** 313-336

67 Troughton EB, Bain CD, Whiteside GM, Nuzzo RG, Allara DL, and Porter MD, (1988) "Monolayer films prepared by the spontaneous self-assembly of symmetrical and unsymmetrical dialkyl sulfides from solution onto gold substrates – structure, properties and reactivity of constituent functional groups" *Langmuir* **4**(2), 365-385

68 Andrade JD, King RN, and Gregonis DE, (1977) "Probing the hydrogel/water interface" in *Hydrogels for Medical and Related Applications* JD Andrade, (ed), *American Chemical Society Symposium Series* **31**, 206-224

69 Bush JF, Huff JW, and MacKeen DL, (1988) "Laser assisted contact angle measurements" *American Journal of Optometry and Physiological Optics* **65**, 722-728

70 Yasuda H, and Sharma AK, (1981) "Effect of orientation and mobility of polymer molecules at surfaces on contact angle and its hysteresis" *Journal of Polymer Science, Polymer Physics Edition* **19**, 285-291

71 Shirafkan A, Woodward EG, Port MJA, and Hull CC, (1995) "Surface wettability and hydrophilicity of soft contact lens materials, before and after wear" *Ophthalmology and Physiological Optics* **15**, 529-532

72 Hamilton WC, (1972) "A technique for the characterization of hydrophilic solid surfaces" *Journal of Colloid and Interface Science* **40**(2), 219-222

73 Hamilton WC, (1974) "Measurement of the polar force contribution to adhesive bonding" *Journal of Colloid and Interface Science* **47**(3), 672-675

74 Young T, (1805) "On the cohesion of fluids" *Philosophical Transactions of the Royal Society* (London) **95**, 65-87

75 Dupré A, (1869) *Théorie Mécanique de la Chaleur* Gauthier-Villars, Paris 369

76 Fowkes FM, (1962) "Determination of interfacial tensions, contact angles and dispersion forces in surfaces by assuming additivity of intermolecular interactions in surfaces" *Journal of Physical Chemistry* **66**, 382

77 Good RJ, and Girifalco LA, (1957) "A theory for the estimation of surface and interfacial energies. I. Derivation and application to interfacial tension" *Journal of Physical Chemistry* **61**, 904-909

78 Owens DK, and Wendt RC, (1969) "Estimation of the surface free energy of polymers" *Journal of Applied Polymer Science* **13**, 1741-1747

79 Tamai Y, Makuuchi K, and Suzuki M, (1967) "Experimental analysis of interfacial forces at the plane surfaces of solids" *Journal of Physical Chemistry* **71**, 4176-4179

80 Adamson AW, (1976) *Physical Chemistry of Surfaces* 3rd Edition, Wiley-Interscience, New York

81 Corkhill PH, (1988) *Novel Hydrogel Polymers*, PhD Thesis, Aston University

82 French KA, (1996) *Novel Cationic Polymers for Use at Biological Interfaces*, PhD Thesis, Aston University

83 Zhang HJ, and Herskowitz R, (1992) "Is there more than one angle to the wetting characteristics of contact lenses?" *Contact Lens Spectrum* **10**, 26-32

84 Raheja MK, and Ellis EJ, (1995) "Achieving new levels of RGP comfort" *Contact Lens Spectrum* **13**(10), 45-48

85 Poster MG, Gelfer DM, and Fernandez NM, (1986) "Wetting angles of rigid contact lens plastics: The effect of contact lens wear" *Journal of the American Optometry Association* **57**(6), 452-454

86 Tretinnikov ON, and Ikada Y, (1994) "Dynamic wetting and contact angle hysteresis of polymer surfaces studied with the modified Wilhelmy balance method" *Langmuir* **10**, 1606-1614

87 Ikada Y, and Uyama Y, (1993) "Contact angle methods" in *Lubricating Polymer Surfaces* Technomic Publishing Company Inc, Pennsylvania, USA, 94-111

88 Uyama Y, Inoue H, Ito, K, Kishida A, and Ikada Y (1991) "Comparison of different methods for contact angle measurement" *Journal of Colloid and Interface Science* **141**(1), 275-279

89 Tonge S, Jones L, Goodall S, and Tighe BJ "*In vivo* versus *in vitro* wettability of group IV hydrogel contact lenses" *Current Eye Research* **22** In press

90 Wenzel RN, (1936) "Resistance of solid surfaces to wetting by water" *Industrial and Engineering Chemistry* **28**(8), 988-994

91 Lecomte du Noüy P, (1919) "A new apparatus for measuring surface tension" *Journal of General Physiology* **1**, 521-524

92 Harkins WD, and Jordan HF, (1930) "A method for the determination of surface and interfacial tension from the maximum pull on a ring" *Journal of the American Chemical Society* **52**, 1751-1771

93 Freud BB, and Freud HZ, (1930) "A theory of the ring method for the determination of surface tension" *Journal of the American Chemical Society* **52**, 1772-1782

94 Adamson AW, (1990) *Physical Chemistry of Surfaces* 5th edition Wiley, New York

95 Addison CC, (1946) "The properties of freshly formed surfaces. Part VI. The influence of temperature and concentration on the dynamic and static surface tensions of aqueous decoic acid solutions" *Journal of the Chemical Society* **149**(2), 579-585

96 Addison CC, and Hutchinson SK, (1948) "The properties of freshly-formed surfaces. Part IX. Expansion of soluble films of sodium dodecyl sulphate at air-water and toluene-water interfaces" *Journal of the Chemical Society* **2**, 943-948

97 Miller R, Fainerman VB, Wüstneck R, Krägel J, and Trukhin DV, (1998) "Characterisation of the initial period of protein adsorption by dynamic surface tension measurements using different drop techniques" *Colloids and Surfaces A: Physicochemical and Engineering Aspects* **131**, 225-230

98 Kuffner RJ, (1961) "The measurement of dynamic surface tensions of solutions of slowly diffusing molecules by the maximum bubble pressure method" *Journal of Colloid Science* **16**, 497-500

99 Lylyk SV, Makievski AV, Koval'chuk VI, Schano K-H, Fainerman VB, and Miller R, (1998) "The effect of capillary characteristics on the results of

dynamic surface tension measurements using the maximum bubble pressure method" *Colloids and Surfaces A: Physicochemical and Engineering Aspects* **135**, 27-40

100 Horozov TS, Dushkin CD, Danov KD, Arnaudov LN, Velev OD, Mehreteab A, and Broze G, (1996) "Effect of the surface expansion and wettability of the capillary on the dynamic surface tension measured by the maximum bubble pressure method" *Colloids and Surfaces A: Physicochemical and Engineering Aspects* **113**, 117-126

101 Fox HW, and Zisman WA, (1950) "The spreading of liquids on low energy surfaces. I. Polytetrafluoroethylene" *Journal of Colloid Science* **5**, 514-531

102 Fox HW, and Zisman WA, (1952) "The spreading of liquids on low-energy surfaces. II. Modified tetrafluoroethylene polymers" *Journal of Colloid Science* **7**, 109-121

103 Fox HW, and Zisman WA, (1952) "The spreading of liquids on low-energy surfaces. III. Hydrocarbon surfaces" *Journal of Colloid Science* **7**, 428-442

104 Ellison AH, and Zisman WA, (1954) "Wettability of halogenated organic surfaces" *Journal of Physical Chemistry* **58**, 260-265

105 Bernett MK, and Zisman WA, (1961) "Wetting properties of polyhexafluoropropylene" *Journal of Physical Chemistry* **65**, 2266-2267

106 Vroman L, and Adams AL, (1969) "Findings with the recording ellipsometer suggesting rapid exchange of specific plasma proteins at liquid/solid interfaces" *Surface Science* **16**, 438-446

107 Leonard EF, and Vroman L, (1991) "Is the Vroman effect of importance in the interaction of blood with artificial materials?" *Journal of Biomaterial Science Polymer Edition* **3**(1), 95-107

108 Vroman L, (1991) "Off into a thinning fog" *Journal of Biomaterials Science Polymer Edition* **3**(1), 109-114

109 Fabrizius-Homan DJ, and Cooper SL, (1991) "Competitive adsorption of vitronectin with albumin, fibrinogen, and fibronectin on polymeric biomaterials" *Journal of Biomedical Materials Research* **25**, 953-971

110 Tonge SR, Goodall S, Jones L, and Tighe B, (1997) "The persistence of surfactants used in multipurpose solutions on the surface of hydrogel contact lens materials. An *in vitro* vs. *in vivo* comparison" Poster presented at British Contact Lens Association (BCLA) Clinical Conference, Bournemouth

111 Tateishi T, Ushida T, Aoki H, Ikeda Y, Nakamura M, Williams DF, Clark B, Stookey G, Christel P, and Pizzoferrato A, (1992) "A round-robin test for standardization of biocompatibility test procedure by cell culture method" *Biomaterial-Tissue Interfaces*, in Doherty PJ, Williams RL, Williams DF, and Lee AJ (eds) *Advances in Biomaterials* **10**, 89-97, Elsevier Science BV, Amsterdam

112 Doane MG, Dohlman CH, and Bearse G, (1996) "Fabrication of a keratoprosthesis" *Cornea* **15**(2), 179-184

113 Corkhill PH, Hamilton CJ, and Tighe BJ, (1989) "Synthetic hydrogels VI. Hydrogel composites as wound dressings and implant materials" *Biomaterials* **10**, 3-10

114 Lydon MJ, Minett TW, and Tighe BJ, (1985) "Cellular interactions with synthetic polymer surfaces in culture" *Biomaterials* **6**, 396-402

115 Imai Y, and Masuhara E, (1982) "Long-term *in vivo* studies of poly(2-hydroxyethyl methacrylate)" *Journal of Biomedical Materials Research* **16**, 609-617

116 Stoker M, O'Neill C, Berryman S, and Waxman V, (1968) "Anchorage and growth regulation in normal and virus-transformed cells" *International Journal of Cancer* **3**, 683-693

117 Verwey EJW, and Overbeek JThG, (1948) *Theory of the stability of lyophobic colloids* Elsevier, Amsterdam

118 Kauzman W, (1959) "Some factors in the interpretation of protein denaturation" *Advances in Protein Chemistry* **14**, 1-63

119 Baier RE, Shafrin EG, and Zisman WA, (1968) "Adhesion: Mechanisms that assist or impede it" *Science* **162**, 1360-1368

120 Altankov G, and Groth TH, (1994) "Reorganization of substratum-bound fibronectin on hydrophilic and hydrophobic materials is related to biocompatibility" *Journal of Materials Science : Materials in Medicine* **5**, 732-737

121 Maroudas NG, (1975) "Adhesion and spreading of cells on charged surfaces" *Journal of Theoretical Biology* **49**, 417-424

122 Underwood PA, and Bennett FA, (1989) "A comparison of the biological activities of the cell-adhesive proteins vitronectin and fibronectin" *Journal of Cell Science* **93**, 641-649

123 Steele JG, Johnson G, Griesser HJ, and Underwood PA, (1997) "Mechanism of initial attachment of corneal epithelial cells to polymeric surfaces" *Biomaterials* **18**, 1541-1551

124 Preissner KT, (1991) "Structure and biological role of vitronectin" *Annual Review of Cell Biology* **7**, 275-310

125 Sack RA, Underwood PA, Tan KO, Sutherland H, and Morris CA, (1993) "Vitronectin. Possible contribution to the closed-eye external host-defense mechanism" *Ocular Immunology and Inflammation* **1**(4), 327-336

126 Fuquay JI, Loo DT, Barnes DW, (1986) "Binding of *Staphylococcus aureus* by human serum spreading factor in an *in vitro* assay" *Infection and Immunity* **52**, 714-717

127 Chhatwal GS, Preissner KT, Müller-Berghaus G, Blobel H, (1987) "Specific binding of the human S protein (vitronectin) to *Streptococci*, *Staphylococcus aureus*, and *Eschericia coli*" *Infection and Immunity* **55**, 1878-1883

128 Neyfakh AA, Tint IS, Svitkina TM, Berahadsky AD, and Gelfand VI, (1983) "Visualization of cellular focal contacts using a monoclonal antibody to 80kD serum protein adsorbed on the substratum" *Experimental Cell Research* **149**, 387-396

129 Tomasini BR, and Mosher DF, (1988) "Conformational states of vitronectin: Preferential expression of an antigenic epitope when vitronectin is covalently and noncovalently complexed with thrombin-antithrombin III or treated with urea" *Blood* **72**(3), 903-912

130 Klebe RJ, Bentley KL, and Schoen RC, (1981) "Adhesive substrates for fibronectin" *Journal of Cell Physiology* **109**(3), 481-488

131 Rosen JJ, and Schway MB, (1980) "Kinetics of cell adhesion to a hydrophilic-hydrophobic copolymer model system" in Lee L-H, (ed), "Adhesion and adsorption of polymers" *Polymer Science and Technology* Vol **12B**, 667-675

132 Tanzawa H, Nagaoka S, Suzuki J, Kobayashi S, Masubichi Y and Kikuchi T, (1980) "Cell adhesion and growth on the surface of synthetic hydrogels" in Goldberg EP, and Nakajima A (eds) *Biomedical Polymers. Polymeric materials and pharmaceuticals for biomedical use*, Academic Press Inc, New York, London, 189-211

133 Thomas KD, (1988) *Biological Interactions with Synthetic Polymers*, PhD Thesis, Aston University

134 Corkhill PH, Fitton JH, and Tighe BJ, (1993) "Towards a synthetic articular cartilage" *Journal of Biomaterials Science, Polymer Edition* **4**(6), 615- 630

135 Kishida A, Iwata H, Tamada Y, and Ikada Y, (1991) "Cell behaviour on polymer surfaces grafted with non-ionic and ionic monomers" *Biomaterials* **12**, 786-792

136 Pettit DK, Horbett TA, Hoffman AS, and Chan KY, (1990) "Quantitation of rabbit corneal epithelial cell outgrowth on polymeric substrates *in vitro*" *Investigative Ophthalmology & Visual Science* **31**(11), 2269-2277

137 Jeon SI, Lee JH, Andrade JD, and de Gennes PG, (1991) "Protein-surface interactions in the presence of polyethylene oxide. 1. Simplified theory" *Journal of Colloid Interface Science* **142**(1), 149-158

138 Jeon SI, and Andrade JD, (1991) "Protein-surface interactions in the presence of polyethylene oxide. 2. Effect of protein size" *Journal of Colloid Interface Science* **142**(1), 159-166

139 Bergethon PR, Trinkaus-Randall V, and Franzblau C, (1989) "Modified hydroxyethylmethacrylate hydrogels as a modelling tool for the study of cell-substratum interactions" *Journal of Cell Science* **92**, 111-121

140 Brandley BK, Weisz OA, and Schnaar RL, (1987) "Cell attachment and long-term growth on derivatizable polyacrylamide surfaces" *Journal of Biological Chemistry* **262**, 6431-6437

141 Peluso G, Petillo O, Anderson JM, Ambrosio L, Nicolais L, Melone MAB, Eschbach FO, and Huang SJ, (1997) "The differential effects of poly(2-hydroxyethyl methacrylate) and poly(2-hydroxyethyl methacrylate)/ poly(caprolactone) polymers on cell proliferation and collagen synthesis by human lung fibroblasts" *Journal of Biomedical Materials Research* **34**, 327-336

142 Sandeman SR, Faragher RGA, Allen MCA, Liu C, and Lloyd AW, (2000) "Novel materials to enhance keratoprosthesis integration" *British Journal of Ophthalmology* **84**, 640-644

143 Smetana K Jr, Lukáš J, Palecková V, Bartunková J, Liu F-T, Vacík J, and Gabius H-J, (1997) "Effect of chemical structure of hydrogels on the adhesion and phenotypic characteristics of human monocytes such as expression of galectins and other carbohydrate-binding sites" *Biomaterials* **18**(14), 1009-1014

144 Smetana K Jr, Vacík J, Soucková D, Krcová Z, and Šulc J, (1990) "The influence of hydrogel functional groups on cell behavior" *Journal of Biomedical Materials Research* **24**, 463-470

145 Lee J, Khang G, and Lee H, (1997) "Interaction of cells on chargeable functional group gradient surfaces" *Biomaterials* **18**(4), 351-358

146 Ma JJ, (1995) *Novel Hydrogel Polymers*, PhD Thesis, Aston University

147 Hubbell JA, (1994) "Chemical modification of polymer surfaces to improve biocompatibility" *Trends in Polymer Science* **2**(1), 20-25

148 Zavala EY, Nayak S, Deg JK, Binder PS, (1984) "Keratocyte attachment to hydrogel materials" *Current Eye Research* **3**(10), 1253-1262

149 Zavala EY, Nayak SK, Dunmire-Deg JK, and Binder PS, (1986) "Human Keratocyte interactions with hydrogel materials" *the CLAO Journal* **12**(1), 54-58

150 Graham CD, (1998) *Cellular Interaction with Novel Biomaterials*, PhD Thesis, Aston University

151 Davis JM, (ed), (1998) *Basic Cell Culture. A Practical Approach* Oxford University Press, Oxford

152 Jones KH, and Senft JA, (1985) "An improved method to determine cell viability by simultaneous staining with fluorescein diacetate-propidium iodide" *Journal of Histochemistry and Cytochemistry* **33**, 77-79

153 Freshney RI, (1994) *Culture of Animal Cells: A Manual of Basic Technique* 3rd Edition Wiley-Liss Inc, 270

154 Wang Y-L, and Taylor DL, (eds), (1989) Methods in Cell Biology Vol 29: Fluorescence Microscopy of Living Cells in Culture, Part A : Fluorescent Analogs, Labeling Cells, and Basic Microscopy, Academic Press Limited, London

155 Braut-Boucher F, Pichon J, Rat P, Adolphe M, Aubery M, and Font J, (1995) "A non-isotopic, highly sensitive, fluorimetric, cell-cell adhesion microplate assay using calcein AM-labeled lymphocytes." *Journal of Immunological Methods* **178**(1), 41-51

156 Rat P, Korwin-Zmijowska C, Warnet JM, and Adolphe M, (1994) "New *in vitro* fluorimetric microtitration assays for toxicological screening of drugs" *Cell Biology and Toxicology* 10(5-6), 329-337

157 De Clerck LS, Bridts CH, Mertens AM, Moens MM, and Stevens WJ, (1994) "Use of fluorescent dyes in the determination of adherence of human leucocytes to endothelial cells and effect of the fluorochromes on cellular function" *Journal of Immunological Methods* **172**(1), 115-124

158 Aparicio CL, Strong LH, Yarmush ML, and Berthiaume F, (1997) "Correction for label leakage in fluorimetric assays of cell adhesion" *BioTechniques* **23**(6), 1056-1060

159 Akeson AL, and Woods CW (1993)"A fluorometric assay for the quantitation of cell adherence to endothelial cells" *Journal of Immunological Methods* **163**(2), 181-185

160 Haugland RP (1999) *Handbook of Fluorescent Probes and Research Chemicals* 7th Edition, Molecular Probes Inc, Eugene, Oregon

161 Burghardt RC, Barhoumi R, Doolittle DJ, and Phillips TD, (1994) "Application of cellular fluorescence imaging for *in vitro* toxicology testing" in *Principles and Methods of Toxicology*, 3rd Edition, Hayes AW, (ed), Raven Press, New York, 1231-1258

162 Lopez-Amoros R, Comas J, and Vives-Rego J, (1995) "Flow cytometric assessment of Escherichia coli and Salmonella typhimurium starvation-survival in seawater using rhodamine 123, propidium iodide, and oxonol" *Applied Environmental Microbiology* **61**(7), 2521-2526

163 Ankarcrona M, Dypbukt JM, Bonfoco E, Zhivotovsky B, Orrenius S, Lipton SA, and Nicotera P, (1995) "Glutamate-induced neuronal death: a succession of necrosis or apoptosis depending on mitochondrial function" *Neuron* **15**(4), 961-973

164 Trost LC, and Lemasters JJ, (1994) "A cytotoxicity assay for tumor necrosis factor employing a multiwell fluorescence scanner" *Analytical Biochemistry* **220**(1), 149-153

165 Vollenweider I, and Groscurth P, (1992) "Comparison of four DNA staining fluorescence dyes for measuring cell proliferation of lymphokine-activated killer (LAK) cells" *Journal of Immunological Methods* **149**(1), 133-135

166 Beletsky IP, and Umansky SR, (1990) "A new assay for cell death" *Journal of Immunological Methods* **134**(2), 201-205

167 Rye HS, and Glazer AN (1995) "Interaction of dimeric intercalating dyes with single-stranded DNA" *Nucleic Acids Research* **23**(7), 1215-22

168 Rye HS, Yue S, Wemmer DE, Quesada MA, Haugland RP, Mathies RA, and Glazer AN, (1992) "Stable fluorescent complexes of double-stranded DNA

with bis-intercalating asymmetric cyanine dyes: properties and applications" *Nucleic Acids* Research **20**(11), 2803-2812

169 Gaugain B, Barbet J, Capelle N, Roques BP, and Le Pecq JB, (1978) "DNA bifunctional intercalators. 2. Fluorescence properties and DNA binding interaction of an ethidium homodimer and an acridine ethidium heterodimer" *Biochemistry* **17**(24), 5078-5088

170 Gaugain B, Barbet J, Oberlin R, Roques BP, and Le Pecq JB, (1978) "DNA bifunctional intercalators. I. Synthesis and conformational properties of an ethidium homodimer and of an acridine ethidium heterodimer" *Biochemistry* **17**(24), 5071-5078

171 Glazer AN, Peck K, and Mathies RAA (1990) "Stable double-stranded DNA-ethidium homodimer complex: application to picogram fluorescence detection of DNA in agarose gels" *Proceedings of the National Academy of Sciences USA* **87**(10), 3851-3855

172 Babich H, and Borenfreund E, (1990) "Applications of the neutral red cytotoxicity assay to *in vitro* toxicology (Review)" *Alternatives to Laboratory Animals* **18**, 129-144

173 Bulychev A, Troyet A, and Tulkens P, (1978) "Uptake and intracellular distribution of neutral red in cultured fibroblasts" *Experimental Cell Research* **115**, 343-355

174 Knox P, Uphill PF, Fry JR, Benford J, and Balls M, (1986) "The FRAME multicentre project on *in vitro* cytotoxicology" *Food Chemical Toxicology* **24**, 457-463

175 Clothier RH, Hulme L, Ahmed AB, Reeves HL, Smith M, and Balls M, (1988) "*In vitro* cytotoxicity of 150 chemicals to 3T3-L1 cells, assessed by the FRAME Kenacid Blue Method" *Alternatives to Laboratory Animals* **16**, 84-95

176 Clothier RH, Hulme LM, Smith M, and Balls M, (1987) "Comparison of the *in vitro* cytotoxicities and acute *in vivo* toxicities of 59 chemicals" *Molecular Toxicology* **1**(4), 571-577

177 Mosmann T, (1983) "Rapid colorimetric assay for cellular growth and survival: application to proliferation and cytotoxicity assays" *Journal of Immunological Methods* **65**, 55-63

178 Jeppesen C, and Nielsen PE (1989) "Photofootprinting of drug-binding sites on DNA using diazo- and azido-9-aminoacridine derivatives" *European Journal of Biochemistry* **182**(2), 437-44

179 Kapuscinski J, (1995) "DAPI: a DNA-specific fluorescent probe" *Biotechnic and Histochemistry* 1995 **70**(5), 220-33

180 British Standard BS EN 30993-5: 1994 ISO 10993-5: 1992, Biological evaluation of medical devices. Part 5. Tests for cytotoxicity, *in vitro* methods, British Standards Institution

181 Dropcova S, Denyer SP, Lloyd AW, Gard PR, Hanlon GW, Mikhalovsky SV, Sandeman S, Olliff CJ, and Faragher RG, (1999) "A standard strain of human ocular keratocytes" *Ophthalmic Research* **31**(1), 33-41

182 Butt ST, and Christensen T, (2000) "Toxicity and phototoxicity of chemical sun filters" *Radiation Protection Dosimetry* **91**(1-3), 283-286

183 Baker D, (1982) *Protein Deposition at Polymer Surfaces* PhD Thesis, Aston University

184 Tonge SR, (1994) *Hypercoiling and Hydrophobically Associating Polymers, Interfacial Synthesis, Surface Properties and Pharmaceutical Applications*, PhD Thesis, Aston University

185 Dean JA (ed), (1992) *Lange's Handbook of Chemistry* 14th edition McGraw-Hill Inc New York

186 McMurry J, (1992) *Organic Chemistry* 3rd Edition Brooks/Cole Publishing Company, Wadsworth Inc, Belmont, California

187 Park J-S, Lim Y-B, Kwon Y-M, Jeong B, Choi Y H, and Kim S W, (1999) "Liposome fusion induced by pH-sensitive copolymer: poly(4-vinylpyridine-co- N,N'-diethylaminoethyl methacrylate)" *Journal of Polymer Science Part A: Polymer Chemistry*, **37**, 2305–2309

188 Lee AS, and Gast AP, (1999) "Characterizing the Structure of pH Dependent Polyelectrolyte Block Copolymer Micelles" *Macromolecules* ***32***, 4302-4310

189 van de Wetering, P, Zuidam NJ, van Steenbergen MJ, van der Houwen OAGJ, Underberg JM, and Hennink WE, (1998) "A mechanistic study of the hydrolytic stability of poly(2-(dimethy- lamino)ethyl methacrylate)" *Macromolecules* 31, 8063–8068

190 Davidson RL (ed), (1980) *Handbook of Water-Soluble Gums and Resins* McGraw-Hill, New York, London

191 Oxley HR, Corkhill PH, Fitton JH, and Tighe BJ, (1993) "Macroporous hydrogels for biomedical applications: methodology and morphology" *Biomaterials* **14**(14), 1064-1072

Appendix I

Sequence distribution simulations for hydrogel copolymers

NVP/MMA 60:40

60 mole % of monomer A, NVP

40 mole % of monomer B, MMA

r (AB) = 0.01 r (BA) = 4.04

Polymerised to 100% conversion

In the simulated copolymer NVP is represented by O and MMA is represented by X

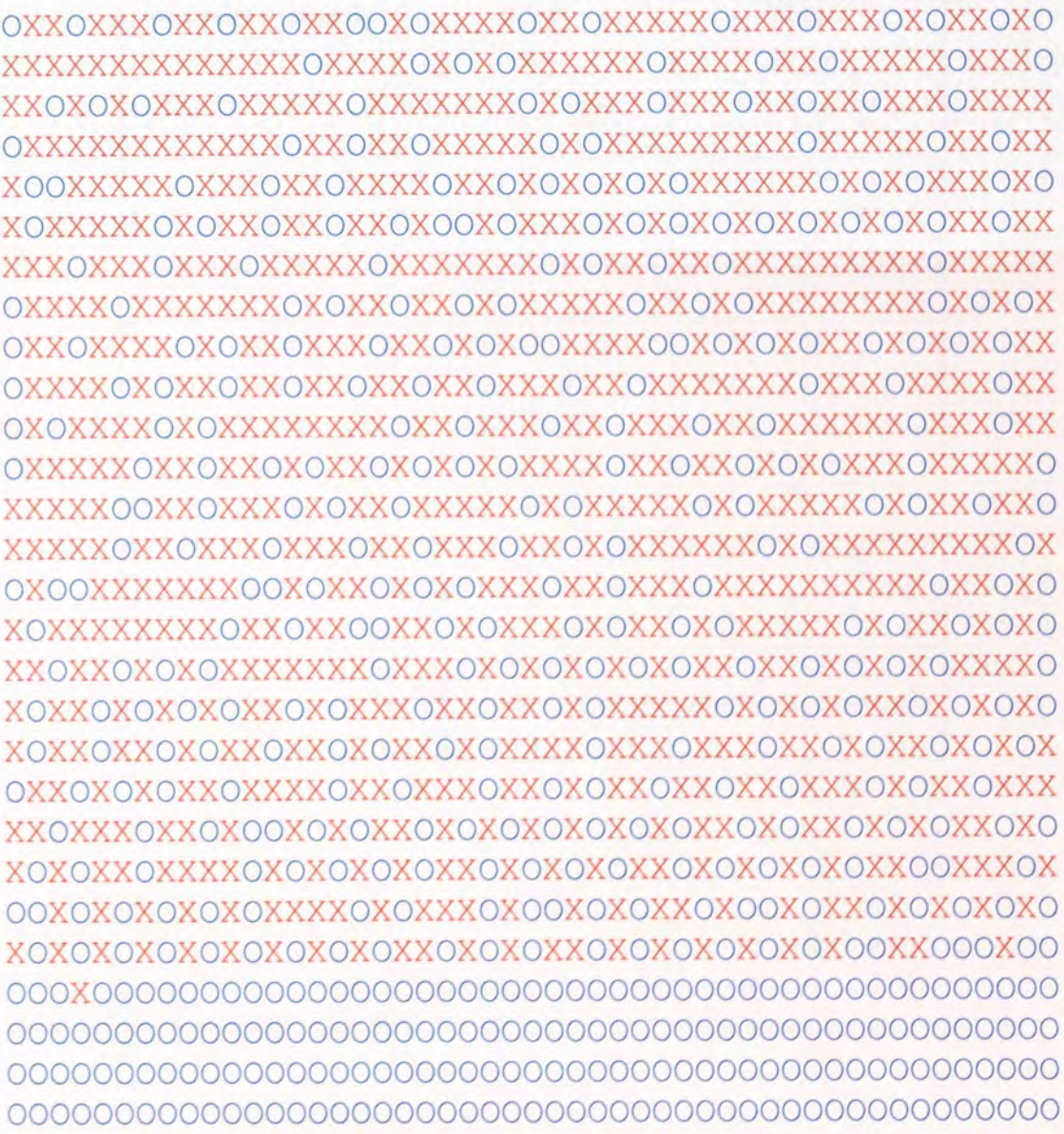

The simulated copolymer contains 1200 NVP units and 800 MMA units

Sequence Length	NVP	MMA
1	342	167
2	15	98
3	1	37
4	00	17
5	1	21
6	0	4
7	0	6
8	0	3
9	0	3
10	0	1
12	0	1
14	0	1
820	1	0

NVP/MMA 70:30

70 mole % of monomer A, NVP

30 mole % of monomer B, MMA

r (AB) = 0.01 r (BA) = 4.04

Polymerised to 100% conversion

In the simulated copolymer NVP is represented by O and MMA is represented by X

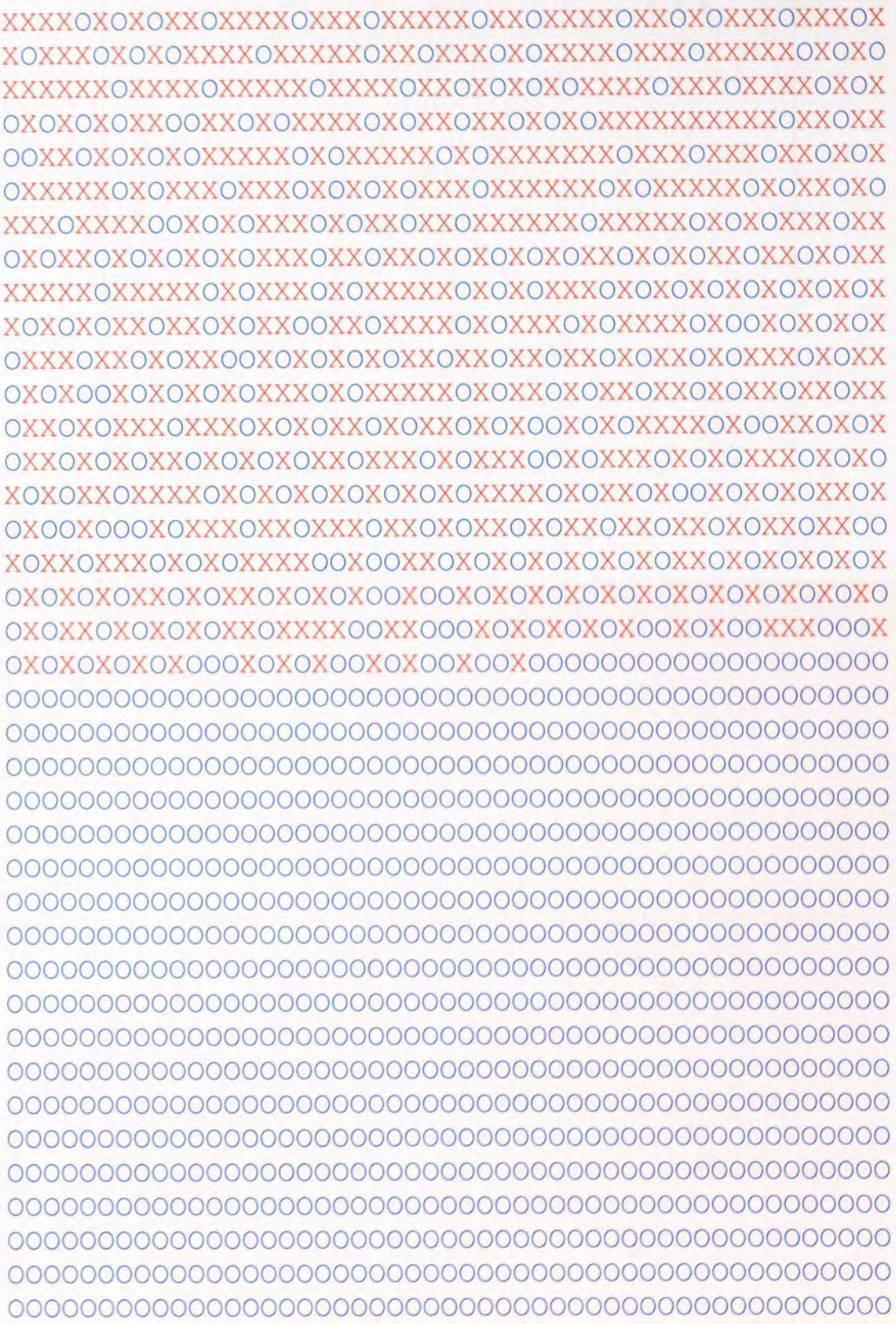

OOOOOOOOOOOOOOOOOOOOOOOOOOOOOOOOOOOOOOOOOOOOOOOOOOOOOOOO
OOOOOOOOOOOOOOOOOOOOOOOOOOOOOOOOOOOOOOOOOO

The simulated copolymer contains 1400 NVP units and 600 MMA units

Sequence Length	NVP	MMA
1	300	192
2	24	69
3	4	32
4	0	18
5	0	12
6	0	3
7	0	2
10	0	1
1040	1	0

NVP/MMA 80:20

80 mole % of monomer A, NVP

20 mole % of monomer B, MMA

r (AB) = 0.01 r (BA) = 4.04

Polymerised to 100% conversion

In the simulated copolymer NVP is represented by O and MMA is represented by X

XXOXOXXXOXXOXOXXXOXOXOOXXOXXOXXXOXXOXXOXXXOXOXOXO
XOXOXXXXOXOXXXXXXXOXXXOXOXXXXXXXXOXXXOXXXOXXOXXXO
XXOXOXXOXOXOXOXXXOXXXXXOXXXOXXOXXOXXXOXOXOXOXOXXX
OXOXOXOXXOXXXXOXXOXOXXOXOXOXOOXOXXOXOXXOXOXXXOXOX
OXOXXXXOXOXOXOOOXOXXOXXOXOXOXOXXOXXXXOXOOXOXXXOXO
XOXXOXXOXOXXXOXXOXXXXXXOXOXOXXOXOXXOXOXXOXOXXXOXX
OXXOXXOXOOXXXXXXOXXOXOXXXXOXOXOXOXOXXOXOXOXOXOXOX
OXOXXOXOXOXOXXXOXXOXOXOXOXXXXXXOXXOXOXXOOXXXXXOXO
XOXXOXXXOXXOXOXXOXOXXXOXXOXOXOXOXOOXXOXOOXOXXXXOX
OXXOXXOXOXOXOXOXOXOXOOXXXOXOXXXOXOXXOXOOXXOXOXXOX

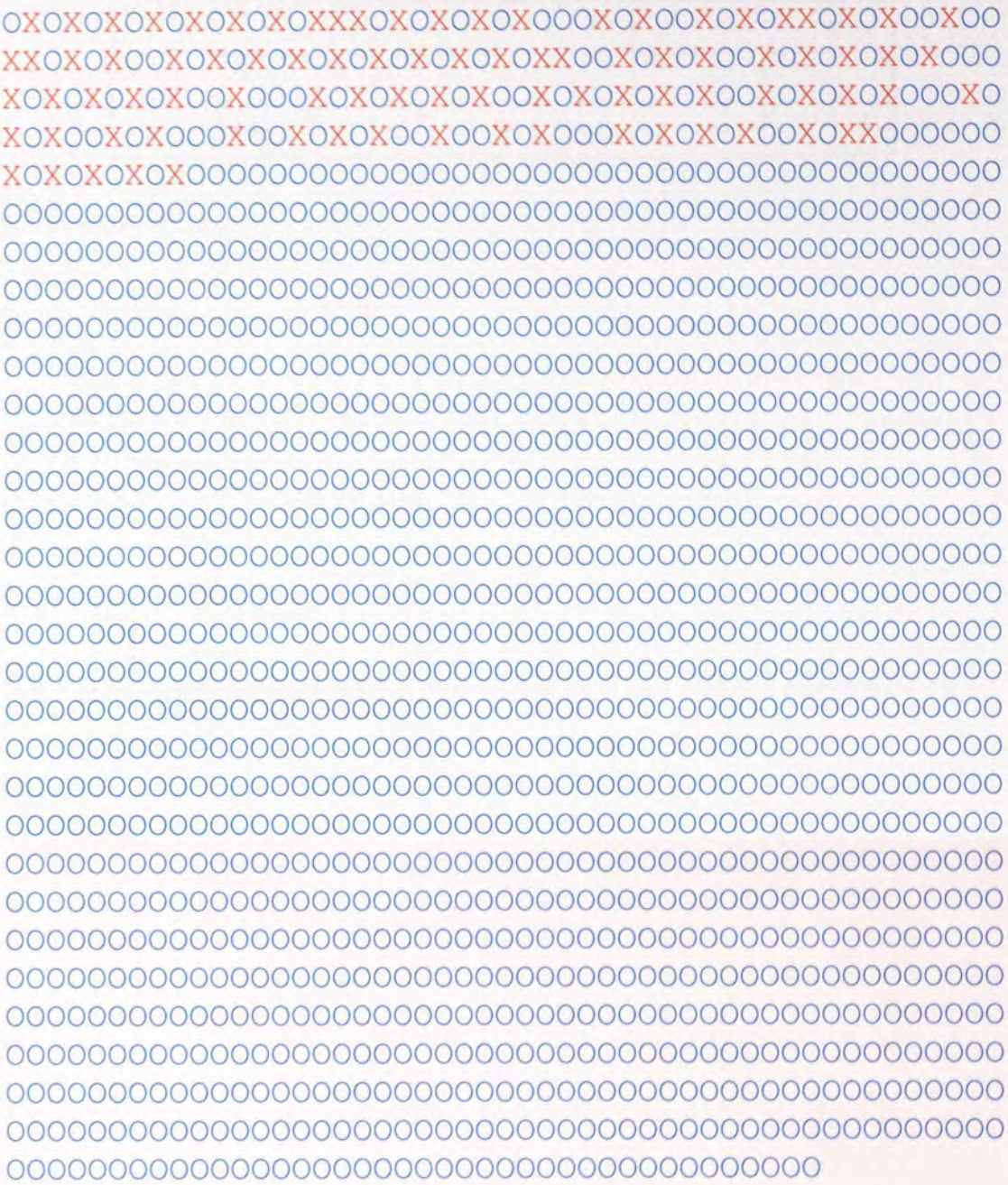

The simulated copolymer contains 1600 NVP units and 400 MMA units

Sequence Length	NVP	MMA
1	222	171
2	23	48
3	7	22
4	0	6
5	0	2
6	1	3

7	0	1
8	0	1
1305	1	0

NVP/MMA 90:10

90 mole % of monomer A, NVP

10 mole % of monomer B, MMA

r (AB) = 0.01 r (BA) = 4.04

Polymerised to 100% conversion

In the simulated copolymer NVP is represented by O and MMA is represented by X

OXOXOXXXOXOXOXOXOXXXOXXOOOXOXXXXOXOXOXOXOXOXOXXXX
OXOXOXOXXXOXOXOXXXOXXOXXXOXOXXOXOXOXXXOOXXOXOXOX
OXOXOXOXXXOXOXOXOXXXOXOOXOXOXOXOXOXOXOXOXXXOXOXOXO
XOXOXOXOOXOOXXOXXOXOXOXOXOXOXOOOXOXOXOXOXOXXOXXXO
XXXOXOXOXOOOXOXOXOXOXOXOXOXOXOOXXOXOXXOXXOXOXOOXO
XOXOXXOXOXOXOXOOXOXXOXOXXXOXOXOXXOXOXOXOOXOOXOXOX
OXOOXOXOXOXOXOXOOXOXOXOXOOOOOOOXOXOXOXOOOXOXOXOXO
XOXXOXOXOOXOXOXOXOXOOXOXOXOXOXOXOXOXOXOOOXXOOOO
OOOOOOOOOOOOOOOOOOOOOOOOOOOOOOOOOOOOOOOOOOOOOOOOOO
OOOOOOOOOOOOOOOOOOOOOOOOOOOOOOOOOOOOOOOOOOOOOOOOOO
OOOOOOOOOOOOOOOOOOOOOOOOOOOOOOOOOOOOOOOOOOOOOOOOOO
OOOOOOOOOOOOOOOOOOOOOOOOOOOOOOOOOOOOOOOOOOOOOOOOOO
OOOOOOOOOOOOOOOOOOOOOOOOOOOOOOOOOOOOOOOOOOOOOOOOOO
OOOOOOOOOOOOOOOOOOOOOOOOOOOOOOOOOOOOOOOOOOOOOOOOOO
OOOOOOOOOOOOOOOOOOOOOOOOOOOOOOOOOOOOOOOOOOOOOOOOOO
OOOOOOOOOOOOOOOOOOOOOOOOOOOOOOOOOOOOOOOOOOOOOOOOOO
OOOOOOOOOOOOOOOOOOOOOOOOOOOOOOOOOOOOOOOOOOOOOOOOOO
OOOOOOOOOOOOOOOOOOOOOOOOOOOOOOOOOOOOOOOOOOOOOOOOOO
OOOOOOOOOOOOOOOOOOOOOOOOOOOOOOOOOOOOOOOOOOOOOOOOOO
OOOOOOOOOOOOOOOOOOOOOOOOOOOOOOOOOOOOOOOOOOOOOOOOOO
OOOOOOOOOOOOOOOOOOOOOOOOOOOOOOOOOOOOOOOOOOOOOOOOOO
OOOOOOOOOOOOOOOOOOOOOOOOOOOOOOOOOOOOOOOOOOOOOOOOOO
OOOOOOOOOOOOOOOOOOOOOOOOOOOOOOOOOOOOOOOOOOOOOOOOOO
OOOOOOOOOOOOOOOOOOOOOOOOOOOOOOOOOOOOOOOOOOOOOOOOOO

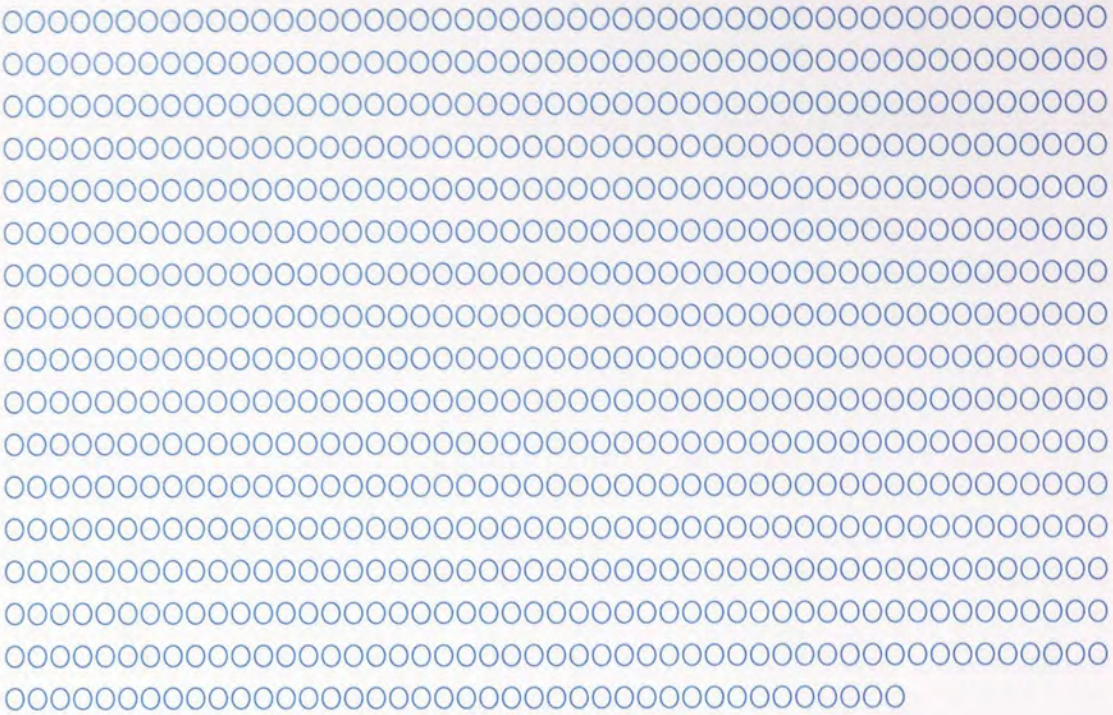

The simulated copolymer contains 1800 NVP units and 200 MMA units

Sequence Length	NVP	MMA
1	140	130
2	13	19
3	5	8
4	0	2
7	1	0
1612	1	0

NVP/MMA/NVI 79:19:2

79 mole % of monomer A, NVP

19 mole % of monomer B, MMA

2 mole % of monomer C, NVI

r(AB) = 0.01 r(AC) = 0.174 r(BA) = 4.04

r(BC) = 4.603 r(CA) = 2.368 r(CB) = 0.067

Polymerised to 100% conversion

In the simulated copolymer NVP is represented by O MMA is represented by X and NVI is represented by *

OOOOOOOOOOOOOOOOOOOOOOOOOOOOOOOOOOOOOOOOOOOOOOOOOOOOO
OOOOOOOOOOOOOOOOOOOOOOOOOOOOOOOOOOOOOOOOOOOOOOOOOOOOO
OOOOOOOOOOOOOOOOOOOOOOOOOOOOOOOOOOOOOOOOOOOOOOOOOOOOO
OOOOOOOOOOOOOOOOOOOOOOOOOOOOOOOOOOOOOOOOOOO

The simulated copolymer contains 1580 NVP units and 380 MMA units and 40 NVI units

Sequence Length	NVP	MMA	NVI
1	223	146	36
2	24	49	2
3	9	22	0
4	1	7	0
5	0	6	0
6	2	2	0
1266	1	0	0

NVP/MMA/NVI 77.5:17.5:5

77.5 mole % of monomer A, NVP

17.5 mole % of monomer B, MMA

5 mole % of monomer C, NVI

r(AB) = 0.01 r(AC) = 0.174 r(BA) = 4.04

r(BC) = 4.603 r(CA) = 2.368 r(CB) = 0.067

Polymerised to 100% conversion

In the simulated copolymer NVP is represented by O, MMA is represented by X and NVI is represented by *

XOXX*XXOXOXOXOXXOXXXXOXOXOXXOXXOXXOOXOXOXXXOXOX
XXXXOXXOXOXXOXOXXOXOXXOXXOXXOXOXOXXOXOXOXOOXXOXOX
XOXXOXXOXOXXXXXXOXX*XOXXXOXOXOXXXOXOXOXXXXOXOXOXOX

The simulated copolymer contains 1550 NVP units and 350 MMA units and 100 NVI units

Sequence Length	NVP	MMA	NVI
1	241	159	90
2	43	54	5
3	14	12	0
4	7	8	0
5	0	3	0
6	2	0	0
8	1	0	0
1133	1	0	0

NVP/MMA/NVI 76.5:16.5:7

76.5 mole % of monomer A, NVP

16.5 mole % of monomer B, MMA

7 mole % of monomer C, NVI

r(AB) = 0.01 r(AC) = 0.174 r(BA) = 4.04

r(BC) = 4.603 r(CA) = 2.368 r(CB) = 0.067

Polymerised to 100% conversion

In the simulated copolymer NVP is represented by O, MMA is represented by X and NVI is represented by *

XOXOXOXXXXX*XOXOXXOXOXXXOXXOXXOXXOXXOXOXXXOXXOXXO
XXOXOXOXXOXXOXOX*XOXXOXXXOXOXX**XXXXOXOXXOXOXXXOX
XOXOXX*OXXOXOXXOXOXXOXXOOXOXOXOXOXXOXOXOXXXOXX*XO
XOXOXXOXOXOXOXXXOXXXOXOXOOXXOXXXOXXOXOX*XOXOXXXXO
XOXXXXOOXXOXOXOXXXOXX*OXOX*XXOOX*X*XOXXXXO*OX*XXX
OXOXOXXOXOXOOO*XOXOXOOX*XOXOXX*OOXOXOXO*XOXXOXXOX
XXOXOXOOXOXXXOXOXOXOXOXXXX*X*XXXOOXXOXOXOXOXOXXOX
XOXOXOXOXO*XOXOXOXOXOOOXX*XOXOXOXXOXOXOXOXOXOOXOX
OXOOXXO*XOXO*XOXX*X*XOOXOXOXO*OXXOXXOXOXO*XXOXOXX

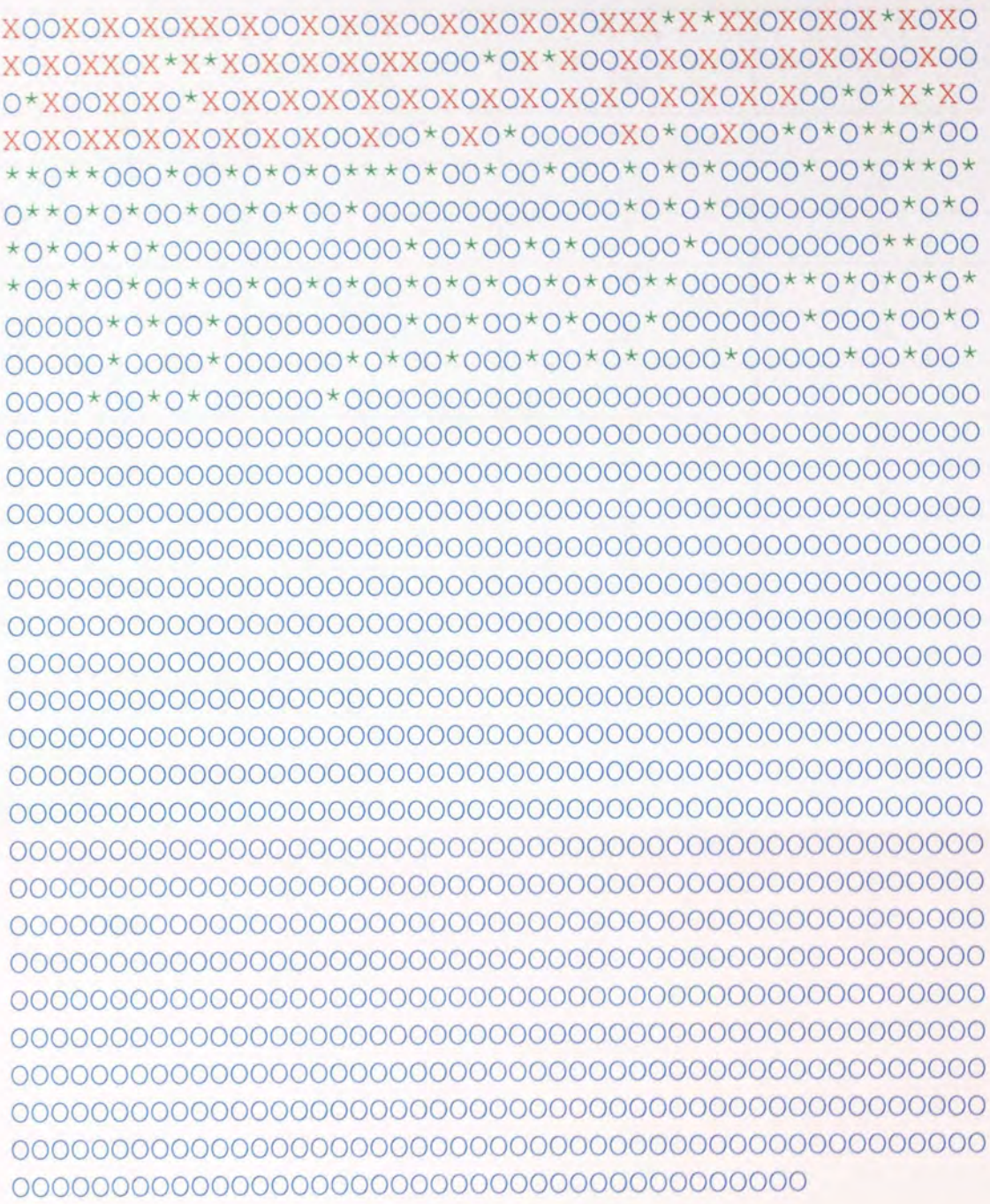

The simulated copolymer contains 1530 NVP units and 330 MMA units and 140 NVI units

Sequence Length	NVP	MMA	NVI
1	228	168	119
2	51	46	9
3	10	15	1
4	4	5	0
5	5	1	0
6	3	0	0
7	1	0	0
9	3	0	0
12	1	0	0
13	1	0	0
1052	1	0	0

NVP/MMA/NVI 75:15:10

75 mole % of monomer A, NVP

15 mole % of monomer B, MMA

10 mole % of monomer C, NVI

r(AB) = 0.01 r(AC) = 0.174 r(BA) = 4.04

r(BC) = 4.603 r(CA) = 2.368 r(CB) = 0.067

Polymerised to 100% conversion

In the simulated copolymer NVP is represented by O, MMA is represented by X and NVI is represented by *

XOXOXOXOXXXOXXOXOXXXOXOXXXOXOXOXOXXXXOXXOXOXX*XXO
XOXOXXOXOXXXOXOXXOXXXX*XOXXXXXXOXOXOXOXOXOXXOXXXX
XOXOXOXX**OXOXOXOOXXOXOXOX*XOXXOXOXOXXOXXOXOXXOXX
XOXOX*OXXOXXOX*XX*XOXXOXXXOXOXOXOXXXOXOXOXOXXOX*O
XXOXXOXOXOXXOXOXOXOXXOXXXO*XOXOOXOXOXXOXOXXOXXXXO

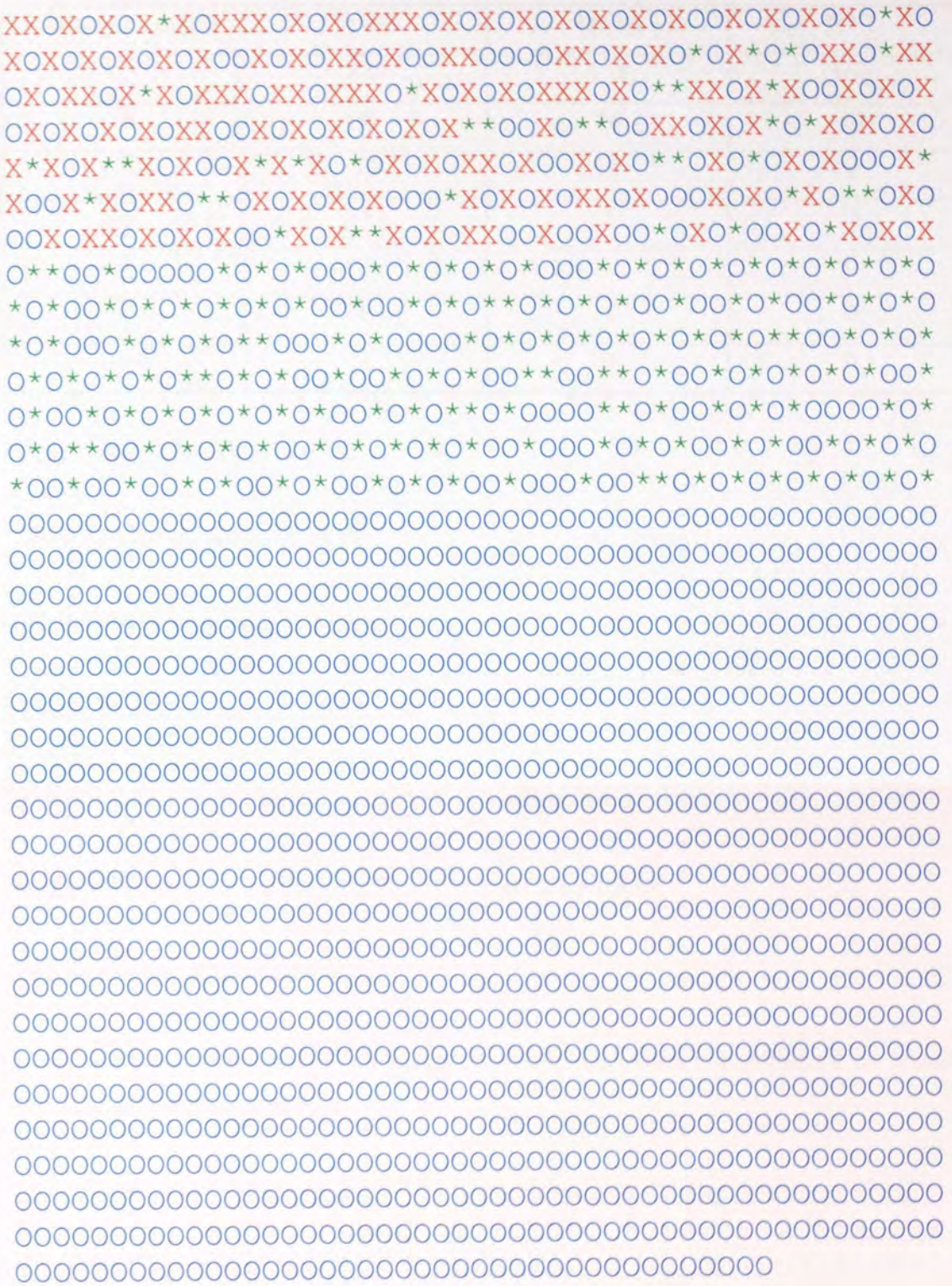

The simulated copolymer contains 1500 NVP units and 300 MMA units and 200 NVI units

Sequence Length	NVP	MMA	NVI
1	288	158	160
2	46	40	20
3	10	13	0
4	4	3	0
5	1	1	0
6	0	1	0
1069	1	0	0

NVP/MMA/DEAEMA79:19:2

79 mole % of monomer A, NVP

19 mole % of monomer B, MMA

2 mole % of monomer C, DEAEMA

r(AB) = 0.01 r(AC) = 0.004 r(BA) = 4.04

r(BC) = 1.184 r(CA) = 2.82 r(CB) = 0.838

Polymerised to 100% conversion

In the simulated copolymer NVP is represented by O, MMA is represented by X and DEAEMA is represented by *

XOXXXO*XO*XXXXXXOXOXXOXOXOXX*XXXXOXOXOXXOXOX*OXOX
XOXOXOXOXOXXOXOX*XXOXO*O*XOXXO*O*XXXXOXXXXXXXOXXX
O*OXXXOXXO*XOOXXO*OXOXXOXXOXOXXXOXXOXXOXOXXXXOXXO
*XOXXXOXOOXXXXOXXOXXOXO*OOX*XOXO*OXXOXXOXOXOXOXOX
OXXXOXXOXXOXOXOXO*OXXOXXXOOXXOXOOXOXOXOXOXOXO*XOX
OXXXOXXXOXXOOXXXOXX*OXXXXX*OXOXOOXX*O*OXOXOXOXOXO
XXOXXO*XXOXOXXOXO*OXXXOXOXOXXOXOXXXOXOX*OXXOO*XXX
OXOXOX*OXXOXO*XXOXXO*O*OXXOXOXOXOXO*O*OXXOXOXOXX*
O*OXXOXXXXO*OXOXOXXOXXOXOXXOXOXOXXOXOXXXOXOXOXOOX
OXXXOOOXXOXO*OXOXOXXXOXXXOXOXOXOXOXXXXOXOXXXXOXXO
XOXOXXXOXO*OXOXOOXOXO*O*OXOXOXOXOXXXXO*OXOOXOXOXO

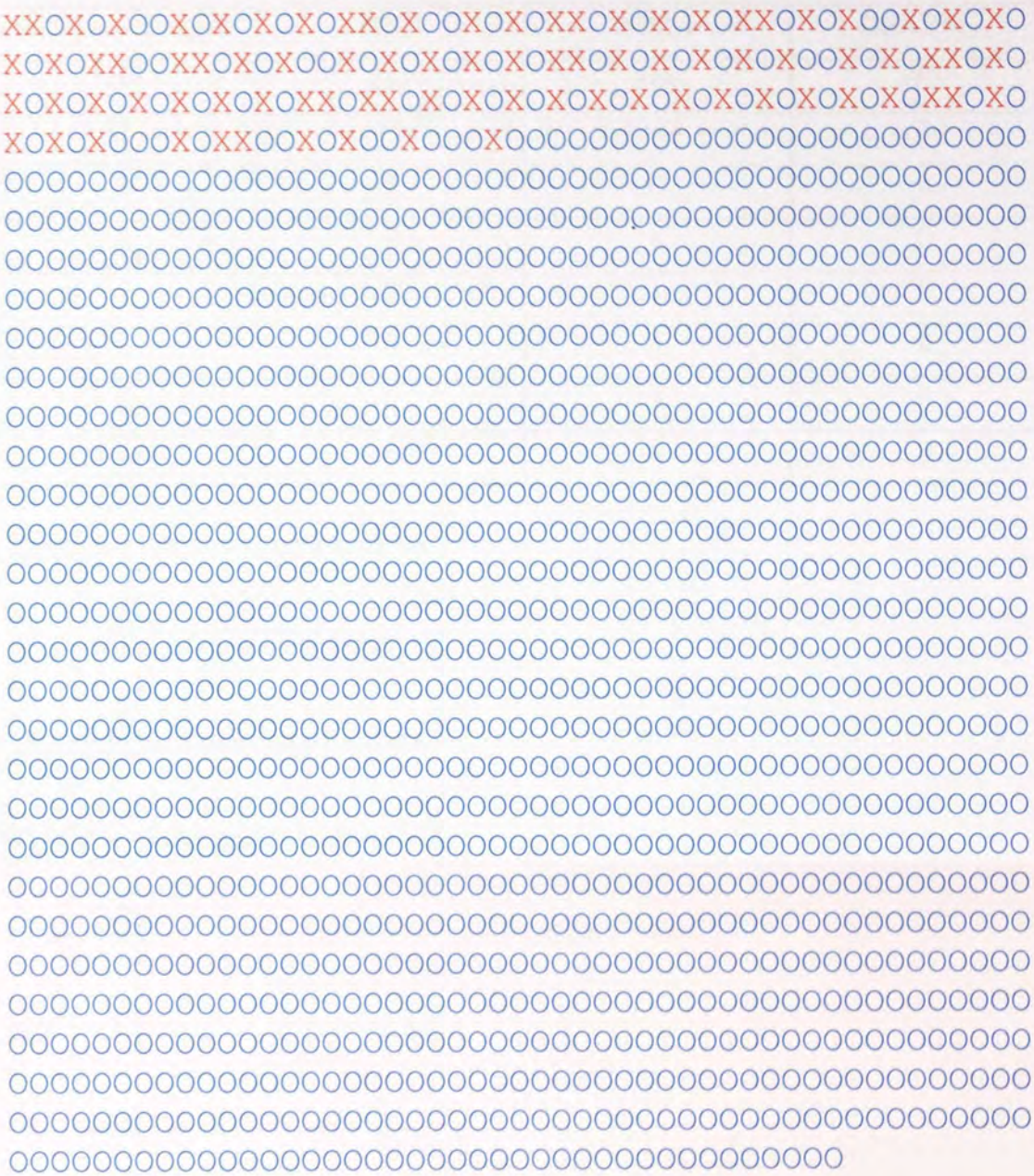

The simulated copolymer contains 1580 NVP units and 380 MMA units and 40 DEAEMA units

Sequence Length	NVP	MMA	DEAEMA
1	243	164	40
2	19	56	0
3	3	18	0
4	0	8	0
5	0	1	0
6	0	1	0
7	0	1	0
1290	1	0	0

NVP/MMA/DEAEMA 77.5:17.5:5

77.5 mole % of monomer A, NVP

17.5 mole % of monomer B, MMA

5 mole % of monomer C, DEAEMA

r(AB) = 0.01 r(AC) = 0.004 r(BA) = 4.04

r(BC) = 1.184 r(CA) = 2.82 r(CB) = 0.838

Polymerised to 100% conversion

In the simulated copolymer NVP is represented by O, MMA is represented by X and DEAEMA is represented by *

XOX*O*XOXXXXO*O*XXO*O*OXXXO*X*OXXOXXXOXO*OXOXXO*O
*XXXO*OXO**XXX*XO*OXO*XXOX*OXXOXXOXO*XXXXO*XXOXXX
O*XXXXO*XO*O**OXO*O*OXXXXO*OXOXOXXOXXO*OOX*XOXO*O
XXOXO*OXXOXX*O*XO*O*XOXXOX*O*OX*XOXOOXXXOXO*O*OXX
XX*OXXOXXXXO*OXOO**OX*OXO*O***OX**OXO*XXOXOXOXOOX
O*XOXOXO*OXXOXO*O*OXOOXXO*OXO**OXOXOXXOXOO*XXXXXO
XXO*O*OX*XXOXXOXXOXOXOXOOXXXXOXOXO*OXOXXOXXOXOXOX
OXOXXOXXXOXXXO*OOXOXOXXO*O*XXOXOXXOXXOXOXXO*OXOXX
OXXX*O*OXXO*OXO*XXOX*XXXOXOOXOXOXOXOXO*OXXOO*OXO*

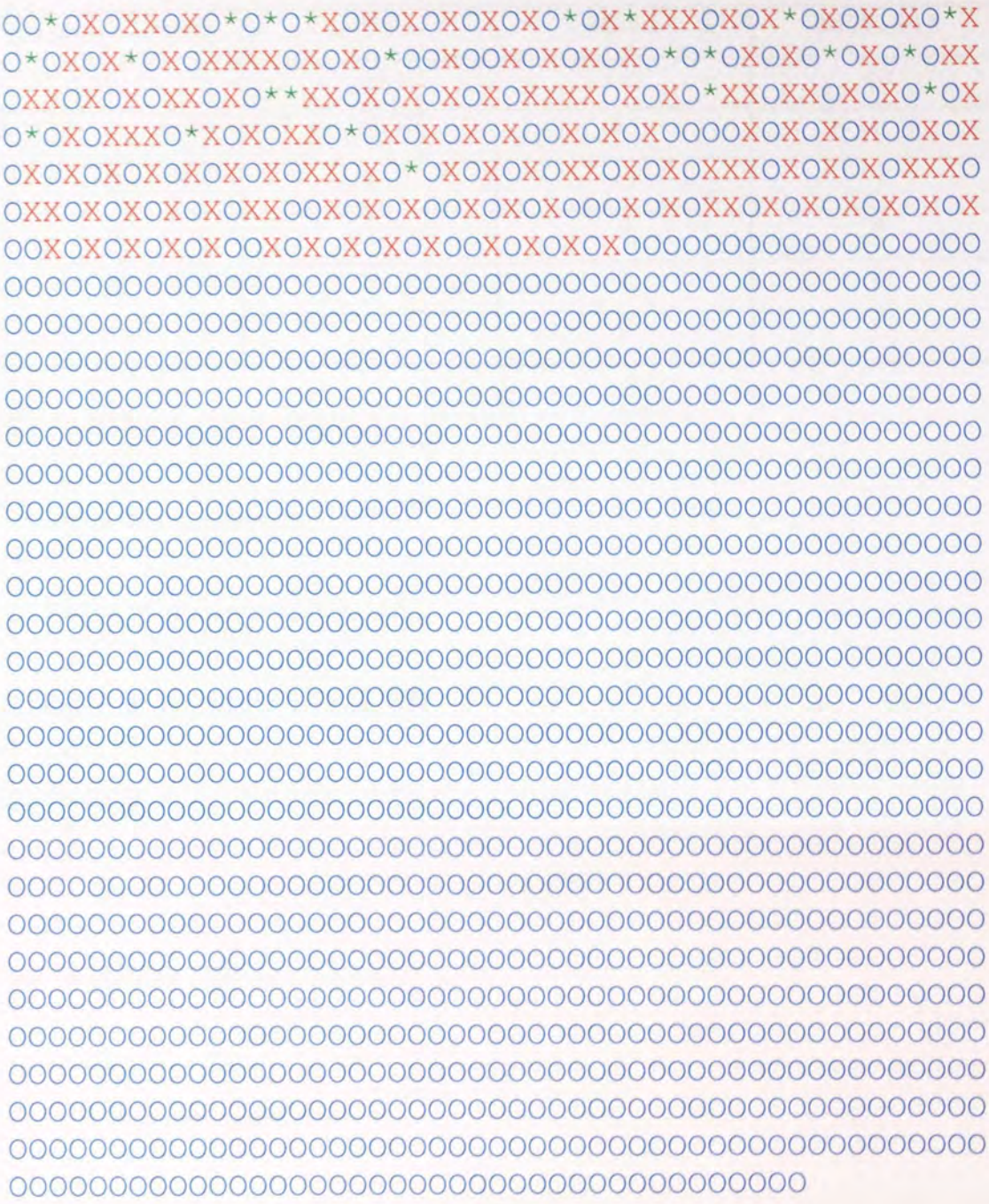

The simulated copolymer contains 1550 NVP units and 350 MMA units and 100 DEAEMA units

Sequence Length	NVP	MMA	DEAEMA
1	267	173	85
2	21	47	6
3	1	14	1
4	1	9	0
5	0	1	0
1234	1	0	0

NVP/MMA/DEAEMA 76.5:16.5:7

76.5 mole % of monomer A, NVP

16.5 mole % of monomer B, MMA

7 mole % of monomer C, DEAEMA

r(AB) = 0.01 r(AC) = 0.004 r(BA) = 4.04

r(BC) = 1.184 r(CA) = 2.82 r(CB) = 0.838

Polymerised to 100% conversion

In the simulated copolymer NVP is represented by O, MMA is represented by X and DEAEMA is represented by *

XO*X*XO*O**XO**OX*O*OXX*XO*XXO*O*OXXOXXXO*XXOXO*O
*OXOXOX*OXXO*O*OX***XXXX*O**OXXOXOXOX*OXOXXXO*XOX
XO*O*O*XOXOXO*XO*XX**XXOXXO*XXX*XOX*OXOXOX*OXOXXO
XO*O*OOXO*OXXOXOXX*OXOXXOXOXO*XOXOXO**XO*OXXX*XOX
OXXO*OO*OXOXXOXXO*XOXXO*OXXXOXXXOXXX*OOXXXOXO*XO*
XO*OXXO*O*XXO*O*OXOXXO*OXXOXOXOOXOO*O*O*O*OXO*O*O
XOXXXOXOXXOO*OXOXXXO*OXO*OXXO*XOXOXXOXX**O**O*O*O
XXXO*XXXXXOX*O*OO*X*O*OXO*O*XOXO**O*O*XOXXXOO*OXX
OXOXOX*XOXO**OO*OXO*XOXOX*XXO*OO**OXO*OXOXO*O*XOX
XXOXX**O*OXOXX*XO*O*O*XOXOXXXOXO*OXXXO*OXXOOXO*XO
XO*O*O*OXOXO*OXOXOXOXXO*XOXO*OXO*OX*OXX*XXOXO*X*X
XOX*XOXXO*O*OXOXXXOXOXOXO*O*O*OXOXXXOXOXOXO*O*X*O

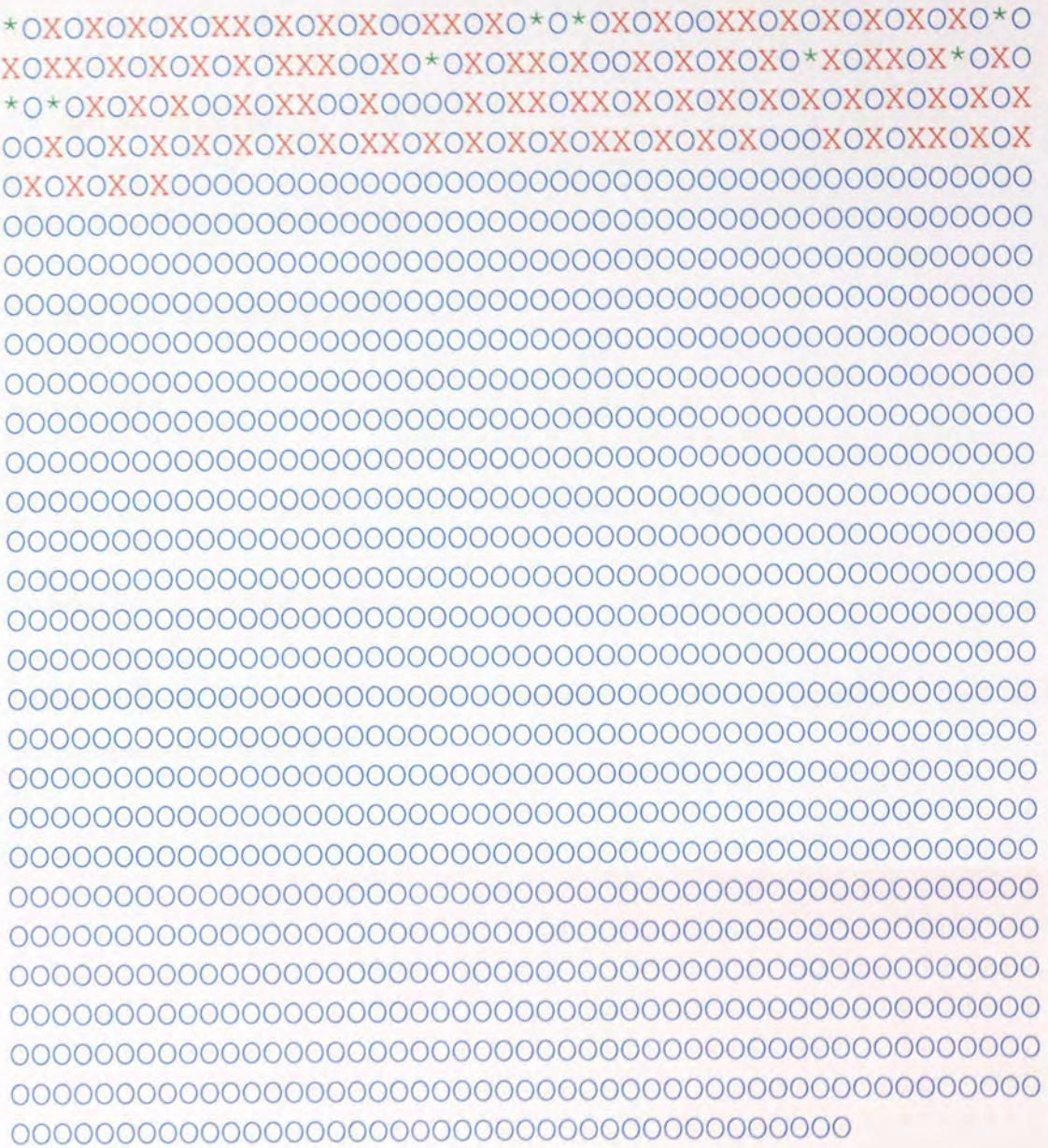

The simulated copolymer contains 1530 NVP units and 330 MMA units and 140 DEAEMA units

Sequence Length	NVP	MMA	DEAEMA
1	277	171	115
2	19	48	11
3	1	18	1
4	1	1	0
5	0	1	0
1208	1	0	0

NVP/MMA/DEAEMA 75:15:10

75 mole % of monomer A, NVP

15 mole % of monomer B, MMA

10 mole % of monomer C, DEAEMA

r(AB) = 0.01 r(AC) = 0.004 r(BA) = 4.04

r(BC) = 1.184 r(CA) = 2.82 r(CB) = 0.838

Polymerised to 100% conversion

In the simulated copolymer NVP is represented by O, MMA is represented by X and DEAEMA is represented by *

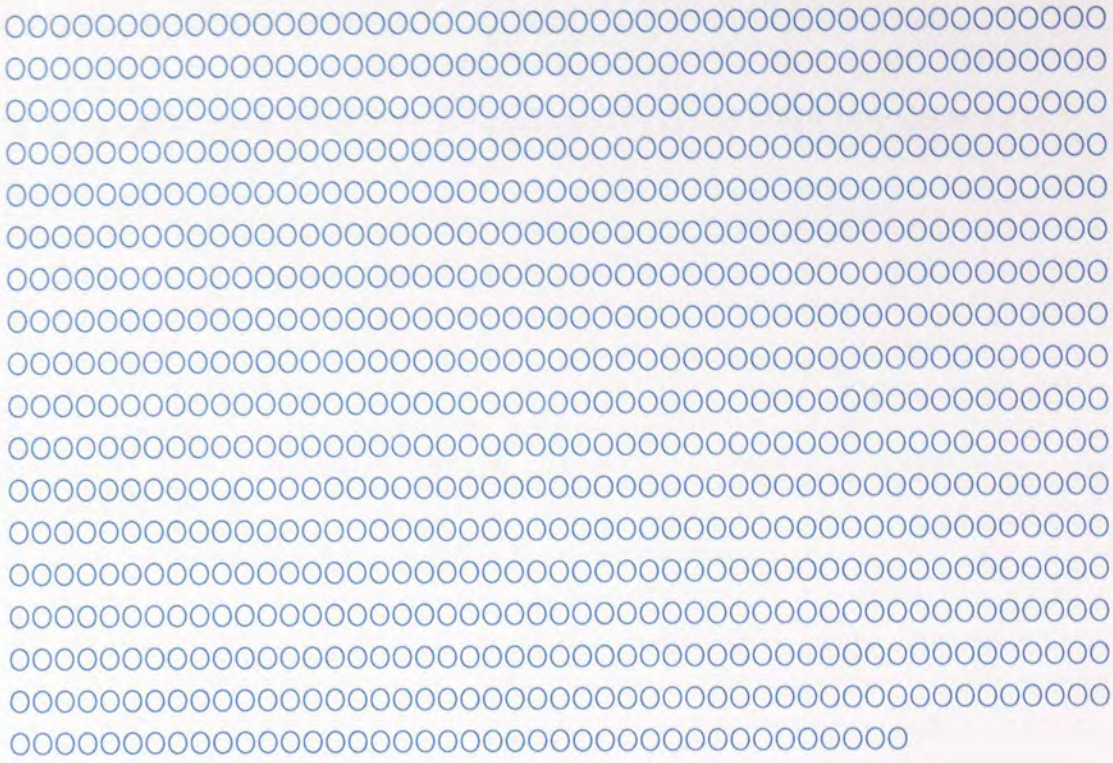

The simulated copolymer contains 1500 NVP units and 300 MMA units and 200 DEAEMA units

Sequence Length	NVP	MMA	DEAEMA
1	297	169	160
2	20	33	17
3	3	14	2
4	0	3	0
5	0	1	0
6	0	1	0
1154	1	0	0

NVP/MMA 25:75

25 mole % of monomer A, NVP

75 mole % of monomer B, MMA

r (AB) = 0.01 r (BA) = 4.04

Polymerised to 100% conversion

In the simulated copolymer NVP is represented by O and MMA is represented by X

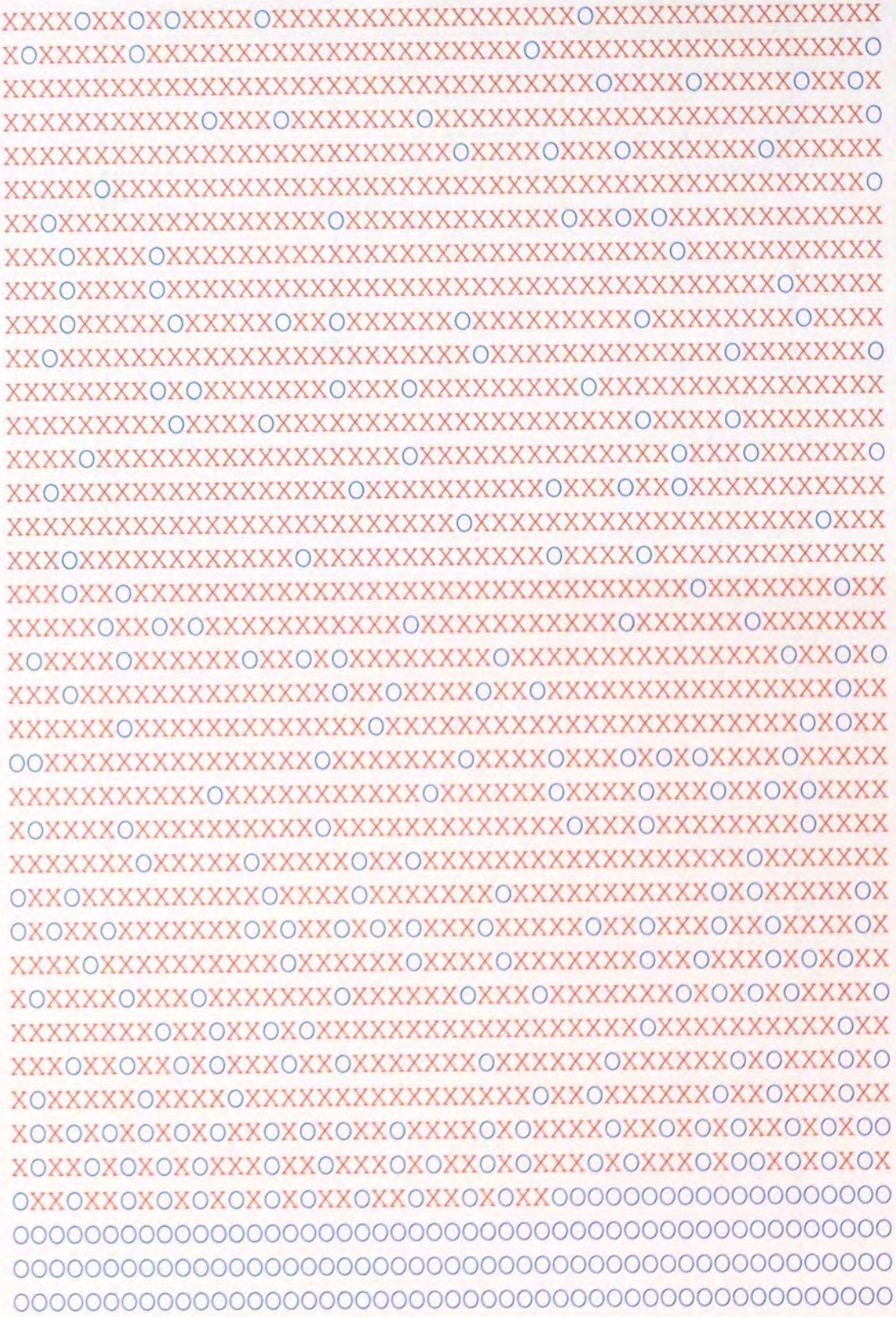

OOOOOOOOOOOOOOOOOOOOOOOOOOOOOOOOOOOOOOOOOOOOOOOOOOOOOOOO
OOOOOOOOOOOOOOOOOOOOOOOOOOOOOOOOOOOOOOOOOO

The simulated copolymer contains 500 NVP units and 1500 MMA units

Sequence Length	NVP	MMA
1	239	56
2	3	42
3	0	23
4	0	23
5	0	12
6	0	12
7	0	14
8	0	8
9	0	2
10	0	5
11	0	6
12	0	4
13	0	4
14	0	3
15	0	4
16	0	5
17	0	3
18	0	3
19	0	1
20	0	1
21	0	1
23	0	2
24	0	1
25	0	2
28	0	1
31	0	1
33	0	1
34	0	1

36	0	1
42	0	1
255	1	0

AMO/MMA 25:75

25 mole % of monomer A, AMO

75 mole % of monomer B, MMA

r (AB) = 0.512 r (BA) = 1.759

Polymerised to 100% conversion

In the simulated copolymer AMO is represented by O and MMA is represented by X

XXXXXXXXXXXXXXXXXXXXXXXXXOXXXXXOXOXXOXXXOXOXXOXXXOXX
XXXOXOOXXXXXOXXXXXXXXXXXXXXXXXXXXOXOXOXXXXXXXXXXXXXO
XXXXXXOXOXOXXXXOXXXXXOXXXXXXXXXXXXXXXXXOOXXXOXXXOXOX
XXXXXXXXXXXOXXOXXOXXXXOXXOXXOOXOXOXXXOXOOXXOXXXXOX
XOXXXXXXOXXXXXXXXXXXXXXXXXXXXXXXXOOXXXOXXXXXXXOXXXXX
XXXXXXXXXOXXXXXOXXOXXOXXXXXXXXXOXXXXOXXXOXOXXXXXXX
XXXOXXXXOXXXOOXXXXXXXXXXXXXXXXXXXXXXXXXXXXXOXXXXXXOXX
XXXOXXXXXXXXXXXOXXXXXOXOOXOXXXXXXXXXOXXXXXXOXOXXX
XXXXXXXOXXXXXXXXXXOXXXXXXXXXXXXXXXXXXXXOXOXXXOXXOXXX
XXXXXXXXXXXXXXXXXOXOOOXXXXXXXXXXXOOXXXXXXXXXXXXXOXXX
OXXXXXXXXXXXXXXXOXXOXXXXXXXXXOXXXXXXXXXXXXXXXXXXXXOX
OXXXXXXXXXOOXOXXXXXXOXXOXXXXXXXXXOXXOXOXXXXXXXXOX
XXXXXXXXXXOXOOXXOXOXXOOXXOXXXXOXOXXOXXXXXXXXXXXXX
XXXXXOXXXXXXOOOOXXXXOXXXXXXOXXXXXXXXXXXXXXOXXXXXXOO
XXXOXXOXXXXXXXXXXXXXOXXXXXXXXXXOXXXXXXXXXXXXXXXXXOXXO
XOXOXXXOOOXOOXXXXXXXXXXXOXXXXOXXXXXXXXXXXXXXXXXXOXOX
OXXOXOOXOXXXXXXOXOXXXXOXOXXXXXXXXOXXXXOXXXXXXXXXXXXX
OXXXXXXOXXOXXXXXXXXXXOXXXXOXXOXXXXXXXXXOXXOXXOOXXOX
XXXXXXXXOXXXOXXXXOXXXXOXXXXXXXXXOXOXXXOXXXXOXXXXXX
OXXXXXXOOXXXXXXXXOXXXOXXXXOXOXOXOXOOXOOXXXXXXOXXXXO
XOXXXXXXXXXXOXXXXXXXXXXXXXXXXXXXXXOXXXXXOXOXOXXXXXXX
OOXXXXOXXOXXXOOXXXXXXXXXXXXXOXOOXXXXXXXXXXXXXXXXOXXOX
XOXXXXOXXXXXXXXOXOOXXXXOXXXXXOOOXXXXXXOXXXXXXXOXXX
XOXXXOXOXXOOXOXXOXOOOXXXXXXXXXXOXXOOXXXXXXOXXXXXXX

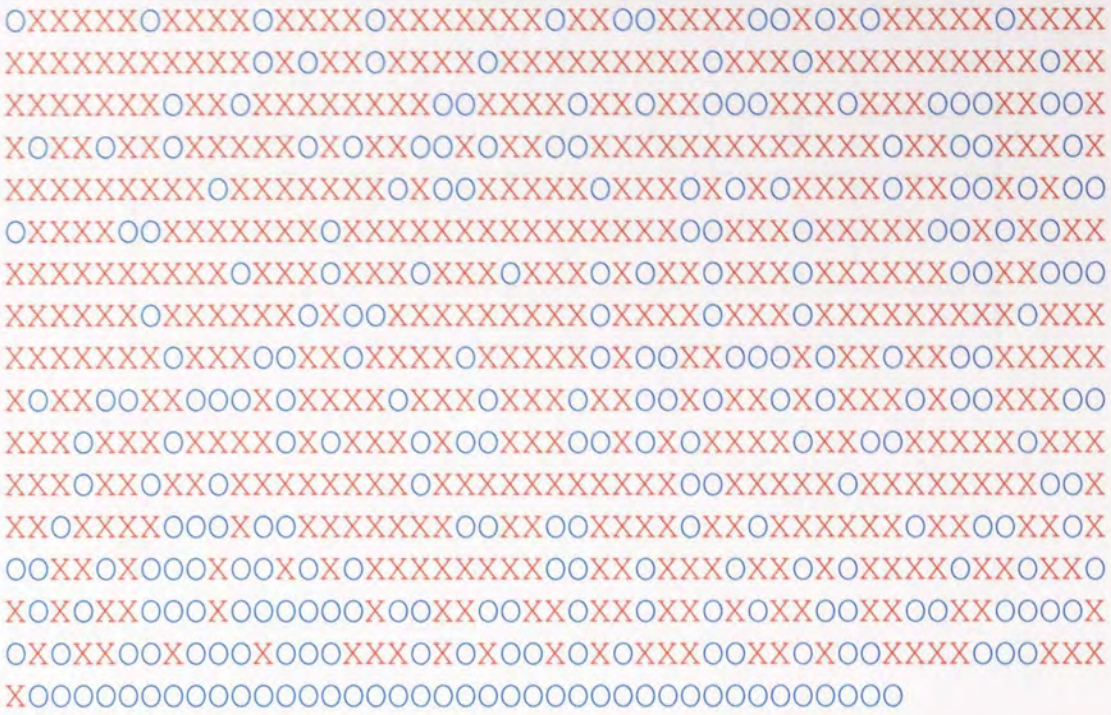

The simulated copolymer contains 500 AMO units and 1500 MMA units

Sequence Length	AMO	MMA
1	269	91
2	65	77
3	16	43
4	2	36
5	0	19
6	1	19
7	0	11
8	0	9
9	0	12
10	0	8
11	0	5
12	0	6
13	0	2
14	0	3
15	0	3
16	0	1
18	0	3

19	0	2
20	0	1
21	0	1
22	0	1
25	0	1
39	1	0

NVP/MMA/MAA 79.5:19.75:0.5

79.75 mole % of monomer A, NVP

19.75 mole % of monomer B, MMA

0.5 mole % of monomer C, MAA

r(AB) = 0.01 r(AC) = 0.002 r(BA) = 4.04

r(BC) = 0.869 r(CA) = 2.777 r(CB) = 1.096

Polymerised to 100% conversion

In the simulated copolymer NVP is represented by O, MMA is represented by X and MAA is represented by *

OXXOXXXOOXXOXOXOXOXOXOXOXXOXXO*OXXOXOXO*OXXOXXOXO
XOXO*OOXOXO*XXXXXXOXXO*OXOXXOXXXXO*OXXXXOXOXXXXOX
XOXOXXOXXOXXXXXXO*XXOXOXXOXOXXOXOXXOXXOXOXOXOXXXO
XOXOXOXOXXXO*OXOXXXO*XOXOXXXXXXXXOXOXXXOXOX*XOXXOX
OXOXOXOXOXOXOXOXOXOXXXOXXOXXXXOXOXXOXXXXXXOXOOXXO
XOXOXOXOXOXXXOXXOXOXOXXXOXXXXOXOXXOXOXOXOXXOXXOXX
OXOXXOXOXOXXXOXXOXOXOXXXOXOXOXXOXOXOXOXOXOXXOXOXO
XOXOXXXXOXXOXXOXOXXXXOXXOXXOXXOXXXOXXXXOXOXOXOXOX
OXOXOXOXXOXOXXXOXOXXOXOXOOXOXOXOXXOXOXXOXOXOXOXOX
OXXOXOXXOXOOOXOXOOXOXXOXOXOOXOXOXOXOXXOXOXOXOXOXX
OXOXXOXXOXOXOOXXOXXOXOXOXOOXOXOXOOXOXOXOXOXOXOOXO
XOXOXOXOXXOXOXOXOOOXOXOXOXXOOOXOOOXOOXOXOXXXOXOXO
XOXXOXOXOXXXOXOXOXOXOXXOOXOOXOXOXOXOXOXOOOXOXOXOX

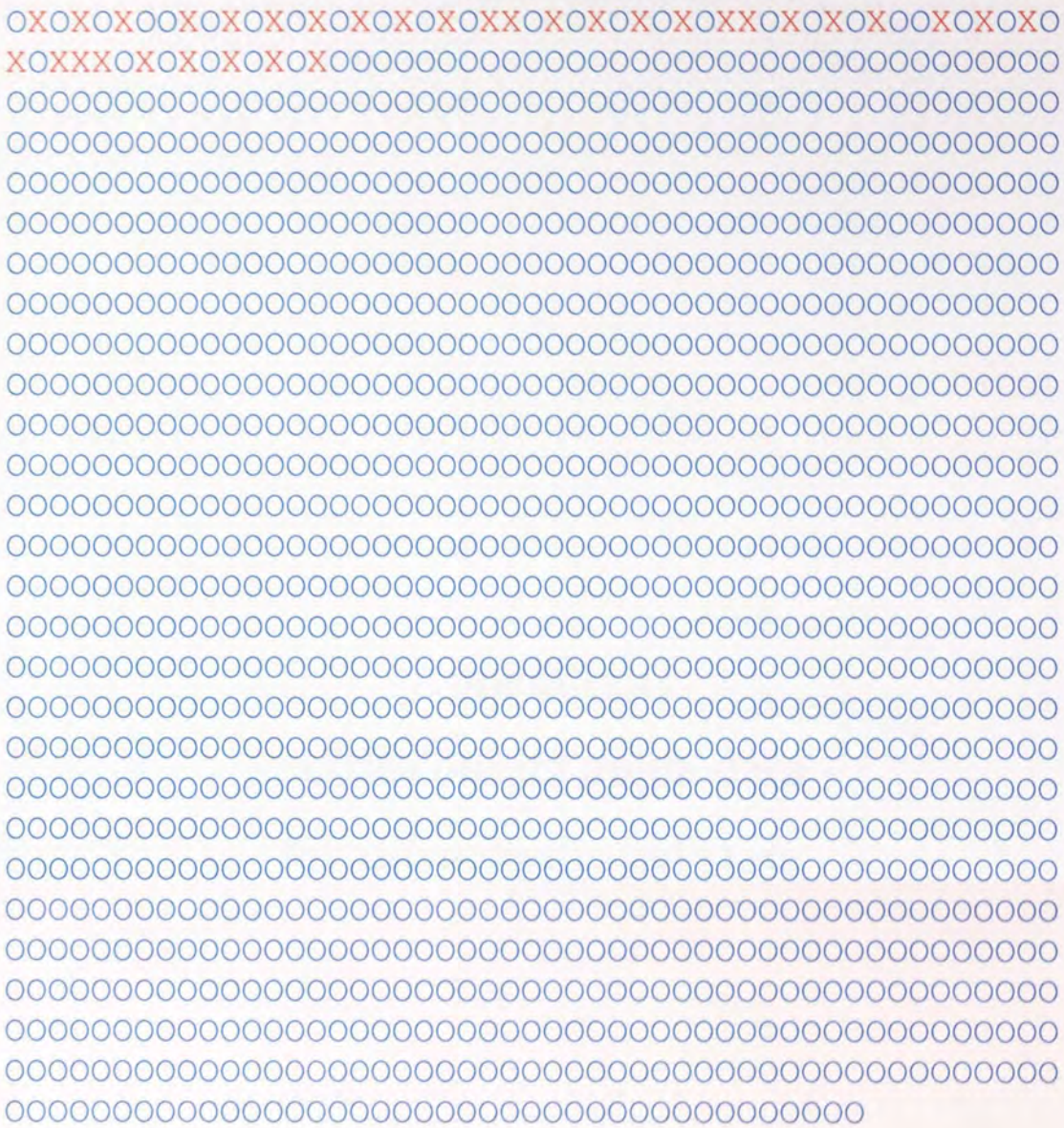

The simulated copolymer contains 1595 NVP units and 395 MMA units and 10 MAA units

Sequence Length	NVP	MMA	MAA
1	251	185	10
2	15	54	0
3	5	15	0
4	0	8	0
6	0	3	0
7	0	1	0
1299	1	0	0

Appendix II

Static contact angle data for the dehydrated state

Copolymer Composition	Water Contact Angle	CH_2I_2 Contact Angle	Polar Component of Surface Energy ± SD (mN/m)	Dispersive Component of Surface Energy ± SD (mN/m)
HEMA	70.7 ± 2	37.2 ± 2	8.5 ± 1.45	35.0 ± 1.55
NVP/MMA 60:40	85.6 ± 2	23.7 ± 2	1.2 ± 0.50	45.6 ± 1.40
NVP/MMA 70:30	82.3 ± 2	23.2 ± 2	2.0 ± 0.70	44.8 ± 1.40
NVP/MMA 80:20	78.8 ± 2	24.5 ± 2	3.2 ± 0.85	43.3 ± 1.35
NVP/MMA 90:10	71.6 ± 2	25.5 ± 2	6.4 ± 1.20	40.8 ± 1.40
NVP/MMA/NVI 79:19:2	77.6 ± 2	32.5 ± 2	4.4 ± 1.05	39.3 ± 1.55
NVP/MMA/NVI 77.5:17.5:5	81.4 ± 2	34.5 ± 2	3.1 ± 0.95	39.3 ± 1.60
NVP/MMA/NVI 76.5:16.5:7	84.4 ± 2	35.8 ± 2	2.2 ± 0.80	39.5 ± 1.65
NVP/MMA/NVI 75:15:10	81.3 ± 2	33.8 ± 2	3.1 ± 0.90	39.6 ± 1.60
NVP/MMA/DEAEMA 79:19:2	69.2 ± 2	22.3 ± 2	7.3 ± 1.25	41.4 ± 1.25
NVP/MMA/DEAEMA 77.5:17.5:5	71 ± 2	32.2 ± 2	7.5 ± 1.35	37.6 ± 1.45
NVP/MMA/DEAEMA 76.5:16.5:7	74.9 ± 2	32.4 ± 2	5.6 ± 1.15	38.6 ± 1.50
NVP/MMA/DEAEMA 75:15:10	84.2 ± 2	32.5 ± 2	2.0 ± 0.75	41.1 ± 1.60
NVP/MMA 25:75	75.1 ± 2	19.2 ± 2	4.3 ± 0.95	44.1 ± 1.20
AMO/MMA 25:75	73.9 ± 2	23.5 ± 2	5.1 ± 1.05	42.2 ± 1.35
NVP/MMA/MAA 79.75:19.75:0.5	90.8 ± 2	19.9 ± 2	0.2 ± 0.23	48.7 ± 1.31
HEMA (control)	83 ± 2	38.3 ± 2	2.9 ± 0.91	37.7 ± 1.68
HEMA (autoclaved)	85.1 ± 2	42.5 ± 2	2.6 ± 0.88	35.8 ± 1.74

Appendix III

Static contact angle data for the hydrated state

Copolymer Composition	Air Contact Angle	Octane Contact Angle	Polar Component of Surface Energy ± SD (mN/m)	Dispersive Component of Surface Energy ± SD (mN/m)
HEMA	37.6 ± 2	134.2 ± 2	36.7 ± 1.09	22.1 ± 2.85
NVP/MMA 60:40	37.9 ± 2	131.9 ± 2	35.5 ± 1.11	23.4 ± 2.99
NVP/MMA 70:30	37.0 ± 2	133.2 ± 2	36.2 ± 1.09	23.3 ± 2.92
NVP/MMA 80:20	35.3 ± 2	138.8 ± 2	39.2 ± 1.03	21.0 ± 2.60
NVP/MMA 90:10	33 ± 2	146.7 ± 2	43.0 ± 0.90	18.6 ± 2.18
NVP/MMA/NVI 79:19:2	37.3 ± 2	141.5 ± 2	40.5 ± 0.99	18.2 ± 2.42
NVP/MMA/NVI 77.5:17.5:5	39.6 ± 2	143.8 ± 2	41.6 ± 0.95	15.5 ± 2.25
NVP/MMA/NVI 76.5:16.5:7	35.9 ± 2	147.2 ± 2	43.2 ± 0.89	16.5 ± 2.14
NVP/MMA/NVI 75:15:10	31.0 ± 2	150.1 ± 2	44.4 ±0.83	18.3 ± 2.02
NVP/MMA/DEAEMA 79:19:2	35.0 ± 2	142.0 ± 2	40.8 ±0.98	19.5 ± 2.42
NVP/MMA/DEAEMA 77.5:17.5:5	35.8 ± 2	144.0 ± 2	41.7 ± 0.95	18.0 ± 2.30
NVP/MMA/DEAEMA 76.5:16.5:7	35.9 ± 2	143.4 ± 2	41.4 ± 0.96	18.2 ± 2.33
NVP/MMA/DEAEMA 75:15:10	32.9 ± 2	144.5 ± 2	42.0 ± 0.94	19.7 ± 2.30
NVP/MMA 25:75	52.7 ± 2	114.7 ± 2	25.6 ± 1.15	22.9 ± 3.73
AMO/MMA 25:75	41.9 ± 2	119.5 ± 2	28.4 ± 1.16	29.7 ± 3.79
NVP/MMA/MAA 79.75:19.75:0.5	35.3 ± 2	140.1 ± 2	39.8 ± 1.01	20.3 ± 2.52
HEMA (control)	44.2 ± 2	127.8 ± 2	33.1 ± 1.14	21.0 ± 3.12
HEMA (autoclaved)	44.7 ± 2	125.6 ± 2	31.9 ± 1.15	22.1 ± 3.26

Appendix IV

Dynamic contact angle data

Composition	water			1% FCS		
	advancing	receding	hysteresis	advancing	receding	hysteresis
HEMA	92.87	26.63	66.24	50.1	47.9	2.2
NVP/MMA 60:40	44.63	0	44.63	107.3	103.3	4
NVP/MMA 70:30	55.64	40.42	15.22	64.5	61.9	2.6
NVP/MMA 80:20	20.27	0	20.27	60.3	58.3	2
NVP/MMA 90:10	32.35	27.38	4.97	34.8	30	4.8
NVP/MMA/NVI 79:19:2	0	0	0	51.1	45.6	5.5
NVP/MMA/NVI 77.5:17.5:5	112.28	91.18	21.1	59.3	56.3	3
NVP/MMA/NVI 76.5:16.5:7	66.41	35.29	31.12	41.5	24.8	16.7
NVP/MMA/NVI 75:15:10	44.63	0	44.63	65.4	54.6	10.8
NVP/MMA/DEAEMA 79:19:2	55.83	41.38	14.45	38.4	32.4	6
NVP/MMA/DEAEMA 77.5:17.5:5	50.78	43.07	7.71	40.7	33.1	7.6
NVP/MMA/DEAEMA 76.5:16.5:7	87.87	48.55	39.32	33.1	24.3	8.8
NVP/MMA/DEAEMA 75:15:10	78.46	23.47	54.99	52.3	33.9	18.4
NVP/MMA 25:75	68.8	14	54.8	36.6	20.1	16.5
AMO/MMA 25:75	83.8	33.7	50.1	36.6	34.5	2.1
NVP/MMA/MAA 79.75:19.75:0.5	33.5	23.8	9.7	33.1	26.4	6.7

Composition	10% FCS			100% FCS		
	advancing	receding	hysteresis	advancing	receding	hysteresis
HEMA	68.2	64.5	3.7	61.04	54.9	6.14
NVP/MMA 60:40	61.3	59.1	2.2	65.2	63.2	2
NVP/MMA 70:30	63.9	60.2	3.7	57.4	55.1	2.3
NVP/MMA 80:20	54.3	48.5	5.8	41.6	28.4	13.2
NVP/MMA 90:10	44.2	36.5	7.7	43.6	30.1	13.5
NVP/MMA/NVI 79:19:2	60.5	57	3.5	59.3	55.3	4
NVP/MMA/NVI 77.5:17.5:5	44.7	44.5	0.2	39.1	27.6	11.5
NVP/MMA/NVI 76.5:16.5:7	56.5	55.2	1.3	49.3	39.2	10.1
NVP/MMA/NVI 75:15:10	40.3	28	12.3	42.8	33.1	9.7
NVP/MMA/DEAEMA 79:19:2	56.8	48.1	8.7	60	58.2	1.8
NVP/MMA/DEAEMA 77.5:17.5:5	39.9	26.7	13.2	39.9	20.6	19.3
NVP/MMA/DEAEMA 76.5:16.5:7	69.9	62	7.9	61.3	53.9	7.4
NVP/MMA/DEAEMA 75:15:10	37.6	26	11.6	39.8	27.1	12.7
NVP/MMA 25:75	48.4	39.2	9.2	53.2	38.8	14.4
AMO/MMA 25:75	39.8	30.1	9.7	52.9	40.2	12.7
NVP/MMA/MAA 79.75:19.75:0.5	42.9	36.2	6.7	46.5	36.8	9.7

Composition	MeOH		
	advancing	receding	hysteresis
NVP/MMA 60/40	42.5	31.8	10.7
	n-octane		
	advancing	receding	hysteresis
NVP/MMA 60:40	38.2	47.1	8.9
NVP/MMA 70:30	26.4	41.6	15.2
NVP/MMA 80:20	59.1	73.1	14
NVP/MMA 90:10	54.7	63.9	9.2
	LiBr		
	advancing	receding	hysteresis
NVP/MMA 60/40	52.2	39.4	12.8
NVP/MMA 70/30	65.7	53	12.7
NVP/MMA/ NVI 79/19/2	54	39.2	14.8
NVP/MMA/ DEAEMA 79/19/2	86.2	40.5	45.7
	autoclave test		
HEMA (control)	116.9	39.8	77.1
HEMA (autoclaved)	119.1	39.9	79.2

Consistency experiments			
HEMA in water	advancing	receding	hysteresis
1	108.6	38	70.6
2	107.5	36	71.5
3	104.7	47.9	56.8
4	109.3	47.8	61.5
5	108.2	44.7	63.5
Range	4.6	11.9	14.7
Standard deviation (SD)	1.78	5.56	6.23

HEMA in 1% FCS	advancing	receding	hysteresis
1	55.2	53.1	2.1
2	75.6	73.6	2
3	63.2	58.4	4.8
4	70.1	66.2	3.9
5	69.7	64.7	5
Range	20.4	20.5	3
Standard deviation (SD)	7.81	7.82	1.44
NVP/MMA in water	advancing	receding	hysteresis
1	56.5	43.8	12.7
2	62.5	50.1	12.4
3	77.1	66.4	10.7
4	63.3	50	13.3
5	77.2	64.8	12.4
Range	20.7	22.6	2.6
Standard deviation (SD)	9.35	10.01	0.97
NVP/MMA in1% FCS	advancing	receding	hysteresis
1	49	42.2	6.8
2	64.3	59.7	4.6
3	59.4	54.8	4.6
4	71.7	65	6.7
5	55.9	48.7	7.2
Range	22.7	22.8	2.2
Standard deviation (SD)	8.57	8.96	1.27

Appendix V

Surface tensions of probe liquids after dynamic contact angle tests

	water	1%	10%	100%
HEMA	71.5	58.6	55.7	57.5
NVP/MMA 60:40	72.2	61.7	54.5	54.7
NVP/MMA 70:30	72	62.6	55.3	55.1
NVP/MMA 80:20	72.4	60.1	56.7	54.8
NVP/MMA 90:10	72.2	61.8	56	54.6
NVP/MMA/NVI 79:19:2	71.7	61.8	58.4	54
NVP/MMA/NVI 77.5:17.5:5	72.2	61.8	60.4	55.3
NVP/MMA/NVI 76.5:16.5:7	72.5	59.3	57.3	55.1
NVP/MMA/NVI 75:15:10	70.3	58.5	56	56
NVP/MMA/DEAEMA 79:19:2	71.4	61.9	57.5	54.4
NVP/MMA/DEAEMA 77.5:17.5:5	71.6	60.6	57	54.9
NVP/MMA/DEAEMA 76.5:16.5:7	71.6	60.3	56.8	54.2
NVP/MMA/DEAEMA 75:15:10	71.8	61.3	55.2	55.4
NVP/MMA 25:75	72.1	64.6	58.7	55.1
AMO/MMA 25:75	71.8	67.9	60.4	56.6
NVP/MMA/MAA 79.75:19.75:0.5	70	64.7	58.7	55.4

	MeOH
NVP/MMA 60/40	24.6
	n-octane
NVP/MMA 60:40	23.1
NVP/MMA 70:30	22.6
NVP/MMA 80:20	23.2
NVP/MMA 90:10	23.2
	LiBr
NVP/MMA 60/40	68.2
NVP/MMA 70/30	61.5
NVP/MMA/ NVI 79/19/2	65.7
NVP/MMA/ DEAEMA 79/19/2	62.5
	water
HEMA (control)	72.2
HEMA (autoclaved)	72.6

consistency experiments				
	HEMA in water	HEMA in 1% FCS	NVP/MMA in water	NVP/MMA in1% FCS
1	72.1	61.4	72.1	62.6
2	71.9	61.6	71.7	63.8
3	71.8	63.8	71.9	62.8
4	71.6	61.6	72.1	65.1
5	71.1	61.5	70.9	62.8
Range	1.0	2.4	1.2	2.5
Standard deviation (SD)	0.38	1.02	0.50	1.05

Appendix VI

Cell adhesion DAPI counts

3T3

composition	EWC %	mean cell count n=6	Standard deviation (SD)	standard error (SEM)
NVP/MMA 60:40	56	2.00	1.73	1.00
NVP/MMA 70:30	64	23.67	17.79	10.27
NVP/MMA 80:20	75	28.00	3.61	2.08
NVP/MMA 90:10	84	19.67	10.07	5.81
NVP/MMA/NVI 79:19:2	76	121.00	60.80	35.10
NVP/MMA/NVI 77.5:17.5:5	78	103.00	89.15	51.47
NVP/MMA/NVI 76.5:16.5:7	79	53.67	20.43	11.79
NVP/MMA/NVI 75:15:10	81	26.33	14.36	8.29
NVP/MMA/DEAEMA 79:19:2	78	6.33	8.50	4.91
NVP/MMA/DEAEMA 77.5:17.5:5	78	13.00	15.39	8.89
NVP/MMA/DEAEMA 76.5:16.5:7	79	31.33	35.28	20.37
NVP/MMA/DEAEMA 75:15:10	79	34.33	33.55	19.37
glass coverslip		1136.67	238.48	137.69
poly(HEMA)	38	393.5	21.92	12.66
NVP/MMA 25:75	14	204.67	18.01	10.40
AMO/MMA 25:75	18	124.67	22.50	12.99

EK1.BR

composition	EWC %	mean cell count n=6	Standard deviation (SD)	standard error (SEM)
NVP/MMA 60:40	56	6.17	8.86	3.62
NVP/MMA 70:30	64	5.33	8.73	3.57
NVP/MMA 80:20	75	0.00	0.00	0.00
NVP/MMA 90:10	84	2.50	5.65	2.31
NVP/MMA/NVI 79:19:2	76	27.83	39.49	16.12
NVP/MMA/NVI 77.5:17.5:5	78	12.67	23.96	9.78
NVP/MMA/NVI 76.5:16.5:7	79	4.33	5.54	2.26
NVP/MMA/NVI 75:15:10	81	12.50	18.82	7.68
NVP/MMA/DEAEMA 79:19:2	78	0.17	0.41	0.17
NVP/MMA/DEAEMA 77.5:17.5:5	78	11.17	11.41	4.66
NVP/MMA/DEAEMA 76.5:16.5:7	79	10.67	16.05	6.55
NVP/MMA/DEAEMA 75:15:10	79	12.33	19.77	8.07
glass coverslip		524.6	289.72	118.28
poly(HEMA)	38	182.4	96.88	39.55